THE EFFECT OF CHEMISTRY AND NETWORK STRUCTURE ON MORPHOLOGICAL AND MECHANICAL PROPERTIES OF DIEPOXIDE PRECURSORS AND POLY(HYDROXYETHERS)

Maggie Marie Bobbitt Bump

Dissertation submitted to the Faculty of the Virginia Polytechnic Institute and State University in partial fulfillment of the requirements for the degree of

Doctor of Philosophy

In

Chemistry

Judy S. Riffle, Chair

John G. Dillard

John J. Lesko

Timothy E. Long

James E. McGrath

Allan R. Shultz

April 2001

Blacksburg, Virginia

Keywords: Phosphine oxide, epoxy, structural adhesive, composite interphase, sizing, water dispersible polyurethane

The Effect of Chemistry and Network Structure on Morphological and Mechanical Properties of Diepoxide Precursors and Poly(hydroxyethers)

Maggie Marie Bobbitt Bump

Abstract

This dissertation research addresses the interrelationships between chemistry and network structure in epoxy networks as well as how mechanical properties of the resulting networks are affected by these relationships. The effects of chemistry and network structure on interphase morphology and performance in vinyl ester/carbon fiber composites have also been investigated on both a macro and nanoscale.

Thermosets were prepared with blends of bisphenol-A and novel phosphine oxide based diepoxide oligomers using a siloxane or a novolac crosslinking agent. In the siloxane cured networks the incorporation of the phosphine oxide group yielded networks with increased glass transition temperatures, from 71°C to 92°C, and water absorption, from 1 wt % to 5.5 wt %, due to the polar nature of the phosphine oxide bond. Higher char yields were also observed with the addition of the phosphorus, 27 wt % compared to 11 wt % for bisphenol-A epoxy networks. The bisphenol-A based epoxy/siloxane network was exceptionally ductile with a fracture toughness (K_{1c}) of 2 MPa-$m^{1/2}$. In networks prepared with the novolac crosslinking agent hydrogen bonding, observed using FTIR, was evident even at temperatures above the network T_g and resulted in increased rubbery moduli with phosphine oxide incorporation. Adhesive strengths to steel increased from ~9.7 MPa with bisphenol-A epoxy to ~13.8 MPa when the phosphine oxide containing epoxy was incorporated into the network.

Within carbon fiber/vinyl ester composites, a series of tough ductile thermoplastics and a series of one-phase polyurethanes were investigated as carbon fiber sizings. The three poly(hydroxyether)s resulted in different interphase morphologies due to their respective interdiffusion into the vinyl ester resin. The unmodified poly(hydroxyether) was miscible with the vinyl ester resin at the elevated cure temperatures and adhesion between the fiber and bulk matrix was increased from 28 MPa with unsized fibers to 45 MPa with sized fibers. The carboxylate modified

poly(hydroxyether) was also miscible at elevated temperatures, however the interdiffused region was narrower, ~5 μm. This system showed an increase in the fiber/matrix adhesion similar to that found for the unmodified poly(hydroxyether)/vinyl ester system and composite cyclic fatigue durability was improved by ~50 %. Using a poly(hydroxyether ethanolamine) interphase material, which was not miscible with the resin, resulted in a sharp interface. While the adhesion was not improved through the use of this sizing, the composite fatigue durability was still increased by a moderate amount, ~ 25%. The one-phase polyurethanes were dispersible in water with incorporation of a minimum of 0.08 equivalents of N-methyldiethanolamine per mole of diisocyanate. Fatigue durability in composite panels was not improved by the addition of the polyurethane sizings due to the miscibility of the sizing and the matrix.

Acknowledgments

I would like to thank Dr. Judy Riffle for her support, guidance and instruction throughout my graduate career. As an advisor, she has been a source of direction and encouragement; as a woman in science, she has been an inspiration. I have been honored to have Dr. James McGrath, Dr. John Dillard, Dr. Allan Shultz, and Dr. Jack Lesko serve on my graduate committee. Not only did these individuals provide invaluable time and assistance regarding polymer chemistry, they have been motivational in their love of science and life.

This work was possible with assistance of many people throughout the chemistry and engineering departments who helped me with both the technical and business aspects of graduate school, including Malcolm Robertson, Nikhil Verghese, Tom Glass and Steve McCartney for their time and energy spent teaching me new techniques. Angie Flynn and Esther Brann have been irreplaceable, helping with everything from submitting papers to planning parties. I have also had the privilege of working with four wonderful undergraduates, Kim Wilson, Sarah Bedsaul, Becky Jelen and Anita Carmichael, each of whom accomplished a great deal.

I thank the Riffle group throughout my graduate career for answering and asking questions on so many occasions. My gratitude also goes to the other organic polymer, polypkem and CASS groups for critical technical discussions that so often took place at the river, on the trail or in the bar. I especially thank 'my girls', old and new for the dancing, hiking, laughter, baking, theme parties and movie clips that have propelled me on throughout my extended academic career. Jen, Ron, Linda and Amy (listed in order of appearance), thank you for making me keep it in perspective!

Most of all, I thank the Lord and my family, for helping me know which path to follow. This dissertation is the product of so much more than five years and my family has supported me through it all. Grandma and Granddaddy, you are my faith. Mom and Dad, you are my heroes. Callie, you are my inspiration. Greg, you are my strength.

There are so many people to whom I am indebted for support and encouragement. I thank you all.

Contents

List of Figures

List of Tables

Chapter 1. Introduction

Bisphenol-A based epoxides are utilized for many applications due the versatility imparted by the strained oxirane ring[1,2,3]. Epoxides can be crosslinked via homopolymerization or reaction with crosslinking agents. Diepoxides are also used as oligomeric precursors for thermoset resins with diverse functionalities, such as vinyl ester resins, and for thermoplastic poly(hydroxyethers).

Epoxy resins and their networks are of interest for use as structural adhesives because of their excellent structural properties, good solvent and corrosion resistance, and their ability to hydrogen bond with a variety of adherends. Different backbone structures can be incorporated into the epoxy oligomer and a variety of crosslinking reagents can be used to cure the resin. In this research a diepoxide has been prepared containing a phosphine oxide functionality. The inorganic nature of the group has improved the flammability properties in thermosets[4,5] while the polarity of the bond increases the hydrogen bonding ability of the resulting epoxy, possibly improving network adhesion to various substrates. This polar resin was blended with a traditional bisphenol-A based epoxy resin at different concentrations to optimize network performance.

Crosslinking agents can further tailor processability and network properties. Amine terminated polysiloxane crosslinking reagents are of particular interest for curing epoxide resins due to their low viscosities, wide service temperature range and ambient cure. Incorporation of a siloxane group can also decrease water absorption and increase

---

[1] H. Lee and K. Neville, Handbook of Epoxy Resins, 1967, McGraw-Hill, Inc., New York.

[2] B. Ellis, Ed., Chemistry and Technology of Epoxy Resins, 1st edition, 1993, Chapman & Hall, New York.

[3] W. G. Potter, Epoxide Resins, 1970, Springer-Verlag, New York.

[4] I.-Y. Wan, J. E. McGrath and T. Kashiwagi, Triarylphosphine oxide containing Nylon 6,6 copolymers, Fire and Polymers II Materials and Tests for Hazard Prevention, ACS Symposium Series (599), G. L. Nelson, Ed., 1995, 29-40.

[5] Y.-L. Liu, G.-H. Hsuie, Y.-S. C, R.-J. Jeng and L.-H. Perng, *J. Appl. Polym. Sci.*, 1996, **61**, 613-621.

network flame retardance[6,7]. Phenolic novolac resins are inherently flame retardant and when reacted with epoxy resins form tough, void-free networks. Due the multifunctional nature of the novolac oligomer, network properties can be tailored to a specific application by varying the epoxide/phenol ratio.

This research addressed the effects of both network chemistry, varied by the epoxy backbone (bisphenol-A based and phosphine oxide based) and the curing agent (amine terminated siloxane and phenolic novolac), and network structure, varied by offsetting the cure stoichiometries, on thermoset properties.

Fiber reinforced composites are used commercially for aerospace and automotive applications. The polymeric matrix provides transverse integrity to the composite while the fibers are the load bearing components. Matrices can be thermoplastics, such as polyethylene and nylon, or thermosets, such as epoxies and unsaturated polyesters. Typical reinforcements include carbon, glass, and polyimide fibers. Between the fiber surface and the bulk matrix resin, a region of finite size exists with properties different from the fiber and the matrix. Research has shown that the composite properties are dependent on the properties of this interphase [8,9,10,11].

The composites investigated in this work were 60 vol % continuous strand carbon fiber and 40 vol % vinyl ester matrix. The vinyl ester resin was a diglycidyl ether of bisphenol-A endcapped with methacrylate groups that allowed the resin to be cured free radically. These oligomers were diluted with 30 wt % styrene. In the carbon fiber/vinyl ester systems, a residual stress developed during the thermal cure due to shrinkage of the resin.

---

[6] C. Tran, Modification of Polymers I. Polysiloxane Modified Epoxies II. Segmented Polyurethane Blends. Virginia Tech Dissertation, 1984.

[7] J.S. Riffle, J. Yilgor, C. Tran, G.L. Wilkes, J.E. McGrath and A.K. Banthia, ACS Symposium Series #221, Epoxy Resin Chemistry, R.S. Bauer, Ed., 21-54 (1983).

[8]J. J. Lesko, A. Rau, and J. S. Riffle, Proc. 10th American Society of Composites, 18-20 Sept., 1995, 53-62.

[9]J. J. Lesko, R. E. Swain, J. M. Cartwright, J. W. Chen, K. L. Reifsnider, D. A. Dillard, and J. P. Wightman, *J. Adhes.*, 1994, **45**, 43, 43-57.

[10]N. S. Broyles, R. Chan, R. M. Davis, J. J. Lesko, and J. S. Riffle, *Polymer*, 1998, **39**(12), 2607-2613.

[11]L. T. Drzal, M. J. Rich and P. F. Lloyd, *J. Adhes.*, 1982, **16**, 1-30.

Sizing the carbon fibers to create a tailored interphase region that can dissipate residual stress is one approach to improving composite performance. Thermoplastic sizings were used in carbon fiber/vinyl ester composites in an attempt to control both the physical properties of the interphase region and fiber/matrix adhesion. The sizing materials were applied to the surface of the fibers from an aqueous bath prior to impregnation with the matrix resin. Tough, ductile poly(hydroxyethers) and low modulus, one phase polyurethanes were investigated to gain a greater understanding of the relationship between interphase properties and composite performance. It was anticipated that composite properties could be optimized by applying a sizing that would 1) improve fiber/matrix adhesion and 2) create an interphase with a gradient of properties to alleviate the residual stress. While adhesion of the fiber to the bulk matrix is necessary to ensure load transfer, increased adhesion may lead to increased residual stress that develops because the two systems (fiber and matrix) are adhered together as the matrix attempts to shrink during cure. Both the sizing/matrix interdiffusion that establishes interphase structure and the adhesion of the sizing to the fiber and matrix are dependent on the sizing chemistry and interaction with the matrix resin before and after cure. Therefore, this research addresses the effect of morphology and adhesion, controlled through sizing chemistry, on cyclic fatigue durability of the composite, a property that is particularly sensitive to changes at the interphase.

Through improvements in continuous strand fiber composite properties, these systems with high strength to weight ratios are now being considered for structural applications, such as infrastructure repair, where steel and concrete have been used traditionally. In order to utilize composites for infrastructure repair, an adhesive that can be applied at the job site to bond new materials to the existing steel structures is necessary. This structural adhesive should have good mechanical properties and be able to hydrogen bond with the heteroatoms and hydroxyl groups on the substrate surface while having a limited affinity for water. With 17 % of the nation's highway bridges

being presently structurally deficient and 13 % functionally obsolete there is a vast market for the use of both composites and adhesives[12,13].

[12] Civil Engineering Research Foundation, Partnership for the advancement of infrastructure and its renewal: transportation component (PAIR-T) technology & investment plan. *Civil Engineering Research Foundation white paper*, 1998a.

[13] U.S. Department of Transportation, Bureau of Transportation Statistics, web site, http://www.bts.gov/aboutbts.html, 2001.

Chapter 2. Literature Review

2.1. Epoxy Resins

2.1.1. Introduction to Epoxy Chemistry

Epoxy resins are a broad class of versatile reactive compounds. The need for a high degree of control over both network properties and resin processability make epoxy chemistry appealing for many applications. The epoxide functionality is stable under ambient conditions and results in an extended shelf life for epoxidized oligomers and polymers. Epoxide rings however can be reacted with a variety of other moieties. The choice of curing agent allows epoxy resins to be cured under ambient conditions, at elevated temperatures, or by exposure to light to yield tough, void-free networks. Both the backbone and cure chemistries can be tailored to provide specific resin processing and network properties.

The freedom offered by epoxy systems to manipulate both resin and network properties has resulted in extensive fundamental research and commercial use of these materials. The following review first discusses the large body of epoxide work that has developed since the 1930s with a focus on industrially significant resins, curing agents and additives. Then novel resins and catalysts that have been investigated over the past decade are addressed. Several excellent epoxy reviews have been compiled and can be referred to for a more detailed study of epoxy research. Epoxy Resins: Chemistry and Technology, edited by C. A. May, discusses a broad spectrum of work including fundamental research regarding the reaction chemistry and cure of epoxies as well as a thorough study of the resulting network properties and applications[14]. Handbook of Epoxy Resins by H. Lee and K. Neville[1] and Epoxy Resins by W. G. Potter[2] include overviews of epoxy resins, curing agents, mechanical behavior and applications such as adhesives, laminates and coatings. A more recent review edited by Bryan Ellis,

[14] C. A. May, Ed., Epoxy Resins: Chemistry and Technology, 1988, Marcel Dekker, Inc. New York.

Chemistry and Technology of Epoxy Resins[2], also discusses the use of epoxy resins as composite matrices. Listings of commercially available epoxy systems[15] and reviews of patent literature[16] have also been compiled.

The term 'epoxy resin' has been applied to a very diverse collection of oligomeric and polymeric materials[17]. While 'epoxy' refers generally to a ring containing an oxygen, the materials called epoxy resins industrially contain specific 1,2-epoxides which are three membered oxirane rings (Figure 2-1). The term *glycidyl* may also be used when naming compounds with epoxy groups. Although the networks formed following the cure of these systems may no longer contain epoxide groups, they are referred to as epoxy networks.

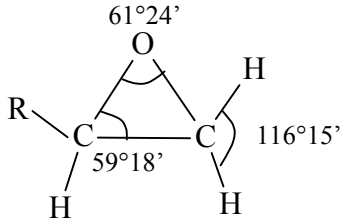

Figure 2-1. Oxirane ring found in common epoxy resins.

Epoxy chemistry was first reported in 1859 when Wurtz synthesized ethylene oxide from ethylene chlorohydrin using aqueous base[18]. This chemistry is similar to that used today to prepare epoxy resins from epichlorohydrin and phenols. In 1909, the Russian chemist Prileschaiev found a new synthetic pathway to the oxirane ring[19]. By reacting vinyl groups with peroxy acids, such as perbenzoic acid, epoxides could be

---

[15] E. W. Flick, Epoxy Resins, Curing Agents, Compounds, and Modifiers, 1987, Noyes Publications, Park Ridge, NJ.

[16] J. I. DiStasio, Ed., Epoxy Resin Technology-Developments Since 1979, 1982, Noyes Data Corp., Park Ridge, NJ.

[17] Y. Tanaka, Synthesis and Characteristics of Epoxides, Epoxy Resins: Chemistry and Technology, C. A. May, Ed., 1988, Marcel Dekker, Inc. New York.

[18] B Ellis, Introduction to the chemistry, synthesis, manufacture and characterization of epoxy resins, Chemistry and Technology of Epoxy Resins, 1st edition, B. Ellis, Ed., 1993, Chapman & Hall, New York, 1-36.

[19] C. A. May, Introduction to Epoxy Resins, Epoxy Resins: Chemistry and Technology, C. A. May, Ed., 1988, Marcel Dekker, Inc. New York.

prepared. Today, this synthesis is used in the production of cycloaliphatic epoxy resins. By 1936, Schlack reported oligomerization of bisphenol-A and epichlorohydrin as well as the reaction of epoxy oligomers with amines and anhydrides[2]. Working independently, Castan in Switzerland and Greenlee in the United States are credited with commercialization of epoxy resins in the 1940s[19]. Castan reacted bisphenol-A with epichlorohydrin and cured the resulting oligomer with phthalic anhydride for potential use as denture materials. Using similar chemistry to a different end, Greenlee at Devoe-Reynolds prepared higher molecular weight poly(hydroxyethers) from epichlorohydrin and bisphenol-A for use as surface coatings. The epoxy chemistry allowed the formation of networks free of hydrolyzable ester linkages. The peroxy acid chemistry to epoxidize alkenes was further developed by Swern and was being used commercially by 1950[1].

The epoxy cure chemistry offers many benefits. Since commercialization of epoxies in 1947, when Devoe-Reynolds released the bisphenol-A based resin, numerous oligomers have been modified through the addition of epoxide rings. Resins ranging from low viscosity liquids to tack-free solids can be prepared by tailoring the backbone chemistry to which the oxirane rings are appended[18]. The epoxide functionality can be cured over a range of temperatures, from 5°C to ~250°C, depending on the crosslinking agent and can be cured without volatile by-products (unlike the phenolic resins) to yield void-free networks with good mechanical properties. The resins have lower cure shrinkage than thermosetting resins which have reactive diluents such as free radically cured unsaturated polyester-styrene resins[20]. For these reasons epoxy materials are used in a wide range of areas including coatings, adhesives and fiber reinforced composites. Epoxy resins, due to the reactivity of the oxirane ring, are also common precursors to higher molecular weight thermoplastics as well as oligomers with different endgroup functionalities.

2.1.2. Epoxide Chemistry

Epoxides are generally synthesized by one of two methods, from phenols and epichlorohydrin or from alkenes and peroxy acids (Figure 2-2)[2,18,23]. The most widely

utilized of these for epoxy resins is the reaction of phenol with epichlorohydrin under basic conditions. In this process, the phenolate anion opens the oxirane ring of the halohydrin through a nucleophilic substitution reaction. Then subsequent intramolecular chloride elimination regenerates an oxirane ring. The substitution occurs most readily at the least substituted carbon, which is consistent with the S_N2 mechanism. Addition at the more substituted carbon or incomplete chloride elimination leads to chlorine remaining in the epoxy resin, typically at a concentration of less than 1 %[18]. More stable 'bound' chlorine results when the phenolate reacts at the more substituted epoxy ring carbon or when the secondary hydroxyl group of the intermediate reacts with epichlorohydrin. When reaction occurs at the more substituted carbon, the 1,3-chlorohydrin is formed and cannot undergo ring closure, resulting in chloromethyl groups. 'Hydrolyzable' chlorine results at reaction sites where the intermediate does not undergo the final chloride elimination step.

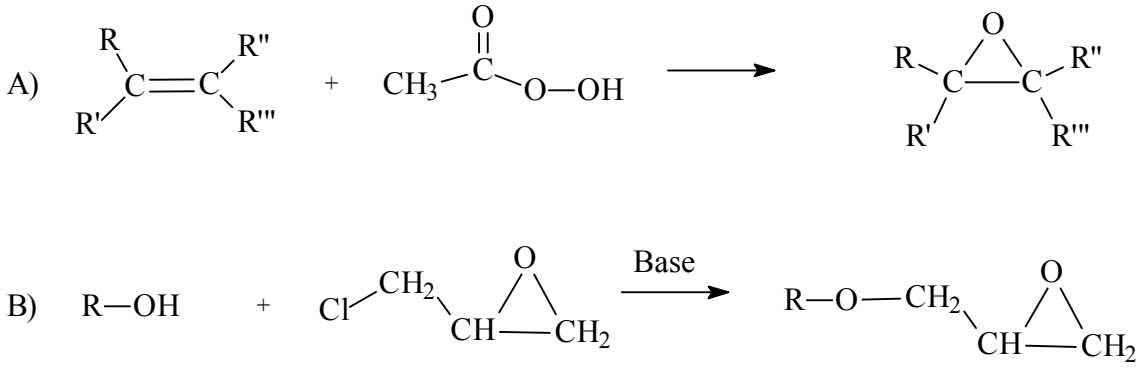

Figure 2-2. Oxirane rings can be formed by reaction of A) a carbon-carbon double bond with a peroxy acid or B) reaction of a phenol group with epichlorohydrin.

In the epoxy synthesis from olefins, increased electron density in the double bond due to electron donating substituents increases the reactivity of the vinyl group with peroxy acids[17]. While the activity of many peracids has been investigated, peracetic acid is commonly used in industry, as in the production of cycloaliphatic epoxy resins[18]. In the epoxidation of alkenes, the reaction product contains no hydrolyzable chlorine or

---

[20]T. D. Juska and P. M. Puckett, Matrix resins and fiber/matrix adhesion, Composites Engineering Handbook, P.K. Mallick, Ed., 1997, Marcel Dekker, Inc., New York, 101-165.

ionic salt byproducts that may be found in reactions involving epichlorohydrin. This leads to materials with improved environmental stability and electrical properties.

The versatile chemistry of the three membered oxirane ring is due in part to the bond strain that makes the ring susceptible to both nucleophilic and electrophilic ring opening reactions[2,17]. Linear ethers typically have a carbon-oxygen-carbon bond angle of ~112° while that of the oxirane ring is ~61°[17]. These small bond angles in the 1,2-epoxide ring results in poor orbital overlap and increased reactivity of the epoxide. The electron density on the oxygen of epoxides is lower than that of typical ethers. Nucleophilic addition to an unsymmetric epoxide ring occurs predominantly at the least hindered site under neutral or basic conditions. The ring opening reaction proceeds through an S_N2 mechanism in which the nucleophile-carbon bond is forming as the carbon-oxygen bond is breaking (Figure 2-3a). Electron donating groups attached to the ring or addition of acid catalyst accelerate the reaction by aiding in the dissociation of this bond. In acid catalyzed reactions, attack can occur at both epoxy carbons. The acid protonates the ether oxygen and a partial positive charge develops on a carbon in the ring. The more substituted carbon will carry this charge. The reaction, however, does not appear to be S_N1, but rather a "borderline" S_N2 reaction[1]. While the nucleophile-carbon bond is forming as the carbon-oxygen bond is breaking, the transition state has a partial positive charge developing on the more substituted carbon in the ring, increasing reactivity at this position (Figure 2-3b). However the product mixture is sensitive to the steric bulk of the substituents, supporting the S_N2 character of the intermediate.

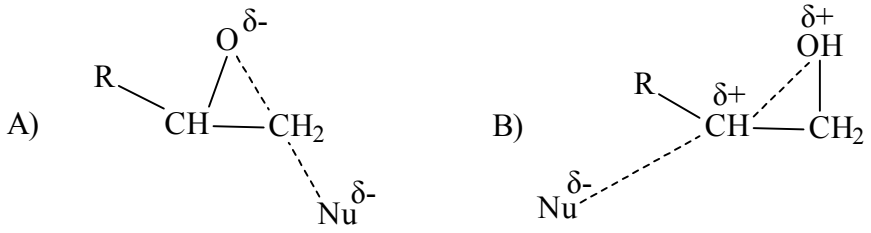

Figure 2-3. Addition mechanism to an epoxide ring; A) S_N2 mechanism under basic and neutral conditions B) borderline S_N2 mechanism under acidic conditions.

The majority of the epoxy resins produced industrially are based on bisphenol-A (Figure 2-4). To synthesize these resins, bisphenol-A is dissolved in a large excess of epichlorohydrin[18]. The reaction is heated to ~65°C and a stoichiometric amount of

sodium hydroxide is added dropwise. Low molecular weight diepoxides are produced within 2-4 hours. The excess of epichlorohydrin is used to minimize the degree of chain extension that occurs during epoxidation. These low viscosity resins are used in a number of applications, one of which is for adhesives. Upon cure of the epoxide with most nucleophiles, polar hydroxyl groups form that can interact favorably with heteroatoms on the surface of adherend substrates. The diepoxide oligomers can be distilled to obtain a monodiperse diglycidyl ether of bisphenol-A with a melting point of 43°C or can be chain extended with diphenols or amines to produce tough, ductile poly(hydroxyether) thermoplastics. In the chain extension reaction, using an excess of either the diepoxide or the chain extender can control the molecular weight and the functionality of the higher molecular weight oligomer or polymer.

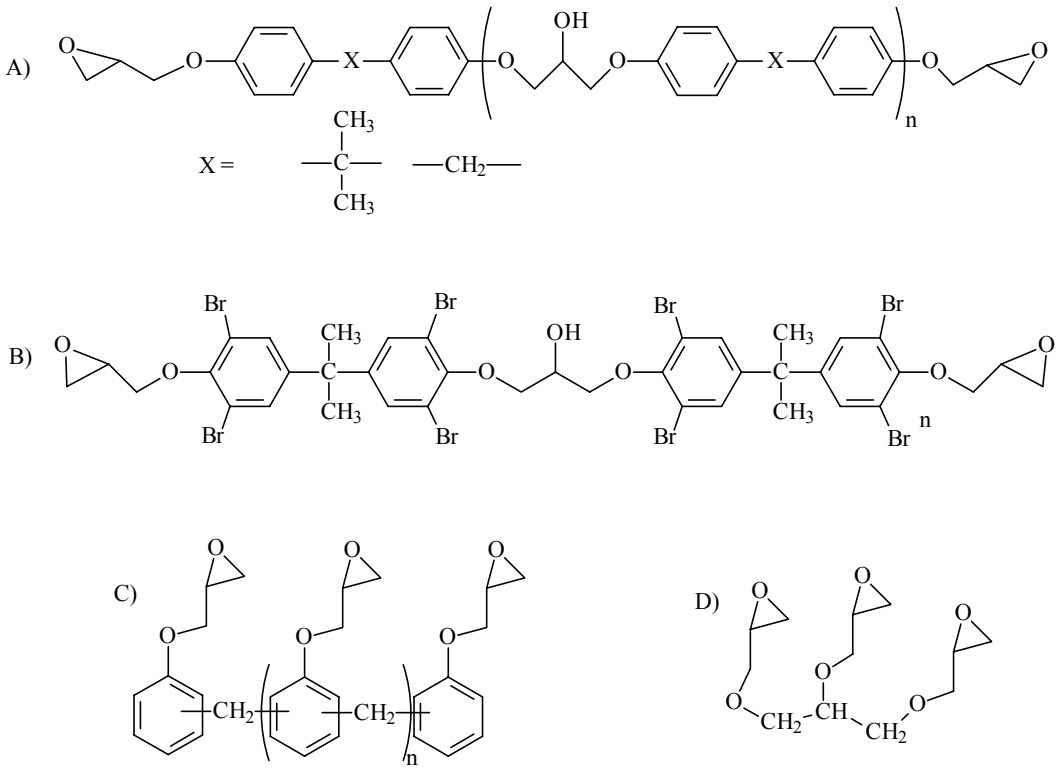

Figure 2-4. Epoxy resins synthesized from A) bisphenol-A and bisphenol-F, B) tetrabromo bisphenol-A, C) phenolic novolac and D) glycerol.

Using similar synthetic approaches, the diepoxides of bisphenol-F (prepared from phenol and formaldehyde) and 3,5,3',5'-tetrabromo bisphenol-A or the multifunctional epoxies of phenolic novolac resins can be prepared (Figure 2-4). Bisphenol-F based resins have lower viscosity than the corresponding bisphenol-A systems at equal

molecular weights. Brominated epoxy resins have good thermal performance and have been used for flame retardant applications. Unfortunately toxic gases, such as hydrobromic acid, are generated and released during burning[38,21]. The current shift away from brominated resins opens the way for other flame retardant systems, including the phenolic networks. Epoxidized novolacs can yield highly crosslinked, high T_g networks and the phenolic nature of the oligomer results in increased network flame retardance compared to that of bisphenol-A materials[120].

Aliphatic epoxy resins are produced from 1) the reaction of epichlorohydrin and an alcohol or 2) the epoxidation of alkenes[18]. A common aliphatic multifunctional epoxy resin is based on glycerol (Figure 2-4) and is synthesized in two steps. The triol is reacted initially with epichlorohydrin in the presence of a Lewis acid, BF_3, to yield the chlorohydrin. Sodium hydroxide is not used due to the similar basicity of the alcohol and secondary hydroxyl formed. The polyetherification reaction can be limited by using a Lewis acid to catalyze the ring opening reaction and sodium aluminate to catalyze the dehydrohalogenation that reforms the ring[1]. The aliphatic resins are often used as reactive diluents to control the viscosity of epoxy systems. Cycloaliphatic resins are epoxidized from alkenes using peracetic acid. This can be accomplished in an aqueous or non-aqueous medium. These systems have superior weatherability over other epoxy resins due to both the aliphatic backbone structure and the epoxidation procedure that does not produce hydrolyzable chlorine.

2.1.3. Epoxy Cure Chemistry

Epoxy resins can be cured via addition reactions or homopolymerizations. During the cure of epoxy resins, there is initially linear growth with a gain in molecular weight[18, 22]. These chains begin to branch and the gel point is reached when a sufficient amount of these branches interconnect to form a continuous three-dimensional network that is insoluble and infusible. In the final stage of the cure reaction most of the remaining sol fraction is incorporated into the network. The viscosity increases with conversion until the gel point is reached and the network becomes infusible. The T_g also increases

[21] S. Wang, Virginia Tech Dissertation, 2000.

[22] J. L. Hopewell, University of Queensland Dissertation, Brisbane, Australia, 1997.

throughout the cure. At cure temperatures above the glass transition of the system the reaction is kinetically controlled. However, as the increasing T_g approaches the cure temperature, the reaction slows, becoming diffusion controlled. The partially cured network can vitrify, arresting the reaction entirely and resulting in a high soluble fraction. To obtain optimum mechanical properties and corrosion resistance, high gel fractions are necessary. Therefore networks are commonly post-cured at a temperature above the network T_g for applications that require maximum mechanical performance.

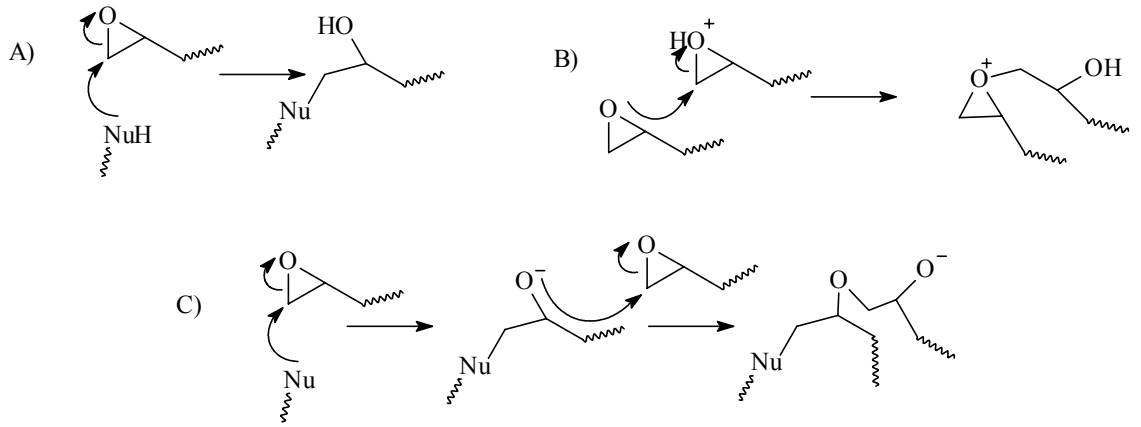

Figure 2-5. Curing mechanisms of epoxy resins, A) nucleophilic addition of a hydrogen active nucleophile, B) cationic polymerization and C) anionic polymerization.

The wide range of cure possibilities further increases the versatility of epoxy resins[23]. Epoxy resins can be cured with a variety of functionalities containing an active hydrogen (Figure 2-5a) such as amines, phenols and carboxylic acids or through etherification of the epoxide rings, which can follow either cationic or anionic pathways. A cationic cure (Figure 2-5b) can occur with the use of photosensitive initiators that generate super acids and an anionic cure (Figure 2-5c) can occur when the resin is crosslinked using imidazoles. The oxirane ring can be either mono- or di- functional depending on the reaction. In the case of nucleophilic addition at the ring, each epoxide has a functionality of one. In the etherification reactions the epoxide ring is difunctional.

[23] Y. Tanaka and R. S. Bauer, Curing Reactions, Synthesis and Characteristics of Epoxides, Epoxy Resins: Chemistry and Technology, C. A. May, Ed., 1988, Marcel Dekker, Inc. New York.

2.1.3.1. Nitrogen Containing Curing Agents

Aliphatic and aromatic amines are commonly used as curing agents. These active hydrogen compounds undergo an addition reaction with the epoxide ring (Figure 2-5a) when added in a stoichiometric ratio and initiate the anionic etherification reaction (Figure 2-5c) when added in a deficiency[24]. Primary amines react more rapidly than secondary amines and the ratio of secondary to primary amine reactivity generally increases with cure temperature. The reactivity ratio of secondary to primary amines for triethylenetetramine increases from 0.25 at 22°C to 0.75 at 50°C[25]. Since a primary amine contains two active hydrogens, it is difunctional. Initially in the diamine cure, chain extension occurs more readily as the primary amines react with the epoxides to form secondary amine linkages. Reaction of these secondary amines then begins to dominate the cure, crosslinking the system. In the crosslinking reaction of a difunctional diepoxide and a tetrafunctional diamine the gel point is reached at ~60% conversion. The reaction of a nucleophile and an epoxide ring is accelerated by hydrogen bonding functionalities, such as hydroxyl moieties[14]. Hydrogen bonding with the epoxy oxygen decreases the electron density of the epoxide prior to ring opening and stabilizes the alkoxide in the transition state[27]. Therefore, the cure reaction initially autoaccelerates due to the formation of the pendant hydroxyl groups from the opening of the oxirane. The degree to which a hydrogen bonding moiety will accelerate the ring opening reaction increases with hydrogen bonding ability or the acidity of the proton. Hydrogen-bond acceptors, such as ethers and carbonyls, slow the amine/epoxy reaction[26].

Aliphatic amines used commercially include ethylene amine derivatives and polyetheramines (Figure 2-6)[27]. When a stoichiometric or larger ratio of active hydrogen is present the epoxy homopolymerization does not occur to any significant degree. However, when excess epoxy groups are present, crosslinking occurs partially via etherification of the remaining epoxides. The etherification reaction is catalyzed by the tertiary amines formed during resin cure. The low molecular weight ethyleneamines provide rapid room temperature cures[1]. Upon postcure, the resulting networks have high

---

[24] U.M.Bokare and K. S. Gandhi, *J. Polym. Sci. Polym. Chem. Ed.*, 1980 **18**, 857-870.

[25] B. Ellis, The kinetics of cure and network formation, Chemistry and Technology of Epoxy Resins, 1st edition, B. Ellis, Ed., 1993, Chapman & Hall, New York, 72-116.

crosslink densities that impart good mechanical strength and corrosion resistance. Unfortunately, these volatile amines are toxic and are often not miscible with the epoxy resin. Hexamethylenediamine, with reduced toxicity, provides good flexibility. Polyetheramines, most commonly amine terminated polyoxypropylene, are less volatile and available in a range of molecular weights including low (230 g/mol) and high (2,000 g/mol) molecular weight oligomers[27]. Incorporation of these amines also increases the flexibility of the network. The etheramine reactivity is lower than that of the alkylene amine so they are often used in combination with other amine curing agents for adhesive applications.

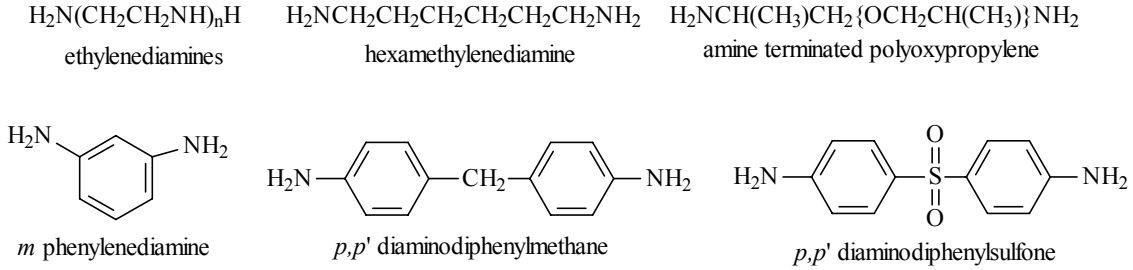

Figure 2-6. Aliphatic and aromatic amine curing agents.

Another approach to improve both the miscibility and safety of the ethyleneamines is to increase the molecular weight[26]. This can be accomplished by prereacting amines with diepoxides. Using an excess of amine, the mixture is reacted at 75°C-100°C to yield amine terminated adducts[20] (Figure 2-7).

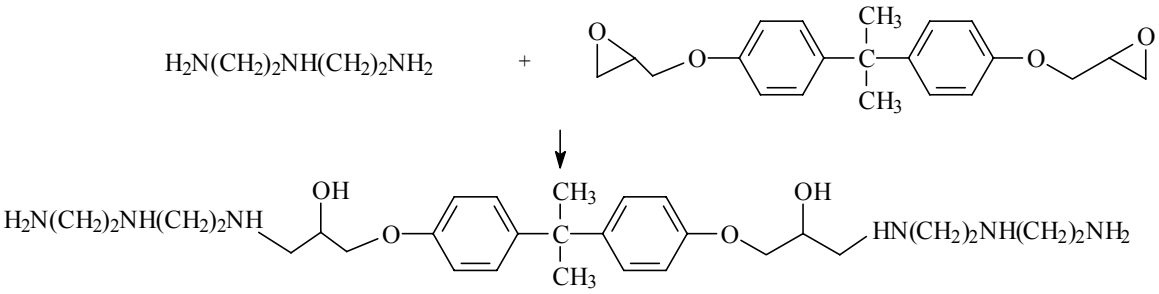

Figure 2-7. An amine adduct prepared by reacting an excess of diethylenetriamine with the diglycidyl ether of bisphenol-A.

[26] T. F. Mika and R. S. Bauer, Curing Agents and Modifiers, Synthesis and Characteristics of Epoxides, Epoxy Resins: Chemistry and Technology, Ed. C. A. May, 1988, Marcel Dekker, Inc. New York.

Amines are also commonly reacted with carboxylic acids to yield polyamides with increased molecular weight and improved resin solubility. Polyamidoamines can be prepared from the dimers and trimers of unsaturated fatty acids, such as the Diels-Alder product of 9,12- and 9,11-linoleic acid[3] (Figure 2-8). The hydrophobic backbones of the aliphatic fatty acids impart good corrosion resistance[27]. While these curing agents are referred to as amides, crosslinking occurs through the amine functionalities. Polyamides are used in concrete primers, adhesives, and coatings but typically are not used alone in epoxy cures.

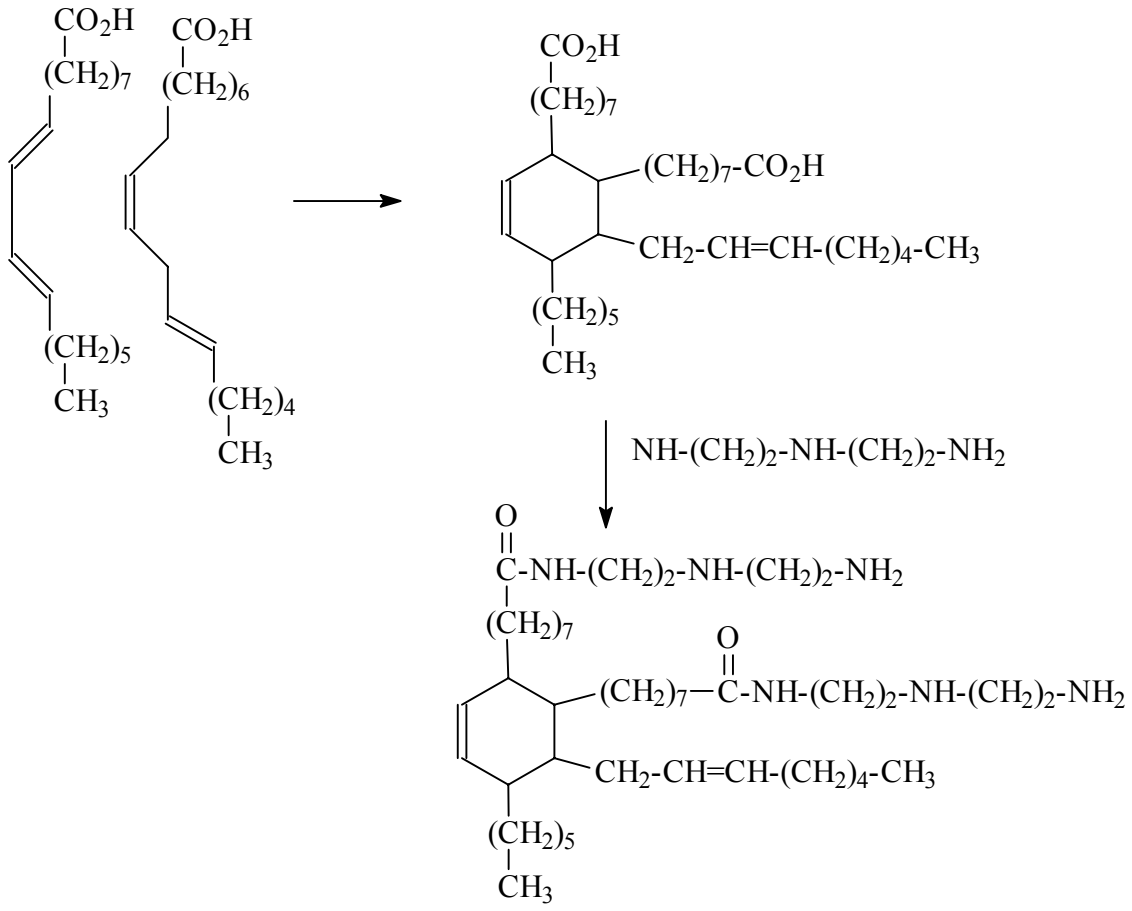

Figure 2-8. Polyamidoamine prepared from a linoleic fatty acid dimer and diethylene triamine.

Ketimines, formed from the reaction of amines and ketones, are blocked amines and, upon addition of water, regenerate the amine and volatile ketone[3] (Figure 2-9).

Therefore these systems offer extended processing windows while curing under ambient conditions but are limited to use in thin films to avoid trapped volatiles.

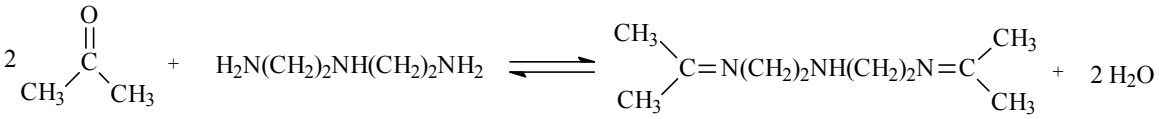

Figure 2-9. Ketimines, blocked amines, are synthesized from acetone and diethylenetriamine.

Aromatic amines have reduced electron density compared to aliphatic amines due to resonance with the adjacent phenyl ring[1,2]. This reduced electron density results in the nitrogen being a weaker, less reactive nucleophile. Processing windows of ~6 hrs can be achieved at 25°C due this relatively slow amine/epoxy reaction. The resins can also be 'B' staged in which the amine and epoxy are allowed to react partially at room temperature and then are further processed and cured at elevated temperatures. In the initial reaction <30% conversion is achieved and the resulting resin is still a fusible and soluble solid that can be heated and molded. These resins are often cured in two stages, such as 2 hrs at ~90°C and a postcure for 2 hrs at ~150°C, to avoid an extreme rise in temperature due the cure exotherm[27]. Networks cured with aromatic amines have improved solvent resistance and performance at elevated temperatures compared to the networks cured with aliphatic amines. Common aromatic amines used as epoxy crosslinking agents include *m*-phenylenediamine, *p,p*'-diaminodiphenylmethane, and *p,p*'- diaminodiphenylsulfone (Figure 2-6). While *m*-phenylenediamine can yield the highest crosslink density, both *m*-phenylenediamine and *p,p'*-diaminodiphenylmethane cured networks are used in electrical insulating materials due to their low polarity and low moisture sorption, ~3 wt %[20]. Thermosets prepared with *p,p'*-diaminodiphenylsulfone have the best thermal performance of the three, however the cure reaction is the slowest due to the electron withdrawing sulfone moiety[2]. For this reason, the Lewis acid monoethylamine-boron trifluoride is frequently added at 1 part per hundred parts of resin (phr) to catalyze the reaction.

2.1.3.2. Oxygen Containing Curing Agents

A variety of hydrogen active oxygen moieties, including carboxylic acids, alcohols and phenols are reactive with oxiranes and are used industrially to prepare epoxy

networks[2,27]. Acid anhydrides, which do not have acidic hydrogens and are therefore less reactive than the carboxylic acids, are also used as epoxy crosslinking agents in combination with accelerators.

Although the anhydrides are more commonly utilized as epoxy curing agents than the carboxylic acids, the chemistry of the anhydride cure involves the chemistry of the carboxylic acid/epoxy reaction. Therefore the carboxylic acids will be addressed first. Cures must be conducted at elevated temperatures, >120°C and under certain cure conditions water is produced as a by-product (Figure 2-10). Therefore, carboxylic acids are used in the preparation of films and coatings. Networks can form through two different mechanisms depending on the epoxy/carboxylic acid stoichiometry and the catalysts utilized. In both reactions the epoxide ring is difunctional. When a deficiency of carboxylic acid is used the acid hydroxyls react with oxirane rings initially. Crosslinking occurs through the subsequent etherification of the epoxy rings. Dibasic saturated acids, such as glutaric acid, and carboxylate terminated polyesters (Figure 2-11) are typically cured with a deficiency of carboxylic acid.

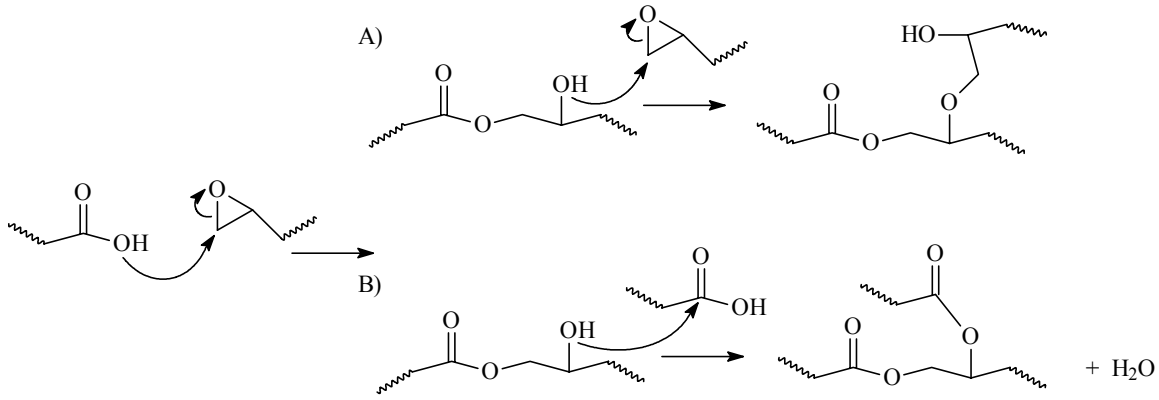

Figure 2-10. Cure process with A) a deficiency of carboxylic acid and B) an excess of carboxylic acid.

In the case of an excess of carboxylic acid, the first step is the same. Then the newly formed secondary hydroxyl condenses with another carboxylic acid moiety and water is produced as a by-product of the esterification. Often a base, such as a tertiary

[27] W. R. Ashcroft, Curing agents for epoxy resins, Chemistry and Technology of Epoxy Resins, 1st edition, B. Ellis, Ed., 1993, Chapman & Hall, New York, 37-71.

amine, is utilized to catalyze the epoxy-carboxylate reaction[1]. The base catalyzes the reaction by deprotonating the carboxylic acid, thereby forming the carboxylate nucleophile. The amine accelerates the reaction and favors the carboxyl-epoxy reaction instead of the epoxy homopolymerization reaction. Triphenyl phosphine also catalyzes the carboxylic acid/epoxy reaction[28]. The phosphine attacks and opens the oxirane ring. The more basic alkoxide anion then abstracts a proton from the carboxylic acid to yield the carboxylate anion. The polyester/bisphenol-A networks show good corrosion resistance and are used as appliance coatings. The tetrafunctional diepoxides are considered the crosslinking agents in these reactions with carboxylate terminated polyesters[27].

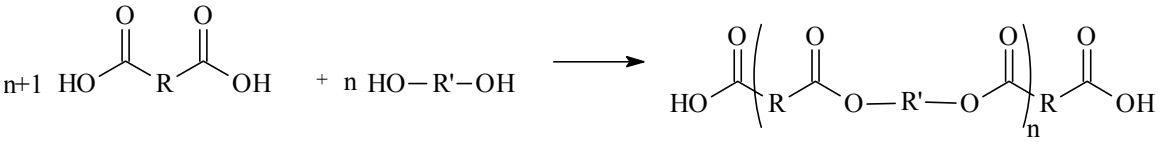

Figure 2-11. Carboxylate terminated polyesters are synthesized using an excess of dicarboxylic acid and a diol.

Acid anhydrides, mainly cycloaliphatic anhydrides (Figure 2-13), can be used to crosslink epoxy resins. Reactivity of these materials is low, providing good processing windows, due to the necessity of a hydroxyl group to initially react with the anhydride and because the carboxylate anion has reduced nucleophilicity compared to the amine curing agents[20]. The ring opening of the anhydride during cure leads to lower cure shrinkage than in other epoxy networks. This, in addition to good electrical insulating properties, makes these systems useful in the electrical industry[27]. Reduced water absorption, ~1 wt %, is another advantage that makes these systems appealing as wet filament winding resins for composites[20].

In the cure reaction, the anhydride reacts with a hydroxyl group to form an ester link and a carboxylic acid. The carboxylic acid formed in the first step reacts with an epoxide ring according to the carboxylic acid/epoxy mechanism shown above (Figure 2-10). Upon epoxy ring opening, the hydroxyl can react with another anhydride or with an oxirane ring. Lewis acids or bases can be used to accelerate the cure reaction. When

[28] B. Starr, E. Burts, J. R. Upson and J. S. Riffle, 2001, submitted to *Polymer*.

acid catalysts are used, the epoxy ring is activated and the epoxy homopolymerization is favored. If a stoichiometric amount of anhydride is added, 20-50% may remain unreacted[20] depending on the flexibility of the networks (eg. M_c) and also on the cure conditions relative to T_g. Due to the etherification reaction that occurs, optimum properties in an uncatalyzed or acid catalyzed system can be obtained with ~0.85 equivalents of anhydride[1].

Lewis bases used as accelerators for the anhydride/epoxy reaction activate the anhydride and produce a carboxylate anion that can open the epoxy ring (Figure 2-12). These materials, such as tertiary amines and imidazoles, limit the amount of etherification and promote alternating reaction between epoxy and anhydride, forming ester linkages[1]. In this system, using a stoichiometric ratio of anhydride to epoxy optimizes the network properties. Tetra-alkyl ammonium salts also catalyze the reaction and yield optimum properties for a stoichiometric ratio of epoxy to anhydride[20]. Electron withdrawing substitution on the anhydride decreases the electron density and results in increased reactivity so that accelerators are not necessary[26].

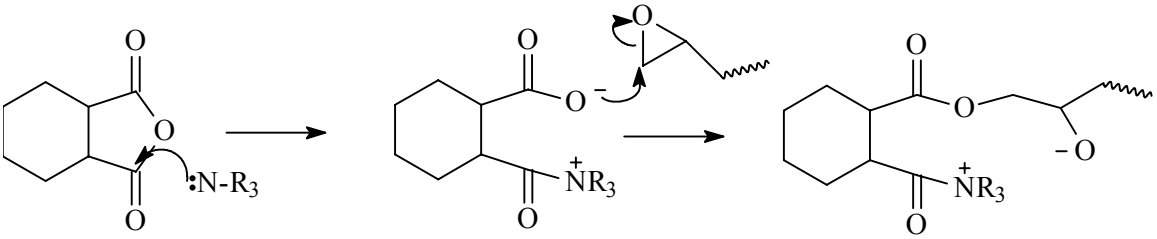

Figure 2-12. Base catalyzed anhydride/epoxy reaction.

Phthalic anhydride has been used as a crosslinking agent (Figure 2-13a). However, it tends to sublime at cure temperatures[27]. Hexahydrophthalic anhydride, with a low melting point of 35°C, can be used to provide low viscosity resins with good processing windows at ambient conditions. Methyl endomethylene tetra-hydrophthalic anhydride, commonly known as nadic methyl anhydride (Figure 2-13c), is also used widely due to the range of properties that can be obtained depending on resin composition and cure conditions[3]. Bisphenol-A epoxy cured with a deficiency of methyl endomethylene tetra-hydrophthalic anhydride at 100°C for 2 hours, followed by a 4 hour postcure at 140°C, has been reported to provide a tough, crack resistant material, while

curing for 2 hours at >220°C yields a network with good heat resistance, due to a heat deflection temperature of 210°C[3].

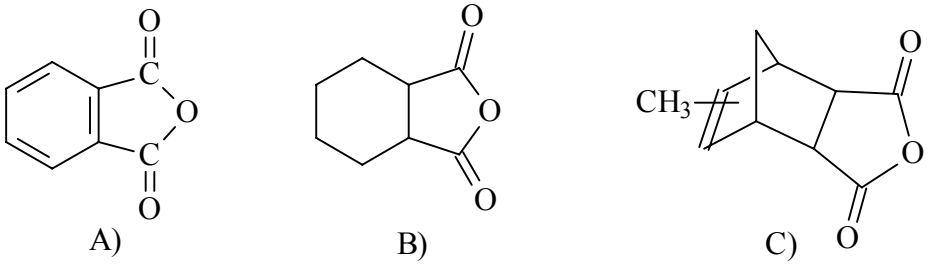

Figure 2-13. Common anhydrides used to cure epoxy resins: A) phthalic anhydride, B) hexahydrophthalic anhydride, and C) methyl endomethylene tetra-hydrophthalic anhydride.

Aliphatic hydroxyl groups react with epoxide resins at >200°C (uncatalyzed), but the resins can be cured at lower temperatures with an acid or base catalyst[1](Figure 2-14). Primary hydroxyl groups are more reactive than secondary hydroxyl groups. They react at rates up to 100 times faster[29]. Tertiary alcohols are even less reactive due to steric hindrance and the reaction proceeds through homopolymerization of the epoxies[1]. The more reactive diphenols and polyphenols are commonly used as crosslinking agents with Lewis base catalysts[1,27]. Diphenols can be utilized with a 1/0.6 epoxide/phenol ratio to allow crosslinking via the etherification reaction[1]. Initially, linear growth takes place as the phenol hydroxyls open the oxirane rings. Upon exhaustion of the phenol groups, epoxy homopolymerization occurs.

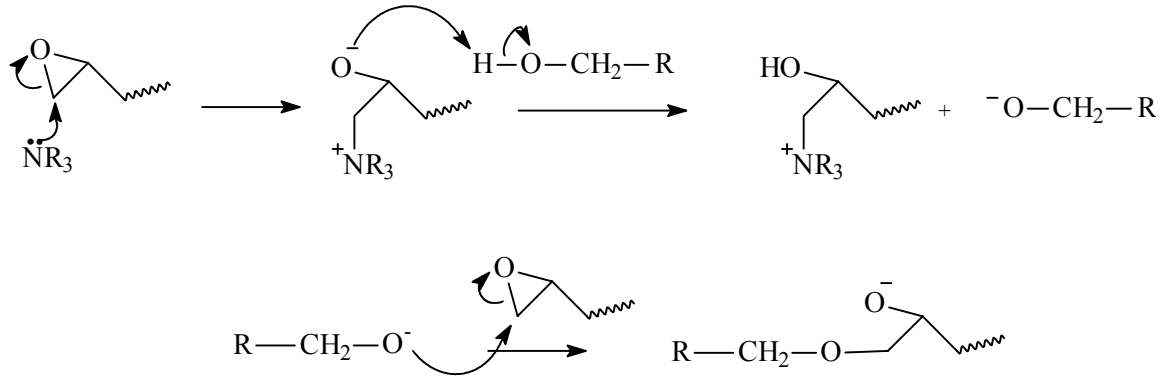

Figure 2-14. Base catalyzed alcohol/epoxide ring opening reaction.

[29]A. Renner and J.-A Cotting, *J. Appl. Polym. Sci.*, 1990, **39**, 789-802.

Polyphenols or phenolic oligomers (Figure 2-15) are prepared from the reaction of phenol and formaldehyde. Novolac resins are synthesized under acidic conditions with an excess of phenol to yield phenol terminated, branched oligomers. Lower molecular weight novolacs are viscous liquids and can be melt mixed with epoxies at ~70°C to yield resins that are stable for several months in the absence of catalyst[1]. When cured with bisphenol-A based epoxy resins at 150°C with ~0.5 wt % benzyldimethylamine as the catalyst, the high glass transition networks can provide good mechanical performance for elevated temperature applications[1]. When phenolic oligomers are prepared under basic conditions with an excess of formaldehyde the resulting resole resins contain methylol units (Figure 2-15). In addition to the epoxide/phenol reaction the hydroxymethyl groups can react with the epoxy oligomers to yield networks with increased crosslink density and chemical resistance compared to novolac cured thermosets[27]. Resoles are commonly used in conjunction with higher molecular weight epoxy oligomers (M_n = 1650-2000 g/mol) as coatings for drums and pails where high cure temperatures can drive off water by-products of the condensation reaction[27].

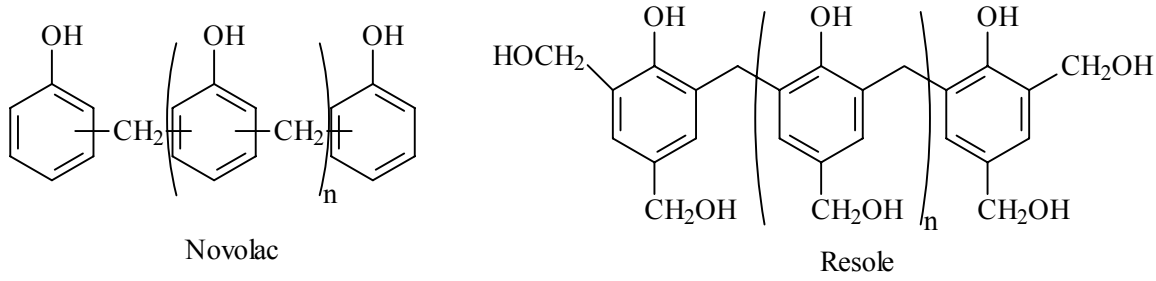

Figure 2-15. Novolac and resole phenolic oligomers.

2.1.3.3. Epoxy Homopolymerization

Polymerization of the epoxide rings is a chain reaction and can occur with either cationic or anionic initiators. For diepoxides, each oligomer is tetrafunctional and this homopolymerization results in crosslinking and network formation. The UV cure of epoxy resins using a photoinitiator involves the generation of superacids and progresses

via a cationic mechanism. Lewis bases and imidazoles are utilized to initiate anionic cure.

Cationic crosslinking occurs thermally with the addition of Lewis acid initiators[27]. The acid associates with the epoxide oxygen. The ring may be activated so that another epoxy oxygen opens the ring, forming a new salt (Figure 2-5b) or the ring may be opened by the catalyst and the anion displaced by an epoxy oxygen (Figure 2-16). The most commonly used Lewis acids are amine complexes of boron trifluoride[1]. Of these the monoethylamine complex has found the most use in epoxy curing because it is more light stable and less hygroscopic than other boron trifluoride compounds. The complex is strong because of the increased basicity of the amine resulting in the aforementioned advantages as well as a reduced rate of reaction with the epoxy group. These complexes serve as latent catalysts. The epoxy reaction is not catalyzed until heated to ~95°C, at which temperature the boron complex dissociates to the catalytic species[3]. While boron trifluoride complexes are more often used as catalysts for aromatic amine and anhydride cured resins, the homopolymerized networks are used as adhesives and electrical varnishes[27].

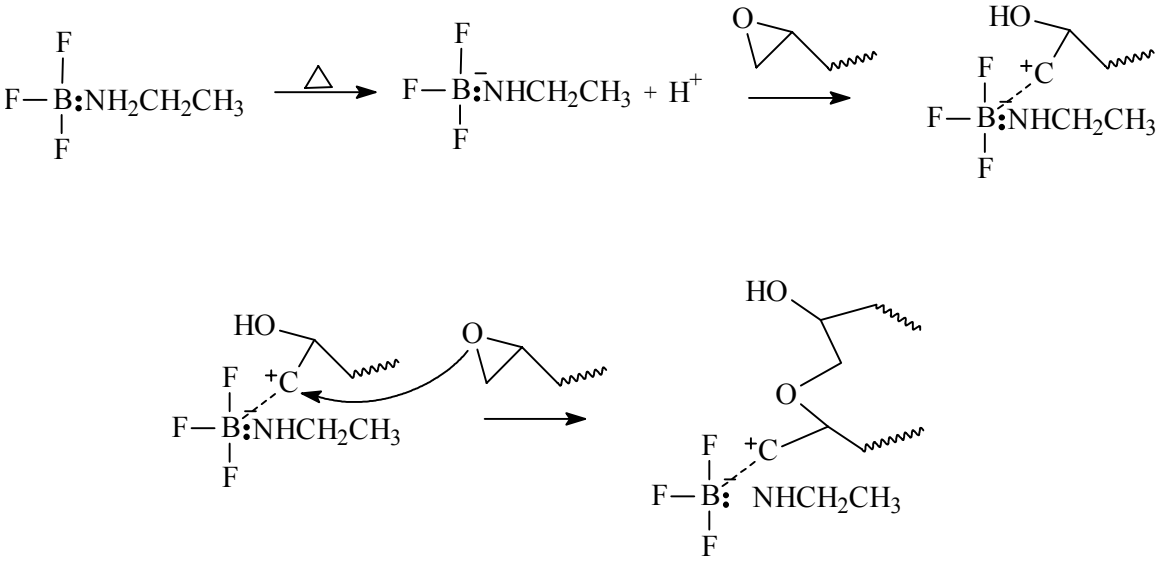

Figure 2-16. Cationic epoxy homopolymerization using boron trifluoride monoethyl amine[1].

Photocuring can be conducted using UV sensitive salts, which generate cations that catalyze the epoxy etherification reaction[27]. The sensitivity of the initiator to photo and thermal energy is determined by the cation utilized, while the cure catalysis is

dependent on the anion structure[30]. Using a non-nucleophilic anion, boron tetrafluoride, early investigations were done with photosensitive aryldiazonium salts[30]. However, the limited thermal stability of the diazonium cation resulted in premature curing of the epoxy resin and the nitrogen gas by-product resulted in defects in the epoxy films.

Diaryliodonium and triarylsulfonium cations (Figure 2-17) have proven more thermally stable and useful for cationic photocuring [27]. Diaryliodonium salts absorb strongly in the 220-250 nm UV region[30]. Upon irradiation, the salt degrades both homolytically and heterolytically to yield cationic and radical species (Figure 2-17). The highly reactive cations, both aryl and aryliodine radicals, react with the resin to yield protonic acids. Triarylsulfonium compounds have higher thermal stability than the iodonium salts due to higher reduction potentials[58]. Common counter ions include BF_4^-, PF_6^-, AsF_6^-, and SbF_6^-, which generate acids with Hammet acidities of –15 to -30[30]. Protons from these superacids associate with the oxirane oxygen and initiate the cationic polymerization. Sulfonium hexafluoroantimonate salts are used commericially due to the ease of initiator preparation and the strong absorption at long wavelengths, ~305 nm[30]. These rapid UV cures are used for coatings and may find applications in lithographic etching processes[27]. The reaction is sensitive to water and the basicity of the resin, which react with the released acid. However, unlike free radical photocuring, the cure is not sensitive to oxygen.

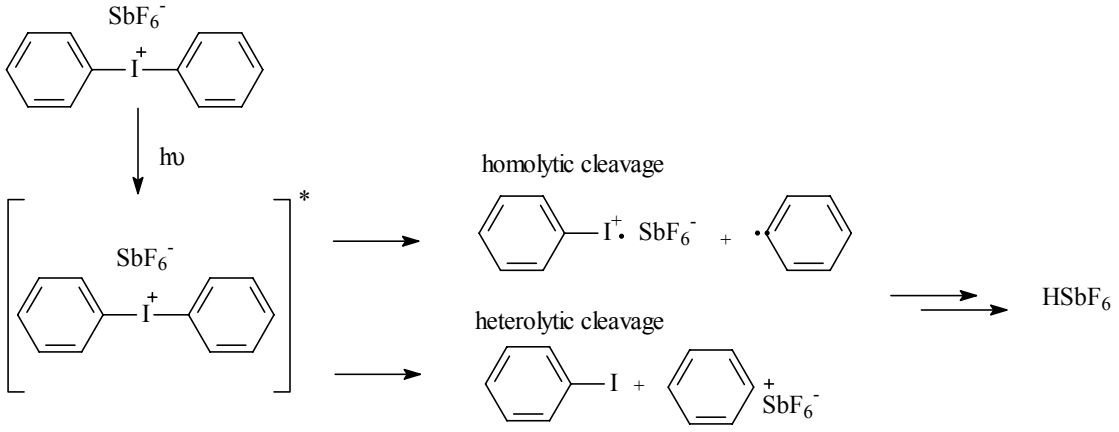

Figure 2-17. Decomposition of diaryl iodonium hexafluoro antimonate salt to yield a superacid[30].

[30] J. V. Crivello, *J. Polym. Sci.*, 1999, **37**(A), 4241-4254.

Two different mechanisms have been proposed for the anionic pathway. One involves a nucleophile attacking the ring and the alkoxide anion propagating the polymerization (Figure 2-5c). In the other proposed route, the nucleophile, such as a tertiary amine, opens the ring and the alkoxide abstracts a proton from an alcohol. A complex may form between an alkoxide and the quaternary amine (Figure 2-18) with the alkoxide as the propagating species[1].

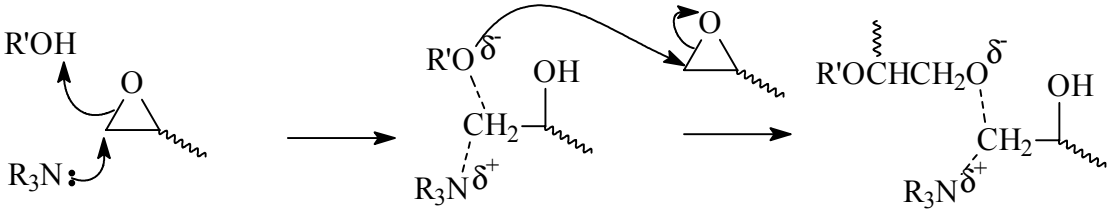

Figure 2-18. Possible mechanism for anionic ring opening with tertiary amine.

A possible side reaction is the abstraction of a proton beta to the ring. The electrons move into the carbon-carbon bond, forming a double bond and opening the epoxy ring[23]. This chain transfer reaction does not terminate the reaction since the alkoxide anion can then react with another oxirane ring. The anionic polymerizations can be catalyzed by tertiary amines and other Lewis bases however the crosslinking requires a long cure cycle.

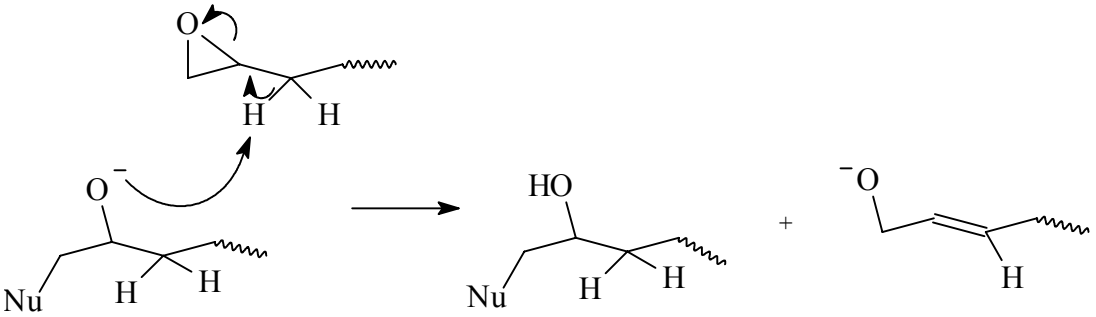

Figure 2-19. Chain transfer reaction during anionic epoxy homopolymerization.

Imidazoles also initiate the anionic polymerization of oxirane groups (Figure 2-20). In the first step, the secondary nitrogen reacts with an epoxy via nucleophilic attack. The next step involves the reaction of the remaining nitrogen with a second epoxy ring that yields the alkoxide ion. Etherification proceeds with the terminal negative charge remaining near the positive nitrogen through bending of the chain.

2-Ethyl-4-methylimidazole (Figure 2-20) can be utilized at a concentration of ~5-15 mol % for the epoxy cure[3]. Bisphenol-A based epoxy resins with imidazole initiators have processing windows in excess of 8 hours at room temperature with improved mechanical performance of the networks at elevated temperatures compared to other anionically cured thermosets. Imidazoles also catalyze the epoxy/phenol and epoxy/anhydride cures via epoxy ring opening[27].

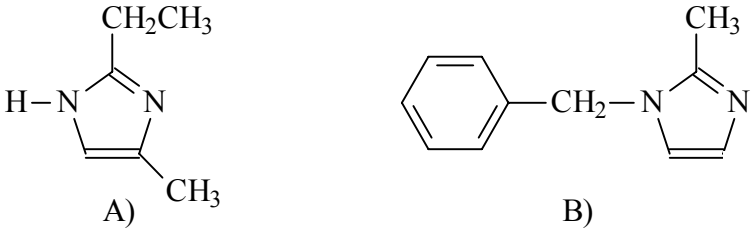

Figure 2-20. Common imidazoles used to catalyze epoxy cures: A) 2-ethyl-4-methylimidazole and B) 1-benzyl-2-methyl-imidazole.

2.1.3.4. Additives

Resins usually contain more than just the epoxy oligomer and crosslinking agent. Viscosity can be modified through the use of either reactive or non-reactive diluents[31]. Both mono- and di- functional epoxies, such as 2,3-epoxyoctane, styrene oxide and *p*-butyl phenol glycidyl ether or 1,2-3,4-butane diepoxide and *p*-benzene diepoxide (Figure 2-21), are used as diluents. Generally glass transition temperatures are elevated when difunctional diluents are used due to increased the network density. Styrene and low molecular weight unsaturated polyesters can also be used to reduce viscosity. In this case, a free radical initiator is added to cure the vinyl diluent into an interpenetrating network[31].

[31] S.J. Shaw, Additives and modifiers for epoxy resins, Chemistry and Technology of Epoxy Resins, 1st edition, B. Ellis, Ed., 1993, Chapman & Hall, New York, 117-143.

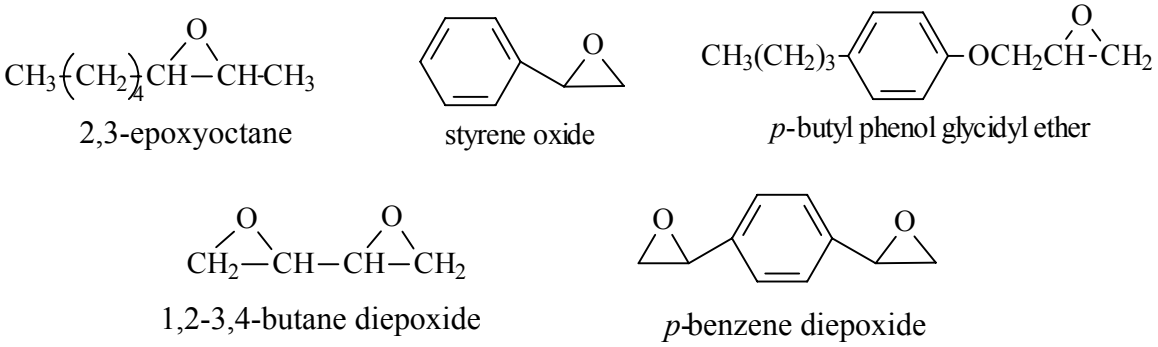

Figure 2-21. Mono- and di- epoxide reactive diluents.

Additives may also be incorporated to tailor network properties, such as flame retardance and toughness. Antimony trioxide, phosphates and halogenated lactones improve thermal performance of the networks[31]. Inorganic particulate fillers, such as alumina, carbon black and silica, are often used for a variety of reasons including reduced cost[31]. Fillers may increase viscosity but offer improved heat transfer. This can reduce exotherms in components with thick cross-sections. Filled thermosets also offer reduced cure shrinkage. While final filled networks may be more dense, leading to increased product weight, the electrical conductivity of the networks can be improved through the addition silver flakes or powder.

Network toughness is often improved with the addition of a second phase, either elastomeric or thermoplastic. Optimum performance is achieved when there is phase separation, which is dependent on the elastomer/matrix miscibility, and good adhesion between the toughening inclusions and the epoxy network[31]. Liquid polybutadiene acrylonitrile, a common elastomeric toughener, is added at 5-20 wt % to improve toughness[1]. The elastomer phase separates into included spheres at these low concentrations and mechanical performance is dominated by the epoxy continuous phase. The rubber reacts with the curing resin through terminal functionalities. While the carboxyl terminated polybutadiene acrylonitrile has been utilized extensively, reactive functional groups such as amines also result in improved adhesion at the phase boundaries[31]. Thermoplastics, such as polyethersulfones and polyetherimides, can also

be used to toughen epoxy networks[32]. The increases in toughness are generally less significant than those with elastomeric tougheners; however, the elastomers can lead to decreases in the modulus and the glass transition temperature of the thermoset. Therefore the inclusion of a thermoplastic phase is typically used for applications where high modulus and T_g are required[31].

2.1.4. Novel Epoxide Chemistry

As industrial use of epoxy resins has grown, research has continued in an attempt to gain a greater understanding of oxirane chemistry and the networks that can be prepared. Novel resins[35], crosslinking agents[59], catalysts[61] and analytical techniques[33] have been developed in the past decade. The extensive body of epoxy research[1,2,14] also helps to simplify investigations of new materials and molecular architectures and has been utilized in the study of reactive monolayers[57] and hyperbranched polymers[56].

2.1.4.1. Organic/Inorganic Epoxy Resins

Recently, epoxy resins have been synthesized containing sulfur, phosphorus and transition metals, chromium, zinc and copper[40]. These heteroatoms were incorporated in an attempt to tailor network properties. The combination of thiocarbonohydrazone (Figure 2-22) and epoxy functionalities was undertaken to impart "ignitability" to a network with good mechanical properties for use as a rocket fuel binder[34]. Incorporation of phosphorus and transition metals, on the other hand, was anticipated to improve flame retardance of the networks. Incorporation of low levels of metals also increased the conductivity of the epoxy network[40].

---

[32] J. C. Hedrick, N. M. Patel, and J. E. McGrath, Toughening of Epoxy-Resin Networks with Functionalized Engineering Thermoplastics, Toughened Plastics I: Science and Engineering, Advances in Chemistry Series (233), C.K. Riew and A. J. Kinloch, Ed., 1993, American Chemical Society, Washington DC, 293-304.

[33] K. Hakala, R. Vatanparast, S. Li, C. Peinado, P. Bosch, F. Catalina, and H. Lemmetyinen, *Macromolecules*, 2000, **33**, 5954-5959.

The nitrogen-nitrogen bond of the thiocarbonohydrazone yielded a high energy backbone[34]. When incorporated into an epoxy oligomer, the resin could be cured and used as a solid fuel binder that would have no ignition delay for solid fuel/liquid oxidizer rocket propellants. Tetraepoxides were synthesized by reacting hydrazones with a ten fold excess of epichlorohydrin (Figure 2-22). While hydroxide salts are typically used to epoxidize phenols, these reactions were refluxed with no catalyst because the use of base resulted in rapid crosslinking. Even without catalyst or base, epoxidized resins were produced within three hours. Both the phenols and secondary amines of the thiocarbonohydrazone reacted with epichlorohydrin to yield tetraepoxides. These materials were cured at 80°C for 48 hrs using thiocarbonohydrazide or ethylenediamine. Networks began to degrade at 125°C. The ethylenediamine crosslinked networks were more stable due to a lower concentration of the high energy nitrogen-nitrogen bond.

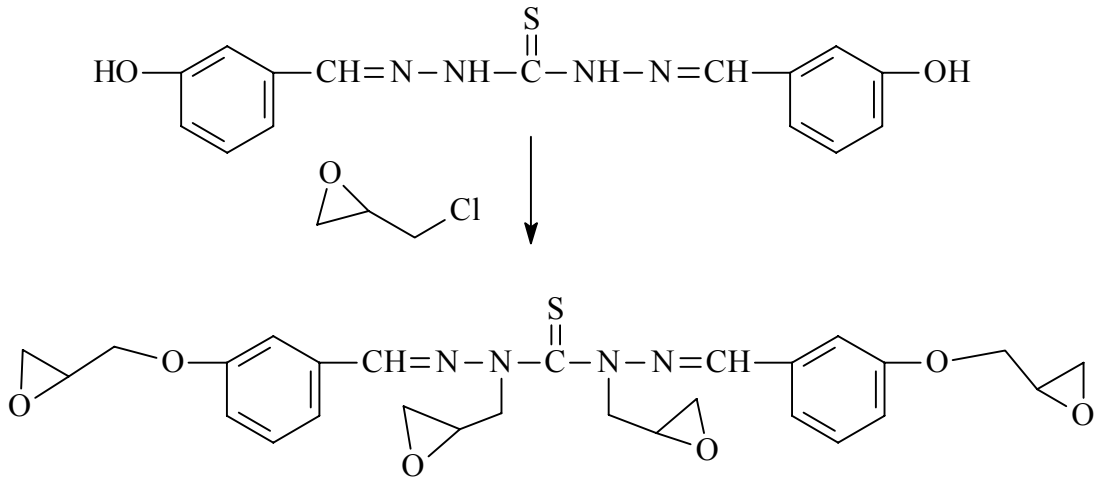

Figure 2-22. Epoxidation of thiocarbonohydrazone without base.

To improve the thermal stability and flame retardance of epoxy networks, 9,10-dihydro-9-oxa-10-phosphaphenanathrene 10-oxide (Figure 2-24A) was incorporated into the epoxy backbone via three different approaches[35,36,38]. Two and four wt % phosphorus were incorporated into *o*-cresol novolac epoxy oligomers by reaction with pendant

[34]P. M. Thangamathesvaran and S. R. Jain, Synthesis and characterization of thiocarbonohydrazone-based epoxy resins. *J. Polym. Sci. Part A Polym. Chem.*, 1991, **29**, 261-267.

oxiranes (Figure 2-23)[35]. Since the phosphorus compound contained an active hydrogen, the phosphorus opened an oxirane ring and this was followed by a proton transfer.

Three different network series were prepared by curing the modified resin with either *p,p*'-diaminodiphenylsulfone, novolac, or dicyandiamide. In each series, increased phosphorus concentration corresponded to decreased epoxide concentration. This led to reduced crosslink density and therefore decreased T_g and rubbery modulus in networks with higher levels of phosphorus. The initial degradation temperatures decreased while the char yield and limiting oxygen content increased. In the dicyandiamide cured networks, the 5 % wt loss temperature in nitrogen decreased from 373°C to 364°C with incorporation of phosphorus but char yield increased from 29 wt % to 35 wt % and the limiting oxygen index increased from 24 to 38. The phosphorus containing networks showed a two stage degradation. This behavior was attributed to lower initial thermal stability and subsequent formation of a phosphorus rich char. The char insulated the sample, improving flame retardance in the second stage of decomposition. The activation energies of the modified novolac epoxy/diaminodiphenyl sulfone cure reaction were also investigated. With increased phosphorus content, the activation energy decreased. Authors attributed this to the increased concentrations of hydroxyl groups that were formed with addition of the phosphorus and could hydrogen bond with oxirane oxygens to activate the ring[36]. However, similar findings of increased epoxy/amine reactivity have been observed in other phosphine oxide resins without elevated hydroxyl concentrations[37]. Hydrogen bonding between the phosphine oxide and the amine may have increased the electron density and reactivity of the nitrogen.

---

[35] C.S. Wang and C.H. Lin, *Polymer*, 2001, **42**, 1869-1878.

[36] C.S. Wang and C.H. Lin, *Polymer*, 2000, **41**, 8579-8586.

[37] Y.-L. Liu, G.-H.Hsuie, Y.-S. Chiu, R.-J. Jneg and L.-H. Perng, *J. Appl. Polym. Sci.*, 1996, **61**, 613-621.

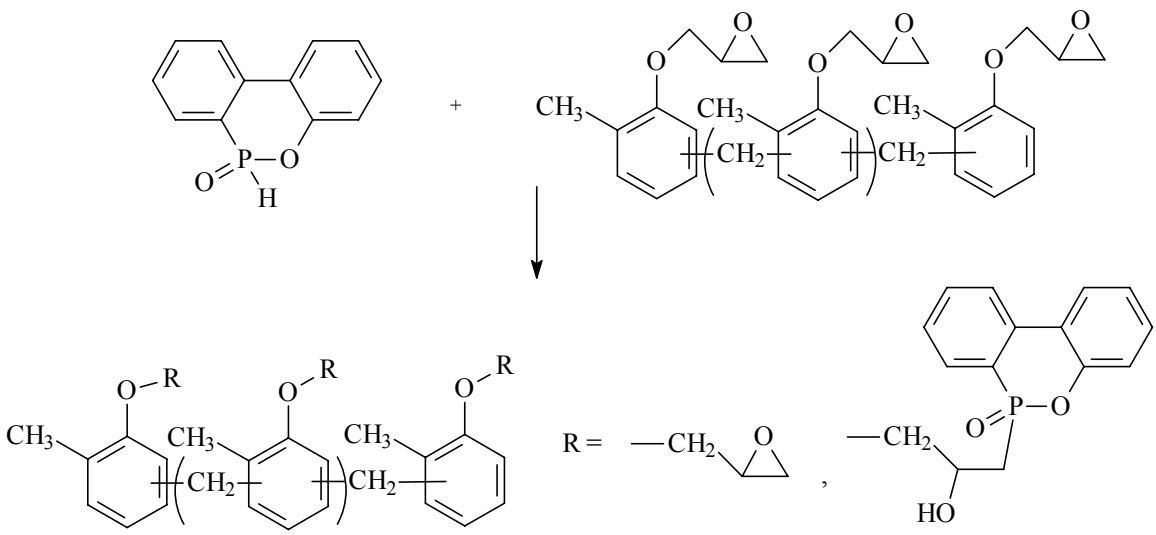

Figure 2-23. Reaction of 9,10-dihydro-9-oxa-10-phosphaphenanathrene 10-oxide with *o*-cresol novolac epoxy.

A diphenol of 9,10-dihydro-9-oxa-10-phosphaphenanathrene 10-oxide (Figure 2-24B) was also prepared by reaction with *p*-benzoquinone[38]. The diphenol was subsequently used to cure a novolac epoxy resin and used to chain extend bisphenol-A epoxy. For comparison tetrabromo bisphenol-A was used in the same manner. Char yields in nitrogen for the novolac epoxy networks increased from 32 wt % to 39 wt % to 49 wt % when novolac, tetrabromobisphenol-A, and the phosphorus diphenol were used as the curing agents, respectively. The burning characteristics of the networks were tested by igniting 127 mm x 12.7 mm x 12.7 mm specimens with a Bunsen burner for two ignition cycles of 10 seconds each. While the novolac cured network burned for 85 seconds, the phosphorus and bromine containing networks did not burn after removal from the igniting flame. The chain extended epoxy resins were cured with methylenedianiline and similar increases in char were found with addition of the phosphaphenanathrene moiety.

[38]C. –S. Wang and J.-Y.Shieh, *Polymer*, 1998, **39**, 5819.

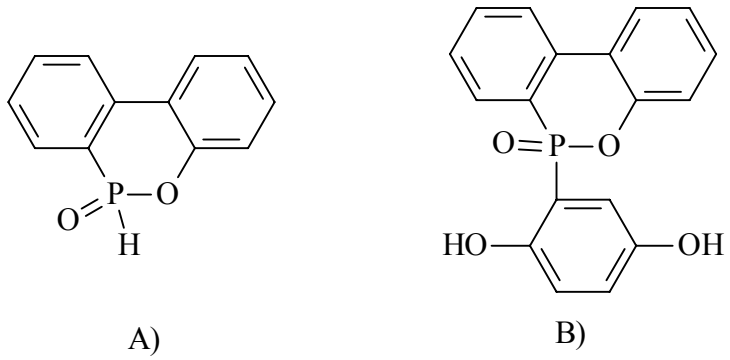

Figure 2-24. A) 9,10-dihydro-9-oxa-10-phosphaphenanathrene 10-oxide and B) diphenol utilized in novolac epoxy networks.

Phosphonates have also been investigated[37]. By reacting phenylphosphonic dichloride with glycidol in the presence of triethylamine and copper chloride a phosphine oxide containing diepoxide was prepared (Figure 2-25). Dicyandiamide, *p,p*'-diaminodiphenylmethane and *p,p*'-diaminodiphenylsulfone were used as curing agents. The phosphine oxide epoxy was more reactive towards the amine curing agents than was the bisphenol-A based epoxy. The phosphine oxide moiety was electron withdrawing which may have resulted in an activated oxirane ring with decreased electron density or the phosphine oxide/amine interactions may have increased the reactivity of the amine. As expected, the most electron dense curing agent, *p,p*'-diaminodiphenylmethane was the most reactive. Char yield in nitrogen increased from18 wt % for bisphenol-A containing networks to 40 wt % for phosphonate based networks. The highest char yield was found in dicyandiamide cured networks, possibly due to a synergistic effect between phosphorus and nitrogen. The nitrogen may have aided the conversion of phosphonate to inorganic phosphate.

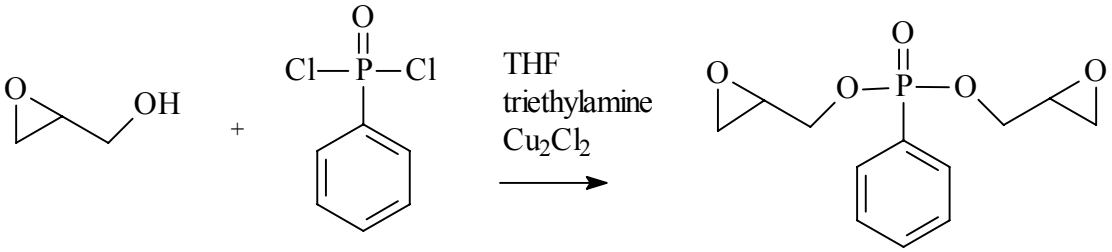

Figure 2-25. Synthesis of bis(3-glycidyloxy)phenylphosphine oxide.

The mechanism of thermal decomposition of phosphonate and phosphate containing epoxy networks was investigated more thoroughly using pyrolysis-gas

chromatography/mass spectrometry[39]. Volatiles were monitored throughout the heating and decomposition of the samples. Phosphonate diepoxides and phosphate triepoxides containing bisphenol sulfone and bisphenol-A units were prepared (Figure 2-26).

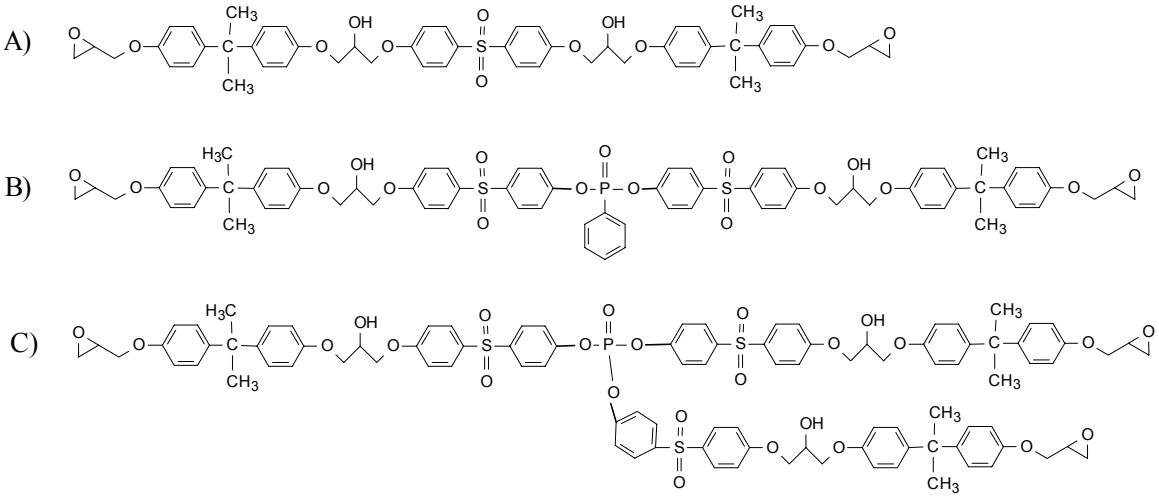

Figure 2-26. A) Sulfone containing diepoxide, B) phosphonate diepoxide and C) phosphate triepoxide.

The resins were cured at 120°C for 1 hour. Similarly to the phosphaphenanathrene materials, the onset of degradation occurred earlier in the phosphorus containing networks; however, these systems resulted in the highest char yield and showed both phosphorus and sulfur residues. The phosphate performed better than the phosphonate, possibly due to a simpler transition to inorganic phosphorus. The phosphonate contained a phosphorus-carbon bond that had to be oxidized to yield inorganic char. In the sulfone/bisphenol-A network, volatiles increased with temperature up to 650°C while in the phosphorus networks the volatiles began to decrease at 500°C as char developed and shielded the sample. The main volatiles in all of the systems were phenolic derivatives.

Transition metals were incorporated into bisphenol-A based diepoxides through a metal complex with the ether oxygen[40,41]. Epoxy resins were prepared via a typical synthesis in which bisphenol-A was refluxed in a ten fold excess of epichlorohydrin as aqueous base was added dropwise over 3.5 hours. This reaction was done without and with metal acrylates. One resin contained 0.004 equivalents of zinc (II) acrylate, 0.003

[39] J.-F.Lin, C.-F. Ho, and S. K. Huang, *Polym. Degradat. Stabil.*, 2000, **67**, 137-147.

equivalents of chromium (II) acrylate, and 0.004 equivalents of copper (II) acrylate[40]. Another series of oligomers were synthesized in the presence of different concentrations of zinc acrylate (0.007-0.02 equivalents)[41]. Molecular weight and chlorine content increased from 380 g/mol to 670 g/mol and from 0.57 wt % to 3.86 wt %, respectively with elevated zinc acrylate concentrations. The metal associated with the phenol and may have inhibited the dehydrohalogenation step slightly, leading to increased chlorine content. The resins were cured with an unspecified polyamide for 24 hours at 30°C and 2 hours at 80°C. Electric conductivity, 1.5×10^{-13} $\Omega^{-1}cm^{-1}$ for the unmodified resin, was increased greatly to 5.45×10^{-10} $\Omega^{-1}cm^{-1}$ for the network containing the blend of all three metal acrylates. Scratch hardness and thermal stability were also improved, increasing with zinc concentration.

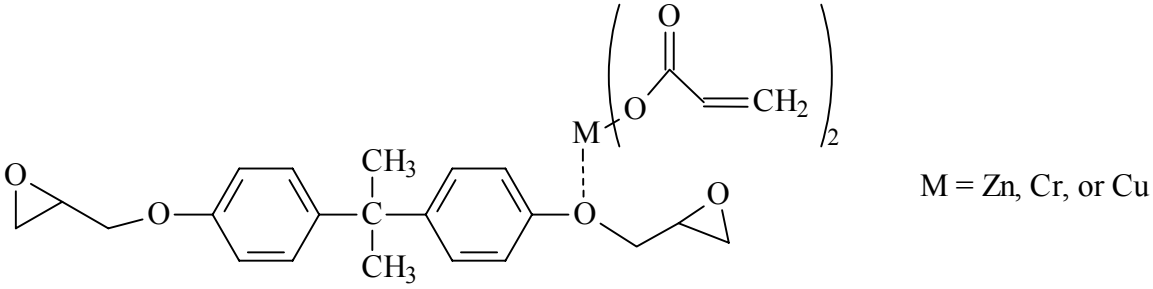

Figure 2-27. Metal acrylate-bisphenol-A based diepoxide complex.

As noted in the above research, inorganic moieties can be used to tailor a number of properties of the epoxy resin and resulting networks. The epoxy/amine cure could be enhanced with the addition of phosphine oxide, possibly due to hydrogen bonding that led to an increased electron density of the nucleophilic amine. Network chemistry could be altered to integrate specific properties such as decreased thermal stability with thiocarbonohydrazone, increased flame retardance with phosphine oxide, and increased electrical conductivity with transition metal acrylates.

2.1.4.2. Aromatic Based Epoxy Resins

Aromaticity within a network increases stiffness without increasing water absorption, in contrast to incorporation of strong hydrogen bonding moieties. Therefore,

---

[40]M. Anand and A. L. Srivastava, *Polymer*, 1993, **34**(13), 2860-2864.

[41]M. Anand and A. K. Srivastava, *J. Appl. Polym. Sci.*, 1994, **51**, 203-211.

incorporation of aromatic moieties has drawn interest for applications that require increased glass transitions with low water absorption such as electronic packaging. Liquid crystal mesogens have also been epoxidized to take advantage of reduced resin viscosity and epoxy cure chemistry that can 'lock in' liquid crystal structure.

Epoxy resins have been prepared with pyrene, anthrylene, and tetramethyl benzene groups along the backbone[42]. Phenolic structures containing the aromatic rings were synthesized and then reacted with an excess of epichlorohydrin with dropwise addition of aqueous sodium hydroxide to yield diepoxide oligomers (Figure 2-28A, B, C). A stoichiometric amount of novolac crosslinking agent was used to prepare the thermosets. A bisphenol-A based epoxy was crosslinked in a similar manner for comparison. Physically increased bulk, from tetramethyl benzene to pyrene, appeared to inhibit chain rotation, both increasing the T_g from 129°C to 137°C and decreasing the coefficient of thermal expansion from $16.6x10^{-5}$/°C to $15.4x10^{-5}$/°C above T_g. Chemically, higher levels of aromaticity improved thermal stability and hydrophobicity. The pyrene containing network had 38 wt % char in nitrogen compared to 18 wt % for the bisphenol-A based thermosets. Moisture uptake was reduced from 2.1 wt % in the bisphenol-A based network to 1.3 wt % in the pyrene based network (determined at 133°C and 3 atm).

To investigate the effect of ether linkages, epoxies were prepared with diphenylether, biphenylene, and phenylene moieties[43]. Diepoxides were prepared by reaction with an excess of epichlorohydrin (Figure 2-28D, E, F). Networks were prepared by curing a phenolic novolac with these low molecular weight oligomers. The increased stiffness of the biphenylene network yielded the highest T_g, 139°C, and, surprisingly high fracture toughness, $K_{1c} = 1.22$ MPa/$m^{1/2}$. This increased toughness may have been due to the high degree of segment stiffness combined with decreased molecular weight between crosslinks. If more free volume was locked into the network structure, plastic deformation could occur more readily during fracture. The char yield was highest for the diphenylether networks, 44 wt %. The coefficient of thermal

---

[42]J. Kaji, K. Nakahara, K. Ogami, T, Endo, *J. Appl. Polym. Sci.*, 2000, 75, 528-535.

[43] M. Kaji, K.Nakahara, K.Ogami, and T. Endo, *J. Polym. Sci. Part A Polym. Chem.*, 1999, **37**, 3687-3693.

expansion was lower for the diphenylether network, 16.9×10^{-5}/°C, compared to that of the phenylene network, 17.3×10^{-5}/°C, and possibly due to ether interactions that resulted in tighter molecular packing.

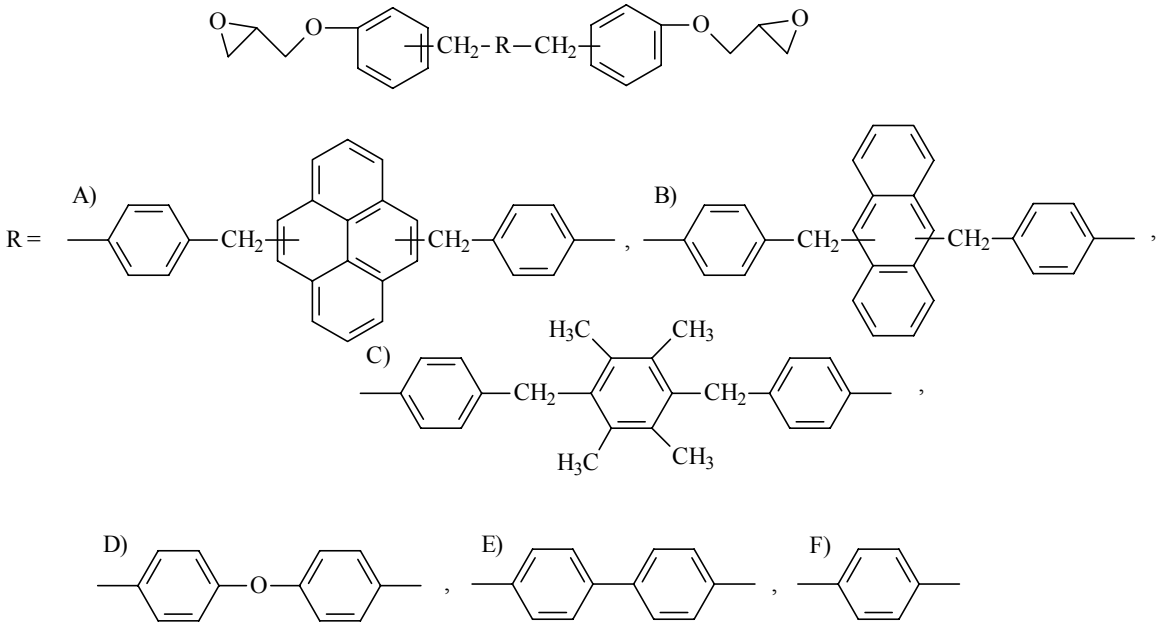

Figure 2-28. Aromatic diepoxides prepared from A) pyrene, B) anthracene, C) tetramethyl benzene, D) diphenylether, E) biphenyl, and F) phenyl functionalities.

Toward a similar end, novel naphthalene and phenyl based epoxy resins were synthesized to increase T_g while limiting moisture absorption[44]. 1-Hydroxynaphthalene or phenol were reacted with 1,4-bis(1-hydroxy-1-methyl-ethylidene) benzene to yield diphenols from which the epoxy resins were prepared by the one step epoxidation with base (Figure 2-29). The diepoxides were crosslinked using a stoichiometric amount of novolac resin. An increase in cure exotherm temperature and a decrease in the heat of reaction for the naphthalene system suggested that steric hindrance reduced molecular mobility and slowed the cure reaction. The resulting network had a lower rubbery modulus than the phenyl based network, indicating lower crosslink density. This may have been due to a reduced degree of conversion because of the reduced mobility. The water absorption was dominated by the chemical composition of the network and even with a more open network, moisture uptake was lower for the naphthalene containing

[44]M. Kaji, T. Endo, *J. Polym. Sci. Part A Polym. Chem.*, 1999, **37**, 3063-3069.

thermoset, 1.3 wt%. This network also provided the highest T_g of these aromatic networks at 157°C.

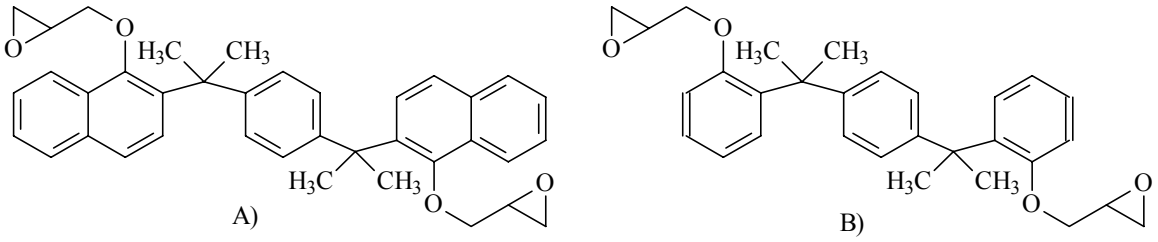

Figure 2-29. Epoxy resins containing A) naphthalene and B) phenyl moieties.

Epoxies were synthesized from aromatic polyimides to improve solubility of the imide and allow photocure of the material[45]. The polyimide was prepared from 4,4'-(1,1,1,3,3,3-hexafluoro-2-propylidene)diphthalic anhydride and 2,2-bis(3-amino-4-hydroxyphenyl)hexafluoropropane. Epoxy groups were grafted quantitatively onto the backbone phenols using epichlorohydrin and a phase transfer catalyst, benzyl(trimethyl)ammonium chloride (Figure 2-30). The traditional hydroxide synthesis could not be used because the imide groups were susceptible to hydrolysis by base. The epoxies were solution mixed with 5 wt % diphenyliodonuim hexafluoroarsenate. Cast films were dried and cured photochemically followed by a 40 minute thermal postcure at varied temperatures, 50°C-195°C. The cure reaction was monitored with FTIR. Due to the immobility of the network, reaction of the oxirane rings was not observed during irradiation, but only upon the heating of the film. The maximum conversion achieved was only 50%. Increased UV exposure time, 0-350 seconds, and higher postcure temperatures both resulted in increased conversion.

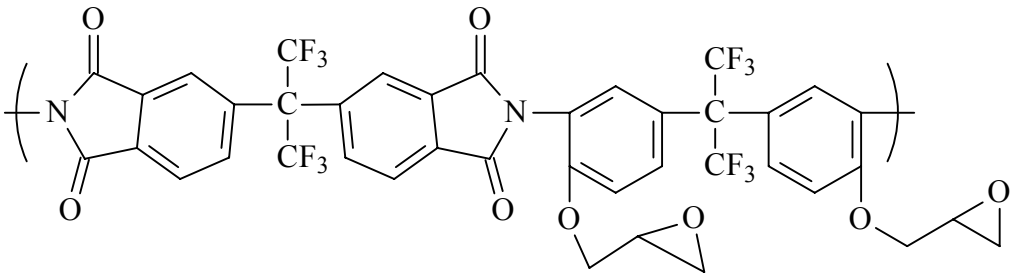

Figure 2-30. Photocurable epoxidized polyimide.

[45]H.S.Yu, T. Yamashita, and K. Horie, *Macromolecules*, 1996, **29**, 1144-1150.

Liquid Crystalline Epoxy Resins

Liquid crystal thermosets were of interest due to their potential for low process viscosities and for "self-aligning" composite matrix materials. The low viscosities of curable oligomers allowed rapid orientation of mesogens in a magnetic field, an advantage over liquid crystalline polymers with higher viscosities.

In an attempt to prepare easily processable oligomers with broad liquid crystalline temperature ranges, epoxy resins were prepared from biphenyl and dibenzoyloxybenzene mesogens with aliphatic spacers of 4 and 6 carbons[46]. Bisphenols were reacted with bromoalkenes to yield divinyl compounds that were then epoxidized using *m*-chloroperbenzoic acid (Figure 2-31). While the divinyl precursors showed smectic liquid crystalline phases, the addition of terminal epoxide groups increased intermolecular attractive forces, disrupting the liquid crystallinity of the epoxies. The epoxy oligomer of 1,4-dibenzoyloxybenzene with 6 carbon spacers did result in a liquid crystal diepoxide with a nematic phase from 107°C to 190°C.

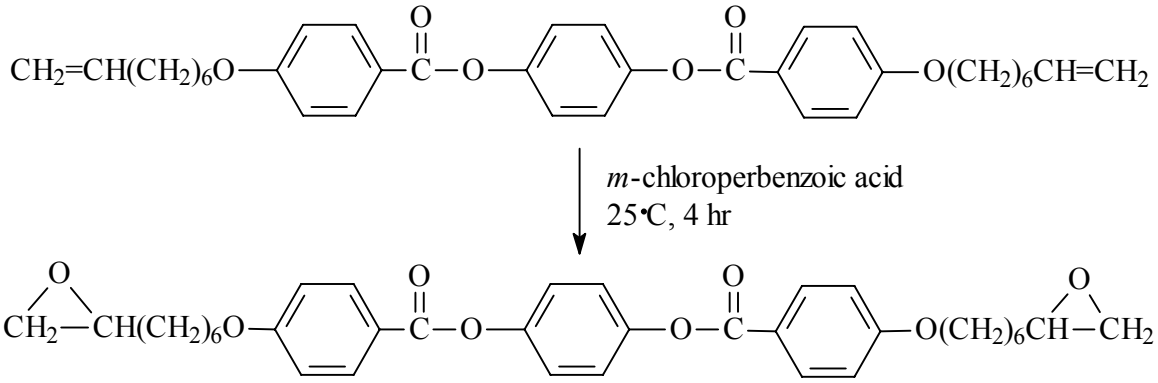

Figure 2-31. Synthesis of 1,4-dibenzoyloxybenzene diepoxide via olefin epoxidation with a peroxy acid.

Networks were prepared from these diepoxides using a stoichiometric ratio of p-phenylenediamine which was chosen because 1) the structure did not disrupt the liquid crystallinity of the epoxy and 2) the cure temperature, 120°C, coincided with the liquid crystalline range of the epoxy. Early in the cure a nematic phase with a clearing temperature was observed but as the molecular weight increased and the resin began to

[46] J. J. Mallon and P. M. Adams, *J. Polym. Sci. Part A Polym. Chem.*, 1993, **31**, 2249-2260.

gel, a smectic phase developed. The final crosslinked material was a smectic liquid crystalline thermoset.

One of the early liquid crystalline epoxy oligomers was based on an α-methylstilbene mesogen (Figure 2-32A)[47,48,49]. Modifying the cure conditions of networks crosslinked with methylenedianiline (Figure 2-32B) altered the liquid crystalline order of the final thermoset[48]. In the melt, smectic, nematic, and isotropic resins were observed at different temperatures. When cured from a nematic melt at 85°C for 3 hours followed by a 2 hour postcure at 180°C, a smectic network formed. Curing at higher temperatures from an isotropic melt produced either a nematic (140°C cure) or an isotropic rigid-rod (180°C cure) network. More ordered networks had higher rubbery moduli, 115 MPa for the smectic, 80 MPa for the nematic, and 59 MPa for the isotropic, because of restrictions on the crosslink points due to the crystal structures that persisted above the glass transition temperatures. Toughness increased with crystalline order up to K_{1c} = 1.59 MPa/$m^{1/2}$ for the smectic network, which showed ductile behavior. The slow stable crack growth was unusual for a thermoset material and may have been due to the isolated fracture of individual crystalline domains. This would have provided voids near the crack tip, relieving strain on neighboring domains and allowing plastic deformation.

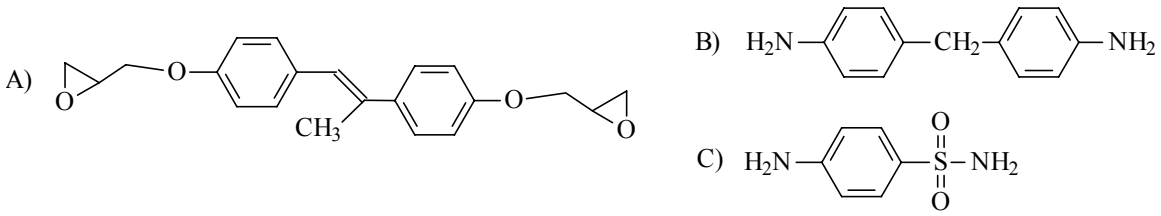

Figure 2-32. Liquid crystalline thermoset components; A) diglycidyl ether of *p,p*'-dihydroxy-α-methylstilbene and curing agents B) *p,p*'-methylene dianiline and C) sulfanilamide.

---

[47] G.G.Barclay, S.G. McNamee, C.K.Ober, K.I.Papathomas, and D.W.Wang, , *J. Polym. Sci. Part A Polym. Chem.*, 1992, **30**(9), 1831-1843.

[48]C. Ortiz, R. Kim, E. Rodighiero, C. K. Ober, and E. J. Kramer, *Macromolecules*, 1998, **31**, 4074-4088.

[49]B. C. Benicewicz, M. E. Smith, J. D. Earls, R. D. Priester, Jr., S. M. Setz, R. S. Duran, and E. P. Douglas, *Macromolecules*, 1998, **31**, 4730-4738.

The stilbene based epoxy was also used to investigate the effect of a magnetic field on crystallinity. Liquid crystal thermosets were prepared with a stoichiometric ratio of sulfanilamide (Figure 2-32C) in a magnetic field of varied intensity[49]. The amine functionalities on the sulfanilamide curing agent had different reactivities. The aniline amine group, being higher in electron density, reacted first with the oxirane rings. This chain extension increased the aspect ratio, improving the likelihood of chain orientation. The resins were cured in the magnetic field from the isotropic phase at 150°C for 1 hour and the gel point was reached within 35 minutes. Using wide angle X-ray light scattering, the network orientation was found to increase with greater field strengths (0 to 18 Tesla). Thermal expansion of the network increased perpendicular to the field and decreased parallel to the field due the differences in bond density in the aligned sample. The higher degree of order also resulted in a tensile modulus of 8 GPa compared to 3 GPa in an isotropic network.

Diphenyl and phenylene benzoate containing diepoxides Figure 2-33) have also been studied in a magnetic field (7 Tesla)[50]. Using *p,p*'-diaminodiphenyl as a curing agent, optimum elongation and strength were found for networks prepared with a 4/1 epoxide/amine ratio due to decreased network density. Resins were cured from the nematic phase at 150°C to yield nematic thermosets. These systems also showed increased modulus with orientation, 3 GPa and 2 GPa for networks cured with and without the magnetic field, respectively. Interestingly, improved performance was achieved with a blend of the two epoxies at a 3/1 benzoate epoxy/phenylene epoxy ratio. An increase in the molecular weight between crosslinks was observed at this composition. When the network density was decreased either through epoxy/amine offset or incorporation of a second oligomer and the network integrity was not lost (as from too great an epoxide/amine stoichiometric offset), strength and elongation increased.

[50]C. Tan, H. Sun, and B. M. Fung, *Macromolecules*, 2000, **33**, 6249-6254.

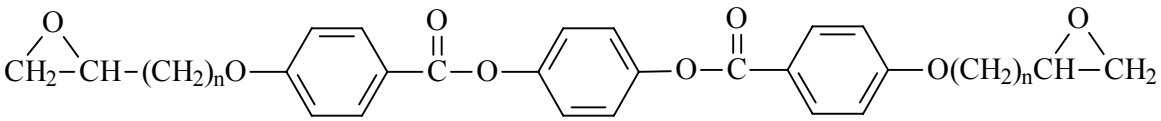

Figure 2-33. Liquid crystal oligomer 1,4-phenylene bis(4-(epoxy) benzoate.

The segmental behavior of epoxy oligomers has been investigated using broad-band dielectric relaxation spectroscopy[51,52]. Dipole dynamics were characterized for molecular transitions in oligomers and networks containing the benzoate mesogen. In the resin, epoxy ring motion and mesogen rotation were monitored. In the cured network, mesogen rotation was still observed while the other transition was not detected because epoxy rings were no longer present. Motion of the epoxy ring segment, requiring 26 kJ/mol, was not sensitive to phase transitions of the resin due to the localized nature of the process. Stepwise increases in dielectric constant however indicated the dependence of mesogen rotation (63 kJ/mol) on phase transitions. In the networks cured with *p,p*'-methylenedianiline at 140°C from a nematic phase, mesogen rotation was still detected and required a similar amount of energy as in the resin, 66 kJ/mol.

In general, the presence of stiff aromatic moieties increased the network glass transition temperature and char yields while reducing moisture absorption. Various levels of molecular order could be achieved in networks by using liquid crystalline oligomers and controlling the processing conditions. Increased liquid crystalline order that resulted in improved rubbery moduli and extreme toughness could be increased with lower cure temperatures and by curing in the presence of a magnetic field.

2.1.4.3. Aliphatic Based Epoxy Resins

This section discusses a broad range of epoxy resins that have been investigated to 1) improve upon the chemistry or reactivity of the resin and 2) study different molecular architectures in which the epoxy moiety's well documented chemistry simplifies the examination of new morphologies.

One advantage of aliphatic epoxy thermosets has been improved network weatherability. Cyclohexanone/formaldehyde condensation resins have been used

---

[51]S. Andjelic and J. Mijovic, *Macromolecules*, 1998, **31**, 8463-8473.

[52]J. Mijovic, X. Chen, and J.-W Sy, *Macromolecules*, 1999, **32**, 5365-5374.

industrially in coating formulations. The following research addressed preparing oligomers with more controlled chemical structures to improve network performance[29]. Reacting cyclohexanone with an excess of formaldehyde, 2,2',6,6'-tetramethylol-cyclohexanol was prepared. Four epoxy resins were investigated, two low molecular weight materials prepared from direct epoxidation of the cyclohexanol and two higher molecular weight materials prepared from the epoxidization of cyclohexanone/ formaldehyde oligomers.

The cyclohexanol/methylol resins were synthesized using two epoxidation routes (Figure 2-34). A one step phase transfer process involved dissolving the cyclohexanol/methylol reagent in a ten fold excess of epichlorohydrin with tetramethylammonium chloride at 55°C and adding aqueous sodium hydroxide dropwise over 3 hours. Higher temperatures were required for the two step process. The multifunctional cyclohexanol/methylol reagent was refluxed in dioxane with a Lewis acid, $SnCl_4$, while epichlorohydrin was added dropwise so as to maintain the reaction temperature. This was allowed to react for 2 hours to form the chlorohydrin. In the second step the reaction was cooled to 55°C and aqueous sodium hyroxide was added slowly. The one step reaction resulted in methylol polycondensation, catalyzed by the basic conditions, yielding 650 g/mol oligomers. Lower molecular weight oligomers, 450 g/mol, were obtained from the second synthesis. In the initial step, $SnCl_4$ did not catalyze the methylol polycondensation. However the Lewis acid did allow secondary hydroxyls to react with epichlorohydrin (to a lesser extent than primary) and this resulted in elevated levels of chlorine, 6.44 wt % compared to 0.75 wt % in the first method. In the first step, the secondary chlorohydrin hydroxyl groups were able to react with epichlorohydrin locking in nonhydrolyzable chlorine. Both resins, cured with a polyaminoamide, outperformed bisphenol-A based epoxy networks when tested as coatings under a xenon-arc weatherometer for 1000 hours. The cyclohexanol/methylol-epoxide networks did not microcrack while the bisphenol-A film completely degraded after 700 hours under the accelerated weathering conditions.

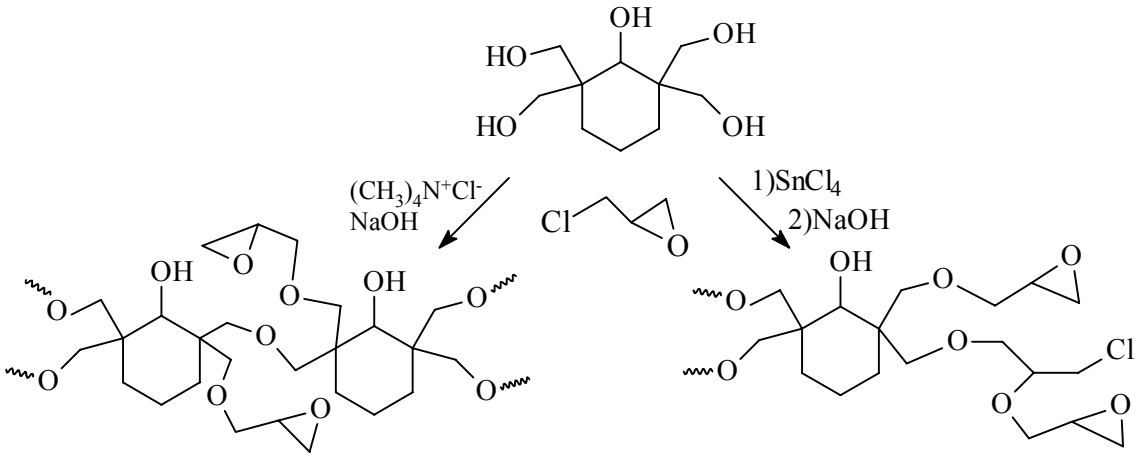

Figure 2-34. Epoxidation of cyclohexanol via a phase transfer process and two step process.

Two higher molecular weight oligomers were also prepared; the condensation product of 1 of equivalent cyclohexanone/1.6 equivalents of formaldehyde containing both pendant and terminal hydroxyl groups and the condensation product of 1.5 equivalents of the cyclohexanol/methylol reagent and 1 equivalent of glutaraldehyde that had only terminal hydroxyl groups. Using the phase transfer process, these alcohols were epoxidized to yield a ~1000 g/mol and a ~2000 g/mol brittle epoxy resin, respectively. After being crushed with carboxyl terminated saturated polyesters, these materials were cured at 200°C. Yellowing occurred in the materials prepared from cyclohexanone due to remaining carbonyl groups. In going to the cyclohexanol system with better control over both the backbone chemistry and oligomer functionality, yellowing was eliminated and tougher coatings were prepared. The terminal epoxide groups on the oligomer prepared from the cyclohexanol/methylol reagent may have allowed reduced network density compared to the cyclohexane/formaldehyde epoxy resin, improving the impact performance of the resulting network.

Novel epoxy resins have been developed which degrade at low temperatures to prepare reworkable networks[53]. To facilitate degradation above the network's T_g, labile tertiary ester moieties were incorporated into the networks. Cycloaliphatic epoxy oligomers were synthesized with internal tertiary esters and with trisubstituted epoxide

[53]S.Yang, J.-S. Chen, H. Korner, T. Breiner, C. K. Ober, and M. D Poliks, *Chem. of Mater.*, 1998, **10**(6), 1475-1482.

rings that formed tertiary esters upon cure with anhydrides. Networks were prepared by curing the epoxy resin with 0.87 equivalents of the crosslinking agent hexahydro-4-methylphthalic anhydride using an ethylene glycol as the initiator and benzyldimethylamine as the catalyst. For comparison, networks were also prepared from 3,4-epoxycyclohexylmethyl-3,4-epoxycyclohexanecarboxylate, which contains no tertiary esters. At ambient temperatures the networks possessed similar moduli, 5 GPa. However, when heated above T_g to 190°C, the network containing the tertiary ester degraded to a brittle network within minutes. This was due to the difference in activation energies for the decomposition of the primary, secondary and tertiary esters, which were 186, 183 and 104 kJ/mol, respectively. While little difference was observed between the activation energy for decomposition of the primary and secondary esters, the tertiary esters were significantly less stable.

Block copolymers containing pendant epoxy groups were synthesized and used as reactive fillers in bisphenol-A based epoxy networks[54,55]. The block copolymers contained one block that was soluble in a bisphenol-A epoxy resin and one block that was insoluble. Due to differences in the epoxide reactivities, the molecular architecture of the phase separated networks were altered. In one series the isoprene block of a butadiene/isoprene block copolymer was selectively epoxidized using a mild alkene epoxidation reagent, dimethyldioxirane prepared in situ from acetone and potassium monopersulfate[55]. The copolymer consisted of an insoluble butadiene block and a soluble isoprene block with 46-95 % epoxidized isoprene. The other block copolymer was polymerized via a nitroxide-mediated living free radical polymerization[54]. The polyepoxy consisted of a miscible block of randomly copolymerized glycidyl methacrylate and methyl acrylate and an immiscible block of polyisoprene. Resin/copolymer blends were cured with *p,p*'-methylenedianiline at 55°C for 48 hr followed by 200°C for 1 hr. Microphase separation was noted when 5 – 40 wt % of the copolymer was added. An epoxy scaffolding developed during cure that locked in the resin morphology before the 200°C postcure. Epoxy groups on the isoprene polymer

[54]R. B. Grubbs, J. M. Dean, M. E. Broz, and F. S. Bates, *Macromolecules*, 2000, **33,** 9522-9534.

[55] R. B. Grubbs, M. E. Broz, J. M. Dean, and F. S. Bates, *Macromolecules*, 2000, **33**, 2308-2310.

block were less reactive towards the amine due to the increased substitution of the oxirane ring and did not become covalently bound to the bisphenol-A network until the high temperature post-cure was performed. During the 55°C cure, the polyisoprene block may have become insoluble as the bisphenol-A resin reacted and increased in molecular weight. This was theorized to result in a layer of excluded polyisoprene block around a polybutadiene block core that crosslinked during postcure. The epoxide rings pendant to the methacrylate chain cured at the same temperature as the resin and probably developed an interdiffused region between the bisphenol-A network and the polyisoprene block core comprised of crosslinked bisphenol-A resin and methacrylate copolymer.

Epoxy chemistry has also been used to develop hyperbranched polymers, which may be useful for low viscosity adhesives and coatings[56]. Through the melt reaction of an excess of diepoxide, 1,2,7,8-diepoxyoctane and triol, 1,1,1-tris(hydroxymethyl)ethane, hyperbranched polymers were synthesized. The polymerization was done at 120°C in the presence of 5 mol % tetra-n-butylammonium chloride. Throughout the polymerization the polydispersity increased with the increase of weight average molecular weight from 1.5 at 1,000 g/mol to 5 at 7,000 g/mol. By stopping the reaction before crosslinking occurred, soluble hyperbranched polymers were achieved with M_w of 5,000-15,000 g/mol. Increasing the ratio of epoxide to alcohol from 1.5/1 to 3/1 increased the final epoxy content and the number of tri substituted ethane units.

Self-assembled monolayers were of interest for potential applications such as molecular lubrication[57]. The epoxide functionality offered a means of preparing a reactive surface to which a tribological layer could be anchored. Silicon wafers were exposed for 0-24 hours to toluene solutions of (3-glycidoxypropyl)trimethoxysilane at concentrations varied from 0.1 wt % to 1 wt %. Monolayer formation occurred only from the 1 % solution and was believed to depend on optimization of the water content. The equilibrium water content in toluene was 0.03 wt %. At low silane concentrations, aggregates formed because the water/silane ratio was high enough to result in hydrolysis of the silanol in solution. At higher concentrations of silane, the water/silane ratio was

[56]T. Emrick, H.-T.Chang, and J.M.J.Frechet, *Macromolecules*, 1999, **32**, 6380-6382.

low and hydrolysis of the silanol occurred at the substrate rather than in the bulk. Carboxylate terminated polystyrene was successfully reacted with the epoxidized surface to form a densely tethered polymer layer.

The increased weatherability of aliphatic networks has continued to be of interest. However, a majority of the current research involving aliphatic epoxy systems has entailed the investigation of physical structures such as hyperbranched polymers and monolayers in the context of well understood epoxy chemistry.

2.1.4.4. Epoxy Cure Chemistry

To further increase the utility of epoxy resins, optimization of epoxy crosslinking has been investigated. Epoxy resin chemistry has been modified to increase the cure kinetics and decrease the cure shrinkage, while novel catalysts have been developed to improve the resin processability.

Interest in increasing the reaction rate of the photopolymerization of epoxide rings has prompted research on 1-propenyl ether containing cyclohexyl epoxies[58]. The cyclohexyl epoxies are the most reactive epoxies towards photopolymerization and the 1-propenyl ether group is the most reactive functionality known at this time. (2-oxapent-4-enyl)-3,4-epoxycyclohexane (**B**) was prepared by the epoxidation of (2-oxapent-4-enyl) cyclohex-3-ene (**A**) using 3-chloroperoxybenzoic acid and reacting at 5°C for 1.5 hours and then 16 hours at 25°C (Figure 2-35). The cyclic alkene double bond was more reactive and selectively epoxidized under these mild conditions with a high yield of 93%. The epoxide was then isomerized to (2-oxapent-3-enyl)-3,4-epoxycyclohexane (**C**) using tris(triphenylphosphine)ruthenium(II) dichloride at 160°C for 9 hours. While isomerization of the (2-oxapent-4-enyl) cyclohex-3-ene (**A**) required 2 hours, the epoxidized compound isomerized much more slowly. This may have been due to competitive complexation of the epoxy with the ruthenium catalyst.

---

[57]I. Luzinov, D. Julthongpiput, A.Liebmann-Vinson, T. Cregger, M. D. Foster, and V. V. Tsukruk, *Langmuir*, 2000, **16**, 504-516.

[58]S.K.Rajaraman, W.A.Mowers, and J.V.Crivello, *Macromolecules*, 1999, **32**, 36-47.

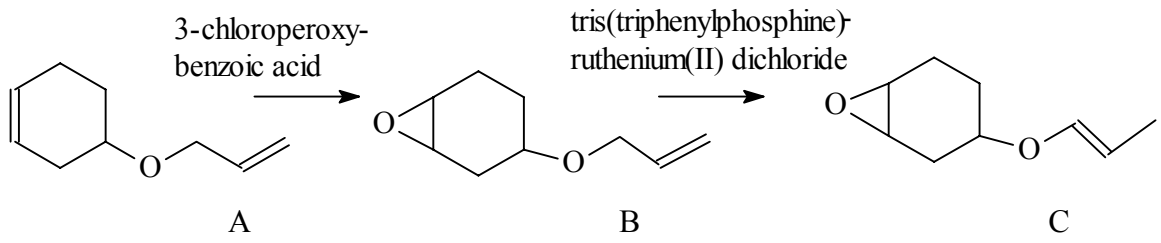

Figure 2-35. Synthesis of propenyl ether epoxy.

The reactivity of the propenyl ether epoxide **C** was investigated with photoinitiators, diaryliodonium (Figure 2-17) and triarylsulfoniom hexafluoroantimonate salts. During photoinitiation both cations and radicals were generated. When iodonium salts were used, the reaction of the epoxide was accelerated while that of the vinyl bond was delayed until all of the epoxy groups were reacted. Essentially, epoxy polymerization occurred initially followed by crosslinking as the vinyl groups reacted. Blends of the unisomerized epoxy (**B**) and an unepoxidized propyl ether showed that the epoxy acceleration still occurred when the two functionalities were on different molecules. A proposed method of acceleration involved the reaction of the propenyl ether with aryl radicals generated by the initiator. Once the propenyl ether radical was formed, it could be oxidized to a cation by reaction with an undecomposed iodonium salt. This cation then initiated further epoxy polymerizations. This theory was supported by the fact that epoxy reaction acceleration was not seen in resins cured with a sulfonium salt initiator. The sulfonium initiator, with a higher reduction potential, did not reduce the propenyl ether radical to generate additional cations.

Anionic cure with bis(γ-lactones) reduced the cure shrinkage of epoxy resins[59]. Polyepoxides were prepared via the free radical polymerization with AIBN of glycidyl methacrylate or 4-glycidylmethylstyrene to yield 25,000 g/mol and 19,000 g/mol polymers, respectively. Each polymer was cured with a stoichiometric ratio of 1,6-dioxaspirol(4,4)nonane-2,7-dione (Figure 2-36) per epoxide group and 2 mol % potassium *tert*-butoxide catalyst. Total conversion of both the spirodicyclic orthoesters and oxiranes was achieved after curing for 72 hours at 120°C. The polyepoxies were cured in a similar manner with no spirodicyclic reactant. The degree of epoxy ring

[59] K. Chung, T. Takata, and T. Endo, *Macromolecules*, 1997, **30**, 2532-2538.

opening was much lower, 27 % for the polymethacrylate and 38 % for the polystyrene and attributed to the reduced reactivity of the epoxide with another epoxide versus the spirodicyclic curing agent. Even with the elevated degree of reaction, shrinkage was reduced from 6.3 % to 4.7 % in the methacrylate network and from 5.4 % to 5.2 % in the styrene network with incorporation of the spirodicyclic monomer. Upon anionic reaction the spirodicyclic reactant underwent two ring openings and there was a corresponding volume increase for this component (Figure 2-36). Crosslinking the methacrylate polymer with a bicyclic orthoester further reduced the cure shrinkage to 2.5 %.

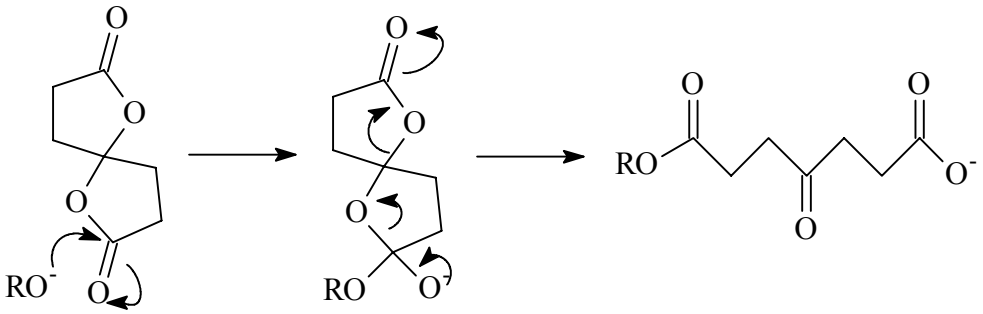

Figure 2-36. Ring opening of 1,6-dioxaspirol(4,4)nonane-2,7-dione during anionic cure of epoxy resins.

To investigate the effect of chain mobility on the epoxy/amine cure, dendrimers were modified with pendant epoxy groups. A third generation dendrimer was reacted with different concentrations of epoxidized methyl undecenoate to yield polyepoxies with epoxy equivalent weights of 1050 g/mol, 560 g/mol, and 410 g/mol. These resins were blended with a stoichiometric concentration of isophorone diamine and the cure kinetics were compared to those of a bisphenol-A based epoxy resin. The low molecular weight bisphenol-A containing system showed an increase in reaction rate up to 15 % conversion. This autocatalysis was due the formation of hydroxyl groups that stabilized other oxiranes during reaction. The dendritic resin did not show any autocatalytic effect. Due to the dense dendritic structure, the mobility of the tethered epoxides was reduced and newly formed hydroxyl groups were not able to associate with and stabilize other epoxy rings. A decrease in percent conversion was also found with increased epoxy equivalent weight of the dendritic epoxies. The higher epoxy equivalent weight corresponded to a greater volume per epoxide group. As the resin cured, dendritic

epoxies with increased equivalent weight excluded more volume in which unreacted epoxide groups were trapped.

New latent catalyst systems have also been investigated[60,61]. Phosphonium ylides with varied electron withdrawing carbon substituents were utilized to investigate the mechanism of catalysis (Figure 2-37). These materials were thermally latent up to 90°C. The more electronegative methoxy acyl substituent polarized the phosphorus-carbon bond more than did the methyl acyl functionality. Therefore the methoxy compound possessed more ylide bond character while the methyl molecule possessed more ylene character. The phosphorus-carbon bond with more ylide character was found to be more catalytic. It appeared that the ylide carbon deprotonated the phenol to become a phosphonium cation. The cation could then associate with the epoxide oxygen and activate the ring to attack by the phenolate anion. Phosphonium salts have also been used as latent accelerators for anhydride cured resins[27]. Triphenylphosphinemethylene boranes also showed thermally latent catalytic activity[61]. Following a similar mechanism, the carbon-boron bond cleaved at elevated temperatures to yield the catalytic ylide. The carbon-boron bond stability increased with more electronegative substituents as seen by the decrease in bond length. The hydrogen substituted boron had a carbon-boron bond length of 1.74 Å while the fluorine substituted boron had a bond length of 1.69 Å. The less stable boranes were more reactive and resulted in increased epoxy conversion upon thermal cure.

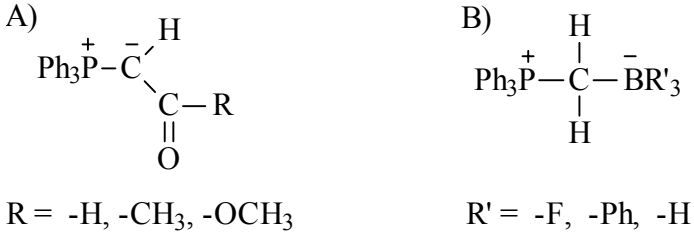

Figure 2-37. Thermally latent catalysts; A) phosphonium ylides and B) boranes.

[60]M. Kobayashi, F. Sanda, and T. Endo, *Macromolecules*, 1999, 32(15), 4751-4756.

[61] M. Kobayashi, F. Sanda, and T. Endo, *Macromolecules*, 2001, **34**, 1134-1136.

Current research into the cure of epoxy resins has increased the understanding of the epoxy reactions to allow faster cures under the desired conditions. By controlling the resin chemistry, including the epoxy oligomer, crosslinking agent and catalyst, properties of the curing system could be tailored for specific applications.

2.1.5. Summary

Epoxy research covers a broad spectrum of chemistries and applications. Due to the varied resin and network properties that can be achieved, the epoxy resins are extremely versatile. These materials have continued to be a focus for research and have found extensive use commercially because of this versatility. A great number of both epoxy oligomers and crosslinking agents have been studied in the past century. A range of additives further increases the flexibility of these materials; viscosity can be reduced without loss of mechanical properties through the use of low molecular weight reactive diluents, toughness can be increased by incorporation of rubber particles, and cure reactions can be accelerated or delayed depending on the catalyst used. Two-part epoxy/amine systems can be purchased at the hardware store and can be cured under ambient conditions to yield strong household adhesives. Using similar epoxy/amine cure chemistry with more rigid aromatic amines and elevated cure temperatures, high T_g networks can be obtained for use as electronic insulators. Epoxy resins will continue to find use in traditional applications such as coatings and adhesives as well emerging technologies such as composites and electronics. The adaptability of the epoxide ring will continue to amaze us, inspiring new avenues of research.

2.2. Fiber/Polymeric Matrix Interphases

2.2.1. Introduction

Composite materials are composed of reinforcing fibers or particles and a matrix material that is designed to bind and protect the fibers. In this review, fiber reinforced polymeric composites will be discussed. In fiber reinforced composite systems, the fibers are principally the load bearing members, while the polymeric matrix provides transverse integrity and transfers the load onto the fiber. Fibers used today include poly(acrylonitrile) (PAN) based and pitch based carbon fibers, aramid fibers, and glass fibers, which are the most commonly utilized. Work is also being done with natural fibers, such as cellulose. Common matrices may be a thermoplastic, e.g. polypropylene (PP), or a thermosetting resin, such as epoxy and vinyl ester resins.

When investigating composite performance, the properties of the matrix and fiber must be taken into account. There is a third component that also plays a crucial role. At the fiber/matrix interface there exists a region with properties different from those of the fiber or the matrix. This region between the bulk fiber and bulk matrix may contain several different layers (Figure 2-38), and can have large effects on the composite properties. Therefore, to design an optimal composite system, it is critical that this interphase region be characterized, including its size, mechanical properties, adhesion to the fiber and to the matrix, and that a determination be made of how these variables affect the overall composite performance.

Different interphase regions can develop. With semicrystalline matrix materials, different crystalline morphologies may arise at the fiber surface than those found in the bulk matrix. Reinforced PP is one example. PP in contact with the fiber surface crystallizes more readily than it does in the bulk, thereby resulting in a highly oriented interphase layer[62]. This transcrystalline layer has a higher modulus and affects the

[62]C. Wang and C.-R. Liu, *Polymer*, 1999, **40**(2), 289-298.

interfacial adhesion between the fiber and the matrix. Much research is being done to understand the effects of the transcrystalline region and to gain control over crystallization within both the interphase and the bulk matrix during processing.

Interphase regions can form in composites with thermosetting matrices due to preferential adsorption of resin components onto the surface of the fibers, resulting in a gradient of cure and mechanical properties[63]. In the case of anhydride cured epoxy resins, a deficiency of epoxy oligomers can occur near the fiber. The resulting interphase region can have a lower crosslink density and glass transition temperature (T_g) than that of the cured bulk epoxy.

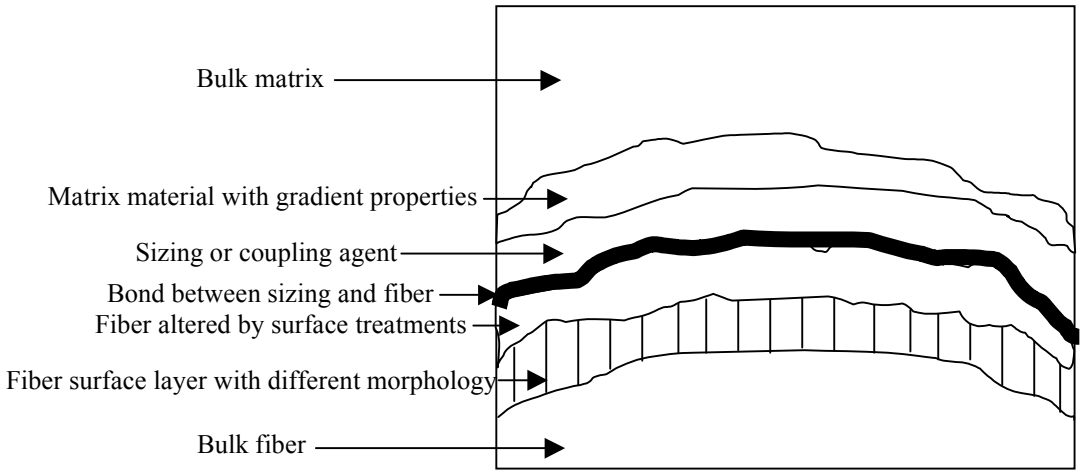

Figure 2-38. Possible layers found within the fiber/matrix interphase region in fiber reinforced polymeric composites, based on the model by Drzal et al. [11]

Treating the fiber surface prior to introducing the matrix material can also modify the interphase region and alter the fiber/matrix adhesion. Surface treatment can remove weak surface layers or introduce new functional groups on the surface that affect the adhesion of the matrix or sizing to the fiber[64]. Polyacrylonitrile based carbon fibers can be electrochemically oxidized prior to use. This relatively harsh environment removes loose crystallites formed on the fiber surface and also increases the surface oxygen concentration. Another common means of surface modification is the reaction of glass fibers with coupling agents[65]. The coupling agent acts to protect the fiber surface from

[63]K. E. Atkinson and C. J. Jones, *J. Adhes.*, 1996, **56**, 247-260.

[64]S. F. Waseem, S. D. Gardner, G. Je, W. Jiang and U. Pittman Jr., *J. Mater. Sci.,* 1998, **33**(12), 3151-3162.

[65]H. R. Wu, D. W. Dwight and N. T. Huff, *Compos. Sci. Technol.*, 1997, **57**(8), 975-983.

hydrolysis and yields desired functional groups on the fiber surface. Treating the surface with polymer chains that diffuse into the fiber and become interpenetrated with fiber polymer chains can also modify the surface[66].

In other cases, sizings can be added to the fiber surface prior to the addition of the matrix resin[67,68]. These components are added to improve fiber processability as well as improve fiber/matrix adhesion, improve fiber wetting, reduce residual stress, and improve composite mechanical damping. Sizings may covalently bond to the fiber surface or they may interact through dipole interactions between polar moieties.

2.2.2. Interphase Characterization Techniques

In an attempt to gain a better understanding of the interphase region, researchers have explored many characterization techniques. The interphase between the fiber and bulk matrix has been evaluated both directly, as in imaging using scanning electron or optical microscopy, and indirectly, as in composite fatigue testing. The atomic force microscope has shown great promise for use as a direct probe of the region, for imaging as well as determination of mechanical properties on a nanometer scale. Other techniques that have been used to evaluate interphase properties include a wide range of fiber debond experiments that characterize the fiber/matrix adhesion. These debond values were often used in conjunction with composite properties such as impact resistance and strength to determine the effect of the interphase on composite performance.

Atomic Force Microscopy

Atomic force microscopy (AFM) or scanning force microscopy analyzes the sample surface by using a stylus that interacts with the surface on an atomic scale. The stylus is located at the end of a cantilever beam that bends due to atomic force interactions between the tip and the surface (Figure 2-39). A laser, reflected off of the end of the cantilever beam, is detected by a photodiode and used to determine the degree of bending of the beam. This deflection is correlated to the surface-tip interactive force.

---

[66]Y. Cohen, D. M. Rein, L. E. Vaykhansky and R. S. Porter, *Composites*, 1998, **30A**, 19-25.

[67]S. Subramaniam, J. J. Lesko, K. L. Reifsnider and W. W. Stinchcomb, *J. Compos. Mater.*, 1996, **30**(3), 309-332.

[68]V. Lacrampe, J. P. Pascault and J. F. Gerard, *Polym. Preprints*, 1995, **36**, 813-814.

Feedback loops sustain a constant force by adjusting the distance between the tip and sample thus maintaining contact between the stylus and surface throughout imaging. Microscopes are configured with either a mobile sample platform or a mobile cantilever. Lead zirconate/titanate piezo-electric ceramic motors direct motion of the movable component in the z direction with 0.5 angstrom resolution and in the x and y direction with 1-2 nanometer resolution.

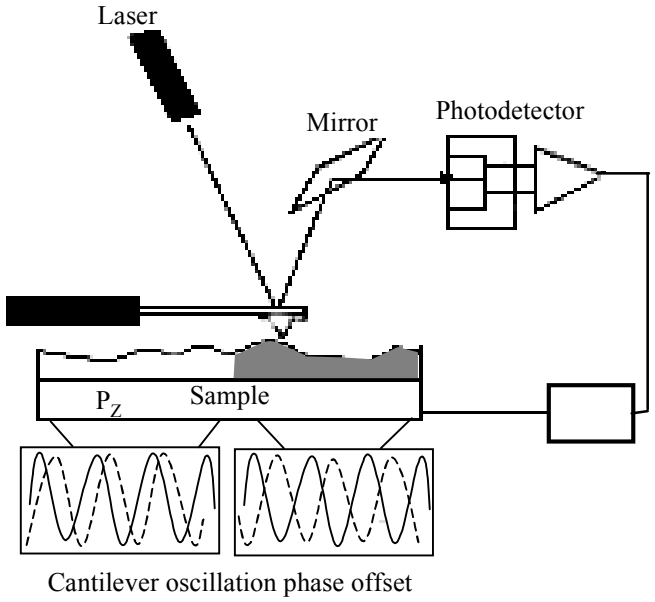

Figure 2-39. Atomic force microscope.

AFM can be used in three different modes that allow surface imaging and analysis of mechanical properties. In the scanning mode the cantilever and the surface are in constant contact. A less destructive imaging mode involves oscillating the cantilever and tapping the surface. In the force mode, the surface is indented, thereby generating a deflection-distance curve rather than an image. AFM can be conducted in air or in a non-gaseous fluid to reduce capillary forces of surface absorbed water layers. These methods can be used to characterize interphases as well as image precursor unsized and sized fibers[69].

In the scanning mode, the stylus is moved across the surface, maintaining contact. Tip deflection involves both bending and twisting. Height images, showing topography,

[69] N. Dilsiz and J. P. Wightman, *Carbon*, 1999, 37(7), 1105-1114.

are generated from the bending data and lateral force images are generated from the twisting of the cantilever. Lateral forces of a relatively smooth surface are attributed to friction. Trace scans, produced when the cantilever moves in one direction, and retrace scans, generated when the cantilever returns across the surface in the opposite direction, result in mirror images. From the deviation between these two scans friction forces can be evaluated[70]. The lateral force image of textured surfaces results from sample morphology. Resolution, which can be estimated by imaging ordered surface features, is limited by the tip-sample contact area. The contact area in the scanning mode is on the order of a few square nanometers[71] and can be minimized by using low forces, ~2 nN. Cantilevers with low spring constants, 0.01-1 N/m, are necessary at these low forces and etched silicon or silicon nitride cantilevers are typically used for scanning mode experiments[72]. Due to the dragging of the stylus over the sample surface, damage may occur on softer materials.

To reduce wear on the surface, displacement modulation can be used. The cantilever is oscillated at its resonance frequency, ~300 kHz. Intermittent tip-sample contact eliminates the destructive shear forces found in the contact mode. Higher forces, 50-100 nN, and stiffer cantilevers with spring constants of 20-100 N/m are used in the tapping mode. Reduction of the cantilever amplitude due to contact with surface features is used to adjust the distance between the stylus and the sample and generates height and amplitude images. Phase lag of the cantilever oscillation relative to the piezo drive (Figure 2-39) results from damping interactions with the elastic component of the sample. In the phase image, variations in surface properties, including stiffness and adhesion, are displayed by contrasting image densities or colors.

In the force mode, surfaces are indented by the stylus. For these experiments a much stiffer cantilever is necessary to withstand the elevated forces, 1-100 μN. A stainless steel cantilever with a stiffer spring constant, 100-300 N/m, and a diamond tip is

---

[70]Y. Han , S. Schmitt and L. Friedrich, *Tribol. Int.*, 1998, **31**(12), 715-725.

[71]S. Magonov, Studies of polymer surfaces with atomic force microscopy. *Application Note*, *Digital Instruments,* October 1995.

[72]C. C. Schmitt and J. R. Elings, Nanoindenting, scratching, and wear testing using scanning probe microscopy. *Application Note, Digital Instruments*, April 1997.

used. Resonance frequencies are in the range of 35-60 kHz and the cantilever is used to image the surface before and after indentation. The level of indentation is controlled by deflection of the cantilever and the indent depths are on the order of tens to hundreds of nanometers. From the deflection-nanoindentation depth curves generated, the stiffness of the material at each indent can be determined (Figure 2-40). Since the cantilever spring constant is in series with the local surface compliance, the curves from these indentations must be corrected to remove tip deflection of the cantilever[73,74]. The tip deflection can be calibrated using a sapphire substrate as an infinitely stiff material. Taking into consideration the AFM tip geometry, elastic and plastic components as well as sample hardness can be calculated from the indents[75]. Plastic deformation results in hysteresis between the extending and retracting deflection curves. The cantilever is positioned at a 12° angle to the sample surface. Application of force in this arc fashion can result in rolling of the diamond tip in combination with cantilever bending. The degree of roll varies for each tip and can make calculation of absolute values of modulus difficult. Nanoindenters have been developed in which a direct controlled force can be applied perpendicular to the sample to generate more reproducible indents[76].

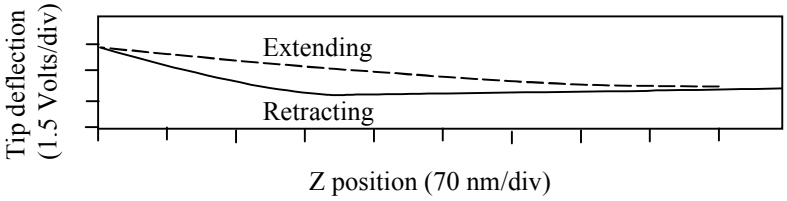

Figure 2-40. Deflection/position curve generated upon indentation of surface.

[73]P. Lemoine and J. McLaughlin, Surface Topography Applications. *Application Note Burleigh Instruments, Inc*., **16**, March 1998.

[74]M. R. Vanlandingham, S. H. McKnight, G. R. Palmese, J. R. Elings, X. Huang, T. A. Bogetti, R. F. Eduljee and J. W. Gillespie Jr., *J. Adhes.*, 1997, **64**, 31.

[75]G. M. Pharr, W. C. Oliver, and F. R. Brotzen, *J. Mater. Res.*, 1992, **7**, 1564.

[76]S. G. Corcoran, Quantitative nanoindentation: bridging the gap between the nanomechanics and AFM communities. *Application Note, Hysitron Inc*.

Displacement modulation in conjunction with AC current measurements was used to evaluate the interphase region in a carbon fiber/polyphenylenesulfide prepreg[77]. The cantilever was modulated sinusoidally. Softer areas, the matrix versus the carbon fiber, resulted in more damping and decreased amplitude of this modulation. Since the carbon fiber was electrically conductive and the polymeric matrix was not, a conductive tungsten coated silicon tip was used to locate the perimeter of the fiber. The sample was cut and polished normal to the fiber axis and adhered to a metal plate with an electrically conductive silver filled epoxy. The stiffness gradient of the interphase region was found simultaneously. In conductivity images, sharp contrast was seen between the fiber and matrix while in the amplitude images an increase in stiffness was seen over tens of nanometers around the fiber edge. In the conductivity image, a dead zone existed in the region near the fiber where current flowed from the fiber edge to the tip flank and yielded an apparent edge (Figure 2-41). A larger vertical difference between the fiber and matrix, therefore, resulted in a larger dead zone because contact between the fiber edge and the tip flank persisted further away from the fiber. For this polyphenylenesulfide system the dead zone was ~15 nm or the apparent fiber edge was 15 nm from the actual fiber edge. In the amplitude image, mechanical data near the fiber edge was also inaccurate. Within 11 nm of the fiber, the lateral extension of subsurface stresses was influenced by the high modulus fiber resulting in stress hardening. Therefore, interphase investigations based on the apparent fiber edge from the conductivity image did not include mechanical effects from the fiber. An interphase region of increased stiffness was found to exist 20-80 nm from the fiber.

[77]M. Munz, H. Sturm, E. Schulz and G. Hinrichsen, *Composites*, 1998, **29A**(9-10), 1251-1259.

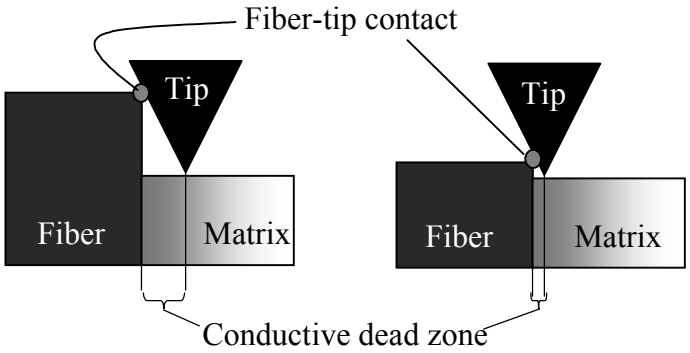

Figure 2-41. A dead zone arises in conductivity images due to fiber edge, tip flank contact; larger dead zones are found with larger steps between fiber and matrix.

Using AFM in the force mode, stiffness across the interphase region of fiber reinforced composites was characterized[73],[78]. Unsized and sized carbon fibers and sized copper fibers were embedded in a low molecular weight epoxy/amine resin and cured for 2 hr at 80°C and 2 hr at 160°C. Copper fibers were used as a model system due to the reduced fiber modulus. Less strain hardening of the indented matrix material near the copper fibers occurred compared to that of the matrix material near the high modulus carbon fibers. The sizing material was a high molecular weight epoxy coating that was 1μm thick on the carbon fibers and 10 μm thick on the copper fibers. Specimens were sectioned normal to the fiber axis and polished. Due to the larger forces (10 μN) used to indent there was more contact area between the sample and the pyramid shaped indenter than when imaging at lower forces. This increase in contact area resulted in an apparently larger region of matrix affected by the presence of the carbon fiber. Data within ~200 nm of the fiber were therefore unreliable[73]. Considering the amine cured epoxy network with unsized carbon fibers, an amine gradient was anticipated to form near the fiber and result in an interphase region. However, finite element models predicted this interphase breadth to be only 3 nm. As expected, no interphase region was seen in the unsized fiber because it would have been too small to be detected with indentation. Surprisingly, no sizing or interphase region was seen in the sized carbon fiber system. This was likely due to diffusion of both the amine curing agent and the

[78]T. A. Bogetti, T. Wang, M. R. VanLandingham and J. W. Gillespie Jr., *Composites*, 1999, **30A**(1), 85-94.

epoxy resin into the sizing. The sizing layer was thin enough that equilibrium was reached and a relatively uniform microstructure was achieved.

In the sized copper fiber system, a 7 μm region with elevated stiffness resulted from the coating and a 1.5 μm interphase region of decreasing stiffness existed between the sizing and bulk matrix[73]. In combination with a heat stage, it was possible to observe the glass transition temperature of the interphase, which was different from that of the sizing and of the matrix material. The stiffness decreases at locations across the interphase was found at different temperatures, 20°C, 65°C, 80°C, and 120°C. An increase in contact depth during indentation was indicative of the material softening as the test temperature approached the T_g of the indent area[79]. At 120°C the stiffness of the interphase region between the sizing and matrix was half of the stiffness of the bulk epoxy.

Interfacial Strength

Another means of investigating the interphase directly involved analyzing the interfacial normal strength[80]. For the single fiber transverse test, an epoxy dog-bone specimen was prepared with a single carbon fiber running through the center perpendicular to the sample draw direction (Figure 2-42a). A 15x15 $m\mu^2$ area was marked with a 7x7 grid of 0.2 μm diameter dots using the electron beam of an SEM. Deformation of the region was monitored during transverse tensile tests and the maximum displacements were smaller for poorly bonded samples. The displacement fields (Figure 2-42c) just before debond initiation were used in a finite element model, along with mechanical properties of the neat cured epoxy resin, to determine the local stresses and strains near the interface. The interfacial normal strength was taken to be the maximum radial stress just before debonding.

---

[79]M. R. VanLandingham, R. R. Dagastine, R. F. Eduljee, R. L. McCullough and J. W. Gillespie Jr., *Composites*, 1999, **30A**(1), 75-83.

[80]P. F. M. Meurs, B. A. G. Schrauwen, P. J. G. Schreurs and T. Peijs, *Composites*, 1998, **29A**(9-10), 1021-1026.

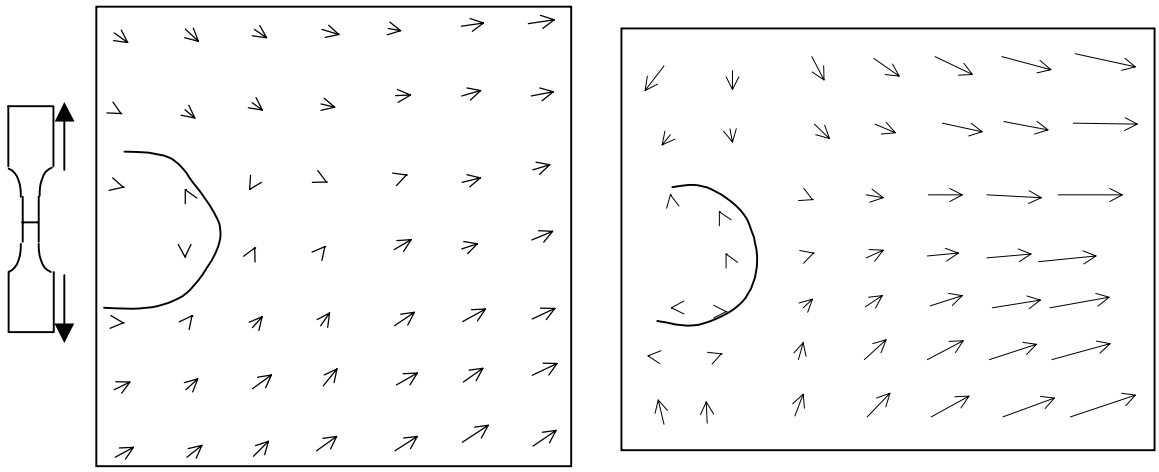

Figure 2-42. Single fiber transverse tensile test A) dog-bone specimen and displacement fields for B) a poorly bonded and C) a well bonded carbon fiber/epoxy interphase[80].

Interfacial shear strength (IFSS) can also be determined. Test methods have been established for both laminate specimens and single fiber model composites[81]. While laminate testing represents the 'real' composite, global composite failure does not necessarily correspond to local fiber/matrix failure, making it difficult to draw conclusions specifically about the interphase performance. In single fiber systems the effect of surrounding fibers on the fiber stress state cannot be taken into account, but these measurements do allow a more localized evaluation of debond failure.

Single fiber model techniques include fiber fragmentation, fiber pull out, fiber debond and fiber indentation. While each technique determines a shear strength value, the results vary both in calculated values and sensitivity to fiber/matrix adhesion because different test geometries result in different stress states at the interface.

[81]K. Jayaraman, K. L. Reifsnider and R. E. Swain, *J. Compos. Technol. Res.*, 1993, **15**(1), 14-22.

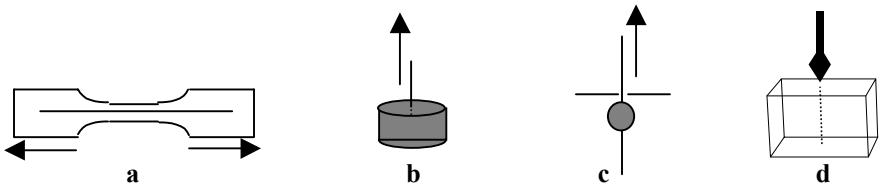

Figure 2-43. Single fiber model composites can be used to determine the interfacial shear strength using A) single fiber fragmentation test, B) fiber pull out test, C) single fiber debond test and D) fiber indentation.

For the single fiber fragmentation test, a single fiber is embedded in a matrix dog-bone (Figure 2-43a)[64,82]. The specimen is then strained in the fiber axial direction until the fiber fragments. Shorter equilibrium fragments result when the shear strength or adhesion between the fiber and matrix is stronger. Using Weibull statistics a critical fiber length (l_c) is calculated from the distribution of the fragmented fiber lengths. Interfacial shear strength (τ) is then calculated from Equation 2-1 using the fiber diameter (d_f) and the fiber tensile strength (σ_f).

$$\text{Equation 2-1} \quad \tau = d_f \sigma_f / 2 l_c$$

The fiber fragmentation is an *in situ* test that allows observation of the debond as failure occurs[85]. However, systems that can be investigated using fragmentation are limited. The strain limit of the matrix must be at least three times that of the fiber and the matrix must be tough enough that matrix failure (dogbone fracture) does not occur with fiber fracture. The stress state of the fiber is affected by the Poisson shrinkage of the matrix, which increases interfacial pressure and frictional force. The maximum shear stress is actually greater than the mean stress used to calculate the shear strength resulting in understated values[83]. This effect was seen in a glass/epoxy system in which fiber pull out yielded higher strengths.

In the fiber pull out experiment, a sample is prepared by embedding the end of a single fiber, typically a length of 50-150 μm, in the matrix material[84]. The fiber is then

---

[82] C. L. Heisey, Adhesion of Novel High Performance Polymers to Carbon Fibers: Fiber Surface Treatment, Characterization, and Microbond Single Fiber Pull-out Test. *Dissertation Virginia Tech,* 1993.

[83]M. R. Piggott, Failure processes in the fibre-polymer interphase. *Compos. Sci. Technol.*, 1991, **42**, 57-76.

[84]V. Rao, P. Herrera-Franco, A.D. Ozzello and L.T. Drzal, *J. Adhes.*, 1991, **34**, 65-77.

pulled out of the matrix network (Figure 2-43b). Assuming uniform shear stress along the length of the embedded fiber, the shear strength can be calculated using Equation 2-2

$$\text{Equation 2-2} \quad \tau = F_d / \pi d_f L$$

where L is the embedded fiber length and F_d is the force required for debond. In a similar technique, fiber debond, the fiber is debonded from a 30-150 μm diameter bead of matrix material, which has been cured onto the fiber (Figure 2-43c). Force is applied to the fiber while the bead is restrained. Shear strength is calculated from the debond force using Equation 2-2. Both of these methods can be used with a variety of fiber/matrix systems and yield a force at the moment of debond. While the fiber debond samples are easier to prepare, the stress state varies with the size and shape of bead. The bead meniscus hinders determination of the matrix-to-fiber contact length and can result in variations in the contact of the sample with the grips[85].

The high surface area of the bead may also affect test results[85]. As much as 40 % of volatile crosslinking agents can be lost during a 125°C cure. In carbon fiber/epoxy systems cured with an amine crosslinking agent, shear strengths determined from microdebond were lower, 39 MPa, than comparative fragmentation values, 70 MPa. Using an extended room temperature cure or a less volatile curing agent resulted in better IFSS agreement. With a higher molecular weight curing agent, strengths of 32 MPa and 33 MPa were obtained by debond and fragmentation, respectively. It appeared that the matrix properties were reduced in the bead because evaporation resulted in reduced curing agent concentration.

Fiber indentation can be conducted on single fiber model composites or actual composite laminates[85]. The specimen is cut and polished perpendicular to the fiber axis and a single fiber is loaded in compression (Figure 2-43d) using a fine diamond tip. The debond load is taken to be the load at which a specified drop in load occurs. Calculation of the shear strength in laminate specimens uses a finite element model to take into consideration fiber diameter, neighboring fibers and the surrounding matrix. When conducted on a laminate, this method allows a relatively easy means of obtaining *in situ* debond strengths. However the fiber/matrix bond can be altered during sample

[85]P. J. Herrera-Franco and L. T. Drzal, *Composites*, 1992, **23**(1), 2-27.

preparation and the fiber or matrix may fail before the fiber/matrix interphase fails. The shear strength values calculated using indentation are usually higher than those determined by other techniques.

Using these means of characterization, investigators are beginning to grasp the complex chemistry and morphology of the interphase and the stresses within this region.

2.2.3. Transcrystalline Interphases

When semicrystalline thermoplastics are used as matrix materials, a transcrystalline region may develop next to the fiber, due to a high nucleation density on the fiber surface. One theory attributes the high nucleation density to thermal stresses near the fiber that align matrix polymer chains. These aligned chains can then act as nucleation sites[62]. This interphase region is highly oriented (Figure 2-44) and has been found to increase the fiber/matrix adhesion in several composite systems. The transcrystalline layer is sensitive to processing conditions[86] and can also be altered through the addition of fiber sizings or matrix additives[87].

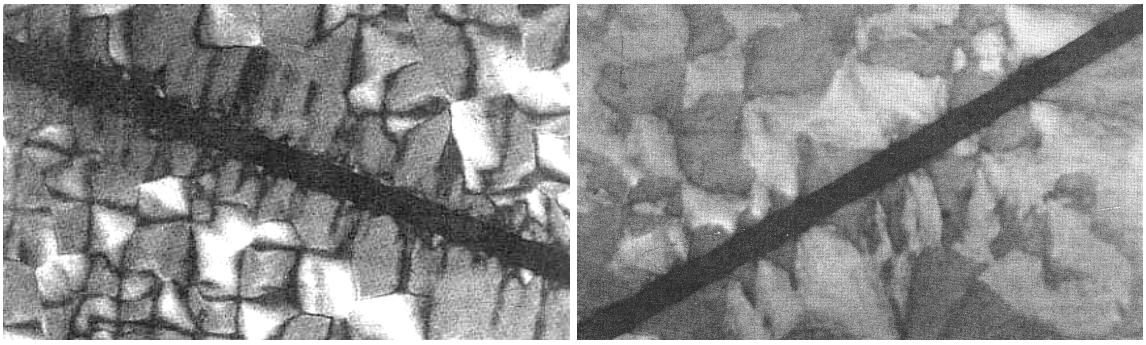

Figure 2-44. Optical microscopy images of carbon fiber/Nylon 66 composite with a transcrystalline layer and PVP sized carbon fiber/Nylon 66 composite without a transcrystalline layer[88].

Fiber reinforced PP is one such system. A variety of fibers and their nucleating abilities have been studied and found to increase in the order of polyethylene terephthalate (PET) < PAN-based carbon < Kevlar < polytetrafluoroethylene (PTFE)[62].

---

[86] T. Vu-Khanh and S. Frikah, *J. Thermoplast. Compos. Mater.*, 1999, **12**, 84-95.

[87] R. L. Clark, R. G. Kander, and B. B. Sauer, *Composites*, 1999, **30A**(1), 27-36.

[88] R. L. Clark Jr., R. G. Kander and S. Srinivas, *Polymer*, 1998, **39**(3), 507-516.

From this work, it was observed that the surface energy of the fiber was not a critical factor in the development of a transcrystalline layer. The PTFE fibers, with the lowest surface energy (lower than that of the PP matrix) would be expected to have the poorest wetting; however, they had the highest nucleating ability. This was attributed to the surface roughness of the fiber. It was theorized that the driving force for this high nucleation density at the fiber surface was due to thermal stress-induced crystallization. The thermal stress developed when the composite was cooled from the melt (200°C) to the crystallization temperature (T_c). The stress was parallel to the fiber surface and resulted in local orientation of the polymer chains. As lower crystallization temperatures were studied, the stress increased. The stress would also have been higher in the troughs of fibers with rough surfaces and lead to different fibers having different nucleating abilities. The kinetic factor considered was that if the oriented chains did not relax, they could serve as nucleation sites. At lower crystallization temperatures, the chains relaxed more slowly and there was more time for the chains to nucleate crystals. Different crystallization temperatures were investigated. With increasing T_c, the induction time to nucleation increased and the nucleation rate after the induction period decreased, resulting in a lower nucleation density at higher T_c for the transcrystalline layer on the surfaces of all fibers.

The toughness of poly(ether ether ketone) (PEEK) composites reinforced with yarn comprised of PEEK and carbon fibers was investigated[86]. It was determined that Mode I toughness was dominated by the matrix properties while Mode II toughness was more sensitive to the interphase region. Since both the matrix and interphase morphology were affected by the processing conditions, Mode I and Mode II toughness varied with molding temperature, residence time, and cooling rate. Composites were processed at different molding temperatures, T_{mold}. At higher molding temperatures, DSC studies showed that the onset of the crystallization temperature, T_o, decreased. This decrease was due to a smaller number of pre-existing crystalline entities. Above a molding temperature of ~400°C the T_o reached a plateau. All pre-existing crystalline entities were absent and the T_o was unaffected by the molding temperature. The heat of crystallization did not vary, therefore, although the number and size of the crystals changed, the level of crystallinity remained the same at each molding temperature. The Mode I and Mode II

fracture toughnesses increased with molding temperature. At T_{mold} = 400°C, different residence times, 1-90 min, resulted in maximums in both Mode I and Mode II toughness. Mode I toughness was highest at a residence time of five minutes, which produced the largest spherulites within the matrix. At this same residence time, the largest transcrystalline interphase region formed, which was necessary for good fiber/matrix adhesion and the Mode II toughness. When the cooling rate was increased from 1°C/min to 20°C/min, Mode I toughness increased because there was less crystallinity within the matrix. Mode II toughness decreased with transcrystalline width, which exponentially decayed with increasing cooling rate. In PEEK/carbon fiber composites, the transcrystalline interphase could be altered by adjusting the molding parameters. Mode I toughness was controlled by the matrix morphology while Mode II delamination was dominated by the interphase morphology which was seen when different cooling rates were investigated.

A transcrystalline region also formed when Nylon 66 was used as the matrix material. Nylon 66/E-glass or carbon fiber composites have been investigated[87]. Poly(vinyl pyrrolidone) (PVP) sizing inhibited the crystallization of Nylon 66, reducing the nucleation density[88]. Through the addition of a 10,000 g/mol PVP sizing to the fiber surface, crystallization at the interface could be inhibited, reducing the width of the transcrystalline layer. A thicker sizing layer or a higher molecular weight PVP sizing, M_n = 360,000 g/mol, inhibited the formation of a transcrystalline region entirely (Figure 2-44). When 1% PVP was blended with the Nylon 66 matrix, crystallization of the bulk thermoplastic was delayed long enough to allow the formation of a transcrystalline layer even when PVP sized fibers were used. Higher interfacial shear strength was obtained for both unsized fibers and fibers coated with PVP that had a transcrystalline interphase. Failure was cohesive within the Nylon 66 matrix.

2.2.4. Fiber Surface Treatment

Altering the fiber surface can modify the interphase and its properties. Fiber treatment may create new functional groups that can interact better with the sizing or matrix material and can also etch away weak surface layers. The most widely utilized fibers are glass and these are typically treated with silane coupling agents to protect the

surface from water absorption as well as improve fiber/matrix interactions. Carbon fibers are electrochemically oxidized to remove weak graphitic crystallites and increase surface polarity. A network structure with altered crosslink density can develop near the fiber and is dependent on surface chemistry. Surface moieties introduced during fiber treatment may activate the curing reaction and result in a higher crosslink density in the interphase or resin components may preferentially adsorb to the fiber, upsetting the cure stoichiometry and resulting in decreased crosslink density. These changes in network structure near the fiber affect the thermal performance and mechanical properties of the interphase and composite as a whole.

2.2.4.1. Coupling Agents

A coupling agent is typically a small molecule that reacts with the fiber surface and has increased interaction with the matrix material. In this manner, fiber/matrix adhesion can be improved. Coupling agents are most commonly used with glass fibers; however, natural fibers can also benefit from their use. These components are often silanes or anhydrides that can react with hydroxyl moieties on the fiber surface to form covalent bonds. Research has been done to elucidate the effect of coupling agents, to determine an optimum level of coupling agents and to ascertain how coupling agents behave in combination with polymeric sizings.

The effects of different levels of γ–amino-propyltriethoxysilane (APS) coupling agent on glass fibers have been investigated[89]. Labile carbon-oxygen-silicon bonds of the coupling agent condensed with silanol moieties on the glass fiber surface. The coupling agent reacted with the fiber surface and with other silane molecules to form a covalently bound network possessing amine functionalities on the fiber surface. These pendent amines were able to react with epoxide rings in the matrix resin. Addition of the coupling agent resulted in an interphase region covalently bound to both the fiber and the matrix. The coupling agent was added from 0, 0.1, 0.5, and 1.0 wt % solutions. The fiber compressive strength increased, possibly due a decrease in sensitivity to flaws on the fiber surface. Within epoxy composites, interfacial transmissibility, defined as the fraction of strain transferred from the epoxy matrix to the fiber, was determined from

[89]N, Oya and H. Hamada, *J. Mater. Sci.*, 1998, **33**(13), 3407-3417.

both tensile and compressive single fiber fragmentation experiments. From the tensile fragmentation test, the highest transmissibility was found for the system containing fibers coated from a 0.5 wt % solution. When compared to compressive fragmentation tests, fibers coated from a more dilute solution, 0.1 wt %, had the highest transmissibility and fiber/matrix adhesion. Maximum adhesion was achieved when there were enough molecules at the interphase to transfer the load, but not so many molecules that the interphase layer was thick enough to behave as a deformable layer. In compression the high transverse tensile stress may have resulted in a thickening of the interphase due to Poisson's effect, resulting in a deformable layer at lower concentrations of coupling agent.

APS was also studied in combination with polymeric epoxy sizings of differing molecular weights and structures[90]. Glass fibers were coated from dispersions of the epoxies both with and without coupling agent. Tensile fragmentation tests in which the fibers were embedded in epoxy matrices were used to examine the fiber/matrix adhesion. Through incorporation of flexibilizers into the epoxy networks, matrix materials of differing moduli were formed and their corresponding effects on IFSS were investigated. The flexibilizer for this epoxy resin was a higher molecular weight chain that was incorporated into the network resulting in a decreased network density and an increased chain mobility. The epoxy sizing of intermediate molecular weight was not soluble in the epoxy resin while the other two sizings were miscible. The highest IFSS value was found in the unsized control sample. All the epoxy sizings resulted in similar reduced strengths and addition of the coupling agent further reduced the IFSS. The lower values may have been due to plasticization of the matrix at the interphase by the silane coupling agent. The primary amine containing coupling agent was difunctional with respect to the epoxy resin. If the silane did not condense with the fiber surface but did react with the epoxy resin, it would behave as a chain extender, increasing the molecular weight between crosslinks and reducing the modulus at the interphase. This theory was supported by the fact that when a lower modulus matrix was used, lower IFSS was found for each composite system.

---

[90]J. Berg and F. R. Jones, *Composites*, 1998, **29A**(9-10), 1261-1272.

Glass fiber/vinyl ester composites were studied to determine the effect of a methacryl functionalized silane coupling agent[91]. Fibers were sized with polyvinyl-alcohol (PVA) to give a weak interphase and with the methacrylsilane/unsaturated polyester blend to provide a well-bonded interphase. Wetting experiments showed poor interaction between the PVA-sized fiber and resin. The silane coupling agent condensed with silanols of the fiber surface and reacted free radically with the vinyl resin. In single fiber transverse tests (Figure 2-42a), PVA sized fibers debonded from the matrix, while the silane/polyester sized fibers did not debond, but rather fractured leading to matrix cracking. The composite system containing the coupling agent had improved transverse cracking toughness, due to the fiber/matrix adhesion and increased ductility of the matrix near the fiber. It was determined that single fiber composite tests were of limited use in characterizing a tough interphase because the matrix cracked before the interphase failed.

The effect of fiber/matrix adhesion on interlaminar fracture behavior was investigated in glass fiber reinforced epoxy composites using silane coupling agents and polyethylene (PE) sizings[92]. Fibers were sized with a coupling agent, a coupling agent/epoxy blend, or PE to yield various levels of fiber/matrix adhesion. Adhesion was highest for the silane/epoxy treatment followed by the coupling agent alone, with the PE yielding the weakest interfacial adhesion. Mode I fracture toughness was examined using a double cantilever beam test and mixed mode I/II toughness was determined from a mixed mode flexure test, Figure 2-45. Both tests showed the highest toughness for composites prepared from fibers with the silane coupling agent alone. However, this was due to fiber bridging and pullout in composites with poor infacial adhesion and therefore could not be used to characterize the interphase properties. Mode II fracture toughness was studied using an end-notched flexure test and was sensitive to the interphase properties. The highest toughness was found for the composite with silane/epoxy treated fibers, followed by those with fibers treated only with the silane coupling agent, and the least toughness was found for the PE sized fiber composites.

---

[91]A. Sjogren, R. Joffe, L. Berglund and E. Mader, *Composites*, 1999, **30A**, 1009-1015.

[92]A. Korjakin, R. Rikards, F.-G. Buchholz, H. Wang, A. K. Bledzki and A. Kessler, *Polym. Compos.*, 1998, **19**(6), 793-806.

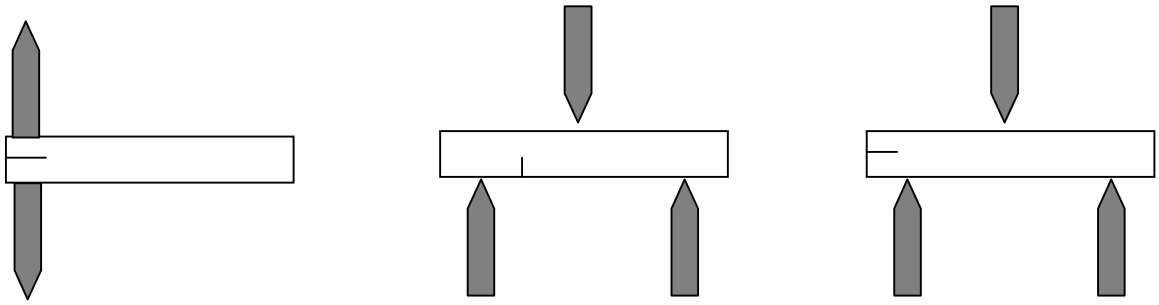

Figure 2-45 Testing mode I, mixed mode and mode II fracture toughness.

Coupling agents with different tails were placed on glass fibers and their effect on hygrothermally aged composites was investigated[65]. The matrix material was a resin containing unsaturated polyester and styrene. Coupling agents had silanol head groups with either methacryloxy or amino tail groups. It was found that when the amine coupling agent was applied both the amino tail and the silanol head adsorbed onto the glass surface. For the coupling agent containing the ester group, the molecules did not orient with respect to the glass surface. In epoxy matrices, integration of amine-silane coated fibers decreased the water content at the surface and resulted in higher IFSS than that found when unsized fibers were used. With a polyester resin, the composite flex strength varied directly with the IFSS and was highest for the system containing the methacryloxy coupling agent, as determined by micro-indentation of a fiber. Apparently chemisorption of the coupling agent was not as influential on adhesion as were fiber/matrix interactions. The polyester resin contained vinyl groups that reacted with the double bond of the coupling agent thereby improving the coupling agent/matrix adhesion. Exposure to boiling water for three days dramatically decreased the composite flexural strength for all compositions.

Coupling agents can also be used on natural fibers[93]. Maleic anhydride grafted PP was coupled to jute fibers, which were embedded in a PP matrix. Hydroxyl groups on the natural fibers were able to react with pendant anhydride moieties on the PP, forming a tethered PP layer around the fibers. Increases in fiber-matrix adhesion, composite strength and modulus resulted from the addition of the coupling agent due to the compatibility of the covalently bound PP at the interphase with the PP matrix. In creep

[93]J. Gassan and A. K. Bledzki, *J. Thermoplast. Compos. Mater*, 1999, **12**, 388-398.

tests, composites with untreated fibers showed 5% strain on the outer fibers. With the sizing, the stress transfer was improved and strain was reduced to 3.5 %.

Addition of silane or anhydride coupling agents can greatly affect interfacial and composite properties. A balance must be achieved between the improved adhesion to the fiber and the plasticizing effect of matrix soluble coupling agents. A decrease in the modulus of the interphase due to either a thick layer of silane coupling agent or plasticization of the matrix has generally been shown to decrease the IFSS and composite properties. Therefore the matrix material must be considered when determining the type and amount of coupling agent to be used to optimize composite performance. Addition of a coupling agent can also result in less water uptake along the fiber and consequently improve weatherability of the fiber/matrix bond.

2.2.4.2. Oxidation of Carbon Fibers

A great deal of work has been done investigating oxidative surface treatments of carbon fibers. Graphitization of polyacrylonitrile fibers results in the formation of graphitic basal planes parallel to the fiber axis[102]. These nonpolar surfaces do not interact strongly with polymeric materials and poor bonds form between the fiber and the matrix. Through the addition of functional groups on the surface of the fiber, covalent and secondary bonding can occur, improving interfacial adhesion. Commercial carbon fiber surface treatments, typically electrochemical, oxidize the fiber surface using aqueous ammonium bicarbonate. This treatment increases the atomic concentration of oxygen on the fiber surface from 1.8 to 9.9[94] and etches away loosely bound crystallites, leaving a more robust fiber surface[11]. The effects of different degrees of treatment as well as alternate surface preparations have been investigated using a variety of techniques.

The effect of both the surface treatment and resin material on network formation was observed when an anhydride cured epoxy system and an amine cured epoxy system were studied[63]. Composites were prepared in both matrix materials from carbon fibers with three different surface oxygen concentrations. In the anhydride system, the composite T_g decreased with increased levels of oxygen while in the amine cured epoxy resin, no difference in T_g was detected. With this in mind, the anhydride curing agent

---

[94]H. Ho, J. J. Lesko, J. Morton, K. L. Reifsnider, S. Wilkinson and T.C. Ward, *J. Adhes.*, 1993, **42**, 39-53.

may have interacted with the functional groups on the fiber surface, offsetting the cure chemistry near the fiber. The disrupted stoichiometry may have resulted in a decreased crosslink density and lower Tg.

Fibers with varied oxidative surface treatments were investigated in an amine cured epoxy matrix[80]. The electrochemical oxidation treatment of the fiber surface was done to different degrees, in which a typical commercially treated fiber was defined as being 100 % treated. Fibers were also investigated with 0, 10, and 50 % of this oxidation. The atomic oxygen surface concentration was expected to increase with elevated degrees of treatment. Interfacial normal strength was measured on a local scale with scanning electron microscopy by placing a 15 x 15 μm^2 grid at the interphase and observing the strain during transverse tensile tests (Figure 2-42). The interfacial normal strengths were determined to be 167, 185, 199, and 240 MPa for the different levels of surface modification. Stress transfer increased with surface treatment due to improved adhesion between the fiber and the matrix. So while little plastic deformation was observed around the untreated fibers, treated fibers showed a maximum strain in the interphase of 22%. On the macro scale, composites with untreated fibers debonded at 1% strain and those with treated fibers debonded at 3.3 % strain.

Commercially oxidized fibers were further electrochemically oxidized using aqueous potassium nitrate[64]. O/C atomic ratios on the surface were increased from 0.21 for the original fibers to 0.21-0.40 depending on the extent of treatment. The number of acidic functions, measured by surface titration with sodium hydroxide, and surface area, determined from nitrogen absorption, increased. The filament tensile strength decreased with oxidation because the process continually etched away the fiber. Adhesion was determined using single fiber fragmentation in an epoxy matrix. Increased interfacial shear strength was found with increasing O/C atomic ratio up to the point where the decreased tensile strength of the fiber dominated the interfacial strength (Equation 2-1). The increased oxygen concentration on the surface improved atomic interactions between the fiber and the matrix resulting in improved adhesion.

Plasma treatment of carbon fibers has also been investigated using composites prepared with an amine cured epoxy matrix[63,95]. The fibers were exposed to an air plasma for 30 seconds. The low power plasma treatment generated a higher concentration of functional groups on the fiber surface than did electrochemical oxidation, but it did not remove loosely bound crystallites. Both treatments improved fiber/matrix adhesion as observed in short beam shear tests. Matrix failure was observed in the electrochemically treated fibers, while interfacial failure occurred in untreated and plasma treated fiber composites. The increase in adhesion resulted in a 100 % increase in transverse tensile strength with both treatments. The composite Mode I toughness increased from 160 J/m^2 with untreated fibers to 276 J/m^2 with electrochemically treated fibers due to improved the interphase performance. A further improvement in Mode I toughness was observed with incorporation of the plasma treated fibers to 436 J/m^2 due to deviation of the fracture path into the matrix. Mode II toughness was highest for electrochemically treated fibers. When end-notched flex tests were used to determine the Mode II toughness, the crack propagated along the fiber/matrix interface with both untreated and plasma treated fibers, while matrix failure occurred in the electrochemically treated fiber composites.

2.2.4.3. Ultra-high-modulus polyethylene fibers

Ultra-high-modulus polyethylene (UHMPE) fibers, while showing high modulus and strength, have low adhesion to matrix materials due to low atomic interactions with the nonpolar PE surface. Fiber surfaces have been altered in an attempt to improve the fiber/matrix adhesion[96]. Both untreated and oxygen plasma treated UHMPE fibers were investigated in a vinyl ester matrix. Micro-pits were observed on the fiber surface following the plasma treatment. The plasma treated fibers yielded composites with higher transverse tensile strengths and higher failure strains. The failure initiation site also changed, shifting from the fiber/matrix interface to within the fiber itself. These improvements were attributed to increased mechanical interlocking with the micro-pits on the fiber surface resulting in better adhesion between the vinyl ester and the fiber

---

[95]K. E. Atkinson and C. Kiely, *Compos. Sci. Technol.*, 1998, **58**(12), 1917-1922.

[96]S. I. Moon and J. Jang, *Compos. Sci. Technol.*, 1999, **59**(4), 487-493.

surface. The plasma treatment may also have increased the oxygen concentration on the fiber surfaces thereby improving fiber/matrix interactions and interfacial adhesion.

UHMPE fibers were also treated in an UHMPE/paraffin oil solution at elevated temperatures under tensile strain[65]. The fibers were swollen by the paraffin and the polymer in the solution became entangled with the UHMPE chains in the fiber surface. Conditions were optimized so that the fibers did not suffer reductions in mechanical properties due to their dissolution. From these fibers, composites with UHMPE matrices were then prepared. The interphase regions contained polymer molecules that were entangled with chains on the surface of the fiber as well as crystallized with the UHMPE matrix material. The resulting novel composite had higher shear and tensile strengths than did the usual UHMPE/PE matrix composites.

2.2.4.4. Natural cellulose fibers

Henequen fibers are among the natural fibers being investigated as composite reinforcement[97,98]. A henequen fiber is a flexible cellulose fiber with high surface roughness and a diameter that varies along the fiber length, typical of the natural fibers. These hydrophilic fibers have poor adhesion to hydrophobic matrix materials. To improve the interaction between fibers and matrices, fibers have been treated with alkaline solutions, impregnated with polymer prior to introduction of the matrix, and modified by grafting polymer chains onto the surface.

Henequen fibers have been investigated as reinforcements in high density polyethylene (HDPE) composites[97]. Fibers were treated with a 2 wt/vol % NaOH solution, 1 wt/vol % vinyl,tris-(2-methoxyethoxy)silane/ 0.5 wt/vol % dicumyl peroxide solution, or impregnated with HDPE. The alkaline solution removed hemicelluloses, waxes, and lignin, leaving a rougher more robust surface with increased surface area to interact with the matrix. The silane coupling agent reacted with alkoxy moieties on the fiber surface while the pendant vinyl functionalities reacted free radically to yield a crosslinked interphase region on the fiber surface. By soaking henequen fibers in a 1.5 wt/vol % HDPE/xylene solution for five minutes, 5 wt % of the polyolefin was deposited on the fiber surface. By introducing the HDPE as a pretreatment, better wetting was achieved.

Fiber/matrix adhesion of the henequen/HDPE composites was investigated using both fiber pull out and fiber fragmentation tests (Figure 2-43)[97]. In the pull out test, a load was applied to the fiber causing Poisson contraction of the fiber but not the matrix. The frictional component of the interfacial strength was reduced by this technique. In the fragmentation test, a tensile force was applied to the matrix, causing Poisson contraction of the matrix and resulting in a radial compressive stress on the fiber. The frictional component of the interfacial strength was increased by this test method. By both methods, adhesion was lowest between the unmodified fibers and the HDPE matrix due to poor fiber/matrix interactions. A slight increase was observed with the alkaline treatment of the fibers. For the pullout test, the impregnated fibers had the highest IFSS, 8 MPa versus 4.5 MPa for the silane treated fibers. However, in the fiber fragmentation experiments silane treated fibers had the highest IFSS (16 MPa) while the impregnated fibers yielded a lower shear strength of 8 MPa. Both the silane coupling agent and the HDPE interphases were more compatible with the matrix material and resulted in increased IFSS. The difference between the fragmentation and the pull out results was attributed to the manner in which the load was applied. For the pull out test in which the fiber undergoes Poisson contraction, the impregnated fibers contracted less due to the incorporation of the HDPE within the fiber. With less fiber contraction, the frictional component was greater in the impregnated fiber composite than the silane treated fibers, so the impregnated fiber composite had a higher IFSS in the pull out test. The results obtained by the fragmentation technique better reflected the composite tensile strength, which was highest for composites containing the silane treated fibers.

Cellulose fibers have also been modified by free radically grafting poly(methyl methacrylate) (PMMA) or poly(butyl acrylate) (PBA) onto the cellulose fibers[98]. Cellulose fibers were reacted with acrylate in an acidic medium using ammonium cerium (IV) nitrate as an initiator. Composites were prepared from these modified fibers and from unmodified cellulose fibers using a plasticized polyvinylchloride (PVC) matrix

---

[97]A. Valadez-Gonzalez, J. M. Cervantes-Uc, R. Olayo and P. J. Herrera-Franco, *Composites*, 1999, **30B**(3), 309-320.

[98]G. Canche-Escamilla, J. I. Cauich-Cupul, E. Mendizabal, J. E. Puig, H. Vazquez-Torres and P. J. Herrera-Franco, *Composites*, 1999, **30A**(3), 349-359.

containing 30 wt % dioctyl phthalate. The miscibility of the grafted side chains with the matrix material resulted in different degrees of fiber/matrix adhesion. PMMA was miscible in the PVC matrix while PBA was not. From SEM images of composite failure surfaces, untreated fibers and PBA grafted fibers pulled out of the matrix smoothly indicating poor fiber/matrix adhesion, while PMMA grafted fibers had matrix particles on the surface because of good interfacial adhesion. At fiber contents up to 15 wt %, all three systems had similar tensile strengths and showed a decrease in strength with increasing fiber content. As more fiber was incorporated, the tensile strength of unmodified cellulose and PBA containing composites was not altered. However, in the PMMA grafted system an increase in strength was observed due to the improved fiber matrix adhesion.

2.2.5. Sizings

Another method for altering the interphase is through the addition of a fiber coating or sizing. Epoxy sizings are often added commercially to improve processability and ease of fiber handling, but sizings may also be introduced to improve composite properties. Fiber wetting and fiber/matrix adhesion can be increased or specific interphase morphologies developed. Different mechanical properties may be imparted to the interphase region through the selection of sizings with specific mechanical properties and interactions with the matrix material. In order to apply the sizing, the fiber tow is pulled through a solution or dispersion of the material. Therefore these materials are typically soluble or dispersible in water.

A brittle thermoplastic, polyvinylpyrrolidone (PVP), has been investigated as a carbon fiber sizing material in a toughened epoxy matrix. The composite included high modulus Apollo carbon fibers and polyethersulfone toughened bisphenol-A based epoxy resin. Interphases were varied in both degree of oxidative fiber surface treatment and sizing. Commercially, fibers were treated with a level of electrochemical oxidation that was defined as 100 % treatment. Fibers with twice this level of oxidative treatment were also used and referred to as 200 % surface treated. Oxygen was found on the fiber surface at a concentration of 14 atomic %, regardless of the oxidative treatment. The elevated level of oxidation resulted in a slight decrease in the tensile strength, from 765

ksi for 100 % treated fiber to 730 ksi for the 200 % treated fiber. The 100 % treated fibers were sized with either a bisphenol-A based epoxy oligomer with no crosslinking agent or with PVP. The 200 % treated fibers were sized with the epoxy[99]. Permanganic etching was used to study the interphase morphology. During this process, material that was not crosslinked was removed. Using SEM, it was observed that an irregular interphase region developed in composites containing the less oxidized (100 %) fibers sized with the epoxy. This structure was due to the fact that the epoxy sizing did not contain any curing agent and therefore did not crosslink. With fibers having the higher level of oxidative treatment (200 %) and an epoxy sizing, no material was etched away. The increase in surface treatment may have increased the reactivity at the fiber surface so that the sizing layer crosslinked, possibly through an epoxy etherification reaction that would not require a crosslinking agent. With the 100 % oxidatively treated fibers and PVP sizing, a different interphase region developed. The PVP sizing was etched away and the cure of the epoxy matrix near the sizing was altered, resulting in a different morphology than in the bulk. The PVP appeared to have little miscibility with the epoxy resin. The sizing remained at the interphase but may have diffused a limited amount into the resin during cure, affecting the epoxy network morphology near the sizing layer.

Fiber/matrix adhesion for these carbon fiber/epoxy systems has been studied using two techniques[67]. From mesoindentation tests, in which a load is applied to the composite surface normal to the fiber axis, the sizing did not alter the fiber/matrix adhesion, but increased oxidative surface treatment increased IFSS. In fragmentation tests, the level of surface treatment did not increase the IFSS, but did result in a change of failure mode from both interfacial and matrix failure with 100 % treated fibers to matrix failure with fibers having a higher level of oxidative surface treatment, suggesting better adhesion between the 200 % treated fibers and the epoxy matrix. Sizing fibers with PVP resulted in interfacial failure and a 20% lower interfacial adhesion. Differences in stress states and failure modes generated by the two test methods may have accounted for the slight discrepancies in adhesive trends. Increased fiber/matrix adhesion was observed by

---

[99]J. J. Lesko, R. E. Swain, J. M. Cartwright, J. W. Chin, K. L. Reifsnider, D. A. Dillard and J. P. Wightman, *J. Adhes.*, 1993, **45**, 43-57.

both methods for the composite containing fibers with increased oxidative treatment. As seen in the SEM images, the interphase region possessed good network integrity and possibly better mechanical properties compared to the uncrosslinked regions observed in the 100 % treated fiber interphases. The improved shear strength in the mesoindentation test may have been due to improvements in the interphase properties that were able to transfer stress onto the fiber. The PVP sized fibers showed the lowest interfacial shear strength. Due to the brittle nature of the sizing, the interphase may not have been able to withstand the shear forces as well as the other two interphase regions.

Longitudinal tensile tests were also used to evaluate these carbon fiber/epoxy composite systems[67]. In unidirectional composites, increased surface treatment did not greatly affect longitudinal properties. Epoxy sized fibers had good fiber/matrix adhesion with both levels of oxidation, which led to stress concentrations at broken fibers, yielding brittle failure. Incorporation of the PVP sizing decreased the composite modulus. This may have been due to poor load transfer from the matrix to the fibers. If the load carrying capacity of the fibers was not reached, the lower composite stiffness would be expected. Tensile strength however increased 10 % and strain to failure increased almost to that of the fiber (1.7%), with increased longitudinal splitting of the failed specimen. This was indicative of composite failure dominated by global strain rather than stress concentration. From a model developed by Gao and Reifsnider, it was predicted that both stress concentration near broken fibers and the ineffective length determined the tensile strength[100]. Therefore, at an optimal, but not necessarily maximum amount of interfacial performance, a maximum tensile strength could be achieved. Below this level ineffective length would dominate failure and above this level stress concentration near broken fibers would be elevated and result in composite failure.

Transverse tensile tests were used to determine the transverse strength and modulus of the above carbon fiber/epoxy composites[67]. Transverse tensile strength increased 24% with higher levels of surface treatment and decreased 8% with the addition of PVP sizing. These differences are attributed to the normal strengths of the interphases and are similar to trends in shear strength determined by mesoindentation

---

[100]A. Gao and K. L. Reifsnider, *J. Compos. Technol. Res.*, 1992, **14**(4), 201-210.

tests. Increased oxidative surface treatment improved the interphase network integrity and strength while incorporation of the brittle PVP sizing yielded a weaker interphase. The transverse modulus was not affected by the interphase strength.

In a separate study carbon fiber/epoxy composites containing fibers with and without oxidative surface treatment were compared[101]. The matrix was a bisphenol-A based epoxy cured with a stoichiometric concentration of amine. Electrochemically oxidized fibers were equivalent to the '100 % treated' fibers in the previous study. Treated fibers were also sized with a bisphenol-A based epoxy without curing agent. Using single fiber fragmentation tests to determine the IFSS of the three systems, different amounts of fiber/matrix bonding and different modes of failure were observed. Untreated fibers failed interfacially at 5.4 ksi, while oxidized fibers failed interfacially and in the matrix at 9.9 ksi. This increase was due to the fact that surface defects and graphitic crystallites were etched away during the surface treatment. Surface treated fibers were also sized with an epoxy oligomer (100-200nm thick), which resulted in the highest adhesion (11.8 ksi) between the fiber and matrix and showed matrix dominated failure. Improved adhesion was attributed to improved stress transfer between the fiber and matrix through the interphase. The sizing layer did not contain amine crosslinking agent. Upon introduction of the matrix resin, amine began to diffuse into the sizing layer as the crosslinking reaction occurred. A gradient in amine concentration developed, becoming more dilute near the fiber. Mechanical properties of epoxy networks with reduced concentrations of curing agent were investigated. Increased modulus and decreased fracture toughness resulted, possibly due to amine catalyzed epoxy homopolymerization that increased the crosslink density. A stiffer, brittle interphase region would have developed next to the fiber, which resulted in improved stress transfer, but also increased the build up of stress concentration at fiber breaks. The concentrated stress induced by the brittle interphase caused the network to crack perpendicular to the fiber and led to matrix failure.

---

[101]L. T. Drzal, M. J. Rich, M. F. Koenig and P.F Floyd, *J. Adhes.*, 1983, **16**, 133-152.

Composite properties in the carbon fiber/epoxy systems described above were also investigated[102]. Inplane shear modulus was found to be insensitive to IFSS. In the linear region of the stress-strain curve debonding did not occur in any of the composites so the fiber/matrix adhesion was not tested. (The in-plane shear modulus was found to be insensitive to fiber surface treatment in a toughened bismaleimide matrix also[94].) However interlaminar shear strength increased with IFSS, while in-plane shear strength increased with surface treatment but not with the addition of the epoxy sizing. No further improvement in in-plane shear strength was observed because, with higher fiber/matrix adhesion, stress concentrations occurred that resulted in brittle interphase failure rather than improved in-plane shear strength. Transverse tensile strength increased ~19% from surface treated fibers to epoxy sized fibers due to the improved fiber/matrix adhesion. Mode I toughness showed the same increase due to similar peel stresses felt in both the transverse tensile and mode I test specimens. Mode II toughness was more responsive to interphase performance and increased 160% for the 83% increase in IFSS from untreated to treated fibers[103]. These findings are similar to the findings for PEEK composites in which the Mode II toughness was more sensitive to the transcrystalline interphase region than was the Mode I toughness[86].

The effect of bisphenol-A based epoxy sizing on discontinuous carbon fiber/epoxy composites has also been researched[104]. The matrix system was an amine cured bisphenol-A based epoxy resin. By conducting fragmentation tests at different strain rates and temperatures, master curves were generated showing interfacial shear yield strength increasing linearly with the log of strain rate. These master curves were compared to curves generated for the epoxy matrix material's shear yield strength and shear strength. Sized fibers produced well bonded systems with interfacial strengths between the shear yield and shear strength of the matrix. The shear strengths for poorly bonded systems in which the epoxy sizing was removed prior to resin impregnation, were lower than the shear yield strength of the resin. This indicated that in the unsized system,

---

[102]M. S. Madhukar and L. T. Drzal, *J. Compos. Mater.*, 1991, **25**(8), 932-957.

[103]M. S. Madhukar and L. T. Drzal, *J. Compos. Mater.*, 1992, **26**, 936-968.

[104]M. Miwa, A. Takeno, K. Yamaguchi, and A. Watanabe, *J. Mater. Sci.*, 1995, **30**(8), 2097-2100.

fiber matrix interaction was through secondary bonding which failed before the matrix yielded.

Semicrystalline nylon 66 has also been studied as a sizing material[105]. Carbon fibers were coated with nylon 66 by two different methods and the interfacial adhesion with a bisphenol-A based epoxy matrix was studied at different temperatures. The epoxy resin was cured with bis(*p*-amino cyclohexyl) methane. The fibers were coated from a formic acid/Nylon 66 solution (M_n=7150 g/mol) or the fibers were dipped in hexamethylenediamine followed by adipoyl chloride so that the nylon was polymerized on the fiber (M_n=2840 g/mol). Interfacial adhesion, determined from fiber fragmentation, decreased with the addition of sizing and continued to decrease with increasing sizing thickness. In unsized fibers, an increase in critical length (decrease in adhesion) was observed between 50°C and 70°C due to passage through the T_g of the epoxy material. Differences in cure chemistry near the fiber may have led to a reduced crosslink density, resulting in a lower T_g material in the interphase. In sized fibers, the glass transition temperature of the polyamide interphase region at 40°C resulted in an initial decrease in IFSS with increasing temperature followed by a second drop as the T_g of the epoxy interphase was reached.

Addition of a rubbery interphase in carbon fiber/epoxy composites resulted in improved impact performance[106]. A 380 g/mol bisphenol-A epoxy was chain extended with 2500 g/mol carboxy terminated butadiene acrylonitrile and 1-8 *p*-menthane diamine, an aliphatic diamine, to yield an epoxy terminated polymer. The functionalized elastomer was able to react with the resin and the glass transition of the resulting interphase was -40°C. The weight of sizing added was determined using thermogravimetric analysis and the sizing thickness was estimated on the basis of the fiber surface area. The level of sizing on the fibers was varied from ~24 nm to ~58 nm. From SEM images of failed surfaces, unsized fibers detached from the matrix while sized fibers had matrix particles remaining on the surface due to improved fiber/matrix

---

[105]P. C. Varelidis, R. L. McCullough and C. D. Papaspyrides, *Compos. Sci. Technol.*, 1998, **58**(9), 1487-1496.

[106]J. F. Gerard, *Polym. Eng. Sci.*, 1988, **28**, 568-577.

adhesion. Incorporation of polar nitrile groups may have improved fiber/sizing interactions. In Charpy impact tests of epoxy composites reinforced with either unsized or sized fibers, the failure initiation energy was found to be at a maximum for fibers with a 24 nm thick elastomeric layer. The flexible interphase was able to absorb impact energy, however increased interphase thickness led to decreased stress transfer from the resin to the fiber and less efficient energy absorption.

Similar impact performance results were found in glass fiber reinforced composites[107]. To improve the impact strength of glass fiber/epoxy composites an elastomeric polyurethane sizing was prepared. A polydimethylsiloxane diol, isophorone diisocyanate, and γ–aminopropyltriethoxysilane (APS) were polymerized to form a urethane prepolymer that was placed on the fiber from a methylethylketone (MEK) solution. Following the sizing of the fiber, the ethoxysilane groups condensed to form an elastomeric network during the fiber drying process at 120°C for 10 sec. Addition of this elastomeric interphase did not affect the longitudinal composite modulus, a fiber dominated property, but the shear modulus was slightly lower (1.4 vs. 1.5 GPa) due the sensitivity of the shear modulus to the interphase properties. The resilience was defined as the absorbed energy per unit area. As measured by the Charpy impact test, the resilience increased with the addition of the elastomeric interphase while the maximum stress was maintained and the deflection was decreased. The improvement in resilience may have been due to increased chain mobility of the elastomeric interphase, which was able to absorb energy as well as alter the stress field around the fiber and inhibit crack propagation.

The effect of the sizing surface free energy on interphase formation and fiber/matrix adhesion was investigated in glass/vinyl ester composites[108]. Glass fibers were exposed to five different sizing solutions containing blends of silane coupling agents and the polymers listed; matrix soluble epoxy, matrix soluble polyester, partially miscible PVA, and insoluble PU. Fibers were also treated with only water. The sized fibers are listed in order of decreasing surface free energy: hydrolyzed water treated

---

[107]M. N. Tillie, T. M. Lam and J. F. Gerard, *Compos. Sci. Technol.*, 1998, **58**(5), 659-663.

[108]B. K. Larson and L. T. Drzal, *Composites*, 1994, **25**, 711.

glass surface > matrix soluble epoxy > matrix soluble polyester ≈ partially miscible PVA ≈ insoluble PU > soluble polyester coated with a mold release agent. Surface energy and resin compatibility decreased with surface polarity from the highly polar silanol surface of the unsized glass fiber to the nonpolar surface of the mold release agent coated fiber. Interfacial adhesion, measured using micro-indentation of a single fiber, increased with increased surface free energy in the case of the intermediate samples due to improved wetting and sizing/matrix interactions. The water treated fiber had the lowest shear strength because a coupling agent did not protect the fibers and the interphase exposed during sample preparation degraded with water uptake. The least energetic surface had a higher shear strength than anticipated. The release agent did not prevent the underlying compatible polyester to interact with the vinyl ester resin. In composite short beam shear experiments, the fibers with the water, epoxy and polyester sizings resulted in composites with shear strengths around 55 MPa while the three low energy surfaces showed a significant drop in shear strength to ~30 MPa. The same trend was seen in longitudinal flexural strength. Decreased fiber wetting resulted in poor composite integrity as reflected in decreased short beam shear and longitudinal flex strengths. It appeared necessary to first have good fiber wetting which could lead to favorable interphase formation when sizings were matrix compatible.

Aramid reinforced epoxy composites were studied with different epoxy sizings in an effort to improve fiber-matrix adhesion[109]. A series of epoxies were prepared with different backbones: a rigid aromatic bisphenol-A based diepoxide, 1,2,7,8-diepoxy octane, a diglydicyl ether of 1,3-propanol, and a polar diglycidyl ether of glycerol (Figure 2-46). The sizing was applied to the fiber from a water/ethanol solution containing the diepoxide and piperazine. The sizings could be crosslinked prior to introduction of the matrix resin by heating to 240°C for 3 sec. Initial chain extension occurred via amine/epoxide reactions and then etherification of the epoxy rings crosslinked the sizing. Bundle pull-out measurements on fibers with uncured sizing showed that treating the fiber with polar propanol and glycerol based epoxies yielded bond strengths of 40 N/mm versus 35 N/mm for the other sizings and unsized fibers. The increases in fiber/matrix

[109]J. Mahy, L. W. Jeneskens and O. Grabandt, *Composites*, 1994, 25(7), 653-660.

adhesion were attributed to the polar ether and hydroxyl functionalities on the propanol and glycerol diepoxides in combination with their chain flexibility. Both imide groups on the fiber and hydroxyl groups in the matrix could interact with the polar groups of the flexible sizings. The digylcidyl ether of bisphenol-A was more rigid, limiting polar interactions due to steric hindrance and the octane diepoxide, while flexible, was less polar and had reduced interaction with both fiber and matrix. When the sizings were cured at 240°C for three seconds, the propylether sized fibers showed even higher strengths, 47 N/mm. Crosslinking the sizing layer may have resulted in an interphase with increased stiffness that allowed improved stress transfer from the matrix to the fiber, increasing pull-out performance.

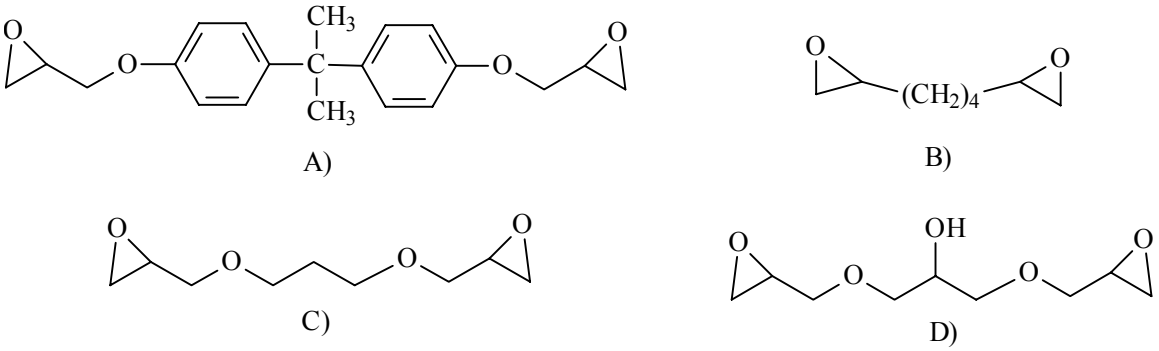

Figure 2-46. Epoxy sizings with varied polarity; A) diglycidyl ether of bisphenol-A, B)1,2,7,8-diepoxy octane, C) diglydicyl ether of 1,3-propanol, and D) diglycidyl ether of glycerol.

Addition of sizing materials altered the interphase region. Interphase and composite performance was dependent on sizing properties as well as sizing/matrix interactions. While some degree of sizing/resin compatibility was necessary to obtain good interfacial adhesion, a limited degree of miscibility resulted in optimum performance. Typically the longitudinal properties of unidirectional composites, which were dominated by the fiber properties were not affected by the interphase. Transverse properties however could be altered. Increased fiber/matrix adhesion occurred when thermosetting or ductile polymeric sizings with limited miscibility with the matrix resin, such as epoxy oligomers, were used and this resulted in increases in the transverse modulus and strength. Addition of a brittle PVP sizing did not improve the IFSS or composite properties. An elastomeric sizing, while decreasing the transverse modulus, did improve the impact performance of the composite. In conclusion, various sizing

materials could be used to tailor the properties of the resulting composites by considering the fiber/resin system and the desired application.

2.2.6. Summary

Research in this field has not only been focused on the properties of the interphase and composites but it has also had to address the validity of the test methods themselves. In these very complex systems, techniques that are generally considered to elucidate the same property, such as interfacial shear strength, may result in contradictory findings. These differences in results are due to differences in stress states and failure modes from one test configuration to another. Therefore it is critical to understand the limitations of the tests to interpret the data correctly.

The small region between the fiber and bulk matrix known as the interphase has a profound effect on composite performance. The incorporation of a transcrystalline region within a composite with a semicrystalline matrix increases adhesion. Fiber surface treatments can alter interactions with the matrix material or modify the interphase structure by changing the cure chemistry of the resin in the immediate vicinity. Sizings may be added to fibers prior to the addition of the matrix resin to develop an interphase with specific properties. The transverse properties are extremely sensitive the fiber/matrix adhesion in unidirectional composites. In crossply laminates, all properties, particularly Mode II fracture toughness, may respond to differences in the interphase.

The chemistry and morphology of the interphase affects composite performance. Sizings and coupling agents must be tailored for specific fiber/matrix systems. Coupling agents bond covalently with the fiber surface and improved coupling agent/resin interaction results in improved interphase performance. In the case of polymeric sizings that are not covalently bound to the fiber surface, it is desirable to have a limited degree of sizing/resin compatibility to ensure good interaction between the sizing and matrix while still maintaining an interphase region near the fiber. Depending on the material properties of the sizing as well as its interactions with the fiber and matrix, a variety of properties can be improved including modulus, strength, fatigue durability, and impact resistance.

Chapter 3. Epoxy Networks

3.1. Introduction

Epoxy resins are of interest as adhesives and composite matrices due to their good shelf life, ease of processability, and excellent network mechanical properties[1,2]. Resulting networks also show good solvent and corrosion resistance and are extremely versatile. Properties of the resin and cured network can be tailored for specific applications by varying both the epoxy chemistry and the crosslinking agent used to cure the epoxy.

The incorporation of phosphonate moieties into the epoxy backbone can improve network flame retardance[110,111]. While phosphorus-nitrogen and phosphorus-oxygen-carbon bonds are hydrolytically unstable, phosphorus-carbon bonds are more stable than the analogous nitrogen-carbon bond[112] and have been shown to impart improved thermal stability and fire resistance over poly(arylene ether sulfones)[113]. The addition of a strongly hydrogen bonding phosphine oxide moiety is anticipated to also increase the adhesive interactions between the resulting thermosets and various substrates.

Crosslinking agents can further tailor processability and network properties. Flexible aliphatic crosslinking moieties, such as aliphatic amine terminated polypropylene oxides are commonly used for tough epoxy adhesives that do not require high glass transition temperatures. Polysiloxane crosslinking reagents are of particular interest for curing epoxide resins due to their low viscosities in combination with their wide service temperature range. Incorporation of a siloxane group can increase network

---

[110] Y.-L. Liu, G.-H. Hsuie, Y.-S. C, R-J. Jeng and L.-H. Perng, *J. Appl. Polym. Sci.*, 1996, **61**, 613-621.

[111] C.-S. Wang and J.-Y. Shieh, , *Eur. Polym. J.*, 2000, **36**, 443-452.

[112] S. Maiti, S. Banerjee, and S. K. Palit, *Prog. Polym. Sci.*, 1993, **18**, 227-261.

[113] D.J. Riley, A. Gungor, S. A. Srinivasan, M. Sankarapandian, C. Tchatchoua, M. W. Muggli, T.C. Ward, J.E. McGrath, and T. Kashiwagi, *Polym. Eng. Sci.*, 1997, **37**(9), 1501-1511.

flame retardance and biocompatibility[114,115]. 1,3-bis(3-aminopropyl)tetramethyl disiloxane has been shown to be miscible with the diglycidal ether of bisphenol-A and to cure rapidly at 100°C[116]. By contrast, rigid aromatic amines are typically reacted with epoxide resins to produce correspondingly rigid, high glass transition temperature networks for structural composites[118]. Multifunctional phenolic novolac oligomers result in networks with high crosslink density. Therefore, novolac resins are widely used as epoxy crosslinking agents to yield high modulus void-free networks. The novolac oligomers also impart flame retardance to the thermoset[117]. Due to the multifunctional nature of these oligomers, the cure stoichiometry can be varied to optimize mechanical performance[118].

One potential application for these epoxy resins is their use as structural adhesives. Due to improvements in continuous glass and carbon fiber reinforced composite properties, these systems are now being considered for structural applications where steel and concrete have been used traditionally. As new materials are being used for structural purposes, new bonding agents are becoming necessary. Adhesives for bonding composite repair materials to existing steel structures should have good mechanical properties and be able to hydrogen bond with the heteroatoms and hydroxyl groups on the steel surface while having a limited affinity for water.

The hypothesis is that tough, ductile, moisture resistant structural adhesives can be developed from a new family of reactive and strongly hydrogen bonding epoxy resins. A low molecular weight epoxy resin containing a phosphine oxide moiety has been

---

[114] C. Tran, Modification of Polymers I. Polysiloxane Modified Epoxies II. Segmented Polyurethane Blends, *Virginia Tech Dissertation*, 1984.

[115] J.S. Riffle, J. Yilgor, C. Tran, G.L. Wilkes, J.E. McGrath and A.K. Banthia, Elastomeric Polysiloxane Modifiers for Epoxy Networks: Synthesis of Functional Oligomers and Network Formation Studies. ACS Symposium Series #221, Epoxy Resin Chemistry, 1983, Ed. R.S. Bauer, 21-54.

[116] E. Yilgor and I. Yilgor, *Polymer*, 1998, **39**(8-9), 1691-1695.

[117] N.B. Sunshine, Flame retardancy of phenolic materials, Flame Retardancy of Phenolic Resins and Urea- and Melamine-formaldehyde Resins, Vol. 2, W.C. Kurlya and A. J. Papa, Eds., 1973, Marcel Dekker, Inc. New York.

[118] C. S. Tyberg, K. Bergeron, M. Sankarapandian, P.Shih, A.C. Loos, D.A. Dillard, J. E. McGrath, J. S. Riffle and U. Sorathia, *Polymer*, 2000, **41**(13), 5053-5062.

synthesized and characterized. The strongly hydrogen bonding phosphine oxide group was incorporated to increase the network glass transition temperature as well as improve adhesive and thermal performance. The phosphorus moiety contains no carbon-oxygen-phosphorus bonds that would be susceptible to oxidation. Networks from both this novel diepoxide and a traditional bisphenol-A based diepoxide have been prepared using 1,3-bis(3-aminopropyl)tetramethyldisiloxane (Figure 3-5) or phenolic novolac (Figure 3-16) as a crosslinking agent. This work addresses the design, synthesis, and adhesion studies for bonding composite panels to pre-existing steel using curable epoxy resins. The phosphorus content and the epoxide/phenol ratio have been systematically varied to allow investigation of the effect of both oligomer chemistry and network structure on thermoset properties.

3.2. Experimental

3.2.1. Materials

Bis-(4-fluorophenyl)phenyl phosphine oxide (BFPPO) was donated by Avecia,. Dimethyl sulfoxide (DMSO), epichlorohydrin, 2-propanol, and potassium hydroxide were purchased from Aldrich and used as received. 1,3-bis(3-aminopropyl)tetramethyldisiloxane was purchased from Gelest. Shell Chemical Co donated Epon-828, a diepoxide prepared from bisphenol-A and epichlorohydrin. This resin had an epoxy equivalent weight of 187 g/mol, which was determined via ^{1}H NMR and titration. The phenolic novolac oligomer with M_n = 788 g/mol, determined by ^{1}H NMR, was donated by Georgia Pacific and used as received. G-10 glass reinforced epoxy composite and A-36 steel were obtained from AIN Plastics and McMaster-Carr, respectively.

3.2.1.1. Purification of Reagents

Bis-(4-fluorophenyl)phenyl phosphine oxide

BFPPO was distilled under a 1.5 mTorr vacuum using a Kugel-Rohr distillation apparatus. The white crystals were then recrystallized from a 5:1 v/v tetrahydrofuran:cyclohexane mixture. The BFPPO was dried under vacuum at 60°C for 24 hours.

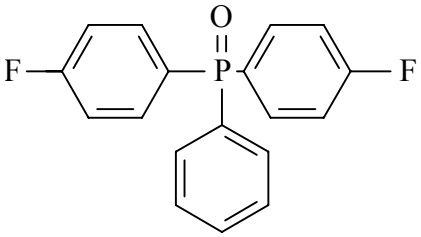

Figure 3-1. Bis-(4-fluorophenyl)phenyl phosphine oxide, molecular weight = 314 g/mol.

1,3-Bis(3-aminopropyl)tetramethyldisiloxane

The disiloxane was distilled under a 1.5 mTorr vacuum at 150°C and then stored under nitrogen.

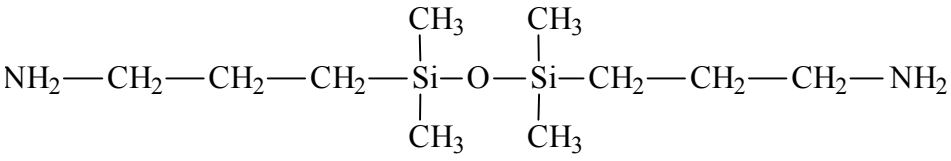

Figure 3-2. 1,3-Bis(3-aminopropyl)tetramethyldisiloxane, molecular weight = 256 g/mol.

3.2.2. Synthesis

3.2.2.1. Synthesis of bis-(4-hydroxyphenyl)phenyl phosphine oxide (BHPPO)

Synthesis of the phosphine oxide diphenol monomer was carried out by nucleophilic aromatic substitution of hydroxide onto the corresponding fluorinated compound following the procedure reported by Riley and McGrath[119] (Figure 3-3). BFPPO (50g, 0.156 moles) was dissolved in 200 mL DMSO to yield a 25% solids solution under nitrogen and heated to 140ºC. Six equivalents of potassium hydroxide in a 20 wt % aqueous solution were added. Due the electron withdrawing nature of the phosphine oxide in the para position to the fluorine, a hydroxide anion was able to attack the aromatic ring. After going through a Meisenheimer intermediate the fluorine was replaced by the hydroxyl group. The newly formed phenol was subsequently deprotonated in the basic reaction solution. The reaction proceeded at 140ºC for 18 hours and was then cooled to room temperature. The monomer was precipitated into rapidly

[119] D. J. Riley, Synthesis and Characterization of Phosphorus Containing Poly(arylene ether)s, *Virginia Tech Dissertation*, 1997.

stirring 10 v/v % HCl/water. The phosphine oxide diphenol was then purified by recrystallizing in boiling 5 % water/methanol. The crystals were dried at 60°C for 24 hours under vacuum.

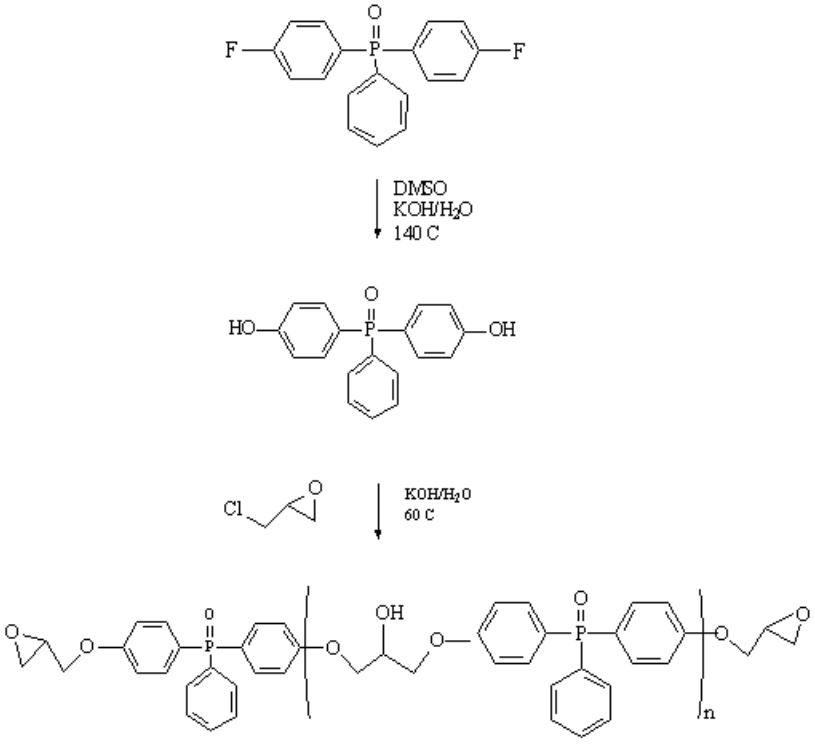

Figure 3-3. Reaction scheme for the hydroxylation of BFPPO and the subsequent epoxidation to yield a diepoxide resin containing a diaryl substituted phenyl phosphine oxide moiety.

3.2.2.2. Synthesis of bis-(4-epoxyphenyl)phenyl phosphine oxide

To synthesize the diepoxide, BHPPO was reacted in an 80/20 v/v epichlorohydrin/2-propanol solution under nitrogen at 60°C (Figure 3-3). A 20 molar excess of epichlorohydrin relative to phenol and 1.05 equivalents of potassium hydroxide per phenol were used. A standard synthesis involved dissolving BHPPO (30g, 0.097 moles) in a mixture of 150 mL of epichlorohydrin and 40 mL of 2-propanol under nitrogen and heating to 60°C. KOH (11.43g, 0.204 moles) was dissolved in 57 mL of deionized water to yield a 20% solution of aqueous potassium hydroxide and was added dropwise by an addition funnel in two aliquots. The first half was added over an hour and then was allowed to react for an additional 15 minutes. The second aliquot of potassium hydroxide solution was added in the same manner. Upon addition of the

hydroxide anion, the phenol was deprotonated. Attack of the oxirane ring by the phenolate anion through a S_N^2 reaction, resulted in the formation of a new ether link with the epoxide ring oxygen as the leaving group. The pendant hydroxide then displaced the chlorine to form a new epoxide ring. Phenolate anions could also attack the oxirane rings of the newly formed phosphine oxide epoxy. This resulted in chain extension of the oligomer. To minimize the amount of chain extension, a large excess (20 fold) of epichlorohydrin was used. After addition of the base, the reaction was continued for 2 hours at 60ºC, then cooled to room temperature. The organic layer of the reaction mixture was washed four times with water to remove unreacted base. It was critical to remove the base so that the epoxide rings would not be opened by any remaining hydroxide anions. The excess epichlorohydrin was vacuum stripped from the round bottom flask at 700 mTorr/50°C for 48 hours. To remove the viscous epoxide, it was dissolved in acetone and then dried in a Teflon dish under vacuum at 60°C for 24 hours. Any remaining epichlorohydrin was removed at this point. ^{1}H NMR in deuterated DMSO was used to monitor the disappearance of the epichlorohydrin peaks and to calculate the average molecular weight of the diepoxide.

3.2.2.3. Network Preparation

Epoxy/Siloxane Networks

Networks were prepared by mixing the appropriate diepoxide resins with 1,3-(3-aminopropyl)tetramethyldisiloxane and curing the mixtures at 100°C or 120°C (Figure 3-5). Epon 828 (30g, 0.08 moles diepoxide) was mixed rapidly with the 1,3-(3-aminopropyl)tetramethyl disiloxane (10.2g, 0.04 moles) at room temperature, degassed under a vacuum for 15 minutes, and cured for 2 hours at 100°C. Networks with blends of the phosphine oxide and bisphenol-A based diepoxides were prepared by initially combining the bisphenol-A epoxy with the disiloxane and degassing. The phosphine oxide diepoxide was heated to 70°C and degassed and then combined with the bisphenol-A/siloxane blend with rapid stirring. The resin was degassed an additional two minutes and then cured as above. The phosphine oxide diepoxide/siloxane networks were prepared by heating the phosphine oxide epoxy (10.2g, 0.017 moles) to 70°C, adding

degassed 1,3-(3-aminopropyl)tetramethyldisiloxane (2.17g, 0.0085 moles) and rapidly mixing. These were cured at 120°C for 2 hours.

Epoxy/Novolac Networks

To prepare 100% bis-A networks for thermal analysis, fracture toughness, and lap shear tests, a novolac resin and ~75% of the required epoxy were heated to 170°C (Figure 3-16). The vacuum was applied incrementally to prevent the material from swelling into the vacuum line during degassing. The bisphenol-A epoxy systems were catalyzed with 0.5 mole % triphenyl phosphine, which was dissolved in the remaining ~25% of the epoxy and then added to the cooled (160°C) solution. These solutions were poured into a heated mold and cured at 200°C for one hour and postcured at 220°C for three hours. Networks containing phosphine oxide epoxy were prepared in a similar manner. Initially novolac and bisphenol-A epoxy were mixed at 170°C and cooled to 160°C. Then bisphenol-A epoxy was added and stirred for <3 minutes and the resin was cured on the above cure schedule. At high loadings of the more viscous phosphine oxide oligomer, processing the epoxy-novolac resin became more difficult. Achieving specimens in optimum condition for flame retardance or fracture toughness could not be done for the 100 % phosphine oxide epoxy thermosets.

3.2.3. Characterization

3.2.3.1. Oligomer Characterization

Nuclear Magnetic Resonance (NMR)

^{1}H NMR and titration were used to determine the molecular weight of the oligomers. Using a Varian 400 MHz NMR, samples were run in DMSO-d_6.

Titration

The epoxy equivalent weights of both the bisphenol-A and phosphine oxide based diepoxide oligomers were determined via potentiometric titration using a MCI Automatic Titrator Model GT-05. Twenty milligrams of potassium hydrogen phthalate were dissolved in 70 mL of glacial acetic acid and this solution was used to standardize a 0.02 molar solution of hydrobromic acid (HBr) in glacial acetic acid. Twenty mg samples of the appropriate diepoxide were mixed with 1.5 g of the phase transfer agent, tetraethylammonium bromide, and then dissolved in 70 mL of glacial acetic acid. The

samples were titrated with the standarized HBr solution until the appearance of the potentiometric endpoint.

Differential Scanning Calorimetry (DSC)

Glass transition temperatures for the oligomers were determined from the second heat using a Perkin Elmer Pyris 1 differential scanning calorimeter equipped with liquid nitrogen coolant at a heating rate of 10°/min.

3.2.3.2. Hydrogen Bonding Analysis

Fourier transform infrared spectroscopy (FTIR) was conducted using a Nicolet Impact 40 infrared spectrometer on sodium chloride salt plates. Dilute solutions of triphenylphosphine oxide, phosphine oxide diepoxide oligomer, amine terminated disiloxane, novolac oligomer, and blends were prepared in acetone and thin films were cast onto the salt plates. The blends were investigated using a heat cell from 25°C to 300°C. The progress of the cure reactions was also followed using infrared spectroscopy. The disappearance of the absorption at 914 cm^{-1} due to the asymmetric stretch of the epoxide ring was monitored.

3.2.3.3. Network Characterization

Gel Fraction

Gel fractions were studied by extracting the cured networks with acetone for three days at 25°C. Both the sol and gel fractions were dried and weighed.

Density

The thermoset's density at ambient temperature was elucidated with a Mettler-Toledo AG204 Balance with a density determination kit. The weight of the solid in air (A) and in water (B) was used with the density of water, $\rho_{(H_2O)}$, to calculate the solid's density, ρ_{RT}, using Archimedes' principle.

$$\text{Equation 3-1} \quad \rho_{RT} = A\,\rho_{(H_2O)}/(A-B)$$

The density in the rubbery regime was calculated using the solid density at 22°C and the coefficient of thermal expansion below and above the glass transition temperature (Figure 3-4).

Water Absorption

Equilibrium water absorption was measured by submersing 1mm thick films of each network in water at both 22°C and 60°C. Films were dried and weighed daily. Equilibrium sorption was reached after 3 months at 22°C and after 1 month at 60°C.

Dynamic Mechanical Analysis

Dynamic mechanical analysis (DMA) was used to determine the glass transition temperatures, coefficients of thermal expansion (CTE), and rubbery moduli of the networks. These measurements were performed using a Perkin-Elmer dynamic mechanical analyzer, model DMA-7. The T_gs were calculated from the peaks in the Tan delta curves. The analyses were conducted using a 15mm span, 3-point bend fixture with 6 mm x 3 mm specimens. Cured samples were heated at 5°C/minute from 25 to 200°C, except the 1 phosphine oxide epoxy/2 novolac system, which was heated to 250°C. The test configuration was used to determine the β-transitions of the networks. The sample chamber was cooled to -110°C using liquid nitrogen and then heated at 5°C/minute to 30°C. Force/displacement curves were generated 45° above the network T_g from which the rubbery modulus was calculated. Specimens were 1.7 mm thick to minimize shear contribution to the modulus. The coefficient of thermal expansion was determined using a quartz stage and probe. Samples were heated from 25°C to T_g+60° at 2.5°/min. From the second heat, CTE values were taken in linear regions below and above T_g.

Dilatometry

CTEs were also determined using a Netzsch dilatometer, model DIL 402C. With the same heating cycle, 4 mm long specimens were analyzed. Samples were heated at 2.5°/min from 25°C to T_g+60°. CTE values were taken from the second heat in the linear region below and above T_g (Figure 3-4).

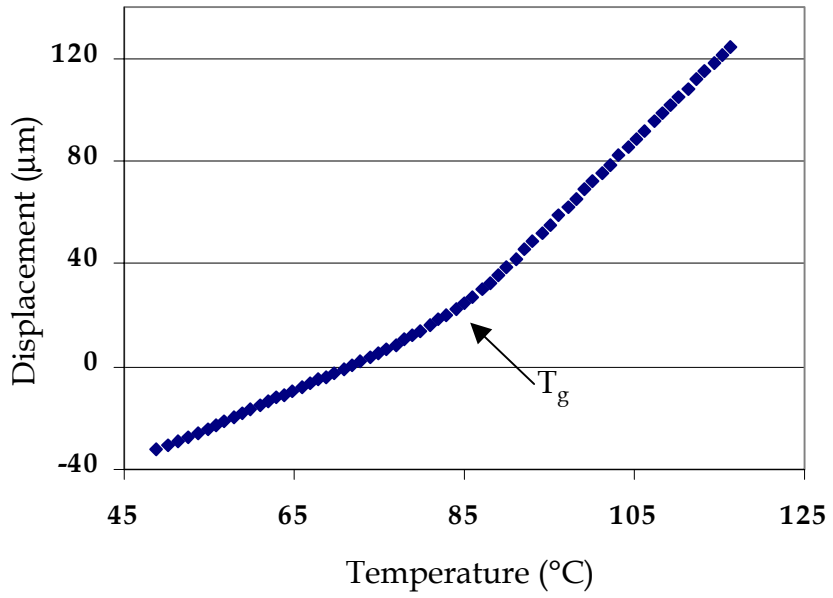

Figure 3-4. Thermal expansion of siloxane network below and above T_g.

Thermogravimetric Analysis

Thermal stability of the networks was investigated with thermogravimetric analysis (TGA). Samples were 8-10 mg of ~0.5 mm particles and heated at 10°C from 50°C to 800°C.

Cone Calorimetry

Flame retardance of the phosphine oxide containing novolac network was investigated with cone calorimetry at the Naval Research Lab in Bethseda, MD. Panels were 6-6.5 mm thick with a surface area of ~0.01 m^2 and were tested in a horizontal orientation. The incident heat flux was 50.00 kW/m^2.

Fracture Toughness

Fracture toughness was evaluated using three point bend tests according to ASTM standard D 5045-91. The specimens had a width of 6.0-6.4 mm and a thickness of 3.0-3.2 mm and were tested on a 25.4 mm span. A minimum of six samples was averaged for each value. The single edge notch bending method was used. First, a notch was created in the sample by sawing. A natural crack was initiated by inserting a cold razor blade (which had been immersed in liquid nitrogen) into the notch and tapping with a rubber hammer. The depth of the crack was between 40 and 60 % of the width. The pre-

cracked notched specimen was loaded crack down, into a three point bend fixture and tested using an Instron model 1123 instrument. The crosshead speed was 1.27 mm/min.

Lap Shear Testing

Glass reinforced epoxy composites and A-36 steel were used as adherends in the lap shear tests following ASTM standard D1009. Both materials were cut into 2.54 cm x 10.16 cm tabs. Adherends were prepared by washing in soapy water, grit blasting, sonicating in 2-propanol, washing with acetone, and drying at 120°C for 30 min. Samples were prepared with a 1.27 cm overlap and 0.05 cm bond thickness using an aluminum step. Siloxane networks were cured following the network preparation cure schedule. Steel lap shear specimens of the novolac networks were also cured following the network preparation cure schedule. However, when composite adherends were used with the novolac systems, specimens were cured at 130°C (below the composite T_g of ~150°C) for 4 hr. Two sets of five lap shear specimens were prepared and averaged for each lap shear value. Samples were failed using an Instron model 1123 with a 22,300 N load cell.

3.3. Epoxy/Siloxane Networks

3.3.1. Synopsis

A novel diepoxide containing a phosphine oxide moiety was synthesized by reacting bis-(hydroxyphenyl)phenyl phosphine oxide with epichlorohydrin. Networks were prepared using novolac and siloxane crosslinking agents. This work addresses the structure-property relationships of the siloxane systems (Figure 3-5). The phosphine oxide containing epoxy resin, as well as a bisphenol-A based diepoxide, was reacted with 1,3 bis-(3-aminopropyl)tetramethyl disiloxane at different stoichiometric ratios. Increasing the molecular weight between crosslinks by offsetting the epoxide/amine stoichiometry resulted in improved the network toughness. The incorporation of the phosphine oxide group yielded networks with increased glass transition temperatures and water absorption due to the polar nature of the phosphine oxide bond. Higher char yield was also observed with the addition of the inorganic phosphorus. The bisphenol-A based epoxy/siloxane network was exceptionally ductile with a fracture toughness of 2 MPa-

$m^{1/2}$. Lap shear analysis was performed to assess the adhesive properties of the epoxy/siloxane networks with steel. Samples prepared with bisphenol-A epoxy and bisphenol-A/phosphine oxide epoxy blends resulted in interfacial failure as observed visually and had strengths in a structural regime, <13.8 MPa (2,000 psi).

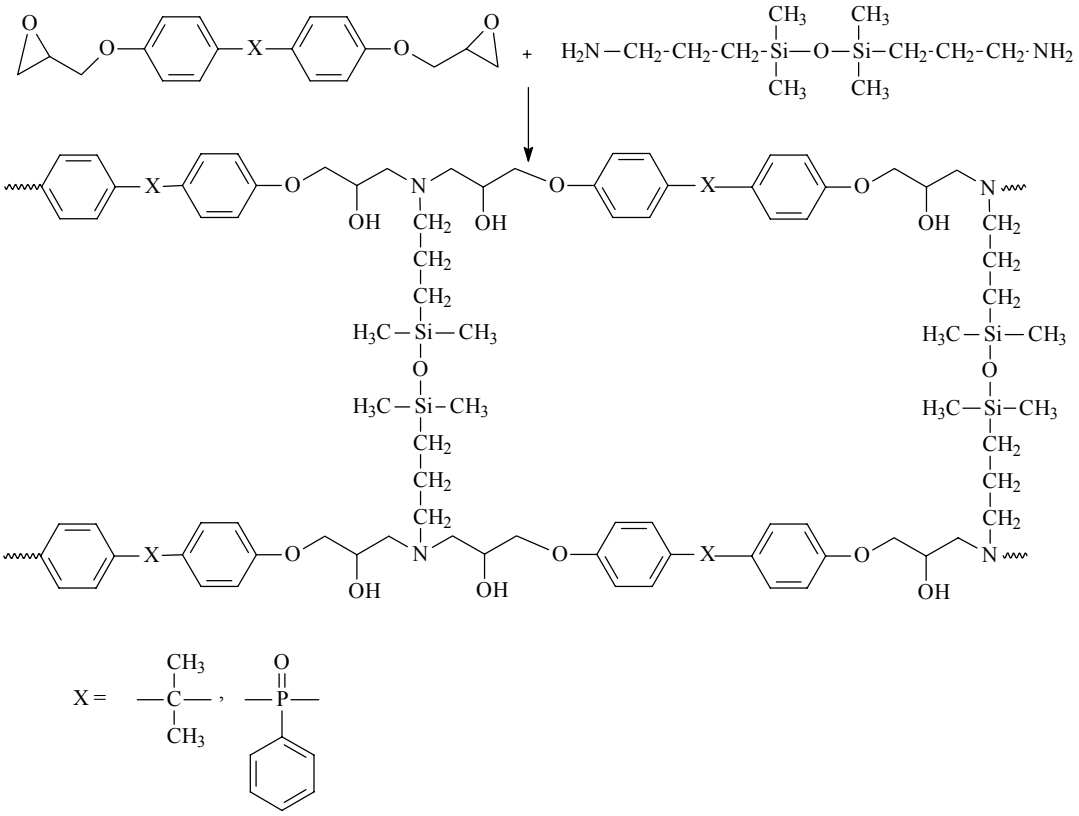

Figure 3-5. Network formation of diepoxides with 1,3-bis(3-aminopropyl) tetramethyldisiloxane

3.3.2. Results and Discussion

This research involved the investigation of chemical and structure/property relationships within networks prepared from both bisphenol-A and phosphine oxide containing epoxy resins. While the bisphenol-A based resin was available commercially, the phosphine oxide epoxy was synthesized in two reactions from bis(fluorophenyl)phenyl phosphine oxide. Epoxy oligomers were difunctional with low degrees of chain extension, between 10% and 30%. A series of networks cured with 1,3-(3-aminopropyl)tetramethyldisiloxane, a low molecular weight amine terminated siloxane, has been investigated (Figure 3-5). The lone pair of electrons on the nitrogen

reacted with the oxirane ring through a nucleophilic substitution ring opening reaction. Since the amines were primary and able to react with two epoxide rings the siloxane component was tetrafunctional. At the stoichiometric ratios investigated, these networks consisted of ~80 wt % epoxy and ~20 wt % siloxane.

3.3.2.1. Preparation of diglycidyl ether of bis(hydroxyphenyl)phenyl phosphine oxide

The phosphine oxide bisphenol, BHPPO, was synthesized via nucleophilic aromatic substitution of a fluorine by a hydroxyl group following the method of Riley and McGrath[119] (Figure 3-3). The substitution reaction was monitored by ^{1}H NMR (Figure 3-6). In going from the fluorinated compound to the phenolate anion, the resonance frequency of the aromatic proton ortho to the reaction site, **a,** shifted upfield due to the increased electron density in the ring and shielding of the hydrogen. By monitoring the formation of this peak, the reaction was followed to ensure complete hydroxylation.

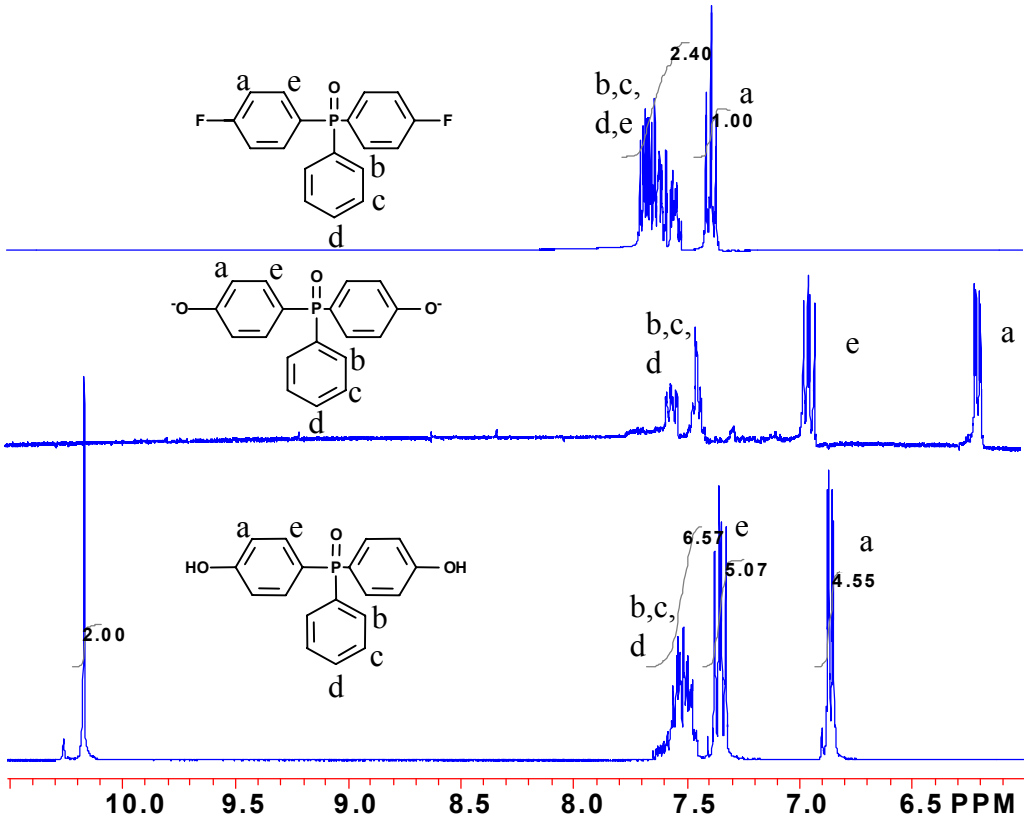

Figure 3-6. ^{1}H NMR's of (from top to bottom) bis(fluorophenyl)phenyl phosphine oxide, phenolate anion formed during reaction, and bis(hydroxyphenyl)phenyl phosphine oxide.

When the phenolate anion was protonated during precipitation in acidic water, the proton was deshielded and peak **a** shifted downfield. Also, the appearance of the hydroxyl group peak at 10.25 ppm following neutralization of the phenolate anions indicated that the desired bisphenol was formed.

The phosphine oxide diepoxide was synthesized under basic conditions by reacting bis(hydroxyphenyl)phenyl phosphine oxide with epichlorohydrin (Figure 3-3). The formation of the epoxide ring was monitored by ^{1}H NMR (Figure 3-7). The integration of the aromatic peaks, found between 7 and 8 ppm, remained constant while peaks **c-g** from the epoxide group increased in intensity.

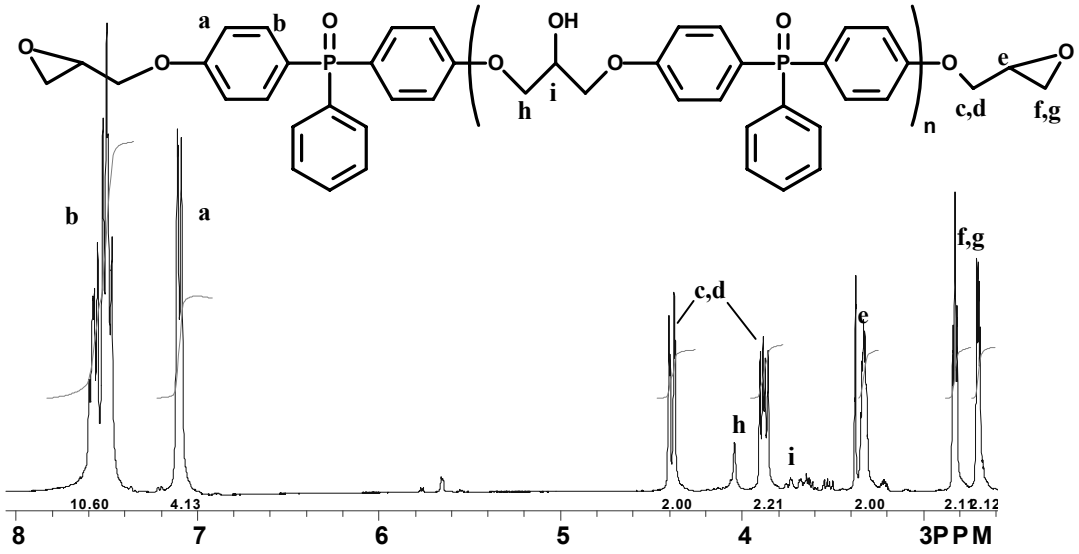

Figure 3-7. ^{1}H NMR of bis-(4-epoxyphenyl-)phenyl phosphine oxide.

The ratio of the aromatic proton peak areas to the epoxide proton peak areas was also used to calculate the molecular weight of the final diepoxide product. It was determined that 30 % chain extension occurred and the molecular weight of the phosphine oxide diepoxide was 554 g/mol. The bisphenol-A based epoxy oligomer was 'shorter' with 10 % chain extension, which corresponded to an average molecular weight of 374 g/mol. The molecular weight was confirmed using potentiometric titration in which the epoxide endgroups were titrated with HBr acid. The epoxy equivalent weights, which would be doubled to give the oligomer molecular weights, were 300 g/mol and 172 g/mol for the phosphine oxide and bisphenol-A diepoxides, respectively. The phosphine oxide epoxy resin had a higher glass transition temperature (T_g), 4°C

compared to the bisphenol-A epoxy T_g of -20°C, and was more viscous because of increased hydrogen bonding and higher molecular weight.

3.3.2.2. Network Series

Networks were prepared by crosslinking blends of the diepoxides with tetrafunctional 1,3-(3-aminopropyl)tetramethyldisiloxane (Figure 3-5). Two series were prepared, (Table 3-1) one with a stoichiometric 2 epoxide/1 amine ratio and the other series with a 2 epoxide/1.2 amine offset ratio. Within each stoichiometric series, the concentration of phosphine oxide was systematically varied. The networks contained 100 mol % bisphenol-A epoxy, 50 mol % bisphenol-A epoxy/50 mol % phosphine oxide epoxy, and 100 mol % phosphine oxide epoxy. The networks containing bisphenol-A epoxy were cured at 100°C for one hour while the networks prepared with 100 % phosphine oxide were cured at 120°C to avoid vitrification of the networks. The reaction between the diepoxide and the amine was monitored with infrared spectroscopy. The oxirane asymmetric stretch at 914 cm^{-1} was dramatically reduced within 30 minutes at 100°C (Figure 3-8). The gel-fractions of the bisphenol-A and phosphine oxide networks were over 99% indicating fully cured networks.

Table 3-1. Network compositions.

Epoxy/Siloxane Network Compositions		**Resin Mixing Temp.**	**Network Cure Temp.**
2 Epoxy/1 SX	**2 Epoxy/1.2 SX**		
100% bisphenol-A epoxy	100% bisphenol-A epoxy	22°C	100°C
50% bisphenol-A epoxy/ 50% phosphine oxide epoxy	50% bisphenol-A epoxy/ 50% phosphine oxide epoxy	70°C	100°C
100% phosphine oxide epoxy	100% phosphine oxide epoxy	70°C	120°C

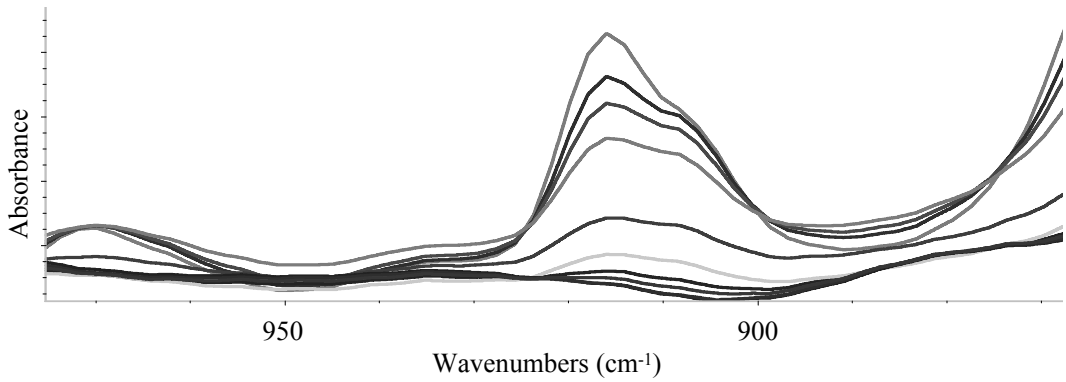

Figure 3-8. Disappearance of FTIR epoxide asymmetric stretch at 914 cm^{-1}over 30 min in the 1 siloxane/2 bisphenol-A cure at 100°C.

3.3.2.3. Crosslink Density

The molecular weight between crosslinks (M_c) can significantly affect network properties[118]. In the glassy regime, a more open network often leads to a tougher network. Increased chain mobility allows increased plastic deformation and decreased stress concentrations at the crack tip. In the rubbery regime, a softer material results with lower crosslink density. Therefore an understanding of the crosslink density for each network composition can aid in the interpretation of network properties. Crosslink points are described as the junction point of three chains and a segment is defined as the chain between two crosslink points. M_c is typically calculated experimentally either from network swelling in a solvent or from the rubbery modulus of the network[120]. Swelling experiments assume a perfect network with no dangling ends and have been found to be most accurate for networks with M_cs of ~5,000 g/mol[121]. For highly crosslinked networks, M_c can be calculated from the rubbery modulus (E') of the network. Based on the statistical theory of rubber elasticity the molecular weight between crosslinks (M_c) is inversely proportional to the rubbery modulus (Equation 3-2) assuming that (1) the system energy is independent of segment conformations, (2) individual segments obey Gaussian statistics, (3) the number of conformations of the network is the sum of the

[120] C. S. Tyberg, Void-Free Flame Retardant Phenolic Networks: Properties and Processability, *Virginia Tech Dissertation*, 2000.

[121] L.E. Nielsen, *J. Macromol. Sci. Rev. Macromol. Chem.*, 1969, **C3**(1), 69-103.

number of conformations of individual segments and (4) the crosslink points deform affinely with deformation of the network as a whole[122].

Equation 3-2 $M_c = 3(\langle r^2\rangle/\langle r_0^2\rangle)RT\rho / E'(1-2M_c/M_n)$

The equation can be simplified by setting $(\langle r^2\rangle/\langle r_0^2\rangle)$ and $(1-2M_c/M_n)$, which is a correction factor for dangling ends, equal to 1. The correction factor would be applicable for high molecular weight polymers that are crosslinked through the reactions of internal sites but was ignored for these systems. However, both of the diepoxides and the amine terminated disiloxane were low molecular weight oligomers and would result in $(1-2M_c/M_n)$ being negative. Setting the correction factor equal to one makes the M_c calculated from the modulus, E', "the effective elastic chain" molecular weight. R, T, and ρ are the gas constant, absolute temperature, and density at 45°C above T_g, respectively. The density of the thermoset at elevated test temperatures is calculated from the density at 22°C and the coefficients of thermal expansion below and above T_g.

The moduli for the epoxy/siloxane networks were determined in the rubbery plateau region using equilbrium stress/strain experiments. At 45°C above the glass transition temperature of the network, a load was applied flexurally to a thin sample and the equilibrium displacement was determined. The absolute modulus was calculated using Equation 3-3 from the slope of the force versus displacement plot (P/Δ), taking into consideration the test span (L) and the sample dimensions, width (w) and height (b).

Equation 3-3 $E' = 9.81\ m/s^2(P/\Delta)(L^3/4wb^3)$

Simplifying Equation 3-2, M_c was calculated for the epoxy/siloxane networks from the rubbery moduli, using Equation 3-4.

Equation 3-4 $M_c = RT\rho / E'$

[122] J.J.Aklonis and W.J. MacKnight, Introduction to Polymer Viscoelasticity, 2nd edition, 1983, John Wiley and Sons, New York.

Table 3-2. Rubbery moduli and molecular weights between crosslinks for epoxy/siloxane networks.

Network Composition	Rubbery Modulus (MPa)	Experimental M_c (g/mol)	Theoretical M_c (g/mol)
2 bisphenol-A epoxy **1** siloxane	14.6	703±33	335
2 bisphenol-A/phosphine oxide epoxy **1** siloxane	9.1	1314±56	410
2 bisphenol-A epoxy **1.2** siloxane	12.4	858±16	439
2 bisphenol-A/phosphine oxide epoxy **1.2** siloxane	7.5	1756±354	534

Using an excess of amine or incorporating the phosphine oxide epoxy component produced softer thermosets with lower rubbery moduli (Table 3-2). Offsetting the stoichiometry or incorporating the longer phosphine oxide epoxy was anticipated to produce a more open network and M_c increased as expected. These values were compared to the theoretical M_cs that were calculated assuming complete conversion and no dangling ends. From an idealized network (Figure 3-9) the total molecular weight of the components was divided by the number of segments to yield the theoretical molecular weight between crosslinks; for the stoichiometric network, $M_c = 2\ M_{n\ epoxide} + M_{n\ siloxane}$ / 3 segments and for the offset network, $M_c = 5\ M_{n\ epoxide} + 3\ M_{n\ siloxane}$ / 7 segments. For this calculation, the tertiary amine was assumed to be the crosslink point and both the aromatic and siloxane chains between two amines to be the segments.

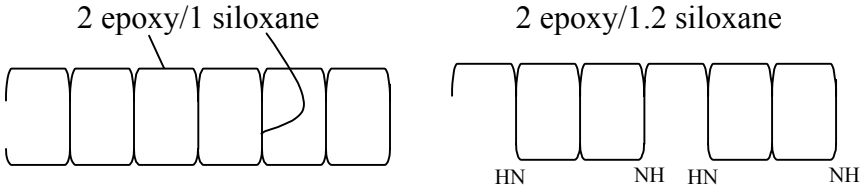

Figure 3-9. Idealized network structures for the epoxy/siloxane networks in which vertical segments represent the amine terminated siloxane and horizontal segments represent the epoxy segments with stoichiometric and with offset epoxide/amine ratios.

In each case the experimentally determined M_c was higher than the theoretical M_c. The difference may have been due in part to linear connections that formed rather than crosslink points when the amines did not react fully. Physically, since these resins had only terminal reactive sites, a linear connection may have developed when a secondary

amine was trapped having no epoxide with which to react. This would have resulted in offsetting the stoichiometry between epoxide and amine groups and opening up the network so that the experimental M_c was larger than the theoretical value.

The bisphenol-A based networks showed experimental M_c's twice as large as the theoretical values in both stoichiometric series. Networks containing 50% bisphenol-A epoxy and 50% phosphine oxide epoxy showed a ratio of experimental M_c to theoretical M_c of over 3 (Table 3-2). The increased M_c of the phosphine oxide containing thermosets may have been due to the strongly hydrogen bonding nature of the phosphine oxide bond which altered the cure chemistry of the resin. The hydroxyl hydrogens would be anticipated to hydrogen bond more strongly than the amine hydrogens due to the more electronegative nature of the oxygen. The hydrogen bonding between the phosphine oxide and the hydroxyl groups (that formed upon ring opening of the epoxy ring) may have increased the electron density of the oxygen, activating these secondary hydroxyl groups and catalyzing the homopolymerization of the epoxy groups. The etherification reaction would lead to an offset in epoxide/amine stoichiometry and open the network, increasing M_c. Reduced chain mobility during the cure due to hydrogen bonding, may have also led to more trapped linear connections. No evidence was observed from FTIR to indicate formation of the phosphazene (phosphorus-nitrogen double bound) from reaction of the phosphine oxide moiety with the primary amine.

3.3.2.4. Hydrogen Bonding

FTIR has proven to be a useful technique for elucidating favorable molecular interactions, such as hydrogen bonding, particularly in the investigation of polymer miscibility[123],[124]. To observe the phosphine oxide bond without the contribution of hydrogen bonding, triphenylphosphine oxide was utilized because the molecule does not have any hydroxyl or phenol functionalities. The phosphine oxide bond stretch with no hydrogen bonding was observed in the FTIR spectrum at 1188 cm^{-1}. Hydrogen bonding

---

[123] X. Yang, P. C. Painter, and M. M. Coleman, *Macromolecules*, 1992, 25(8), 2156-2165.

[124] S. Wang, Q. Ji, C. T. Tchatchoua, A. R. Shultz, and J. E. McGrath, *J. Polym. Sci. Part B Polym. Phys.*, 1999, **37**(15), 1849-1862.

in the cured network between the phosphine oxide and aliphatic hydroxyl groups resulted in a shift to a lower frequency, 1175 cm^{-1} (Figure 3-10).

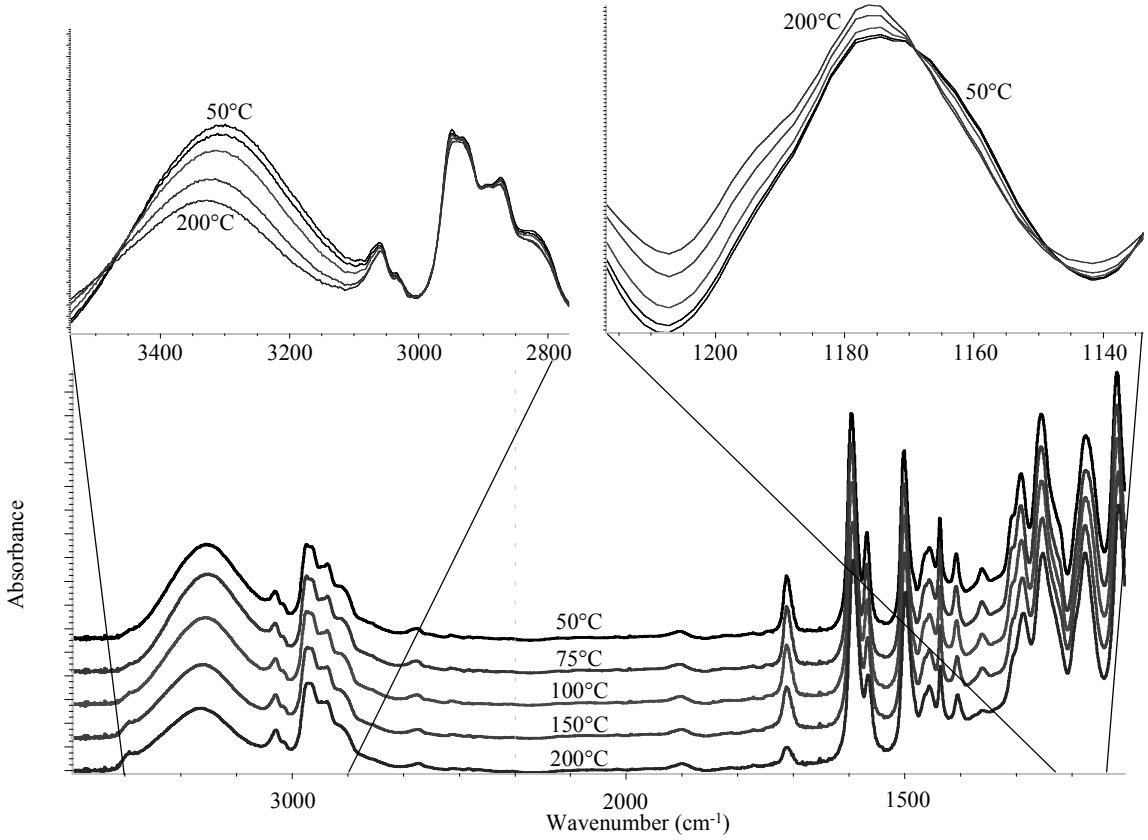

Figure 3-10. Hydrogen bonding of the hydroxyl and phosphine oxide in epoxy networks with increasing temperature.

A similar FTIR peak frequency shift of the phosphine oxide bond stretch was observed in blends of polyhydroxyether and poly(arylene ether phosphine oxide/sulfone)[125],[124] due to the same combination of secondary hydroxyl group and phosphine oxide moiety interactions. In phosphine oxide containing polyimides, hydrogen bonding with polyhydroxyether hydroxyl groups was observed in ^{31}P CP-MAS NMR[126]. With increased temperature hydrogen bonding decreased, as seen by the shift of both the hydroxyl stretch and phosphine oxide stretch to higher frequencies. However

[125] S. Wang, Q. Ji, C. T. Tchatchoua, A. R. Shultz, and J. E. McGrath, *Am. Chem. Soc. Div. Polym. Chem. Prepr.*, 1998, **39**(2), 410-411.

[126] S. Wang, T. E. Glass, H. Zhuang, M. Sankarpandian, Q. Ji, A. R. Shultz, and J.E. McGrath, *Am. Chem. Soc. Div. Polym. Chem. Prepr.,* 1998, **40**(2), 744-745.

hydrogen bonding still persisted at the cure temperatures. Hydrogen bonding at elevated temperatures, 230°C, was also observed in polyhydroxyether/poly(arylene ether phosphine oxide) blends[21].

As will be seen in the next section, hydrogen bonding between the phosphine oxide and phenol hydroxyl groups in the novolac cured network was stronger and did not decrease, even at 200°C. The novolac's aromatic hydroxyl groups hydrogen bond more strongly than the aliphatic hydroxyl groups found on the epoxy segments in the siloxane cured network. In the novolac systems, strong hydrogen bonding served as physical, non-covalent bond cross-link points and incorporation of phosphine oxide resulted in a reduced experimental M_c.

3.3.2.5. Network Characterization

The glass transition temperatures of the networks were expected to decrease as network density decreased and chain mobility increased; however, this was not the case with incorporation of the phosphine oxide epoxy. Higher concentrations of the phosphine oxide, which increased M_c, resulted in significant increases in network glass transition temperatures (Table 3-3). The elevated T_gs were due to enhanced hydrogen bonding within the network with no loss of segment stiffness between the bisphenol-A and phosphine oxide moieties. Network systems prepared with increased concentrations of phosphonate based epoxies, in which the oxygen-phosphorus-oxygen bond possessed more flexibility then the bisphenol-A epoxy, had lower glass transition temperatures[37]. Therefore, the increased T_g due to hydrogen bonding was achieved when the segment stiffness was not reduced. Phosphine oxide/hydroxyl interactions dominated the network chain mobility rather than the network crosslink structure. T_gs for a given chemical composition were similar regardless of the epoxide/amine ratio. The slight offset in the network stoichiometry did not increase the chain mobility enough to affect T_g.

Table 3-3. Glass transition temperatures and density for the epoxy/siloxane networks.

Network	2 Epoxy/1 SX			2 Epoxy/1.2 SX	
	T_g (°C)	Water Uptake (wt %)	Density (g/ml)	T_g (°C)	Density (g/ml)
Bisphenol-A	71	1	1.13	67	1.12
50% Phosphine oxide	84	2.2	1.18	86	1.16
Phosphine oxide	92	5.5	1.23	96	1.18

Beta transitions due to secondary in-chain motions were observed in both the bisphenol-A based network and the phosphine oxide network[1] (Figure 3-11). However, the bisphenol-A system showed a broad relaxation over 100° from -100°C to 0°C while the phosphine oxide containing network possessed a much narrower transition at -85°C.

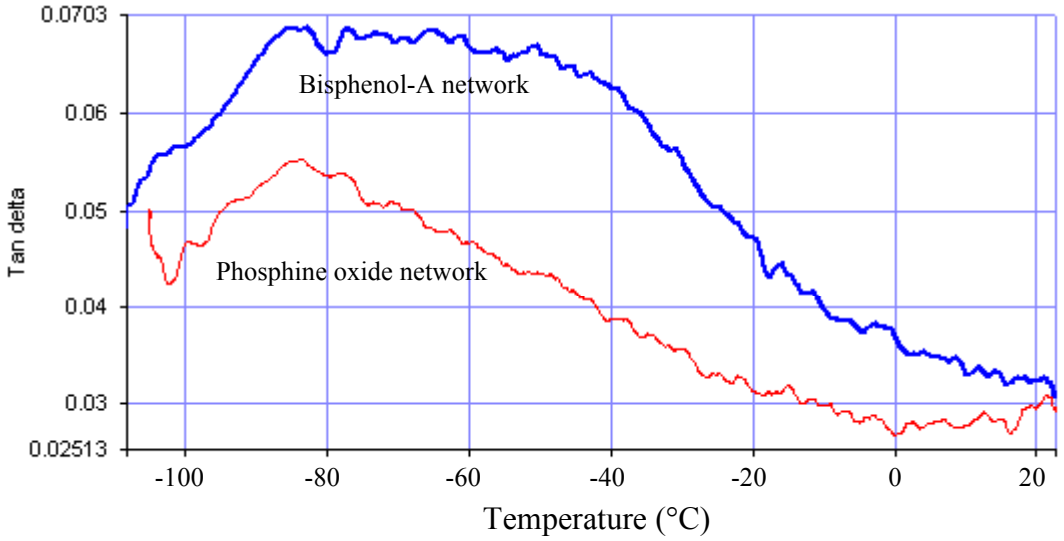

Figure 3-11. DMA of beta transition for the bisphenol-A and phosphine oxide networks.

The β-transition of the aliphatic segment typically occurs between -60°C and -30°C[132]. The transition of the bisphenol-A based thermoset was due to the motions of both the –$[CH_2CH(OH)CH_2O]$- aliphatic segments and the siloxane segments. In the phosphine oxide network, hydrogen bonding of the phosphine oxide with the pendant hydroxyl groups limited motion of the aliphatic segment. The narrower beta transition of the

phosphine oxide containing system was likely due to the motion of the siloxane segment alone at -85°C.

Water absorption of the networks was also dominated by chemical structure (Table 3-3). While a decrease in network density yielded a more open network to accommodate solvent, it was anticipated that a polar solvent, such as water would be more sensitive to network polarity than crosslink density. Within the 2 epoxide/1 amine series, the bisphenol-A based network reached equilibrium saturation at 1 wt % water while the more polar phosphine oxide epoxy/disiloxane network absorbed 5.5 wt % water.

Density was affected by both chemical composition and network structure (Table 3-3). For a given chemical composition networks prepared with a stoichiometric cure ratio that had a higher crosslink density were more dense solids. The increased frequency of crosslink points resulted in more tightly packed segments and reduced the free volume within the network. Incorporation of phosphine oxide also increased the thermoset's density. While the crosslink points were further apart, hydrogen bonding between the phosphine oxide and hydroxyl groups resulted in the chains being pulled closer together. Density of the material along with water absorption and glass transition temperature was more sensitive to the polar phosphine oxide concentration than to the network crosslink structure.

Networks prepared from the bisphenol-A diepoxide and 1,3-(3-aminopropyl)tetramethyldisiloxane were found to be extremely tough (Figure 3-12). Typical thermosets show brittle fracture that results in a sharp drop in energy absorption during fracture toughness testing. The bisphenol-A networks however tore rather than catastrophically failing; yielding a fibril debond surface and a force vs. displacement curve that resembled those found for ductile thermoplastics rather than thermosets. The incorporation of flexible diglycidal ether of bisphenol-A chains and siloxane chains provided enough chain mobility, observed as a broad β relaxation below 0°C, to dissipate energy at the crack tip, similar to that observed due to plastic deformation of thermoplastics. The addition of the siloxane segment also increased the impact energy of the bisphenol-A epoxy network[116]. For each chemical composition the more open network, formed with an offset in stoichiometry, was tougher. Again, these

improvements in toughness could be attributed to more chain mobility as the number of crosslink points decreased.

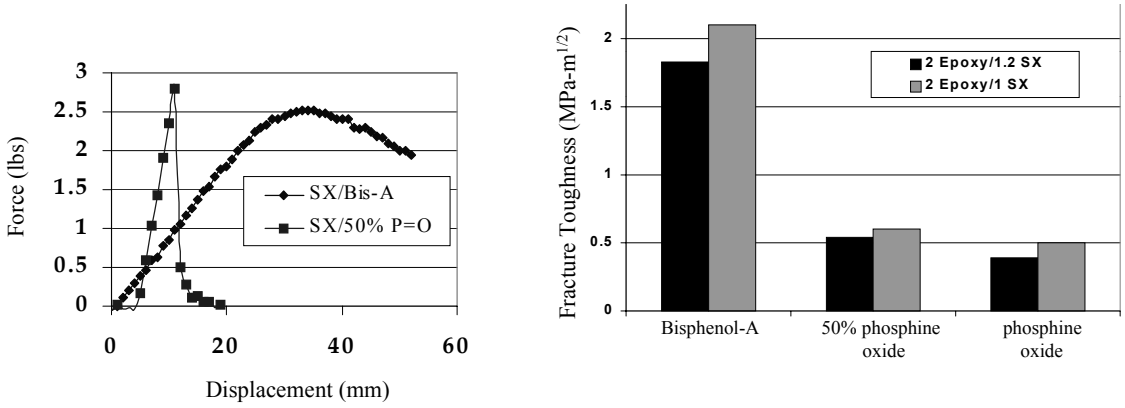

Figure 3-12. Force displacement curves for tearing of tough bisphenol-A/siloxane network and brittle failure of 50 % phosphine oxide/siloxane network and fracture toughness of the networks.

Incorporation of phosphine oxide lowered the toughness. This was not surprising given the decreased β relaxation in these networks. Epoxy toughness has been attributed to the localized segmental motion of the aliphatic linkages in epoxy networks. The increase in hydrogen bonding inhibited chain mobility and thus the network's ability to dissipate energy. These observations are in agreement with the network density, where more dense networks with tighter chain packing would have decreased chain mobility.

3.3.2.6. Network Thermal Stability

The thermal stability of the networks was studied using thermogravimetric analysis. Network samples were heated at 10°/min to 700°C in both aerobic and anaerobic conditions (Table 3-4). In air, no significant differences in the 5 % wt loss temperature were seen; however, in nitrogen, increased levels of phosphine oxide resulted in 5 % wt loss at slightly lower temperatures. This behavior in which the 5 % wt loss temperature decreases with phosphorus content has been seen in other phosphine oxide containing epoxy networks[127,128] and indicated lower thermal stability of the phosphorus-carbon bonds relative to carbon-carbon bonds. However, both stoichiometric

[127] Y.-L.Liu, G-Ho Hsiue, Y.-S. Chiu, R. –J. Jeng, and L.-H. Perng, *J. Appl. Polym. Sci.*, 1996, **61**, 613-621.

[128] C. H. Lin and C. S. Wang, *Polymer*, 2001, **42**(5), 1869-1878.

series showed increased char yield at 700°C with higher concentrations of phosphorus under air or nitrogen atmospheres. It appeared that there was a two stage degradation of the phosphorus containing networks (Figure 3-13). The phosphine oxide component had lower thermal stability than the bisphenol-A oligomer initially. However, as the network degraded, volatilized phosphine oxide radicals may have been generated that could terminate flame propagating radicals, such as HO• and H•[129] and inorganic phosphorus char developed. This char then thermally insulated the network and restricted the flow of oxidant to the network, thereby improving the thermal performance of the network beyond that of the bisphenol-A containing network at temperatures above 500°C. The solid phase mechanism has been found to dominate flame retardation in thermoplastics containing the triphenyl phosphine oxide moiety[130]. The char of polyimides containing triphenyl phosphine oxide groups were analyzed using XPS[131]. The atomic concentration of phosphorus in the surface of the char was over twice the phosphorus concentration in the polymer surface. The binding energy of the phosphorus 2p electron increased from 132.4 eV in the polymer to 133.7 eV in the char, due to the increased oxidation state of the phosphorus, indicating a phosphate type surface layer.

---

[129] J. C. Salamone, Ed., Polymeric Materials Encylopedia, 1996, CRC Press, Boca Raton, 2400-2402.

[130] I.-Y. Wan, J. E. McGrath and T. Kashiwagi, Triarylphosphine oxide containing Nylon 6,6 copolymers, Fire and Polymers II Materials and Tests for Hazard Prevention, ACS Symposium Series (599), G. L. Nelson, Ed., 1995, 29-40.

[131] H. Zhuang, Synthesis and Characterization of Aryl Phosphine Oxide Containing Thermoplastic Polyimides and Thermosetting Polyimides with Controlled Reactivity, Dissertation Virginia Tech, 1998.

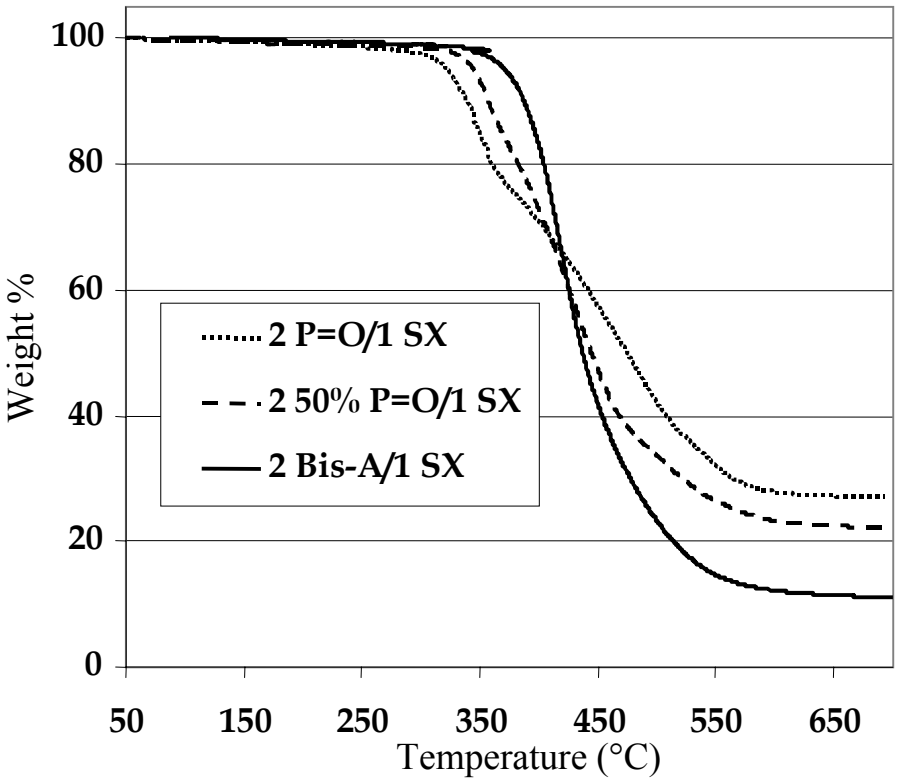

Figure 3-13. Thermogravimetric analysis of stoichiometric networks in nitrogen heated at 10°/min.

Table 3-4. Thermal degradation properties of the epoxy/siloxane networks in air and nitrogen heated at 10°/min.

Network (Epoxy/SX)	5% wt loss temperature in air	Char yield in air (700°C)	5% wt loss temperature in air N_2	Char yield in N_2 (700°C)
2 Bisphenol-A/1 SX	308°C	7%	372°C	11%
2 50% phosphine oxide/ 1 SX	314°C	27%	345°C	22%
2 phosphine oxide/1 SX	302°C	28%	321°C	27%
2 Bisphenol-A/1.2 SX	322°C	5%	371°C	10%
2 50% phosphine oxide/ 1.2 SX	310°C	26 %	311°C	30%
2 phosphine oxide/1.2 SX	299°C	29%	311°C	24%

3.3.2.7. Adhesion Properties of Networks

The adhesive properties of the epoxy/siloxane networks were investigated on glass reinforced epoxy composite and steel adherends. The adhesive strengths for the networks prepared from 100 % bisphenol-A epoxy and 50 % bisphenol-A/50 % phosphine oxide epoxy on composite adherends were the same (~13.8 MPa) with failure within the composite adherend (Figure 3-14). The composite epoxy failed before the adhesive network, making it impossible to compare the adhesive properties of these two systems. Although it was not possible to differentiate between the two adhesive networks containing bisphenol-A units, they both were quite satisfactory for bonding the composite surfaces with regard to interfacial adhesion. The adhesive strength of the 100 % phosphine oxide epoxy network was significantly lower, 10.35 MPa (1500 psi), and mixed mode failure occurred at the gritblasted composite surface and within the adhesive network. The low fracture toughness of this system resulted in poorer adhesive performance than the tougher bisphenol-A containing networks and cohesive failure. While the polar phosphine oxide moiety was expected to increase network/adherend adhesion, no conclusions could be drawn. Failure was not dominated by adhesion at the interface but rather by composite adherend strength for the bisphenol-A containing networks and adhesive network properties for the most brittle phosphine oxide containing network.

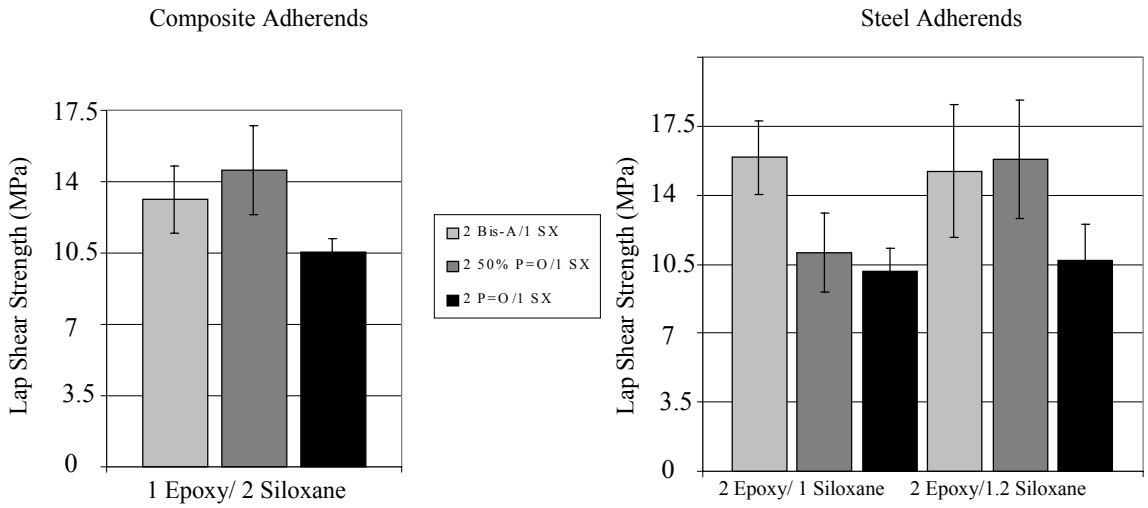

Figure 3-14. Lap shear strengths to both composite and steel adherends.

On steel adherends, network toughness dominated adhesive performance. In the 2 epoxide/1 siloxane stoichiometric series, a decrease in the maximum lap shear strength occurred when the phosphine oxide epoxy was incorporated at either 50 % or 100 %. The tougher 2 epoxide/1.2 siloxane series was less sensitive to the addition of phosphine oxide. The bisphenol-A and 50 % phosphine oxide systems resulted in adhesive strengths of ~15.5 MPa (2300 psi) with interfacial failure, while the phosphine oxide failed both interfacially and cohesively at 10.35 MPa (1500 psi). While incorporation of phosphine oxide resulted in mixed mode failure, the strengths were lower. A minimum degree of network performance was necessary to sustain a load. From Figure 3-15, the linear correlation between network fracture toughness and lap shear strength can be seen for lap shear specimens that failed via mixed mode. Above a threshold network toughness, adherend/adhesive bond strength dictated the adhesive strength and interfacial failure occurred.

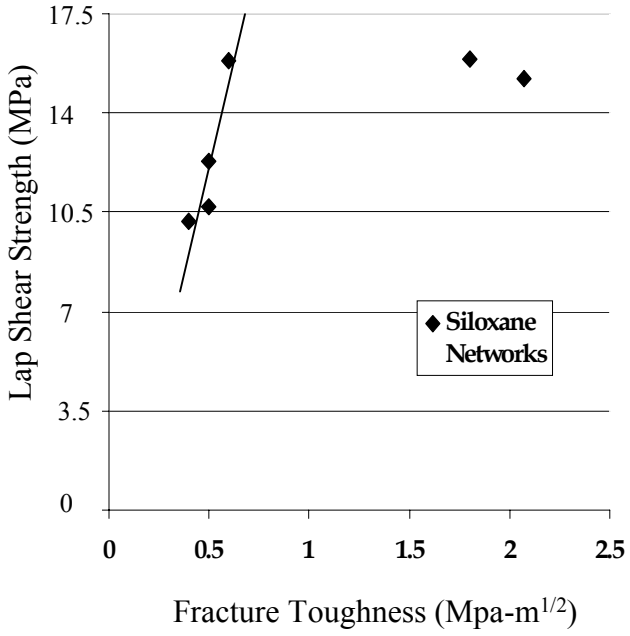

Figure 3-15. Linear correlation between lap shear strength and fracture toughness in adhesives that failed via mixed mode.

3.3.3. Conclusions

The epoxy/disiloxane networks were systematically varied by incorporating a phosphine oxide group and altering the epoxide/amine ratio. Addition of the strongly

hydrogen bonding phosphine oxide group to the network increased the glass transition temperature, water uptake, density, and char yield. Offsetting the stoichiometry resulted in a more open network with a lower rubbery modulus and higher toughness for each chemical composition. The fracture analysis of the bisphenol-A epoxy/siloxane network exhibited extreme ductility for a thermoset, tearing rather than catastrophically failing, as typically seen in thermoset materials. The adhesive strengths and failure modes as determined from lap shear specimens were related to the adhesive toughness. In fact, a linear correlation was found between the fracture toughness of the adhesive network and the lap shear strengths for samples with mixed mode failure. Extremely tough bisphenol-A networks resulted in interfacial failure with the steel adherend. The adhesive strength could be improved by increasing the adhesion between the steel adherend and the epoxy network, which requires further investigation of the surface preparation of the steel adherend.

3.4. Epoxy/Novolac Networks

3.4.1. Synopsis

With the improvements in composite properties, these materials are now finding use in infrastructure applications. For composites to be used in structural repair, an adhesive is necessary to bond the composite material to the existing steel structure. A bisphenol-A based epoxy resin and a novel phosphine oxide containing epoxy resin have been investigated. Networks have been prepared with both diepoxide oligomers using a phenolic novolac crosslinking agent. Glass transition temperatures increased with phosphine oxide concentration due in part to hydrogen bonding of the phosphine oxide to pendant hydroxyl groups, which was observed using FTIR. Hydrogen bonding was evident even at temperatures above the network T_gs and resulted in increased rubbery modulus. Adhesion to both composite and steel adherends was investigated using lap shear tests. The lap shear experiments conducted using composite tabs broke within the composite adherends at ~15 MPa (2200 psi). The steel lap shear specimens prepared from bisphenol-A had adhesive strengths of ~10 MPa (1400 psi), with interfacial failure.

Adhesive strengths to steel increased to ~14 MPa (2000 psi) and cohesive failure was observed when the phosphine oxide containing epoxy was incorporated into the network.

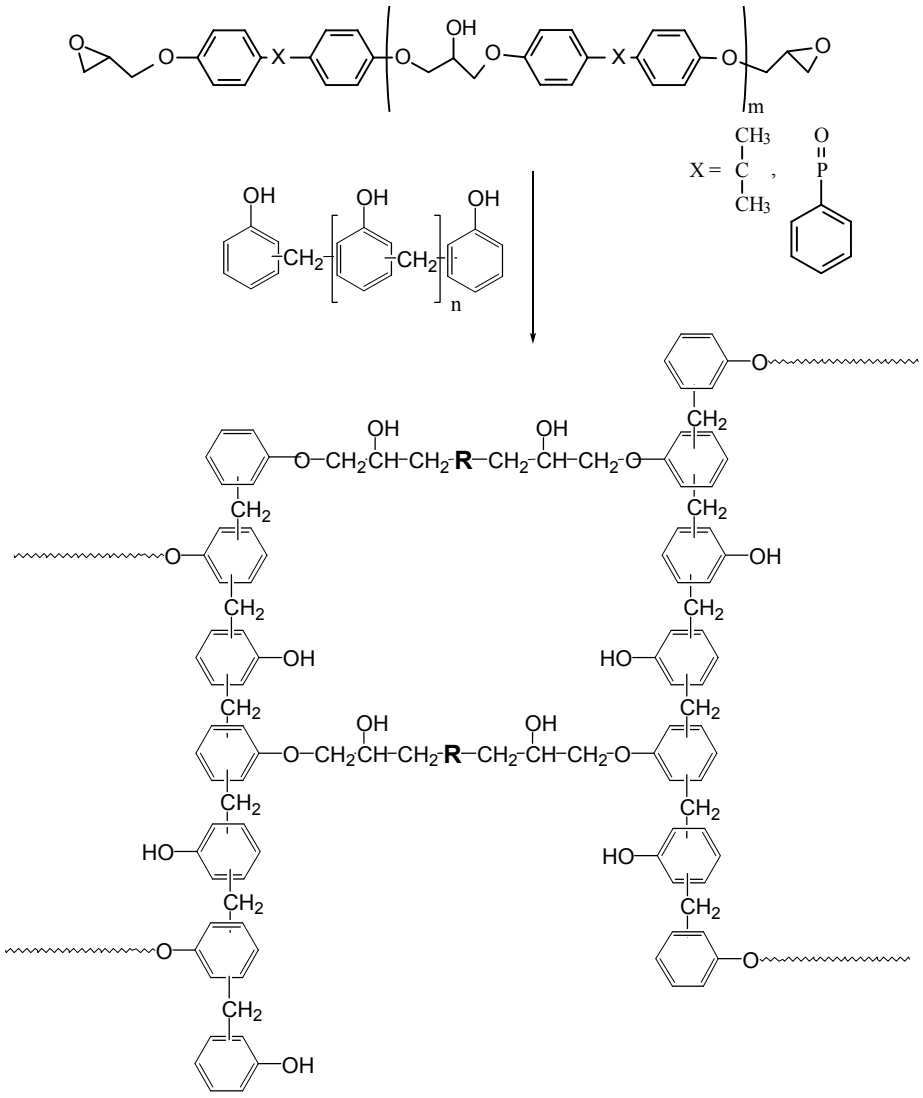

Figure 3-16. Epoxy-novolac network structure represented with bisphenol-A based epoxy.

3.4.2. Results and Discussion

Research has been done to establish the chemical and structure/property relationships of networks containing both a traditional diglycidal ether of bisphenol-A and an innovative triphenyl phosphine oxide epoxy resin. Thermosets have been prepared using a 741 g/mol novolac resin as the curing agent (Figure 3-16). The epoxy

systems were difunctional, while the novolac oligomers had an average functionality of 7.3 phenols/chain. The epoxide/phenol ratio was systematically varied to optimize network properties, such as toughness, and the epoxy structures have been tailored to improve flame retardance and adhesion.

The phosphine oxide diepoxide was synthesized via nucleophilic substitution of epichlorohydrin by a phenolate anion as discussed in section 3.3.2.1. It was determined that 30 % chain extension occurred and the molecular weight of the phosphine oxide diepoxide was 554 g/mol. The bisphenol-A based epoxy oligomer was 'shorter' with 10 % chain extension, which corresponded to an average molecular weight of 374 g/mol.

3.4.2.1. Network Series

A commercial novolac oligomer donated by Georgia Pacific was used to cure the epoxy resin. The phenolic novolac resin was formed by the condensation of phenol and formaldehyde under acidic conditions. The branched oligomer had an average functionality of 7.3 phenols/chain. In the cure reaction, the phenolic oxygen opened the oxirane ring via a substitution reaction and was followed by a proton transfer that resulted in an ether linkage. Since there were no by-products from the reaction a void-free network was formed. Networks have been prepared with different epoxide/phenol ratios and different concentrations of phosphine oxide. All resin systems were melt mixed at ~170°C and cured at 200°C for 1 hour and 220°C for 3 hours. Networks prepared with a 1/5 or 1/6 epoxide group/phenol group ratio had equivalent gel fractions of ~85 wt %.

To investigate the effect of the cure stoichiometry, two chemical series were investigated. Epoxide/phenol ratios were varied from 1/2 to 1/7 and epoxy content was 100 % bisphenol-A based epoxy resin or 100 % phosphine oxide containing epoxy (Table 3-5). These ratios corresponded to high levels of novolac loading, from 50 to 80 weight %. To investigate the effect of diepoxide oligomer chemistry, networks with 1/5 and 1/6 epoxide/phenol ratios were studied with varied concentrations of phosphorus. Within each series, networks were prepared with 100 mole % bisphenol-A epoxy, a 75 mole % bisphenol-A epoxy/25 mole % phosphine oxide epoxy blend, or a 50 mole % bisphenol-A epoxy/50 mole % phosphine oxide epoxy blend.

Table 3-5. Epoxy/novolac network compositions.

Bisphenol-A epoxy/ Phosphine oxide epoxy (mole %)	Epoxy/Novolac (weight ratio)				
	1 epoxide/ 7 phenols	1 epoxide/ 6 phenols	1 epoxide/ 5 phenols	1 epoxide/ 3 phenols	1 epoxide/ 2 phenols
100 % bis-A	20/80	22/78	26/74	35/65	50/50
75 % bis-A/25 % P=O	--	24/76	27/73	--	--
50 % bis-A/50 % P=O	--	26/74	28/72	--	--
100 % P=O	24/76	26/74	30/70	42/58	51/49

3.4.2.2. Hydrogen Bonding

To understand the effect of phosphine oxide on network properties, it was first necessary to understand the interactions between this polar functionality and the phenol groups in the network. Hydrogen bonding was observed in a model system using infrared spectroscopy (Figure 3-17). Triphenyl phosphine oxide was used during this study to view the phosphine oxide bond free of hydrogen bonding. Blends were prepared with the phenolic novolac resin in a 1/1 ratio of -P=O/-OH. The hydroxyl stretch of the novolac phenol unit shifted from 3345 cm^{-1} to a lower frequency, 3148 cm^{-1}, with the introduction of the polar phosphine oxide bond. A corresponding shift was noted for the phosphine oxide stretch from 1188 cm^{-1} for the triphenyl phosphine oxide to 1169 cm^{-1} when the phosphine oxide oxygen was interacting with the hydroxyl hydrogen on the phenol group. A larger shift was seen in the novolac networks compared to the siloxane networks (1175 cm-1) due the increased acidity of the phenolic proton. Hydrogen bonding persisted even at elevated temperatures. Upon heating the blend, the hydrogen bonded phosphine oxide peak was evident at 200°C (Figure 3-18).

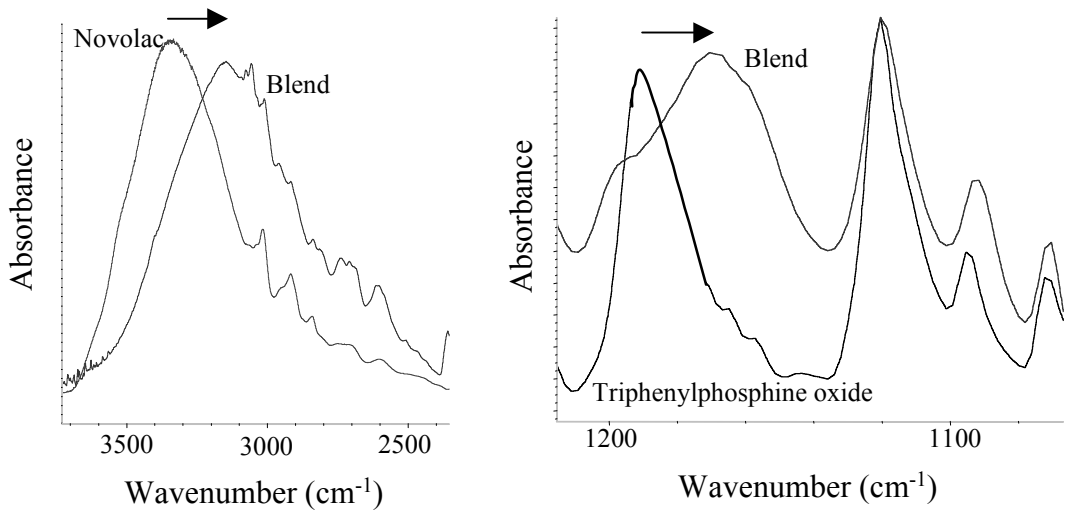

Figure 3-17. Both the phenol hydroxyl (left) and phosphine oxide (right) stretch shift to lower frequencies upon hydrogen bonding.

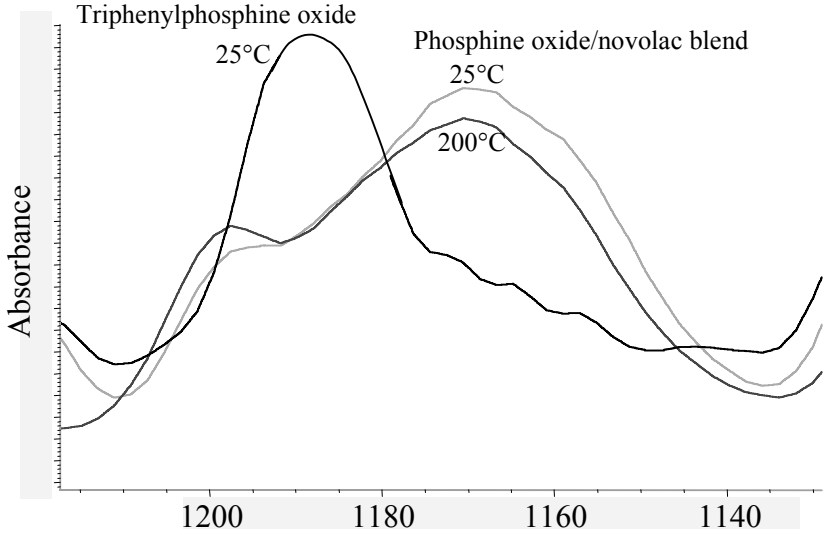

Figure 3-18. FTIR of phosphine oxide stretch without (triphenylphosphine oxide) and with (phosphine oxide/novolac blend) hydrogen bonding that persists at 200°C.

3.4.2.3. Crosslink Density

Properties of the networks were investigated in the rubbery regime, 45°C above the glass transition temperature of the networks. A further offset of the epoxide/phenol stoichiometry from 1/5 to 1/6 resulted in lower rubbery moduli (E') in each chemical series, while incorporation of the phosphine epoxy increased the E' of the thermosets (Figure 3-19). According the theory of rubber elasticity, E' was inversely proportional to the molecular weight between crosslinks (M_c) as discussed in section 3.3.2.3. This

approach considered only the physical structure of the network, not the chemical composition of the material[132]. The M_c increased as expected with a further offset in stoichiometry from 1/5 to 1/6. The molecular weights between crosslinks, determined experimentally also increased with stoichiometric offset for the 1/2, 1/3, and 1/7 bisphenol-A epoxy/novolac networks[120].

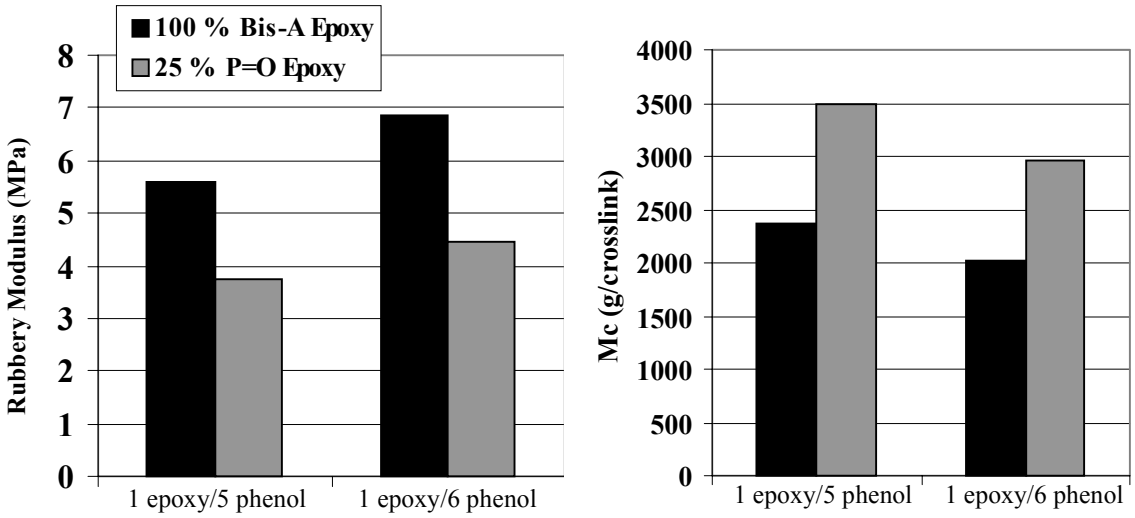

Figure 3-19. Rubbery modulus and molecular weight between crosslinks for 1/5 and 1/6 epoxy/phenol networks.

Based on the different molecular weights or "lengths" of the bisphenol-A and phosphine epoxy oligomers, incorporation of a longer phosphine oxide epoxy chain would be expected to result in an increase in M_c and a softer network above T_g. Instead, a stiffer network was obtained which corresponded to lower molecular weight segments. Ordinarily, the molecular weight of the segments between covalently bound crosslink points could be determined when intermolecular interactions were not contributing to the network properties above T_g. However, in this case strong hydrogen bonding occurred between the phosphine oxide and pendant phenol groups in the network. From FTIR, hydrogen bonding was observed at these elevated temperatures. In the phosphine oxide containing system the chemical nature of the network dominated the properties, even at >150°C, and effectively created crosslink points. Interestingly, this increased rubbery

[132] D.H. Kaelble, J. Moacanin and A. Gupta, Physical and Mechanical Properties of Cured Resins, Epoxy Resins: Chemistry and Technology, C. A. May, Ed., 1988, Marcel Dekker, Inc., 603-651.

modulus was not observed in epoxy networks formed with a siloxane crosslinking agent, which did not have strongly hydrogen bonding phenol moieties.

3.4.2.4. Network Characterization

The effect of epoxy/novolac composition on the network glass transition temperature (T_g) was studied in networks prepared with 100 % bisphenol-A epoxy or 100% phosphine oxide epoxy (Table 3-6). Within both chemical series, as the ratio of novolac to epoxy was increased, the glass transition decreased. The lower T_gs were due to the decrease in crosslink density with the larger offset in stoichiometry in going from 1 epoxide/2 phenols to 1 epoxide/7 phenols[118]. Chain mobility was increased with formation of more open networks. When the isopropylidene group was replaced with the strongly hydrogen-bonding phosphine oxide moiety, a large increase in the network T_g was seen at each epoxy/novolac composition (Table 3-6). For the 1/5 and 1/6 epoxy/phenol networks in which bisphenol-A epoxy/phosphine oxide epoxy blends were used, higher levels of phosphine oxide resulted in increased glass transitions (Table 3-7). In each of the networks, there was an excess of phenolic moieties that was able to hydrogen bond with the polar phosphine oxide functionality resulting in decreased chain mobility and elevated network glass transition temperatures.

Table 3-6. Effect of composition on T_g and fracture toughness.

Equiv Epoxide/ Phenol	Bis-A		P=O
	T_g * (°C)	K_{1c} (MPa-$m^{1/2}$)	T_g * (°C)
Epoxy control^	\	0.62	\
1/7	117	0.70	151
1/6	120	0.62	---
1/5	125	1.03	172
1/3	127	0.85	170
1/2	151	0.64	206

* T_g determined using DMA from peak of Tan delta

^ Bisphenol-A epoxy cured with DDS

The beta relaxations due to motion of the –[$CH_2CH(OH)CH_2O$]- segment[132] were observed at -35°C in the 1 epoxide/5 phenol networks. The β-transition of this aliphatic segment, often observed between -60°C and -30°C, occurred at -35°C in the bisphenol-A and phosphine oxide containing networks. These localized motions were removed not sensitive to hydrogen bonding of the phosphine oxide and phenol functionalities.

Fracture toughness of the networks was measured by determining the plane-strain stress intensity factor, K_{1c}. In previous studies, the bisphenol-A containing series toughness was found to improve with increasing offset in stoichiometry to a maximum of 1.03 MPa-$m^{1/2}$ for the ratio of 1 bisphenol-A epoxy/5 phenols[120], Table 3-6. This increase followed a decrease in network density. With larger molecular weight segments between crosslink points, chain mobility increased, allowing the network to absorb more energy and inhibit crack growth. However, when the stoichiometric offset became too large (1/6 and 1/7), the toughness decreased. For each epoxy blend, the toughness was lower for networks prepared with a 1/6 epoxy/phenol ratio than with a 1/5 epoxy/phenol ratio (Table 3-7). At the low epoxy/phenol ratios the three-dimensional structure of the network did not form sufficiently. More dangling ends and unconnected phenolic chains resulted in poor mechanical properties.

Table 3-7. Effect of phosphine oxide content on T_g and fracture toughness.

	100% Bisphenol-A		75/25		50/50	
Equiv Epoxy/ Phenol	T_g (°C)	K_{1c} (MPa-$m^{1/2}$)	T_g (°C)	K_{1c} (MPa-$m^{1/2}$)	T_g (°C)	K_{1c} (MPa-$m^{1/2}$)
1/6	120	0.62±0.09	124	0.46±0.02	129	0.31±0.04
1/5	125	1.03	140	0.68±0.05	119	0.43±0.05

The toughness of the 1/5 and 1/6 epoxide/phenol networks decreased with increased phosphine oxide concentration in both series (Table 3-7). This loss of toughness also corresponded to a decrease in the apparent M_c of the network. Epoxy network toughness has been attributed to the motion of the –[$CH_2CH(OH)CH_2O$]- segment[132]. These β-relaxations were evident in both the bisphenol-A and phosphine oxide containing networks at -35°C. It appeared that hydrogen bonding between the

phosphine oxide and aliphatic hydroxyl groups was not significant enough to damp this segmental motion. Phenol hydroxyl groups however were more strongly hydrogen bonding than aliphatic hydroxyl groups. Hydrogen-bonding between the phosphine oxide and the unreacted phenols may have led to a decrease in novolac chain mobility, reducing the fracture toughness.

Another benefit of phenolic resins was their flame retardance. However, the flame retardance of the phenolic network decreased with increasing levels of the epoxy component[118]. Replacing the isopropylidene group in the epoxy with a phenyl phosphine oxide resulted in a smaller loss of flame retardance in the 35 wt % epoxy/65 wt % novolac networks. To allow processing of the 15.24 x 15.24 x 1 cm^3 thermoset panels, a 23 wt % phosphine oxide epoxy/12 wt % bisphenol-A based epoxy blend was used. The flammability of two networks was investigated by cone calorimetry. The heat release, which is a vital consideration during a fire because it can affect the rate of burning, mass loss, and ignition of the surrounding environment was determined. The heat release rate decreased more rapidly in the phosphine oxide containing network, so while the peak heat release rate was the same for both compositions the total heat release was reduced from 132 MJ/m^2 in the bis-A network to 94 MJ/m^2 in the network containing phosphorus. Less CO_2 was evolved and the CO/CO_2 ratio was higher for phosphine oxide containing epoxy networks. The inorganic phosphorus resulted in a char layer that may have smothered the burn. No difference in char yield for the networks was apparent from thermogravimetric measurements. This may have been due to the inherently flame retardant nature of the phenolic component. A more pronounced effect of phosphorus improving thermal stability has been reported in networks with 75 wt % epoxy/25 wt % siloxane. In these predominantly epoxy networks, thermal properties were not governed by a high concentration of a flame retardant novolac component.

Water absorption was investigated at 22°C and at 60°C by monitoring the weight gain of submerged thin films. The offset in stoichiometry appears to affect the water uptake while the concentration of phosphine oxide did not. At 60°C networks prepared with the 1 epoxy/5 phenol ratio absorbed ~4 wt% water at equilibrium saturation and those with 1 epoxy to 6 phenols reached saturation at ~5.5 wt%. Two factors may have contributed to this increase in water uptake. With further offset in stoichiometry 1) M_c

increased resulting in a more open network and 2) the concentration of unreacted phenols was higher increasing the network polarity. Water absorption was anticipated to increase as the network polarity increased; however, no significant difference was seen with incorporation of phosphine oxide in either series. The inherently polar nature of the epoxy/novolac networks may have overshadowed additional effects of phosphine oxide or there may have been competing effects driving water absorption. With the addition of phosphine oxide, the apparent molecular weight between crosslinks decreased, which would decrease water absorption, so the increase in polarity is balanced by the decrease in M_c.

3.4.2.5. Adhesion Properties of Networks

Adhesion to glass/epoxy composites and to steel was studied using lap shear measurements. Bis-A epoxy/novolac networks with stoichiometries of 1/3, 1/5, and 1/7 epoxide/phenol ratio were investigated initially. The adhesive strength for the 1/3 and 1/5 networks on the composite adherends was the same (~15 MPa) with failure within the composite adherend (Figure 3-20).

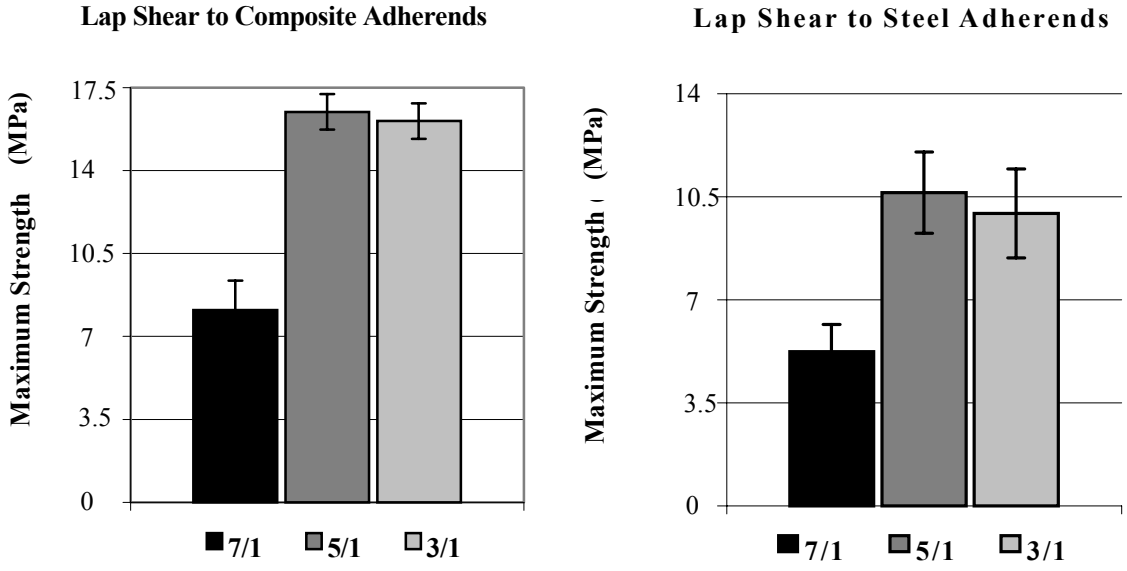

Figure 3-20. Maximum lap shear strength of bisphenol-A based networks to composite and steel adherends.

The epoxy composite failed before the adhesive network or the interfacial adhesion failed, making it impossible to compare the adhesive properties of these two

systems. The 1 epoxide/7 phenol network strength was significantly lower, 7.6 MPa (1100 psi), and cohesive failure occurred within the adhesive network. This performance difference can be attributed to poor network properties for the 1 epoxide/7 phenol system because of the large offset in stoichiometry. A similar trend was seen when steel adherends were used. The 1/7 bisphenol-A based network yielded a significantly lower bond strength than those of the 1/5 and 1/3 networks. From visual inspection, the mode of failure was also different, cohesive for the 1/7 and adhesive for the 1/5 and 1/3 systems.

The adhesion of the phosphine oxide containing 1/5 and 1/6 epoxy/phenol networks was also probed using lap shear tests to steel adherends (Figure 3-21). When 25% of the bis-A epoxy was replaced with phosphine oxide epoxy in the 1/5 network, adhesion to the steel was improved from 10.3 MPa (1500 psi) up to 14.5 MPa (2100 psi) with mixed mode failure. This improved adhesion to the steel is probably due to the increased hydrogen bonding capability of the network containing the phosphine oxide group. A further increase in phosphine oxide concentration resulted in a decrease in maximum sustained load and cohesive failure. At this level of phosphine oxide, the network is significantly more brittle and no longer had the mechanical integrity to sustain the load. Within the 6/1 series, all of the networks are more brittle and with addition of phosphine oxide, the adhesive strength decreases.

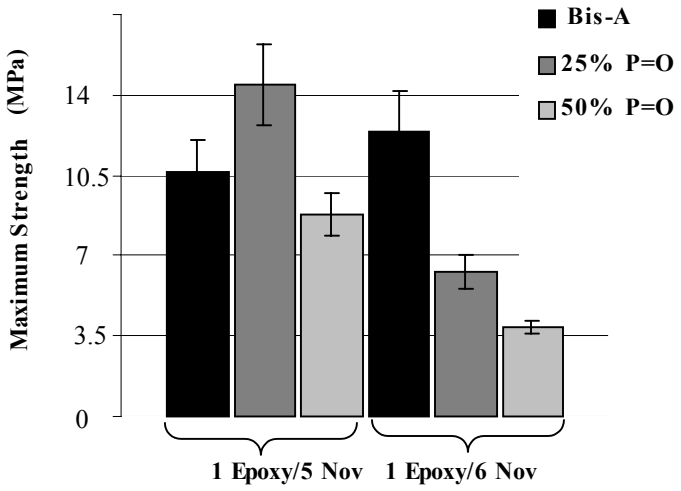

Figure 3-21. Maximum lap shear strength in 1/5 and 1/6 epoxide/phenol series with varied chemical composition.

A linear correlation was observed between the network fracture toughness and the lap shear strength of systems that failed cohesively (Figure 3-22). To improve the lap shear strength, it was necessary that the adhesive have a certain degree of mechanical integrity as well as adhesion to the surface being bonded.

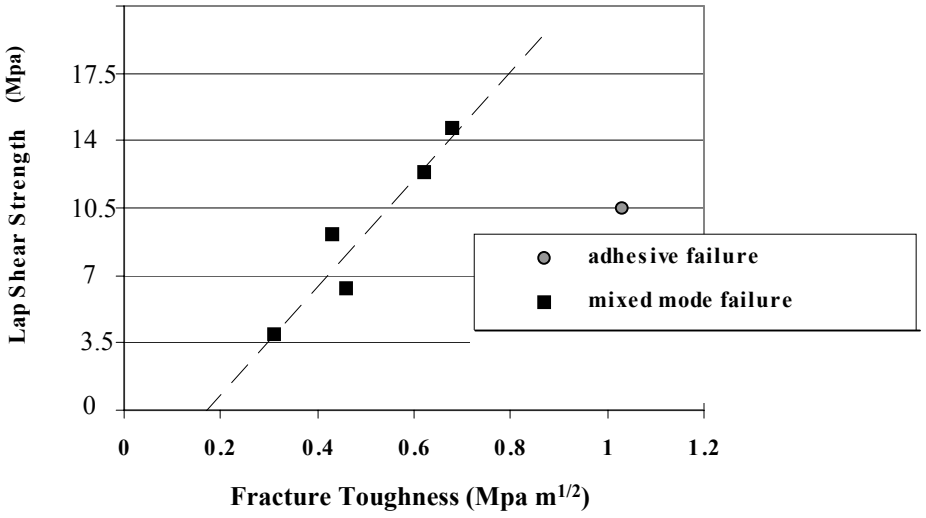

Figure 3-22. Linear correlation between maximum lap shear strength and fracture toughness for specimens showing mixed mode failure.

3.4.3. Conclusions

Incorporation of the strongly hydrogen bonding phosphine oxide diepoxide into epoxy/novolac networks resulted in a 40-50°C increase in the network T_g. The apparent M_c, as determined from the rubbery modulus, increased as expected with an increased offset in phenol/epoxide stoichiometry while it decreased with incorporation of the longer phosphine oxide oligomer. This decrease is likely due to the hydrogen bonding that occurs between the phenol groups and the polar phosphine oxide bond that is evident in the infrared spectrum. Increased bis-A epoxy concentration resulted in greater flexibility in the network corresponding to improved fracture toughness. The incorporation of the phosphine oxide group increased adhesion to steel adherends and improved the maximum load when the adhesive network had the mechanical integrity to sustain the load.

3.5. Conclusions

The siloxane and novolac crosslinking agents resulted in networks with varied properties. Incorporation of the siloxane yielded tough networks with rapid cures, while novolac thermosets possessed elevated glass transition temperatures and increased flame retardance.

The hydrogen bonding that occurred in the novolac networks was stronger than in the siloxane networks, as seen in the phosphine oxide FTIR peak shift (Figure 3-23). A phosphine oxide bond free of hydrogen bonding, as in triphenylphosphine oxide, was observed at 1188 cm^{-1}. The increased acidity of the phenol proton resulted in a stronger interaction (phosphine oxide IR peak shift to 1169 cm^{-1}) than that observed in the siloxane crosslinked network (peak shift to 1175 cm^{-1}).

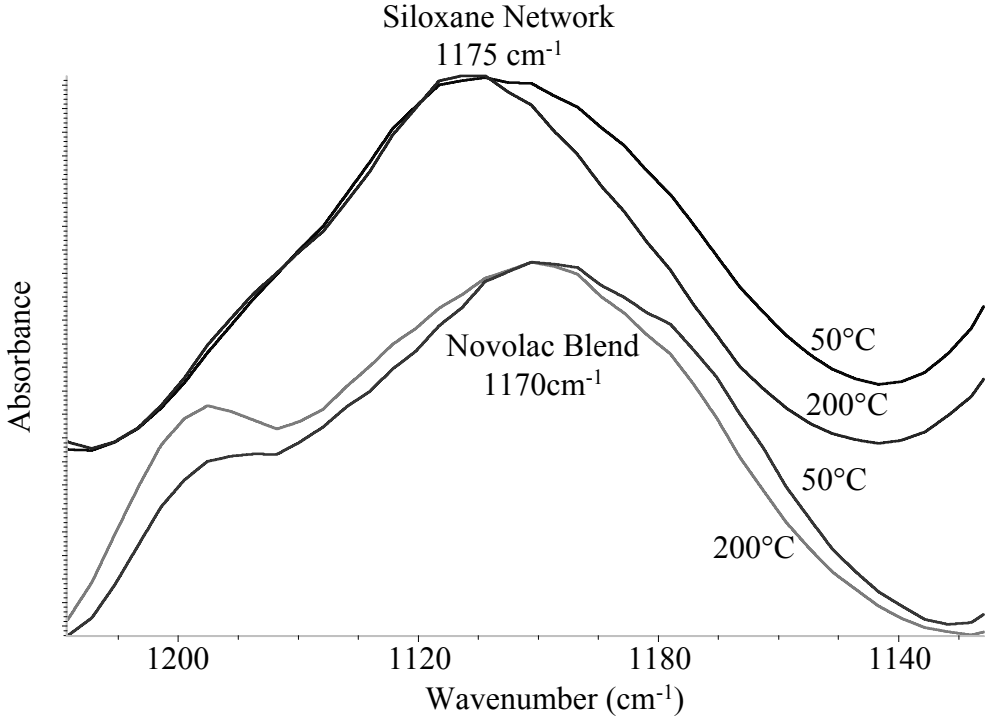

Figure 3-23. Phosphine oxide stretch in siloxane and novolac networks.

The weaker hydrogen bond in the siloxane network was more sensitive to increasing temperature. With a 150°C increase in temperature, the phosphine oxide peak narrowed more in the siloxane network than in the novolac system. The systems compared include two different phosphine oxide moieties. In the novolac spectrum, a blend of novolac and triphenylphosphine oxide was investigated. In the siloxane

network, the phosphine oxide epoxy was used because it was necessary for the epoxy/amine reaction to occur to liberate secondary hydroxyl groups to hydrogen bond. However, the trends were still valid. The ether groups of the epoxy increased the electron density of the phosphine oxide, shifting the peak to a lower frequency. The novolac blend still showed a shift to lower wavenumbers even with a less electron rich phosphine oxide.

The glass transition temperatures for the novolac networks were 120-200°C while the siloxane networks were much lower, 65-100°C. This was due to the difference in flexibility and wt % of the crosslinking agent. The novolac and siloxane networks contained ~75 wt % and ~20 wt % crosslinking agent, respectively. The stiff, hydrogen bonding novolac oligomer resulted in decreased network mobility even though the M_c was greater for these networks (2000-3500 g/crosslink) than the siloxane networks (700-1700 g/crosslink).

The increased weight % of phosphine oxide in the siloxane networks led to significant increases in water absorption while in the polar novolac networks, water uptake was not altered by addition of the phosphine oxide. In the novolac networks, phosphine oxide hydrogen bonded more strongly with unreacted phenols, which may have limited its interaction with water. Water absorption increased in the siloxane networks from 1 wt % in the bisphenol-A network to 5.5 wt % with incorporation of phosphine oxide. In the siloxane networks there was a greater concentration of phosphine oxide and there were no phenol groups with which to interact.

The bisphenol-A based siloxane networks were much tougher (2 MPa $m^{1/2}$) than the corresponding novolac networks (1 MPa $m^{1/2}$). The incorporation of the flexible siloxane segment increased chain mobility, as seen in the broader β-relaxation and the decreased network density (1.13 g/ml versus 1.25 g/ml for the novolac network). While toughness decreased with increasing phosphine oxide concentration, the siloxane toughness was more sensitive to the incorporation of 50 mol % phosphine oxide epoxy with a drop of ~1.5 MPa $m^{1/2}$ compared to a ~0.3 MPa $m^{1/2}$ decrease in novolac networks. This was due to phosphine oxide damping of the β-transitions in the siloxane networks. The phosphine oxide interacted with the secondary hydroxyl groups, while in

the novolac networks, the phosphine oxide hydrogen bonded with phenol groups rather than the aliphatic hydroxyl moieties.

Interestingly, the lap shear strength to steel adherends in the phosphine oxide containing thermosets was dominated by network toughness, regardless of the crosslinking agent used (Figure 3-24). Lap shear specimens to steel that failed either cohesively or in mixed mode exhibited a linear relationship between adhesive strength and fracture toughness. With tougher systems, above a threshold toughness, failure was dominated by interfacial strength. This suggests that by improving the surface preparation of the steel adherends to promote cohesive failure in the tough adhesives, much higher shear strengths could be achieved.

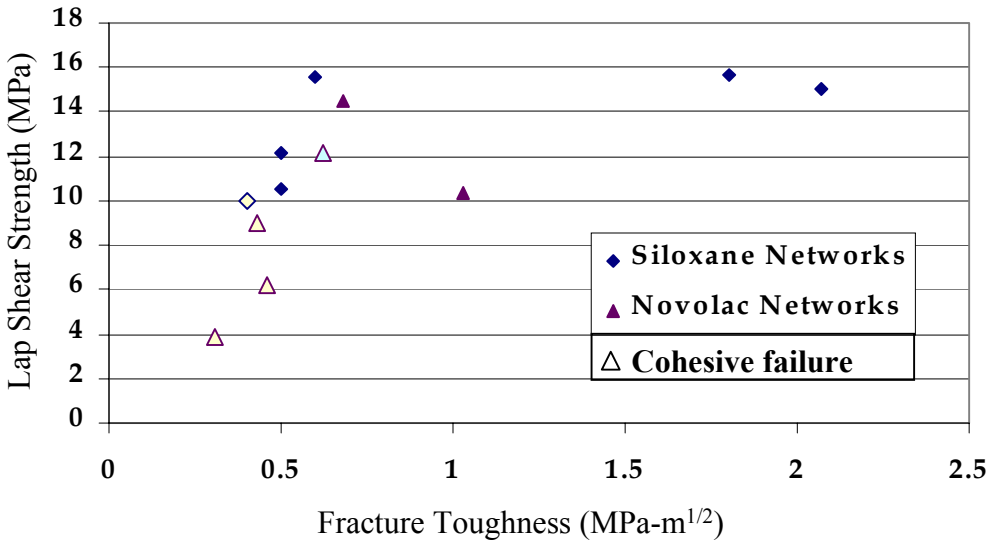

Figure 3-24. Linear relationship between lap shear strength to steel and fracture toughness.

The increased wt % of novolac, the increased hydrogen bonding between the phosphine oxide and phenol protons, and the lower flexibility of the novolac segment resulted in the properties of these systems being less sensitive to incorporation of phosphine oxide than were the properties of the siloxane crosslinked networks. The increased concentration of phosphine oxide, hydrogen bonding with aliphatic hydroxyl groups, and the flexibility of the siloxane segment resulted in the siloxane systems showing increases in glass transition temperatures, water absorption and thermal stability and decreases in fracture toughness and density.

Chapter 4. Vinyl Ester/Carbon Fiber Composites

4.1. Introduction

Polymer composites consisting of continuous reinforcing fibers embedded in polymeric matrices are becoming increasingly important as structural components for the infrastructure and construction industries due to their improved corrosion resistance and high strength/weight ratios compared to traditional metallic materials[133]. Carbon and glass reinforcing fibers with high moduli and strengths are typically used in these composites as the primary load bearing constituents. Rapidly processable polymer matrix resins include thermosetting materials such as epoxies, vinyl esters (dimethacrylate oligomers diluted with styrene), and unsaturated polyesters (polyester oligomers diluted with styrene). The matrices protect the brittle reinforcing fibers, bind them together, and transfer loads to the fibers via fiber-matrix adhesion.

The fatigue performance of these composites has been shown to be particularly sensitive to the structure of the fiber-matrix interphase regions[8,9,10,11]. This interphase can be defined as the region of finite thickness between the fiber and matrix with properties different from either the fiber or the matrix[11]. One method for controlling both fiber-matrix adhesion and the physical properties of the interphase region is to apply a sizing (i.e., a polymer coating on the fiber deposited from a polymer solution) to the surface of the fibers prior to impregnation with the matrix resin. The sizing may or may not form a gradient in chemical composition moving outward from the fiber due to interdiffusion of the fiber sizing with the matrix resin before and/or during the cure reaction (Figure 4-1). The durability and lifetime of vinyl ester matrix composites consisting of fibers sized with two dissimilar thermoplastics have been tested[134]. The carboxylate modified poly(hydroxyether) sizing, a ductile engineering thermoplastic, showed a 20-fold increase in the notched fatigue life of the vinyl ester composite compared to the unsized case, while that sized with the brittle poly(vinylpyrrolidone) exhibited only a 6-fold increase.

---

[133] G. Gray and G. Savage, *Metals Mater.*, 1989, **5**, 513.

[134] N. S. Broyles, K. E. Verghese, S. V. Davis, H. Li, R. M. Davis, J. J. Lesko, and J. S. Riffle, *Polymer*, 1998, **39**(15), 3417-3424.

Addition of a butadiene acrylonitrile based elastomeric interphase resulted in increased composite impact toughness when the sizing layer was <24 nm[106]. Increased interphase thickness resulted in poor stress transfer from the matrix to fiber and reduced composite performance. Relationships between the structure of these fiber-matrix interphase regions and the properties of the composites are not adequately understood. For example, the relative roles and importance of fiber-sizing adhesion, sizing-matrix adhesion, interphase morphology and interphase mechanical properties are not clear. This research addresses the design and characterization of carbon fiber-vinyl ester interphase regions. Data defining the relationships between interphase structure and composite performance are presented.

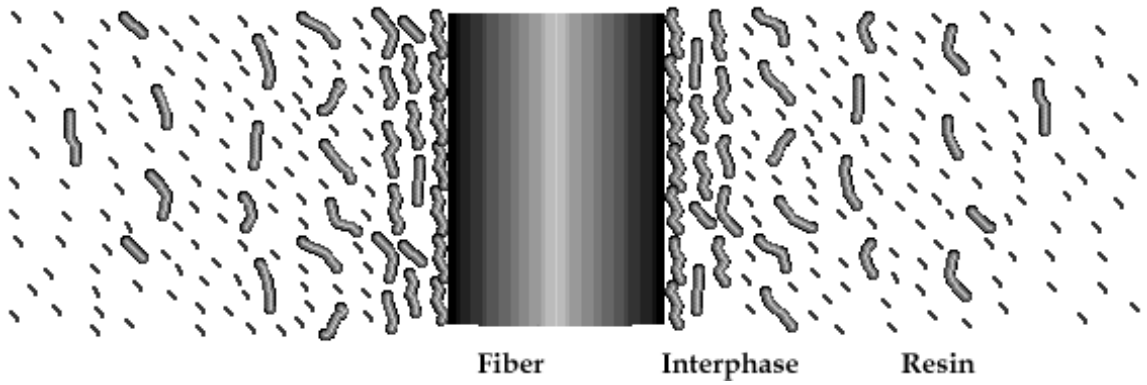

Figure 4-1. Ideal interphase development in fiber reinforced polymeric composite.

Interphase regions have been designed by tailoring tough ductile thermoplastic sizings to partially diffuse into a thermosetting matrix resin during cure to enhance sizing-matrix adhesion. The chemical and physical interactions between the fiber, sizing, and resin during composite fabrication result in an interphase region with a gradient in chemical composition and mechanical properties. One-phase polyurethanes containing polar phosphine oxide were synthesized and were also investigated as sizings. It was anticipated that incorporation of the strongly hydrogen bonding phosphine oxide moiety would increase adhesion between the fiber and sizing and promote interaction between the sizing and matrix.

4.2. Experimental

4.2.1. Materials

The carbon fibers were Hexcel AS-4 carbon fibers, which were oxidatively surface treated but unsized in a 12k tow. Polyaramid Nomex fibers and vinyl ester matrix material were kindly donated by DuPont and the Dow Chemical Co., respectively. The resin was 70 wt % vinyl ester oligomer (M_n of ≈700 g/mole) terminated with methacrylate groups diluted with 30 wt % styrene (Figure 4-2). Benzoyl peroxide (Aldrich) was used as received as the initiator for the free radical cure reaction.

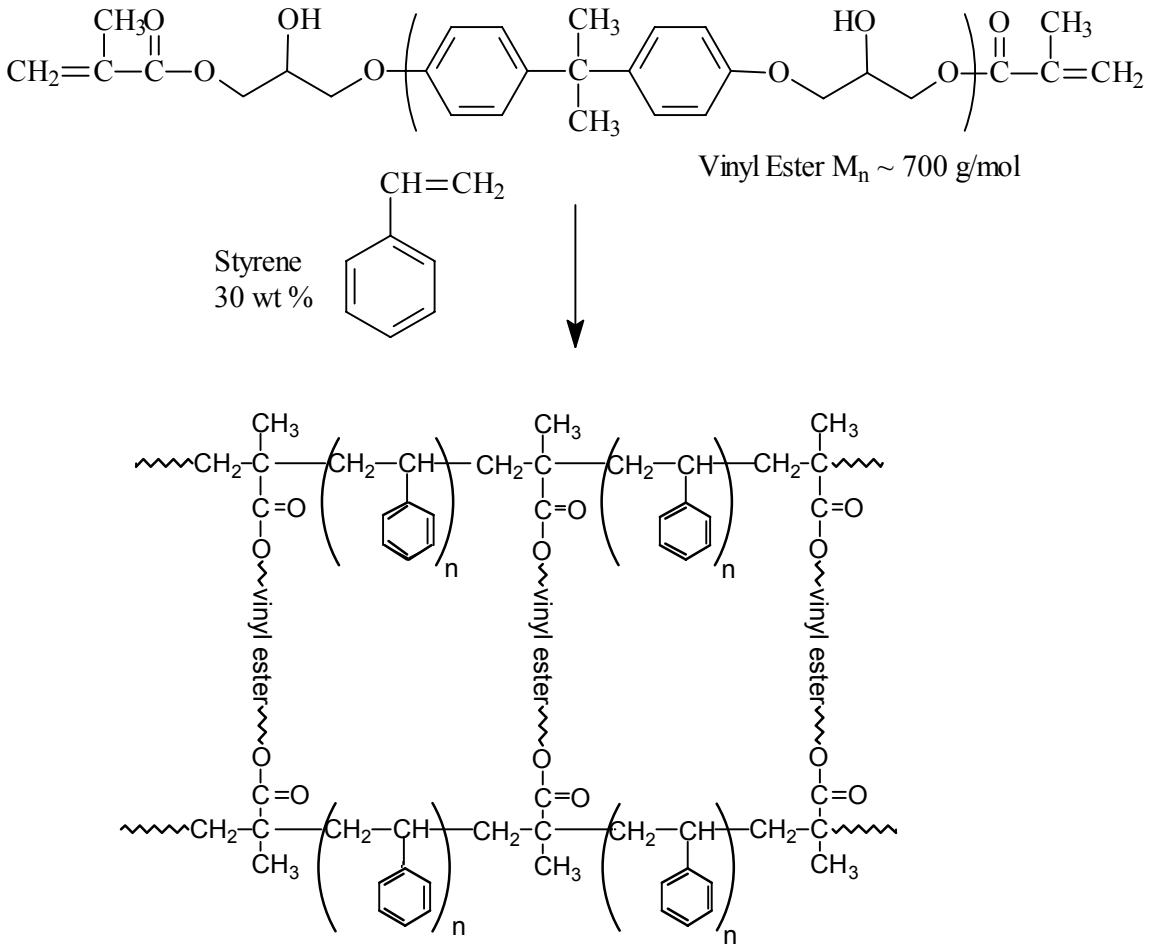

Figure 4-2. Vinyl ester network formation.

Reagent grade hexane, glycerol, and diiodomethane, were purchased from Aldrich and used as received. Deionized water was used for the dynamic contact angle analysis. The poly(hydroxyether), PKHH Phenoxy Resin, and the modified poly(hydroxyether)

sizing (PKHW-35 Phenoxy Resin), Figure 4-12, were kindly donated by Phenoxy Associates in Rock Hill, SC. The poly(hydroxyether) has been modified by grafting carboxylic acid groups on ~10 % of the repeat units to aid in obtaining a stable dispersion in water. The carboxylic acid grafted poly(hydroxyether) was obtained as a 35 wt % aqueous dispersion of ~1μm average diameter particles which was diluted to 2 wt. % with water for application to the carbon fibers. The poly(hydroxyether ethanolamine) thermoplastic, an ethanolamine chain extended bisphenol-A epoxy resin was also kindly supplied by the Dow Chemical Company. A 2 wt % solution was prepared for the sizing process by heating 3 vol % acetic acid in water to ~45°C and dissolving the thermoplastic in this solution.

For the polyurethane synthesis, two soft segment materials were investigated. The 1,170 g/mol Union Carbide polycaprolactone (PCL) and the 930 g/mol BASF polytetramethylene oxide (PTMO) were dried overnight at 70°C under a 500 mTorr vacuum. Methylethylketone (MEK) and isophorone diisocyanate (IPDI) were purchased from Aldrich. Di(3-hydroxypropyl) isobutyl phosphine oxide (DPPO) was donated by Avecia. Chain extenders, N-methyldiethanolamine (MDEA), and 1,4-butanediol (BD) and catalyst, dibutyltin dilaurate, were purchased from Aldrich.

4.2.1.1. Purification of Reagents

Methylethylketone

The MEK was dried over phosphorus pentoxide overnight. It was then distilled at ambient pressure at 79°C in a 110°C oil bath. Stored under nitrogen, the MEK was subsequently syringed into the reaction roundbottom flask.

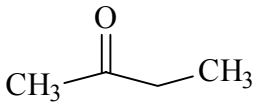

Figure 4-3. Methylethylketone (2-butanone).

Isophorone diisocynate

IPDI was distilled under 1 Torr vacuum at 140°C.

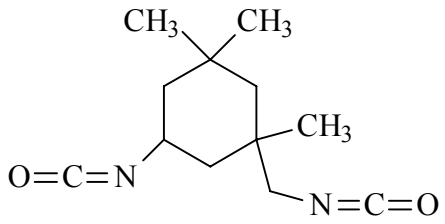

Figure 4-4. Isophoronediisocynate, mw = 222.29, density = 1.049 g/ml.

Di(3-hydroxypropyl) isobutyl phosphine oxide

DPPO was dried under a 1 Torr vacuum for 18 hours at ambient temperature prior to heating. The diol was then heated in a heating mantle to ~210°C and distilled.

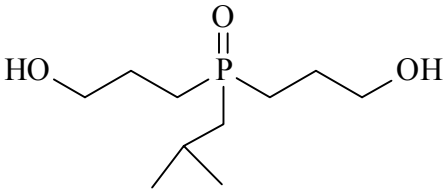

Figure 4-5. Di(3-hydroxypropyl) isobutyl phosphine oxide, mw = 222.26 g/mol.

N-Methyldiethanolamine

Molecular sieves were dried 18 hours at 200°C under vacuum. The MDEA was then dried over these sieves 3 hours and decanted into a roundbottom flask for distillation. The amine distilled at 89°C under a 1.5 Torr vacuum. The MDEA was stored under nitrogen and syringed into the reaction mixtures.

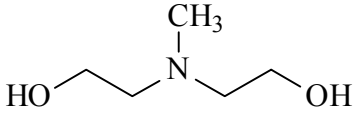

Figure 4-6. N-Methyldiethanolamine, mw = 119.16 g/mol, density = 1.038 g/ml.

1,4-Butanediol

The diol was distilled under 1 Torr vacuum at 180°C.

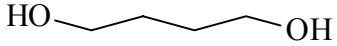

Figure 4-7. 1,4-Butanediol, mw = 98.19 g/mol, density =1.017 g/ml.

4.2.1.2. Network Preparation

The vinyl ester resin was cured via a free radical process. Benzoyl peroxide was used as a free radical initiator and added at 0.5 mole % per vinyl bond. The resin was degassed by applying a vacuum to remove oxygen, which inhibited the free radical reaction. The systems were cured at 140°C for one hour unless otherwise noted.

4.2.1.3. Aqueous Dispersions of Polyurethanes

Each polyurethane was dissolved in MEK to make a 10 weight % polyurethane solution. For each equivalent of the amine chain extender in the polyurethane, 1.1 equivalents of acetic acid were added. While stirring, water was added dropwise until the dispersion formed. With the addition of water the mixture began to grow cloudy at 2 % water due to immiscibility of MEK and water. The mixture became opaque at 6 % water due to formation of dispersed particles. At that point, water could be added quickly without disturbing the dispersion. The MEK was evaporated using a rotary evaporator with a water aspirator and a water bath at 60°C. Water was added to dilute the dispersion to yield an ~2 wt % solids dispersion. The dispersions were stable. However, as a precaution, the dispersions were used within 24 hours of preparation to size the fibers. Molecular weights of the dispersed polyurethanes were confirmed after three days. The dispersions were dried under vacuum at 80°C and by GPC no molecular weight loss or degradation of the polyurethanes were observed.

4.2.1.4. Sizing Carbon Fiber

The fiber tow was sized on a custom made small scale sizing line (Figure 4-8)[135]. The PKHW-35 Phenoxy Resin was obtained as a 35 wt % aqueous dispersion of ~1μm diameter particles and then diluted to ~2 wt % with water for sizing. A 3 % aqueous acetic acid solution was heated to 45°C and then poly(hydroxyether ethanolamine) was added and dissolved at a concentration of 2 wt % for the sizing process. Fibers were also sized with the polyurethane dispersions discussed above. The sized tow was wound onto a drumwinder and cut to 16.5 cm length plies. The plies were then dried at 150°C for 3 hours.

---

[135] Broyles, N. S., Chan, R., Davis, R. M., Lesko, J. J., and Riffle, J. S., *Polymer*, 1998, **39**(12), 2607-2613.

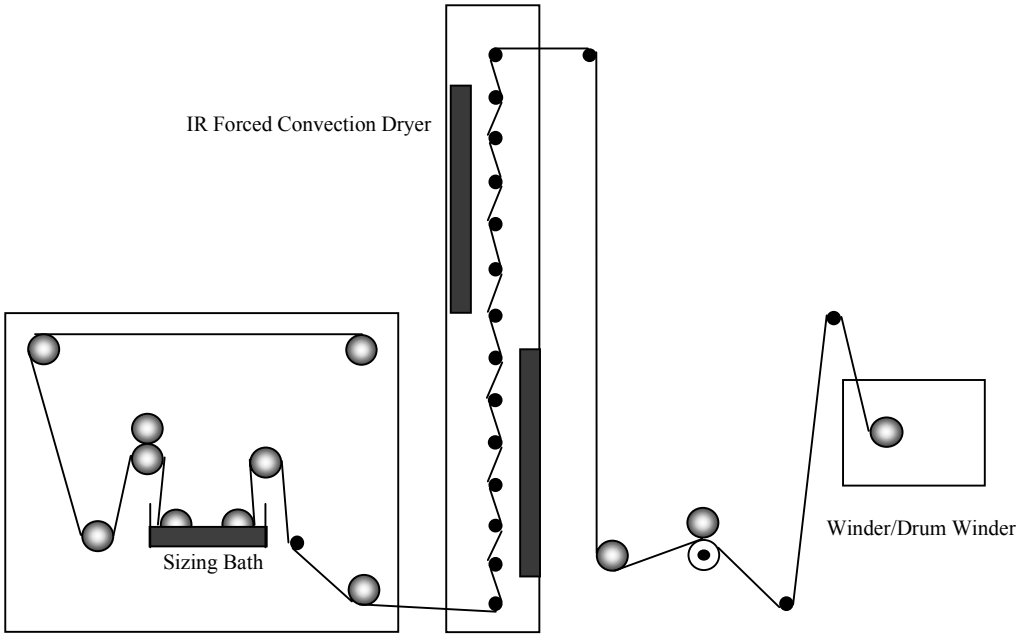

Figure 4-8. Small scale laboratory sizing line.

4.2.1.5. Single Fiber and Bilayer Model Composite Preparation

Model systems of the sizing materials and the vinyl ester matrix were prepared to study sizing-matrix interactions (Figure 4-9). Single fiber model composites were prepared by sizing Nomex fibers individually and drying. Fibers were coated with the sizing material from a 20 wt % solution in NMP for the poly(hydroxyether) and poly(hydroxyether ethanolamine) and from a 20 wt % aqueous dispersion of the carboxy modified polyhydroxyether. The fibers were then mounted on a copper frame and dried at 150˚C for 3 hours. A single fiber was embedded in the vinyl ester resin, which was then cured at 140°C for 1 hr with 0.5 mol % benzoyl peroxide.

Bilayers of both the poly(hydroxyether) and polyurethane thermoplastics were prepared. First, a thin film of the poly(hydroxyether) sizing material was cast and dried in a small silicone rubber mold. The carboxy modified poly(hydroxyether) and the poly(hydroxyether ethanolamine) films were cast from water while the poly(hydroxyether) film was cast from THF and dried under vacuum at 80°C for 18 hours. The polyurethane sizing material was cast from dichloromethane and dried under vacuum at 60°C for 18 hours. Then the vinyl ester (with benzoyl peroxide initiator) was

poured into the mold on top of each sizing material. This was immediately placed in a preheated oven (140°C) for 1 hour to cure.

Samples were then cut perpendicular to the fiber axis and investigated using TEM and AFM.

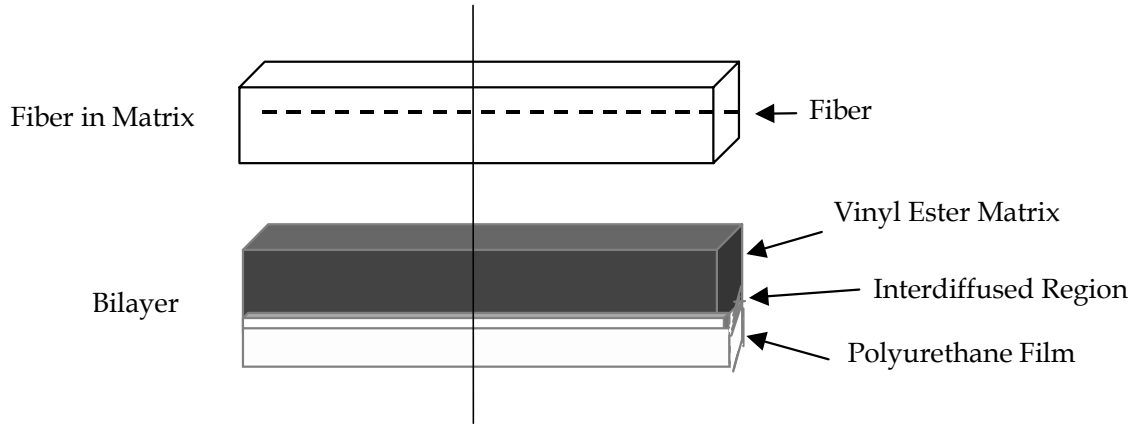

Figure 4-9. Single fiber and bilayers model composite systems.

4.2.1.6. Composite Preparation

To prepare the composite panels, the sized carbon plies were stitched at 3.8-5 cm intervals to hold the fibers in place. The amount of carboxy modified poly(hydroxyether) sizing based on fiber weight was 1.12%. At 64 % fiber volume in the composite panel, this corresponds to 0.8 % by weight sizing based on the weight of the total composite. The amount of poly(hydroxyether ethanolamine) sizing based on fiber weight was 1.5 wt %. At 60 vol % fiber in the panels, this corresponds to 0.7 wt % sizing based on the total composite weight. The vinyl ester matrix resin was prepared for the cure reaction by dissolving 0.5 mol % benzoyl peroxide in the vinyl ester resin at room temperature, then degassing under mild vacuum. No accelerator was used. Seven ply (crossply symmetrical about the center ply), 16.5 cm x 16.5 cm panels were cured using a resin infusion process on a Wabash model 9112 vacuum hot press by heating from 25°C to 150°C over 30 min., holding at 150°C for 20 minutes, then cooling to approximately room temperature over a period of 1 hour under pressure.

Fiber volume fractions of the composite panels used in these experiments were calculated by measuring their densities in air and in isopropyl alcohol. An ~4 gram sample of each composite was weighed in air, then immersed in isopropyl alcohol and

reweighed. The density of the composite was calculated using Archimedes' principle and Equation 4-1

$$\text{Equation 4-1} \quad \rho_{composite} = W_{air}\,\rho_{IPA} / (W_{air} - W_{IPA})$$

where $\rho_{composite}$ was the density of the composite, ρ_{IPA} was the density of isopropyl alcohol, W_{air} was the weight of the sample in air and W_{IPA} was the weight of the sample in isopropyl alcohol. The fiber volume fraction was then determined using the rule of mixtures where ν was the fiber volume fraction calculated from Equation 4-2,

$$\text{Equation 4-2} \quad \nu = (\rho_{composite} - \rho_{resin})/(\rho_{fiber} - \rho_{resin})$$

ρ_{fiber} was the density of the carbon fiber, and ρ_{resin} was the cured network density. The fiber volume fractions were estimated to be 0.60-0.62. The densities used for the fiber and resin were ρ_{fiber} = 1.78 g/ml (8) and ρ_{resin} = 1.18 g/ml[136].

As a quality control precaution, linear ultrasonic C-scans were conducted on all the composite materials. These tests were done using a Sonix HS1000 HiSPEED instrument. A 15 MHz, 32 mm focal length sensor was used. The data were analyzed using the FlexSCAN-C software provided with the instrument. The scans were gated both to the midplane as well as to the bottom surface of the specimens. These scans indicated a larger dissipation in the poly(hydroxyether ethanolamine) composite samples as compared to those with the carboxy modified poly(hydroxyether) sizing. This was postulated to be caused by poor interface adhesion in the former case as all the other material constituents were the same and no unusual porosity was observed by the C-scans in either of the composite systems.

4.2.2. Characterization

4.2.2.1. Scanning Electron Microscopy (SEM)

An ISI SX-40 scanning electron microscope was used to image the samples. Imaged fibers were secured using a conductive pressure sensitive adhesive. Polymeric

---

[136] H. Li, E. Burts, K. Bears, Q. Li, J.J.Lesko, D.A. Dillard, and J.S. Riffle, *J. Compos. Mater.*, 2000, **34**(18), 1512-1528.

bilayers and composite materials were sputter coated with gold and secured with a conductive silver-filled epoxy adhesive.

4.2.2.2. X-ray Photoelectron Spectroscopy (XPS)

Fibers were analyzed using a Perkin Elmer PHI 5400 X-ray photoelectron spectrometer operating at 17.9 V analyzer pass energy with a sampling angle of 45°. Peak binding energy positions were referenced to carbon at 285.0 eV binding energy as 532.9, 102.1, and 400.3 eV for oxygen, silicon, and nitrogen respectively. The atomic concentration of each element was analyzed based on peak areas. Two samples each were analyzed from three different spools.

4.2.2.3. Fiber Surface Energy

Using a method established by Good et al., the acidic and basic contributions to the fiber surface free energy were determined[137]. Individual carbon fibers were prepared for wettability analysis by attaching a 1.5 cm length of fiber to a copper hook with a cyanoacrylate adhesive. The wetting force was measured on a Cahn DCA balance at a stage speed of 20 μm/s to submerse and withdraw the fiber from the liquid (Figure 4-10).

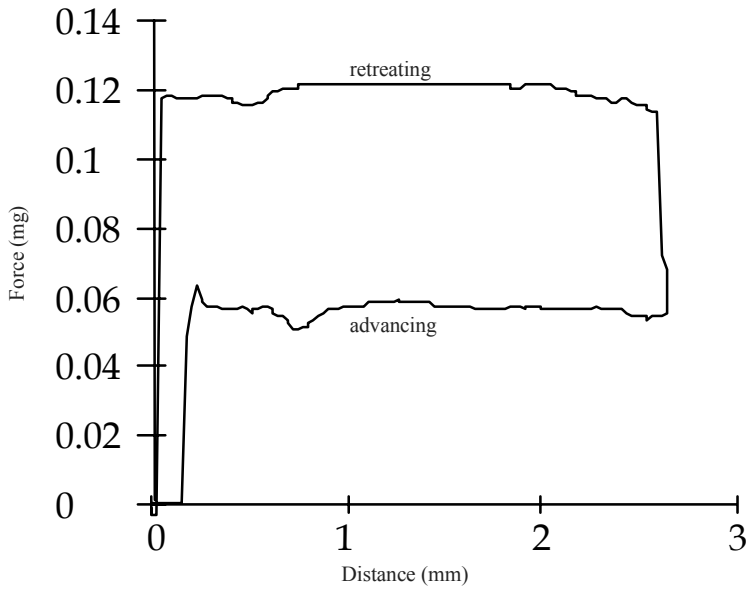

Figure 4-10. Force-displacement curve generated by the DCA.

[137] R.J. Good, N.R.Srivatsa, M. Islam, H. T. L. Huang and C.J. Van Oss, *J. Adhes. Sci. Technol.*, 1990, **4**(8), 607-617.

To reduce the error due to differences in fiber diameter, six fiber specimens were prepared and tested in each solvent. Fibers were cleaned with an acetone rinse and allowed to dry for 30 minutes under an infrared lamp in between wetting experiments. The perimeter of the fiber was determined using hexane and assuming total wetting. The acidic and basic components of the surface free energy were estimated by analyzing contact angles of water, glycerol, and diiodomethane on the fibers, discussed in section 4.3.2.

4.2.2.4. Gel Fraction Determination

To investigate the crosslinking reaction of the carboxy modified poly(hydroxyether), particles were precipitated from the aqueous dispersion. The 35 wt % dispersion was diluted to 10 wt % with dionized water. An equivalent volume of isopropanol was added to the dispersion while stirring. The precipitated particles were recovered via filtration, washed with water and dried in a vacuum at 60°C for 18 hours at which point the carboxylate modified poly(hydroxyether) was soluble in NMP. The particles were then cured at 150°C for 1 hour and 3 hours, similar to the drying process of the carboxy modified poly(hydroxyether) sized fibers, and weighed. The samples were extracted with dimethyl acetamide for three days and redried in a vacuum oven at 100°C for 18 hours. The remaining gel fractions were weighed.

4.2.2.5. Molecular Weight Determination

The molecular weights of the polyurethanes were determined via gel permeation chromatography (GPC). GPC was run on a Waters 150C equipped with refractive index and viscosity detectors, which allows for universal calibration, so that absolute molecular weights were measured. Samples were run at 60°C in NMP stirred over P_2O_5.

4.2.2.6. Thermal Analysis

A Perkin Elmer Dynamic Mechanical Analyzer 7e was used to measure the glass transitions in polyurethanes and polyurethane/vinyl ester blends using the three point bend mode at a frequency of 1 Hz. The temperature was ramped at 2.5˚C/min. The glass transition was taken as the onset of the drop in modulus for the neat polyurethanes and blends prepared with polytetramethylene oxide containing polyurethanes. The tan δ peak was observed for the blends prepared with the polyurethane having the polycaprolactone

soft segment. Blends were made in solution by dissolving vinyl ester, polyurethane, and 0.5 mol % benzoyl peroxide per vinyl bond in dichloromethane. To maintain integrity during the thermal scan, the polyurethanes and their blends were cast onto aluminum tabs from a dichloromethane solution and dried at 100˚C for 16 hours under vacuum. The blends were then cured at 140˚C for one hour. Modulus values, therefore, were not accurate because they represented the aluminum/polymer composite rather than the polyurethane or blend.

4.2.2.7. Atomic Force and Transmission Electron Microscopy

Atomic force microscopy (AFM) was utilized to image fibers, bilayers and composites as well as investigate the mechanical properties of the fiber/matrix interphase. Imaging was done using the Tapping Mode™ and nanohardness was determined using the force mode. Transmission electron microscopy (TEM) was used to image the interphase region of single fiber composites.

Individual carbon fibers, imaged using AFM, were adhered to the microscope stage with a pressure sensitive adhesive. Single fiber and bilayer model composites were also prepared for AFM imaging. These were cut through the middle perpendicular to the fiber axis (Figure 4-9) and microtomed to smooth the surface for AFM imaging and remove thin films for TEM imaging. The samples were initially trimmed with a razor blade to obtain a trapezoidal shape ~1 mm in length with the interface near the middle of the trapezoid. The single fiber model composites with the poly(hydroxyether) sized fibers were microtomed with a Reichert-Jung Ultracut E apparatus with a diamond knife at room temperature. Polyurethane/vinyl ester bilayers were cryotomed below 25°C due to the low glass transition temperature of the polyurethane. A Digital Instruments Dimension 3000 instrument with a Nanoscope IIIa controller was used to obtain the AFM images. The phase images were collected in the Tapping Mode™ using etched silicon tapping tips with spring constants in the 20-100 N/m range.

4.2.2.8. Nanoindentation

The nano-mechanical properties of the bilayer samples were also studied using the AFM apparatus. Digital Instruments indentation software and a diamond tipped cantilever with a 325 N/m spring constant was used to produce nanometer size

indentations in the cut surfaces of the cross-sectioned samples. Force-nanoindentation depth curves from these indentations were then corrected to remove tip deflection of the cantilever [78]. The tip deflection was calibrated using a sapphire substrate as an infinitely stiff material; then this component was removed from the data collected from the samples under study.

Force-distance curves were generated from the deflection-displacement data (Figure 2-40). The nanohardness (force at the maximum load per unit surface area of the indent) was calculated by converting the indentation depths to indentation surface areas from the known shape of the indenter.

4.2.2.9. Microhardness

Vicker's hardness, force per unit surface area of the indent using a four sided oblique pyramid, was found using a Tukon microhardness tester according to ASTM E384. Vinyl ester samples were prepared by curing films with 0.5 mol % benzoyl peroxide at 140˚C for one hour. Films of the poly(hydroxyether) and polyurethanes were cast from tetrahydrofuran and dichloromethane, respectively and dried at 80°C under vacuum for 18 hours. A four sided Vicker's diamond pyramid with a 136˚ angle between opposite sides was used to indent the samples at varied forces ranging from 0.01 N to 1 N.

4.2.2.10. Interfacial Shear Strength

The interfacial shear strength was obtained from microbond tests. A microbead of material was placed onto sized and unsized fibers. A micro-vise was used to hold the bead and was placed on a Mettler BB2400 balance connected to a personal computer. The fiber was pulled from the bead using an Instron 5567 at a speed of 0.3 mm/min. This adhesion study was conducted at the Kwangju Institute in Korea under the guidance of Dr. T. –H. Yoon.

Fibers, both sized and unsized, were used in micro-debond tests to determine the interfacial shear strength between the fibers and the matrices. Vinyl ester/carbon fiber samples for micro-debond tests were prepared by applying a small droplet of the vinyl ester resin containing 0.5 mol % benzoyl peroxide onto the carbon fiber that had been sized with each respective sizing (and also the unsized fiber). Then the droplets were

cured at 130°C for 20 min in nitrogen to avoid oxygen inhibition of the free radical reaction. Thermoplastic polymer/carbon fiber specimens were prepared by flowing a notched thin polymer film around the fiber above the polymer's glass transition temperature to form a droplet. The interfacial shear strength was calculated from the debonding load, fiber diameter and embedded fiber length using Equation 2-2, as the load required to debond the droplet per unit of fiber surface area covered by the droplet. At least 50 droplets were debonded for each material and the results were averaged

4.2.2.11. Quasi-static Compression

Quasi-static compression tests were conducted on an MTS test frame to assess composite strength. A loading rate of 91 kg per second was applied. This loading cycle was programmed into the Microprofiler that controlled the machine once a test was begun. A 5.08 cm test gauge length was used. The specimens were loaded into the grips at a grip pressure of 7 MPa and specimen alignment was ensured with a spirit level. Emory cloth (100 grit) was wrapped around the grip sections of the specimens to prevent slip.

4.2.2.12. Fatigue Tests

Fatigue tests were conducted using a sinusoidal, fully reversed tension-compression (R = -1) mode at a frequency of 10 Hz. Specimens were 15.2 cm x 2.54 cm x 0.25 cm. A 6.4 mm diameter hole was drilled in the center of the specimens to create a notch prior to testing. An MTS Model 632 extensiometer with a gauge length of 2.54 cm and a maximum strain limit of 4% was used to monitor strain. Aluminum extensiometer tabs were adhered to the composite specimen and used to hold the extensiometer in place. The signal from the extensiometer was amplified using a 2310 Vishay Measurements Group amplifier.

4.3. Carbon Fiber Surface Analysis

4.3.1. Synopsis

Composite materials were prepared from vinyl ester resin and continuous strand carbon fibers. Composite panels contained both sized and unsized fibers. In order to better understand the interaction between the fiber and the sizing materials or matrix

resin, the fiber surface was analyzed. X-ray photoelectron spectroscopy (XPS) was used to establish the atomic concentrations at the surface and Goode's surface energy analysis was used to determine the acidic and basic components of the surface free energy.

4.3.2. Results and Discussion

The surface of AS-4 unsized carbon fibers from Hexcel, used as vinyl ester composite reinforcing fibers, were characterized. Fibers, as seen by SEM (Figure 4-11), were ~7 μm in diameter. AFM showed surface striations parallel to the fiber axis, which has been reported previously[69]. These striations are due to graphitic ribbons of crystallites that developed during graphitization of the polyacrylonitrile at 1500°C[102].

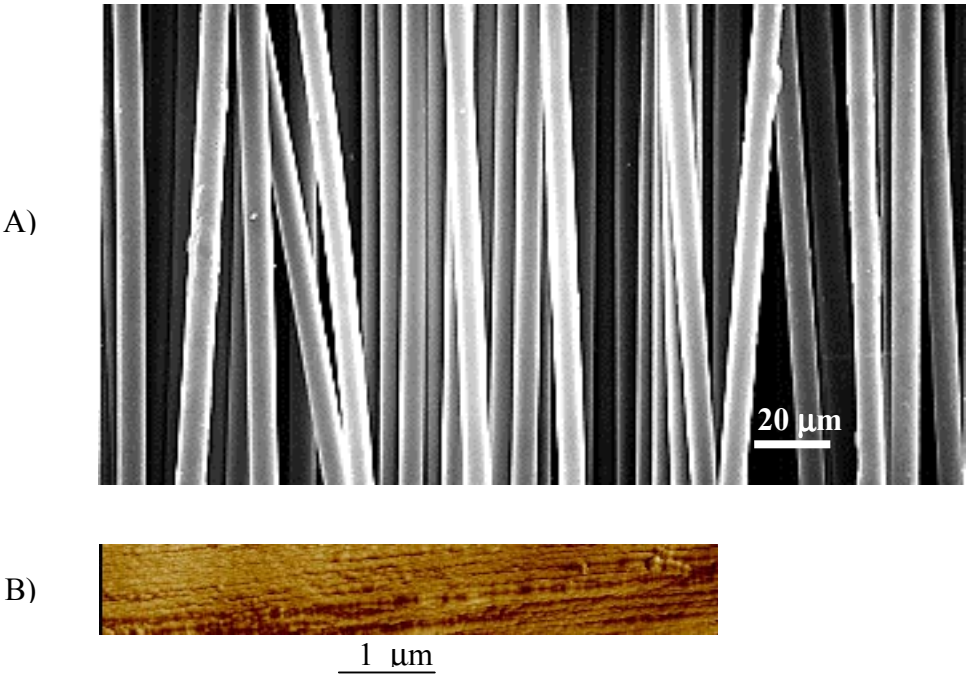

Figure 4-11. A) Scanning electron micrograph and B) atomic force micrograph of AS-4 surface treated, unsized carbon fibers.

The surface chemistry of the fibers was investigated using XPS and wettability measurements. The XPS showed that the fiber surface was 81-85 atomic % carbon. Nitrogen and silicon were on the surface at ~2-3 atomic % along with a significant amount, 10-13 atomic %, of oxygen. The atomic concentrations did not vary significantly between bundles. The oxygen was believed to be bonded to carbon as ether linkages or hydroxyl groups because no higher binding energy shoulder on the oxygen

peak, representing doubly bonded oxygens, were observed. It is assumed that the relatively high oxygen concentration originated from the proprietary electrochemical oxidative surface treatment applied by the supplier.

For this study, the surface free energy of a solid, γ_s, is considered to have an apolar, γ^d_s, and an acid-base component, γ^{AB}_s, as seen in Equation 4-3.

Equation 4-3 $\gamma_s = \gamma^d_s + \gamma^{AB}_s$

The apolar component is due to the dispersive, dipole-dipole, and induction forces; however, the dipole-dipole and induction forces are small compared to the dispersive force. The acid-base energy is due to interactions between two species and therefore differs from the dispersive energy, which is a property of a single material. However the acid-base energy is composed of two components, acidic (γ^+_s) and basic (γ^-_s), that are properties of the material. According to Equation 4-4

Equation 4-4 $\gamma^{AB}_s = 2\sqrt{\gamma^+_s \gamma^-_{fs}}$

the acid-base component is evident only in bipolar materials. A monopolar surface, either acidic or basic, would have an acid-base component of zero.

Using hexane and assuming total wetting of the fiber or a contact angle (θ) of zero, the perimeter (P) was calculated using the following equation.

Equation 4-5 $P\ (\mu m) = F\ (mg) * 9.8 \times 10^{-3} (mN/mg) / \gamma_l\ (mJ/m) * \cos\theta * 10^{-6}\ (m/\mu m)$

The calculated fiber diameter, equal to P/π, varied from 6.8±0.06 to 7.8±0.06 μm which is in good agreement with the diameter observed by SEM.

Table 4-1. Surface free energies for test liquids (mJ/m^2) [137].

	γ_l	γ^{LW}_l	γ^{AB}_l	γ^+_l	γ^-_l
Hexane	18.4	18.4	0	0	0
Water	72.8	21.8	51.0	25.5	25.5
Glycerol	64	34	30	3.9	54.7
Diiodomethane	50.8	50.8	0	0	0

Using contact angle analysis, a better understanding of the surface heteroatoms was obtained. The acid-base components of the surface free energy were calculated by analyzing contact angles of water, glycerol, and diiodomethane on the fibers, Table 4-2. Rearranging Equation 4-5, the contact angles of the liquids on the fibers were determined from the force experienced by the advancing and retracting fiber. From the contact angles in nonpolar diiodomethane, the non polar component of the surface free energy of the fiber was found using Young's equation

$$\text{Equation 4-6} \quad \gamma^d_f = \gamma^d_l (1+\cos\theta)^2 / 4$$

where γ^d_f and γ^d_l are the nonpolar components of the surface energy for the fiber and diiodomethane, respectively. θ is the contact angle of the liquid on the fiber.

Using the nonpolar components of the fiber and liquids, the acidic and basic parameters were calculated using Equation 4-7:

$$\text{Equation 4-7} \quad \gamma_l (1+\cos\theta) = 2(\sqrt{\gamma^d_l}\,\gamma^d_f + \sqrt{\gamma^+_l}\,\gamma^-_f + \sqrt{\gamma^-_l}\,\gamma^+_f)$$

where γ_l is the total surface free energy of the liquid while γ^+_l and γ^-_l are the acidic and basic components, respectively. Using data generated with two liquids having both acidic and basic contributions to their surface free energy, glycerol and water, two equations could be solved simultaneously to find the acidic (γ^+_f) component and basic (γ^-_f) component of the fiber surface free energy.

Table 4-2. Acidic and basic parameters of surface free energy of AS-4 fibers.

	Acidic contribution (δ^+)	Basic contribution (δ^-)
Advancing	19 mN/m	57 mN/m
Retreating	17 mN/m	59 mN/m

These parameters suggest that the fiber surface has both acidic moieties, such as hydroxyl groups and basic moieties, such as ether linkages, which is in agreement with XPS oxygen peaks. Therefore, the significant basic component suggests that adhesives with an acidic component such as a hydroxyl group, or a urethane might be particularly effective in forming hydrogen bonds with the fiber surface. The acidic component would

also be anticipated to interact favorably with electron donating functionalities, such as amine or phosphine oxide groups. The advancing and retreating energies were similar indicating the chemical homogeneity of the fiber surface.

4.3.3. Conclusions

The carbon fiber surface was analyzed. The fibers were ~7 μm in diameter, as determined from SEM, AFM and contact angle analysis. The surface chemistry of the carbon fiber would be expected to affect fiber-sizing adhesion. Therefore the atomic composition of the unsized carbon AS-4 fibers was characterized using XPS. As anticipated the surface was predominantly carbon with high levels (~10 atomic %) of oxygen. From the oxygen peak in XPS, the oxygen appeared to have only single bonds. The surface energy analysis revealed both acidic and basic moieties on the fiber surface, which may be attributed to hydroxyl and ether linkages, respectively. The high surface energy of the fiber should result in good wetting of the fiber by either sizing materials or the matrix resin and good interaction is possible with sizing materials containing either acidic or basic functionalities.

4.4. Polyhydroxyether Sizings

4.4.1. Synopsis

Fiber reinforced polymer matrix composites are finding increased use in structural applications where long term mechanical and environmental durability are key issues. This has prompted impetus for fundamental studies to determine relationships between the structure of fiber/matrix interphase regions and composite durability. The following research describes interphase and composite properties for a series of carbon fiber reinforced vinyl ester matrix composites wherein the fiber sizing chemical structure has been varied systematically in a series of ductile poly(hydroxyether)s (Figure 4-12). The mechanical properties of the sizings were similar. The primary difference among the systems studied was the amount of sizing-matrix interdiffusion and hence the microstructure of the interphase regions. The vinyl ester matrix consisted of a 700 g/mol vinyl ester oligomer diluted with 30 wt % styrene (Figure 4-2). A number of techniques

were used to evaluate both the "macro and micro" properties of the composites as a function of interphase structure. These include atomic force microscopy and nano-indentation to map sizing/matrix interdiffusion compositional gradients and the resulting mechanical properties across bilayer films comprised of the fiber "sizings" and vinyl ester matrices. Micro-debond tests were carried out to probe adhesion between the sized fibers and matrices. Fatigue cycling proved to be particularly useful in highlighting the influence of the tailored interphases on the durability of the carbon fiber/vinyl ester composites.

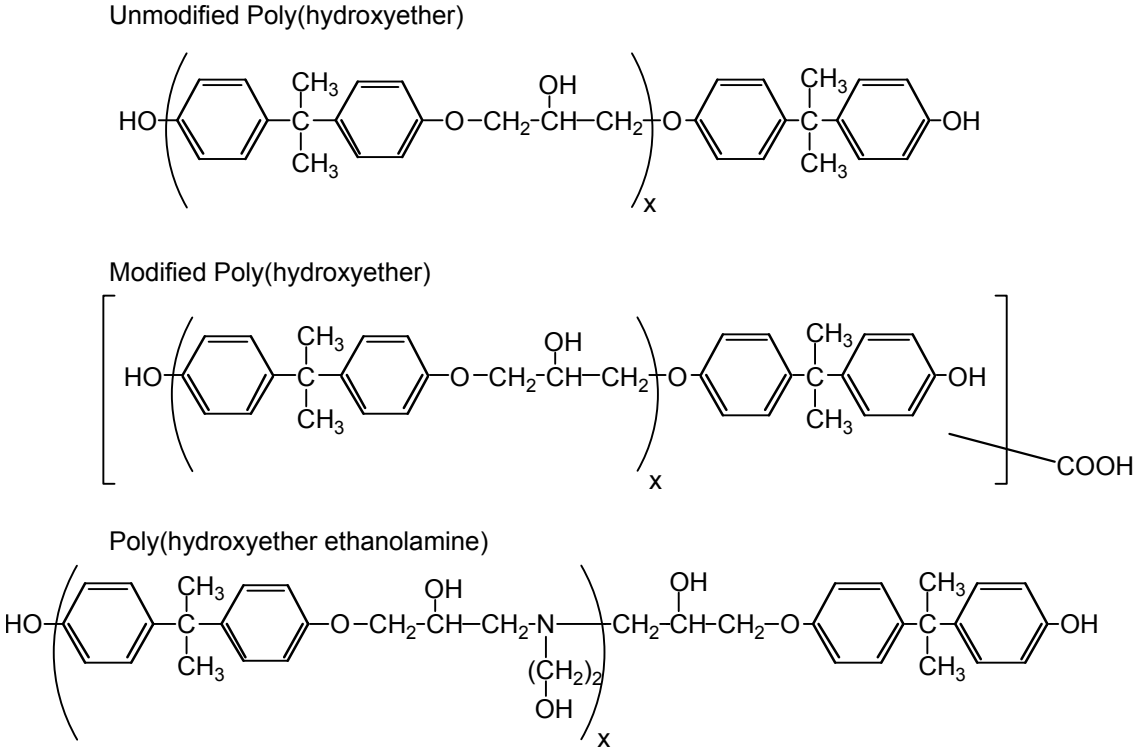

Figure 4-12. Poly(hydroxyether) sizing materials, unmodified poly(hydroxyether), carboxylate modified poly(hydroxyether), and poly(hydroxyether ethanolamine).

Composite fatigue properties of AS-4/vinyl ester composites having a tough, ductile polyhydroxyether thermoplastic in the "interphase" region were improved dramatically (relative to using unsized fibers) with <1 wt. % of the sizing in the composite. The thermoplastic sizing became miscible in the thermoset resin at the cure temperature, but microphase separated into ~90 nm diameter inclusions during matrix curing. A gradient in chemical composition and morphology resulted moving outward from the fiber into the thermoset matrix. It is hypothesized that the unusually good

fatigue resistance of composites from these materials can be at least partially attributed to this interphase gradient.

4.4.2. Results and Discussion

The objective of the following research was to relate composite fatigue properties and interfacial shear strengths of a series of carbon fiber reinforced vinyl ester matrix composites to sizing and interphase structure. Carbon fibers derived from a poly(acrylonitrile) precursor were surface treated by the supplier (Hexcel), sized in this study with a series of physically similar poly(hydroxyether) thermoplastics, and used as the reinforcing fibers with a vinyl ester-styrene matrix. It should be noted that the term "vinyl ester" refers to a family of matrix resins comprised of oligomeric poly(hydroxyether) backbones having methacrylate endgroups which are diluted with styrene monomer. The molecular weights of the vinyl ester prepolymers and the amount of styrene can be varied. For this research, the number average molecular weight of the dimethacrylate (vinyl ester) prepolymer was ~700 g/mole and this was diluted with 30 weight percent styrene. It is important that the constituents and concentrations of the particular resin composition are specified because the solubility of the sizings in the resin (and hence, the amount of sizing-resin interdiffusion) may differ as the resin composition is varied within the "vinyl ester" family.

The choices of sizing materials (Figure 4-12) were based on the anticipated need for (1) limited (but finite) solubility in the matrix resin during cure, (2) tough, ductile mechanical properties in the interphase region, and (3) to have strongly hydrogen bonding groups (e.g., acidic hydroxyl groups) in the polymer chain to enhance fiber-sizing adhesion. The "limited solubility" characteristic between sizing and matrix resin was an attempt to control sizing-matrix interdiffusion to maintain an interphase region containing the ductile polymeric sizing, yet have sufficient interdiffusion to achieve good sizing-matrix adhesion. The sizings, the poly(hydroxyether), the carboxy modified poly(hydroxyether) and the poly(hydroxyether ethanolamine), had similar chemical structures to the vinyl ester prepolymer component of the matrix resin but the polymers were not soluble in the matrix resin at room temperature.

Interphase regions between the sizings and matrix were examined in the attempt to relate the structure of these regions to composite fatigue performance. The interdiffusion and resultant morphologies of interphase regions between each sizing and the vinyl ester network were examined by constructing single fiber model composites, then microtoming cross-sections and studying them using atomic force microscopy and transmission electron microscopy (Figure 4-13). Model composites were prepared using polyimide Nomex fibers. Carbon fibers were brittle and shattered during microtoming while tougher Nomex fibers allowed the interphase region to remain intact during microtoming, so that it could be imaged. The relative size of the interphase regions where visible interdiffusion between the sizings and the vinyl ester matrix occurred, decreased in the order unmodified poly(hydroxyether) > carboxy modified poly(hydroxyether) > poly(hydroxyether ethanolamine) (no visible interdiffusion).

The interdiffused sections of the interphase region for the unmodified poly(hydroxyether) sizing consisted of a homogeneous dispersion of relatively spherical inclusions 80 - 90 nm in diameter of the poly(hydroxyether) material embedded in the vinyl ester continuous matrix. It is believed that this sizing partially dissolved in the matrix resin at the elevated cure temperature and phase segregated as the network formed (i.e., as high molecular weight was achieved for the ester resin). The small size of the inclusions may have been related to the fact that full cure took place within 3-5 minutes under the conditions used and the rapid reaction kinetics inhibited growth of the poly(hydroxyether) domains. With the addition of carboxylate groups, the sizing material became reactive. When the composite panels investigated were prepared, the plies were "pre-dried" for three hours prior to panel fabrication. Gelation studies on the carboxy modified poly(hydroxyether) sizing material suggested that during the 3 hour ply drying process, this sizing crosslinked. Cure studies showed that after one hour at 150°C, there was a 44 % gel fraction and after three hours, there was a 65 % gel fraction. This light crosslinking probably limited the mobility of this sizing as panels were prepared, and thus a significant fraction of sizing material was maintained in the interphase region. The interphase region derived from the carboxylate modified poly(hydroxyether) interphase showed a morphology with ~ 1 micron diameter "droplets" embedded in a mixed continuous phase. The droplet formation was attributed to light crosslinking of the

dispersed carboxy modified poly(hydroxether) particles, which were similar in size to the morphological features observed at the interphase. This interphase composition and morphology may be related to the enhanced composite properties found for this system.

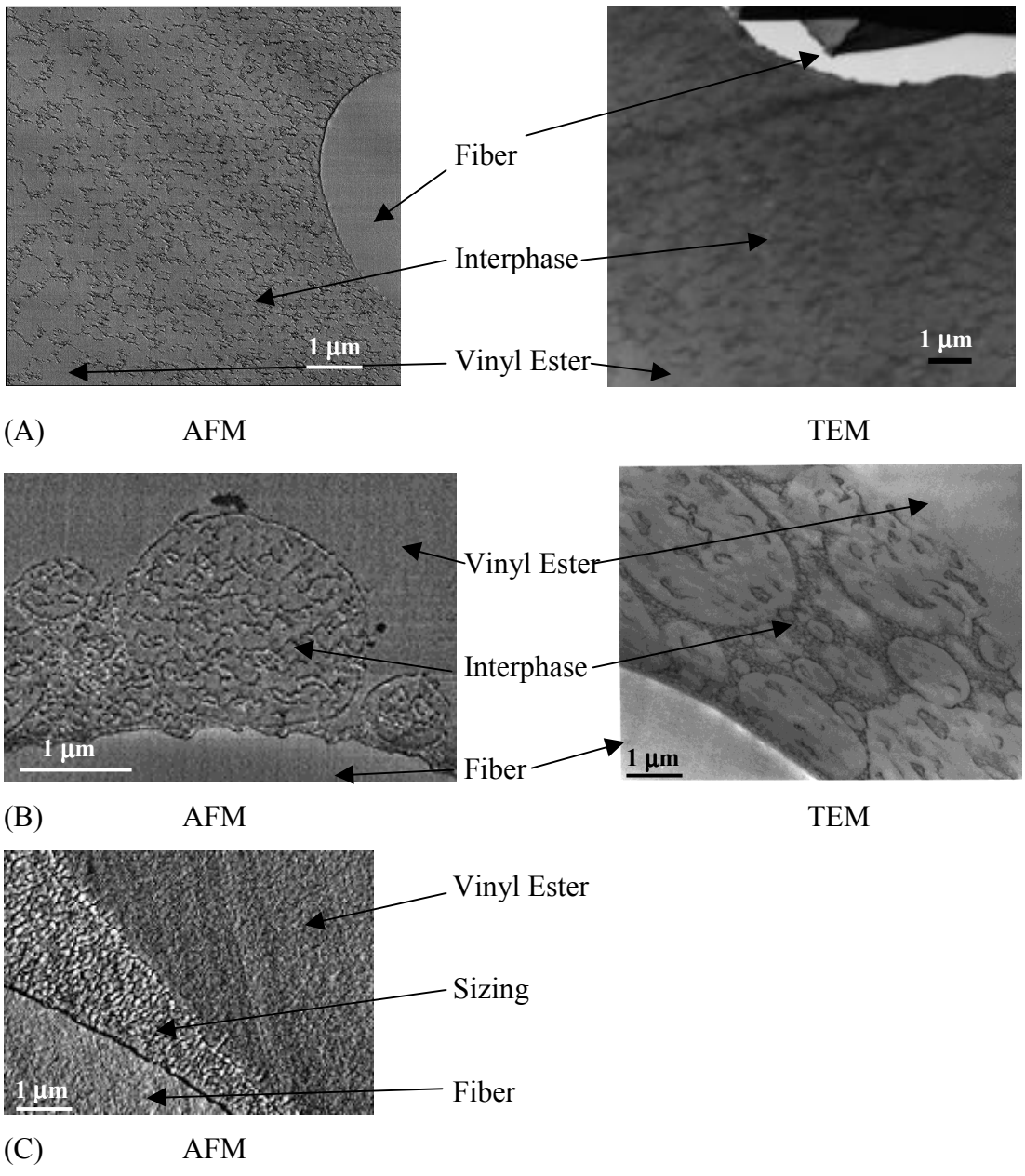

Figure 4-13. Atomic force and transmission electron microscopy images of Nomex/vinyl ester single fiber composites illustrating relative interdiffusion of the adhesives with the matrix; (A) poly(hydroxyether), (B) carboxy modified poly(hydroxyether) and (C) poly(hydroxyether ethanolamine).

The poly(hydroxyether) became miscible with the vinyl ester resin at elevated temperatures while the poly(hydroxyether ethanolamine), which had an amine group in every repeat unit, did not. A sharp interface was observed between the amine sizing and vinyl ester matrix because there was little interaction between the two components during the matrix cure. The carboxylate modified poly(hydroxyether) lightly crosslinked during the drying of the sized fiber. The breadth of the interdiffused region decreased in the order unmodified poly(hydroxyether) > carboxy modified poly(hydroxyether) > poly(hydroxyether ethanolamine). An ~ 10 μm wide compositional gradient was evident in the unmodified poly(hydroxyether)/vinyl ester model composite as compared to the much smaller gradient region for the carboxy modified poly(hydroxyether), and no interdiffusion was evident for the more polar poly(hydroxyether ethanolamine) sizing in the vinyl ester resin. The sizing materials had similar mechanical properties. The difference lies in the interphase structure formed, which allowed comparison of the composite performance versus the structures of the different interphase regions. As will be discussed later in this chapter, the fatigue properties of composites from these materials were far superior for the carboxy modified poly(hydroxyether) sizing case. Thus, the enhanced composite fatigue results may indeed be dependent on having a sizing with limited, but finite, interdiffusion with the matrix resin during cure.

4.4.2.1. Interphase Property Variations

One property of particular interest is the variation of yield strength across the interphase region because information about yield strength within the interphase region can assist in establishing failure criteria for assessing the onset of damage via maximum shear stress failure criteria. Interphase profiles for sizing-matrix bilayers (no fibers present) have been probed and nanohardness as a function of position is reported.

A nano-indentation technique using the AFM apparatus was used to profile the compositions in the interphase regions for the vinyl ester - poly(hydroxyether) bilayers and the nanohardness was calculated[75]. An example of this is depicted in Figure 4-14, which shows a number of indentations across an interphase region. Force-indentation depth curves for each point across the interphase regions were derived from these measurements by programming the apparatus to indent until a set tip deflection was reached, retract, then to repeat the same process 750 nm removed. This spacing ensured

that each successive indent was well removed from the stress field of the preceding indent.

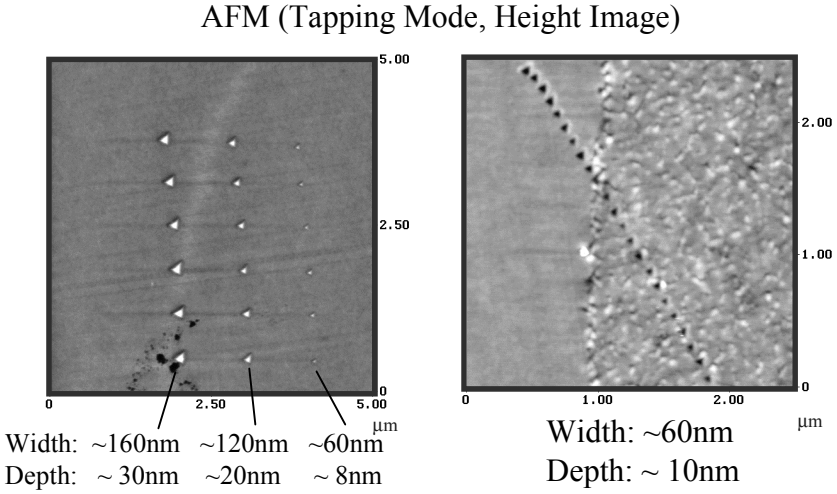

Figure 4-14. Nanoindentations at three decreasing forces (left) and across an interphase (right).

Figure 4-15 depicts examples of force-distance curves from indentations across a carboxy modified poly(hydroxyether) sizing-vinyl ester matrix sample. The force-distance curves for the poly(hydroxyether ethanolamine) were similar to those for the carboxy modified poly(hydroxyether). This was expected because of the chemical similarity of these two materials. As each position was indented, the force increased with depth due to a combination of plastic and elastic deformation; then the force decreased as the tip was retracted. Hysteresis between the indention and retraction curves was attributed to plastic deformation[138]. As expected, the data indicated that the depth of the indents were greater for the thermoplastic carboxy modified poly(hydroxyether) and that it also had a larger degree of plastic deformation relative to the thermoset vinyl ester.

It was noticed that for all indents there was a "pile-up" of material around the top of the indentations. The degree of "pile-up" varied across the interphase regions with the thermoplastic sizing materials showing a larger amount than the thermoset matrices. This

[138] M.F. Doerner and W.D. Nix, *J. Mater. Res.*, 1986, **1**, 601.

phenomenon was attributed to material actually being moved out of the hole during indentation. It was reasoned that this might affect the absolute values of the depths since attempts were made to differentiate the elastic and plastic components of the indentation responses. However, it is not expected to change the general trends for each component across the interphases[139,140].

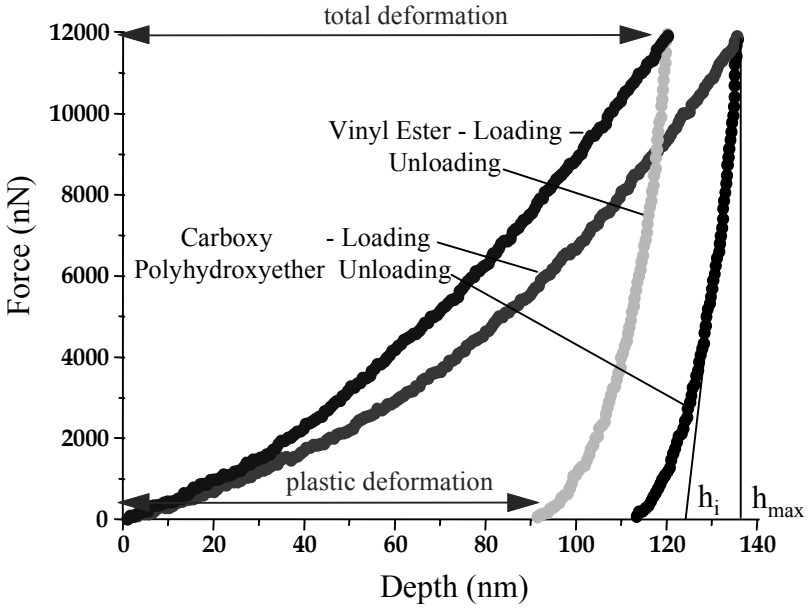

Figure 4-15. Force-depth curves for nanoindents of vinyl ester matrix and carboxy modified poly(hydroxyether).

Nanohardness was calculated from deflection-displacement curves generated by the AFM instrument. The deflection of the cantilever was removed from the data to give the force/distance curve seen in Figure 4-15. Extrapolating the intercept depth (h_i) and the maximum depth (h_{max}) from the force/distance curve, Equation 4-8 was used to calculate the contact depth (H_c).

$$\text{Equation 4-8} \quad H_c = h_{max} - \varepsilon (h_{max} - h_i)$$

[139] Tsui, T. Y., Oliver, W. C., and Pharr, G. M., *Mat. Res. Soc. Symp. Proc*. 1997, **436**, 207-212.

[140] Bolshakov, A., Oliver, W. C., and Pharr, G. M., *Mat. Res. Soc. Symp. Proc*. 1997, **436**, 141-146.

The constant ε was a function of the shape of the indenter tip (0.75 for a 3 sided pyramidal indenter). Knowing the shape of the diamond tip (a three sided pyramid with a face to vertex angle of 60º), the contact area was calculated. Dividing the force by the contact area yielded hardness, 1.3 GPa for pure vinyl ester and 0.8 GPa for poly(hydroxyether).

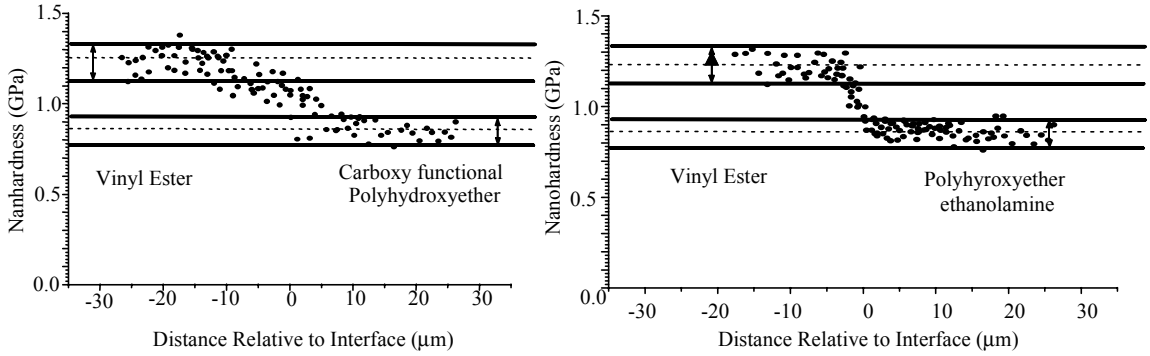

Figure 4-16. Nanohardness across carboxy modified poly(hydroxyether)/vinyl ester and poly(hydroxyether ethanolamine)/vinyl ester bilayers.

The nanohardnesses of the indentations made across the interphase region of the carboxy modified poly(hydroxyether)-vinyl ester bilayer are depicted in Figure 4-16. The dotted lines in Figure 4-16 represent average values (for at least 10 indentations) for indentation in the vinyl ester and the specific polyhydroxyether, while the solid lines represent 2 standard deviations from these average values. The indents increased in depth from the vinyl ester to the carboxy modified poly(hydroxyether) side of the bilayer, indicating the expected decrease in hardness from the brittle crosslinked vinyl ester matrix to the ductile thermoplastic sizing. The data also indicated a gradient across the interphase extending ≈10-15 μm from the vinyl ester to the interface and ≈5 μm into the carboxy modified poly(hydroxyether) side of the bilayer. The zero point on the graphs was arbitrarily set as the point where the themoset-thermoplastic interface was observed via an optical microscope. The gradient characterized using nano-indentation on the vinyl ester side of the interphase corresponded well with the AFM image of this system. The process of interphase formation probably consisted of the uncured vinyl ester resin

swelling the carboxy modified poly(hydroxyether) and then for the latter to diffuse out into the vinyl ester material. Following this course, it was expected that the gradient in properties extended into the carboxy modified poly(hydroxyether) side of the interphase region as seen in the nano-mechanical data. In contrast to the ≈15-20 μm interphase observed in the carboxy modified poly(hydroxyether) - vinyl ester bilayer, the interphase region for the poly(hydroxyether ethanolamine) and the nano-mechanical data showed a sharper interphase with a breadth of only ≈1-2 μm. This was consistent with the qualitative observation that very poor adhesion existed between these two materials in the bilayers.

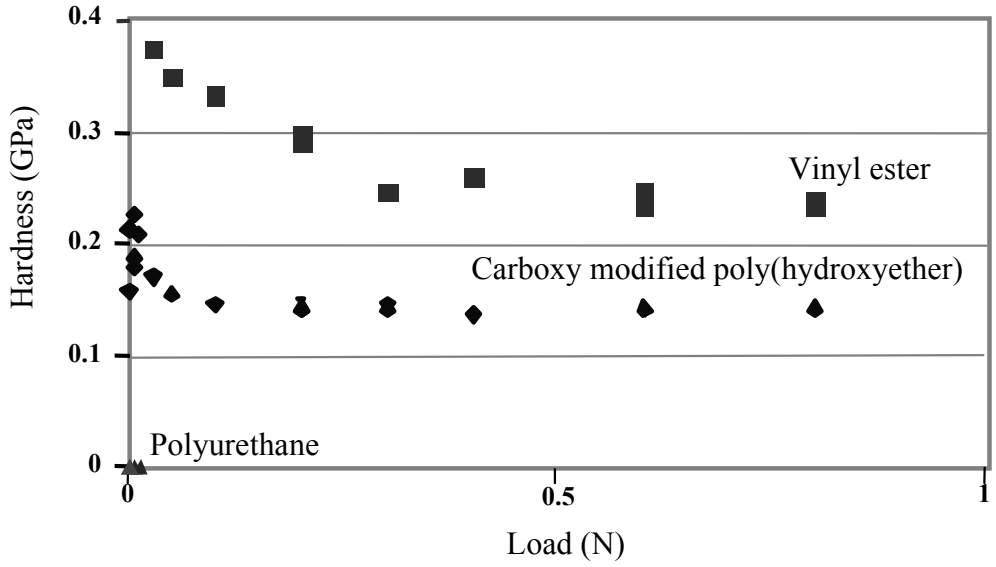

Figure 4-17. Microhardness as a function of indentation load.

The nanohardness values calculated from nanoindentation were higher than 'bulk' hardness values for crosslinked networks and ductile thermoplastics. This was due to the very small forces (10^{-5} N) used to indent the surface. Apparent hardness increased with decreasing indentation depth[141] and this was observed with the poly(hydroxyether) and vinyl ester systems using microhardness indentations. Vickers microhardness measurements were done at varied forces from 10 mN to 1 N. The apparent

[141] E.T. Kang, Z. H. Ma, K. L. Tan, O. N. Tretinnikov, Y. Uyama, and Y. Ikada, *Langmuir*, 1999, **15**(16), 5389-5395.

microhardness decreased as indents were made with increasing force until a plateau region was reached (Figure 4-17). At a minimum force, 0.3 N for the vinyl ester network and 0.1 N for the carboxy modified poly(hydroxether), the hardness value determined was a property of the bulk and not dependant on indent depth. Thus, it may be that below this minimum force surface characteristics become significant and the apparent hardness is no longer a bulk property. Forces used for the nanoindentation of the bilayers, 10^{-5} N, were well below the minimum force necessary to observe bulk properties, 10^{-1} N.

4.4.2.2. Interfacial Shear Strength

Interfacial shear strengths (IFSS) on "model" single fiber composites were measured using a microdroplet debond method at the Kwangju Institute within Dr. T.-H. Yoon's research group. The average IFSS of the control carbon fiber - vinyl ester samples prepared with unsized carbon fibers was 28 MPa (Table 4-3) whereas the values almost doubled for the fibers coated with the poly(hydroxyether) and carboxy modified poly(hydroxyether) engineering thermoplastics. This was consistent with good adhesion between these sizings and the vinyl ester matrix promoted by interdiffusion of these layers during cure (observed using AFM).

Table 4-3. Interfacial shear strength from microdebonding of a single fiber from (A) a bead of sizing and (B) a bead of resin.

Thermoplastic	(A) IFSS (MPa) -thermoplastic bead / unsized fiber	(B) IFSS (MPa) -vinyl ester bead / sized fiber
No sizing	---	28±8
PHE	55.2±6.7	45.2±8.3
CPHE	---	44.4±7.3
PHEA	53.2±7.4	22

The interfacial shear strengths found for debonding droplets of the thermoplastic sizings from the carbon fiber were significantly higher than for debonding the vinyl ester from the unsized fiber. It is hypothesized that acidic protons from the hydroxyl and carboxyl groups on the sizing backbones can interact with heteroatoms on the fiber surface and contribute to this enhanced adhesion. The adhesion of the carboxy modified poly(hydroxyether) sizing could not be tested because the powder would not flow into an

~100μm bead, but rather consisted of a bead of ~1μm particles due to the crosslinking of the dispersed particles upon heating.

The lightly crosslinked carboxy modified poly(hydroxyether) was less soluble in the resin than the unmodified poly(hydroxyether). The interdiffused interphase region observed by AFM was narrow and it yielded a high IFSS between the sized fiber and vinyl ester matrix. This suggests a necessity to control interdiffusion in the composites to ensure that a substantial amount of sizing indeed remains at the interface. In contrast to the encouraging results obtained with the carboxy modified poly(hydroxyether) sized fibers with the vinyl ester droplets, the samples prepared from the fibers sized with the poly(hydroxyether ethanolamine) and vinyl ester droplets provided almost the same IFSS as the control samples with the unsized fibers. This suggested poor adhesion, probably between the vinyl ester network and the poly(hydroxyether ethanolamine) sizing layer due to the lack of miscibility between the two materials even at elevated temperatures. While the sizing adheres well to the fiber, the bead of matrix material was able to slide off the poly(hydroxyether ethanolamine) surface. (Poly(hydroxyether ethanolamine)/ vinyl ester bilayers peeled apart during handling.) Consistent with this result, the AFM micrographs indicated little to no interdiffusion between this polar sizing and the vinyl ester thermoset.

Similar adhesion results were found with poly(arylene ether phosphine oxide) (PEPO), poly(arylene ether sulfone) (PES), and Ultem polyimide sizings[142,143]. Adhesion of the thermoplastic sizings to the carbon fiber was characterized and found to be higher (>45 MPa) than that of the vinyl ester resin to the fiber (30 MPa) as determined by debonding beads of thermoplastic or vinyl ester from unsized fibers. IFSS between vinyl ester resin and sized fibers was found to increase as follows; unsized (30MPa) ≈ polyimide sized (29 MPa) < PES sized (45 MPa) < PEPO (56 MPa) sized. The PEPO and PES were partially miscible with the vinyl ester resin and an interdiffused region was seen both cases, while the polyimide was insoluble in the vinyl ester resin. Without interdiffusion between the matrix and sizing, no increase in adhesion was seen.

---

[142] I.-C. Kim and T.-H. Yoon, *J. Adhes. Sci. Technol.*, 2000, **14**(4), 545-559.

[143] H. M. Kang, T. H. Yoon, M. Bump, and J. S. Riffle, *J. Appl. Polym. Sci.*, 2001, **79**(6), 1042-1053.

4.4.2.3. Composite Characterization

While the adhesion of the sizing to the fiber seemed unaffected by the subtle changes in polarity of the poly(hydroxyether)s from the unmodified to the ethanol amine thermoplastic, a large difference in cyclic fatigue properties of the resulting composites was found. Composite panels $(0°/90°)_{7S}$ were prepared with each of the two water dispersible sizings, the carboxy modified poly(hydroxyether) and the poly(hydroxyether ethanol amine), and fully reversed (R = -1) notched fatigue tests were used to compare the as-processed fatigue lives as a function of the amount of sizing-matrix interdiffusion. Composite fatigue performance had previously been identified as being particularly sensitive to changes in the fiber-matrix interface[8]. Improved fatigue performance is noted by a decrease in the slope of the S-N curve and increases in the stress level that defines the fatigue limit, i.e. the stress level at which the material survives 10^6 cycles. Significantly, by placing only 0.8 wt. % of the carboxy modified poly(hydroxyether) at the interface, an ~50% increase in fatigue limit resulted as compared to the unsized material (Figure 4-18). By comparison, the poly(hydroxyether ethanolamine) interphase increased the fatigue performance of the composite relative to the unsized case, but did not lead to similar levels of durability enhancement. Fatigue limits for both sets of sized fiber composites relative to those for the unsized case were measured even though fiber-matrix adhesion for the poly(hydroxyether ethanolamine) materials was low. The slopes of the S-N curves were reduced for both sized systems relative to the unsized case. However, one can clearly see that at low cycle fatigue, the composite with the poly(hydroxyether ethanolamine) sizing did not outperform the unsized case. This could be associated with strength issues where the interface was so poor that it could not prevent microbuckling at the stress concentrations. However, at lower stress levels, the weak interface facilitated the growth of splits at the notch and effects of the stress concentration were reduced; therefore, the stress levels in the material were not high enough to cause compression failure.

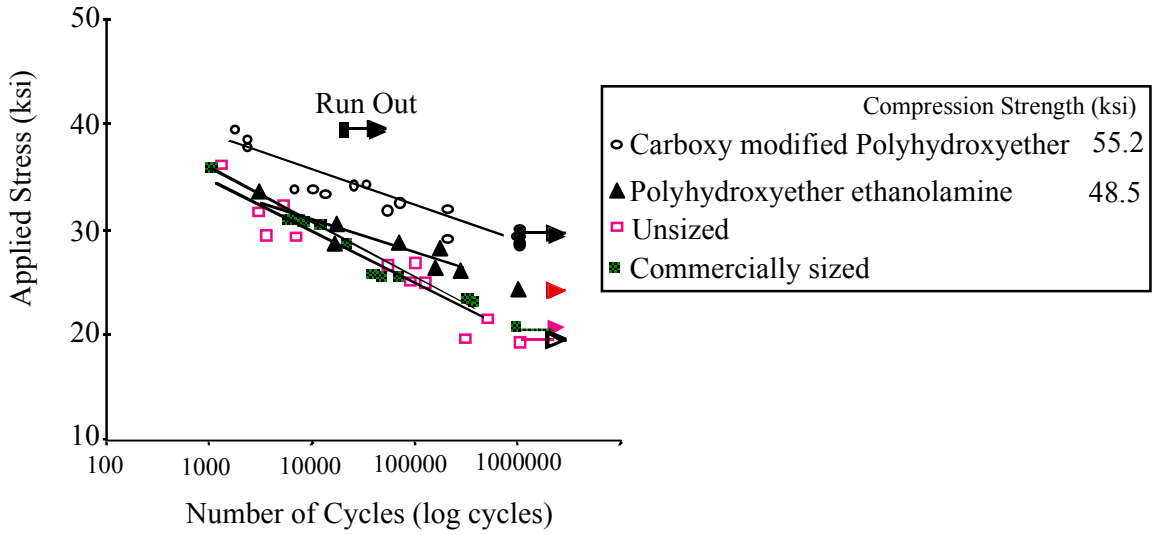

Figure 4-18. Cyclic fatigue durability for poly(hydroxyether) sized carbon fiber composites.

The greatest improvement in durability was observed when the sizing material remained at the fiber surface but did interact with the vinyl ester resin, so that adhesion was improved on both sides of the interphase region.

4.4.3. Conclusions

Interphase regions were designed for carbon fiber reinforced vinyl ester matrix composites with a series of tough, ductile, thermoplastic sizings that interdiffuse into the matrix to varying degrees. Adhesion between the matrix and fiber was improved from 28 MPa in the unsized case to 45.2 and 44.4 MPa in the unmodified and carboxylate modified poly(hydroxyether) cases, respectively. Consistent with the adhesion data, atomic force microscopy showed interdiffused interphase regions with poly(hydroxyether) inclusions for both of these systems. By contrast, the interfacial shear strength was not improved by sizing the fiber with poly(hydroxyether ethanolamine), a sizing which did not interdiffuse with the matrix during cure. The relative amounts of sizing-matrix interdiffusion could also be qualitatively correlated with composite fatigue properties. Addition of <1 wt % poly(hydroxyether ethanolamine) to the composite improved fatigue durability (the stress limit where the samples endured a million cycles) from ~20 ksi in the unsized case to ~25 ksi. However, with as little as 0.8% by weight of the carboxylate modified poly(hydroxyether) sizing in

the composite, the fatigue limit for applied stress was improved by ~ 50% over the unsized fiber case, to ~32 ksi. Compilation of this adhesion, AFM imaging, and composite fatigue data suggests that tough ductile sizings designed for both fiber adhesion and matrix interdiffusion can significantly improve selected mechanical properties of these composites.

4.5. Polyurethane Sizings

4.5.1. Synopsis

Novel polyurethane thermoplastics were synthesized from isophorone diisocyanate with either polycaprolactone or polytetramethylene oxide soft segments. Chain extenders containing a basic amine, phosphine oxide, or aliphatic functionality were incorporated at tailored concentrations in efforts to obtain water dispersible polyurethanes with limited interactions with the dimethacrylate matrix resin. Adhesion between the carbon fiber and vinyl ester matrix was improved by incorporating selected polyurethane sizings. All of the polyurethanes were miscible with the vinyl ester resin at low, < 20 wt %, and high, > 80 wt %, concentrations of polyurethane at 25°C. The composites prepared from polyurethane sized fibers resulted in similar fatigue performance to those prepared from unsized carbon fibers, probably due to dissolution of the sizing into the matrix so that no interphase region formed.

4.5.2. Synthesis of Polyurethanes

In a typical synthesis, the polyurethane was prepared by first reacting the soft segment with the diisocyanate (Figure 4-19). One equivalent of polycaprolactone was dried in the reaction round bottom flask at 70°C under vacuum for 18 hrs. Three equivalents of IPDI and 1000 ppm by weight dibutyltin dilaurate were added, and the melt reaction was stirred under N_2 for two hours at 70°C. Due to the excess of isocyanate, the prepolymer formed in the melt was isocyanate endcapped polycaprolactone or polytetramethylene oxide. The prepolymer was diluted to 30 weight % concentration with MEK, and one equivalent of N-methyldiethanolamine and one equivalent of di(3-hydroxypropyl) isobutyl phosphine oxide were added. The oxygen of

the hydroxyl group attacked the central carbon of the isocyanate (Figure 4-20). Proton transfer from the diol nucleophile to the isocyanate nitrogen yielded the carbamate linkage. Dibutyltin dilaurate was used to catalyze the hydroxyl-isocyanate reaction[144]. The mechanism involved tin associating with the isocyanate oxygen, thereby decreasing the electron density on the carbonyl oxygen and activating the isocyanate toward nucleophilic attack.

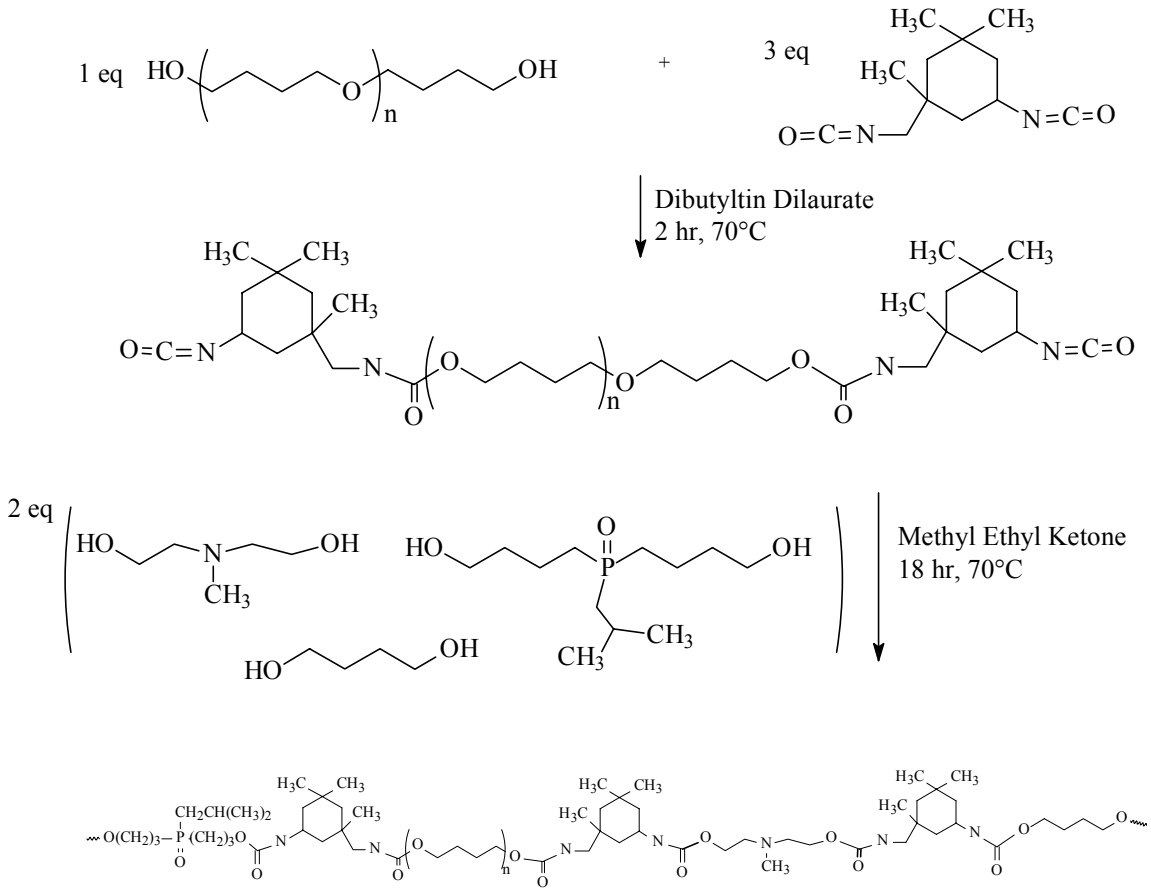

Figure 4-19. Synthesis of polyurethane thermoplastics.

This reaction was allowed to react for 18 hours at 70°C and was monitored using FTIR to observe the disappearance of the isocyanate peak at 2270 cm^{-1}. Due to the reactivity of the isocyanate group with water, the reaction was conducted under anhydrous conditions. To promote high molecular weight a stoichiometric ratio of isocyanates to hydroxyl groups was used, all reagents were purified, and the

[144] M. Bikales, Ed., Encyclopedia of Polymer Science and Engineering, **13**, John Wiley & Sons, New York,

disappearance of the isocyanate peak was monitored to ensure complete conversion. The block copolymer was precipitated into basic water and washed with neutral water. The polyurethane was dried under vacuum at 50°C for 24 hours.

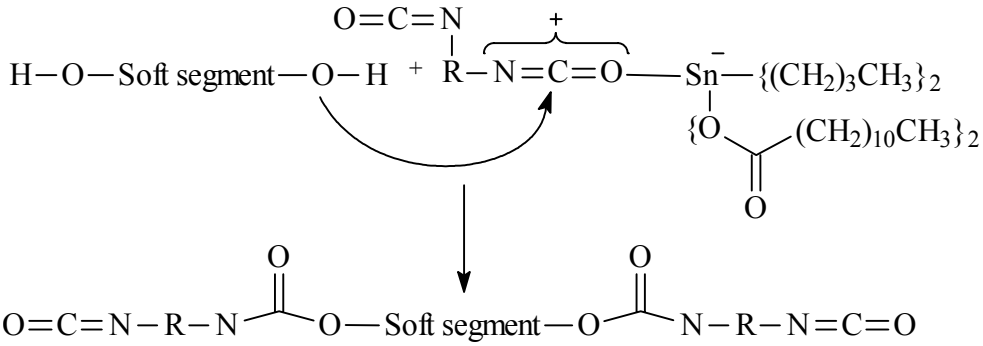

Figure 4-20. Reaction of aliphatic hydroxyl with isocyanate catalyzed by Lewis acid[145].

A series of polyurethanes were also synthesized containing polytetramethylene oxide soft segments. The diol chain extenders were varied to control dispersibility in water and interaction with the vinyl ester matrix. A similar synthesis was utilized with combinations of the three chain extenders, N-methyldiethanolamine, di(3-hydroxypropyl) isobutyl phosphine oxide, and 1,4-butanediol.

4.5.3. Results and Discussion

To explore the effect of a low modulus interphase on composite performance in carbon fiber/vinyl ester composites a series of one-phase polyurethanes was synthesized. As in the case of the poly(hydroxyether) sizings, it was anticipated that limited interdiffusion with the matrix was desired. The vinyl ester matrix consisted of a 700 g/mol methacrylate endcapped diglycidyl ether of bisphenol-A diluted with 30 wt % styrene, to reduce resin viscosity. The vinyl ester was free radically cured using benzoyl peroxide at 140°C and the reaction reached 85% conversion within 5 minutes (Figure 4-2). Interactions between the matrix and sizing are specific to this resin composition and cure.

243-252.

[145] J. C. Salamone, Ed., Polymeric Materials Encylopedia, 1996, CRC Press, Boca Raton, 6942-6944.

The components incorporated into the polyurethane included a 1,170 g/mol M_n polycaprolactone (PCL) or a 930 g/mol M_n polytetramethylene oxide (PTMO) as soft segments and N-methyldiethanolamine (MDEA), di(3-hydroxypropyl) isobutyl phosphine oxide (DPPO), and 1,4-butanediol (BD) as the chain extenders. Isophorone diisocyanate (IPDI), an aliphatic isocyanate, was chosen due to its increased ultra-violet stability.

Initial work was begun using the polycaprolactone soft segment based on its well established miscibility with the vinyl ester backbone structure. In an attempt to tailor the interdiffusion of the sizing and matrix, a polytetramethylene oxide segment was also investigated. While polycaprolactone oligomer contained a carbonyl group to hydrogen bond with the hydroxyl groups of the vinyl ester, the polytetramethylene oxide did not have this hydrogen bonding capability. Hence, it was reasoned that the lack of these interactions might reduce the interdiffusion between the polyurethane and vinyl ester resin, forming a distinct interphase region.

The amine chain extender was incorporated to promote water dispersibility, which was considered necessary for sizing of carbon fibers. The polar phosphine oxide group of the phosphorus chain extender was incorporated to improve adhesion between the carbon fiber and the polyurethane. It was reasoned that both the amine and phosphine oxide chain extenders would hydrogen bond with the vinyl ester hydroxyl groups. Improved miscibility between vinyl ester oligomers and poly(arylene ether)s was observed with incorporation of triphenyl phosphine oxide moieties along the backbone and was attributed to strong hydrogen bonding[21]. Therefore two series of polyurethanes (Table 4-4) were synthesized with systematically reduced concentrations of either the amine or the phosphine oxide chain extender in an effort to decrease interdiffusion into the matrix resin and reduce the size of the interphase region. Butanediol was utilized to maintain the isocyanate/hydroxyl stoichiometry.

4.5.3.1. Polyurethane Characterization

The polyurethanes were synthesized with an amine functionality to facilitate water dispersibility of the sizing. To disperse the polymer, the tertiary amine was protonated using acetic acid to form the carboxylate salt. Initially, a 10 weight % solution of each polyurethane in methyl ethyl ketone was prepared. For each equivalent

of the amine chain extender in the polyurethane solution, 1.1 equivalents of acetic acid were added. The solution was stirred rapidly as water was added dropwise and the mixture began to grow cloudy with ~2 % water due to immiscibility of MEK and water. The mixture became opaque with the addition of ~6 % water and the formation of dispersed particles. After the particles formed, water could be added quickly without disturbing the dispersion. The organic solvent was removed under vacuum to yield aqueous dispersions.

The dispersibility of each polyurethane was investigated and it was observed that the concentration of amine chain extender could be reduced to 0.25 equivalents per diisocyanate while still maintaining dispersibility. The dispersions were stable for >3 days and no degradation of molecular weight occurred. Bimodal distributions of particles were observed in the dispersions, in the range of 0.5 - 5 μm and 30 - 200 μm. The most prevalent particle size in the dispersions was 3 μm. Particle size and distribution was likely affected by both the chemical composition of the polyurethane and the dispersion process. When the amount of amine chain extender was reduced to 0.15 equivalents, the polyurethane was no longer dispersible. While the phosphine oxide moiety was strongly hydrogen bonding, the concentration of phosphine oxide in the polyurethane did not affect the dispersibility of the polymer. Molecular weights of the dispersed polyurethanes were confirmed after three days. Dispersions were dried under vacuum at 80°C and by GPC no weight loss or degradation was observed.

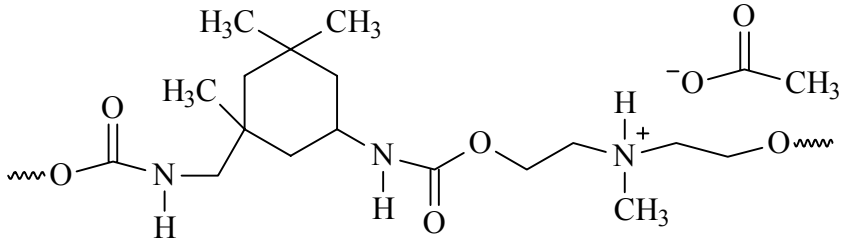

Figure 4-21. Protonation of tertiary amine within polyurethane backbone.

Table 4-4. Compositions of polyurethanes synthesized.

Soft segment	DPPO	BD	MDEA	M_n(g/mol)	Tg	Dispersible in Water
Polycaprolactone	1	0	1	47,000	3˚C	Yes
Polytetramethylene oxide	1	0	1	7,000	-5˚C	Yes
	0.5	0.5	1	10,000	-8˚C	Yes
	0	1	1	29,000	-10˚C	Yes
	1	0.5	0.5	7,000		Yes
	1	0.75	0.25	16,000	-3˚C	Yes
	1	0.85	0.15	---	-3˚C	No

Each of the polyurethanes synthesized showed a single glass transition near room temperature indicating that these materials were one phase polyurethanes. If they had been two phase elastomeric polyurethanes, a lower glass transition should have been observable around –80°C for the soft segment, and a higher glass transition above 100°C would have been anticipated for the hard segment. The single phase was not surprising given the low molecular weight of both soft segments used, ~1,000 g/mol. The segment lengths were too short to achieve effective phase separation; yielding a one phase system with an intermediate T_g. Chemical composition of the polymers affected the glass transitions. The highest molecular weight polyurethane, as determined by GPC, possessed the highest T_g. This polymer also contained the more polar polycaprolactone soft segment and the highest concentration of phosphine oxide, contributing to the increased transition temperature. Decreasing the phosphine oxide content resulted in lower T_gs. The polyurethane synthesized with no phosphine oxide possessed the second highest molecular weight but had the lowest glass transition due to the lack of the strong interactions of the polar phosphine oxide bond.

4.5.3.2. Interphase Properties

Miscibility between the polyurethanes and the vinyl ester resin (VER) was investigated via thermal analysis. Vinyl ester/polyurethane blends were solution mixed in dichloromethane with 0.5 mol % benzoyl peroxide per vinyl bond. To maintain

integrity during the thermal scan, polyurethanes and blends were cast onto aluminum tabs and dried at 100˚C for 16 hours under vacuum. The blends were then postcured at 140˚C for one hour. Figure 4-22 shows the results of dynamic mechanical analysis of blends prepared with the polyurethane containing 0.5 equivalent of phosphine oxide containing chain extender and polytetramethylene oxide soft segment. The moduli values were for polyurethane blend/aluminum supported composites and cannot be compared to each other.

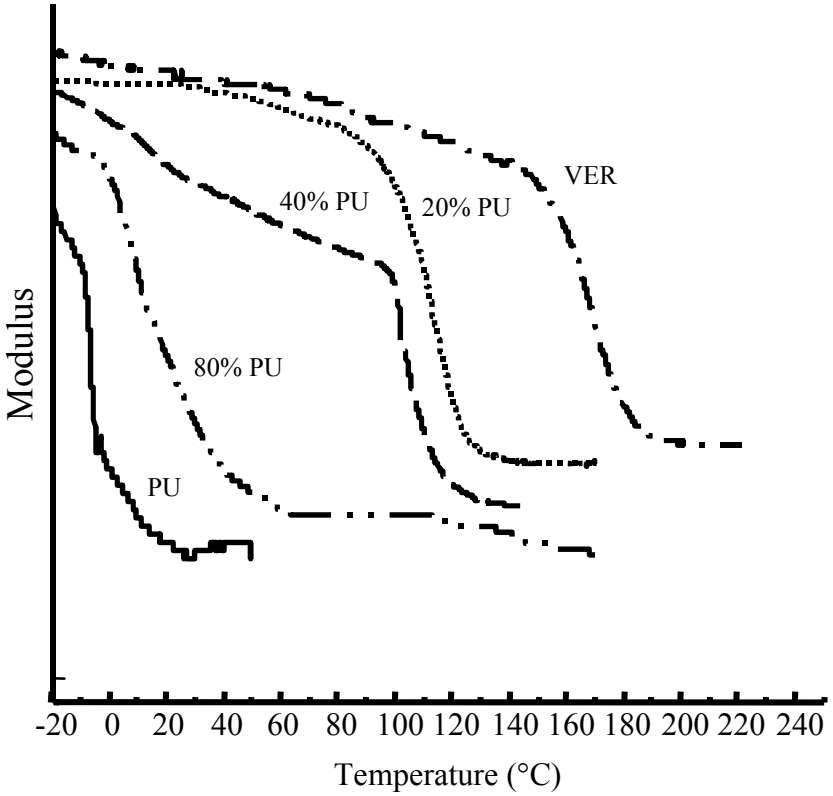

Figure 4-22. Thermal transitions for a series of polyurethane/vinyl ester blends show at least partial miscibility at all compositions.

The pure polyurethane had a glass transition at –8°C while the pure vinyl ester resin had a glass transition at 156°C (Table 4-5). The 20 weight %, 40 weight %, and 80 weight % polyurethane blends had intermediate glass transition temperatures. At the 20 % and 80 % polyurethane compositions, only one glass transition was detected for each of the blends, 100ºC and –2ºC respectively. The Fox-Flory equation (Equation 4-9) can be used to predict the glass transitions of miscible blends, $T_{g\ Blend}$.

Equation 4-9 $$1/ T_{g\ Blend} = \text{wt \% PU}/ T_{g\ PU} + \text{wt \% VER}/ T_{g\ VER}$$

The predicted glass transitions for the blends would be 109ºC for the 20% and 14ºC for the 80 % polyurethane blends, which were close to those found using DMA. These single transitions that corresponded with the Fox-Flory values indicate miscibility, at least in the cured networks. At the 40 weight % polyurethane composition, two glass transitions were found, a low glass transition corresponding to a phase rich in polyurethane at 15ºC and a higher glass transition corresponding to a phase rich in vinyl ester at 96ºC, neither of which corresponded to the predicted value of 71ºC (for components which were miscible across the composition range). This phase separation indicated that at a 40% polyurethane composition, the polyurethane and vinyl ester were only partially miscible. Similar trends in miscibility were observed when no phosphine oxide chain extender was used and when the polycaprolactone soft segment was used (Table 4-5). Since the polyurethane and vinyl ester resin were at least partially miscible at all compositions of polyurethane and vinyl ester, some interdiffusion within the composite was expected.

Table 4-5. Glass transitions temperatures for polyurethane/vinyl ester blends.

Polyurethane				Glass Transition Temperature (°C)					
Soft Segment	Chain Extender (eq)			PU	80% PU	40% PU		20% PU	VER
	DPPO	BD	MDEA			Lower	Upper		
PCL*	1	0	1	26	35	29	90	150	176
PTMO^	0.5	0.5	1	-8	-2	15	96	100	156
	0	1	1	-10	12	-7	87	---	156

* T_g obtained from tan δ peak
^ T_g obtained from onset of drop in modulus

Polyurethane/vinyl ester bilayers were prepared with each of the polyurethanes and the interphase regions between the polyurethane and vinyl ester were investigated with AFM. The polycaprolactone containing polyurethane, which possessed carbonyl bonds that were anticipated to interact with the vinyl ester resin hydroxyl groups, showed a broad interdiffused region, which was too large to be imaged by AFM (which could image 20 μm spans) and did not possess enough contrast to be imaged by TEM. Using nanoindentation as discussed in section 4.4.2.1, a gradient in hardness was mapped across

the interphase showing a >60μm region of a broad, gradual transition from polyurethane to vinyl ester (Figure 4-23). It appeared that the entire breadth of the interphase was not indented because the pure vinyl ester hardness, 1.3 GPa, was not reached in these measurements. The bulk polyurethane nanohardness was 0.3 GPa. As expected, this was significantly lower than the nanohardness found for the glassy poly(hydroxyether) interphase materials, 0.8 GPa. The polyurethane was partially miscible in the vinyl ester matrix at 25°C and at the elevated cure temperatures the polyurethane diffused rapidly over 60μm, a great deal further than the poly(hydroxyether) interdiffusion which spanned ~10 μm.

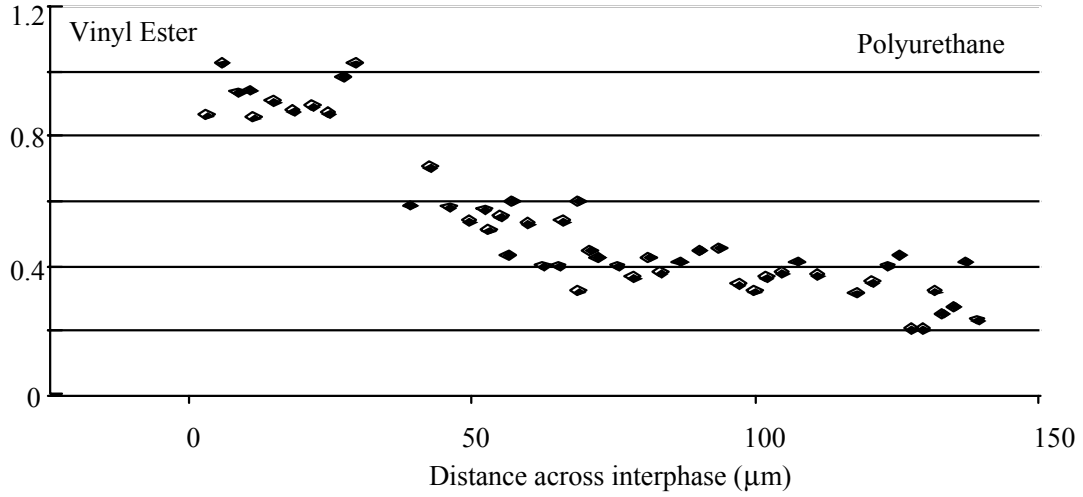

Figure 4-23. A gradient in nanohardness was seen across a polyurethane/vinyl ester interphase.

Broad interdiffused regions also developed in bilayers prepared from vinyl ester resin and the polyurethanes in the series containing a polytetramethylene oxide soft segment and one equivalent of amine (Table 4-4). Across the interphase region of each of the three bilayers, the conversion from the pure vinyl ester matrix to the pure polyurethane was too broad, 60-100 μm, to be imaged by AFM and too gradual to be imaged by TEM. As the phosphine oxide concentrations were reduced within the polyurethane series, from 1 to 0.5 to 0 equivalents, the amount of interdiffusion between vinyl ester and polyurethane and the morphology of the interphase were not visibly affected.

However, as the amount of amine chain extender was reduced, the microstructure of the interphase region was altered. In the polytetramethylene oxide polyurethane series synthesized with one equivalent of phosphine oxide, a change was observed in going from 1 to 0.5 equivalent of amine chain extender. Instead of a gradual transition, a relatively sharp interface occurred where the continuous phase changed from a vinyl ester rich phase to a polyurethane rich phase. Bilayers prepared with the polyurethanes containing 0.5 and 0.25 equivalents of tertiary amine both resulted in an interdiffused region containing an interface between two continuous phases. However, large regions of interdiffusion (>60μm) were also observed, with inclusions of polyurethane in the vinyl ester side (Figure 4-24). A decrease in the amine/hydroxyl interaction with lower amine concentrations may have reduced miscibility of the polyurethane significantly enough to alter the interphase morphology. At the cure temperature, the polyurethane diffused rapidly into the vinyl ester resin. As the resin cured and the vinyl ester molecular weight increased, there were regions with high concentrations of polyurethane that phase separated.

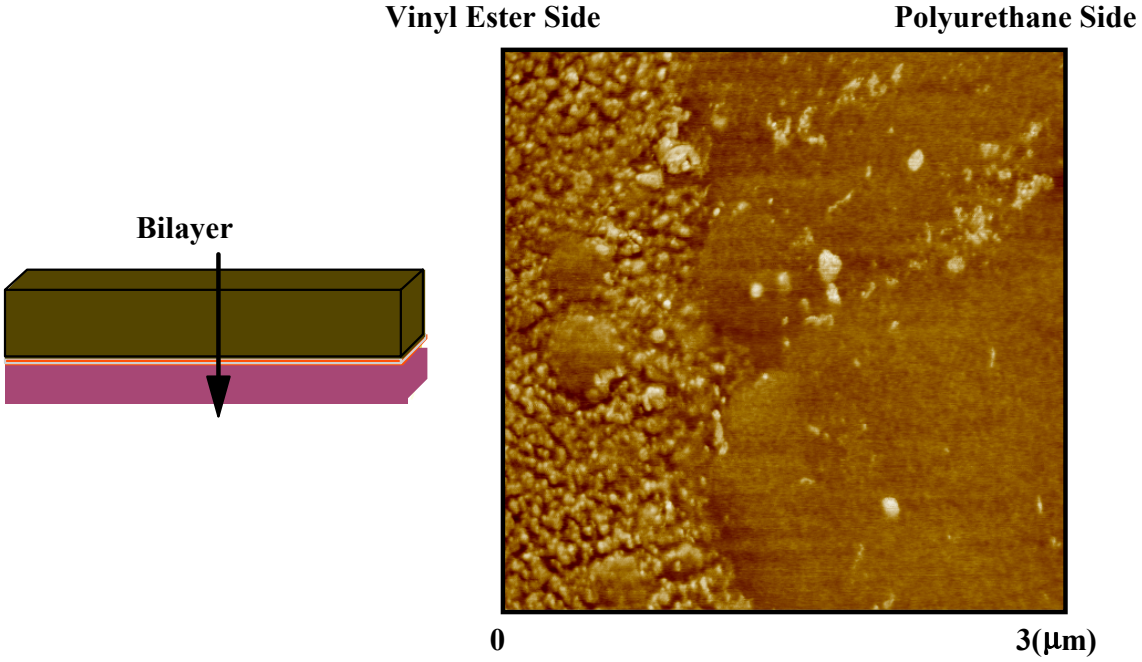

Figure 4-24. In this AFM Image of the polyurethane (with PTMO and 0.25 eq. MDEA)/vinyl ester resin bilayer, the phase inversion can be observed from a vinyl ester rich phase to a polyurethane rich phase.

Interdiffusion appeared to occur too extensively between all of the polyurethanes in the series and the vinyl ester matrix to develop an interphase region on the composite scale. Within a composite panel with 60 vol % fibers, there would be ~2μm between fibers. The rapid diffusion of the polyurethanes may have resulted in no sizing at the fiber surface and no interphase region.

4.5.3.3. Interfacial Shear Strength

The interphase region was investigated at the Kwangju Institute within Dr. T.–H. Yoon's research group using microdebond testing to find the interfacial shear strength between the carbon fiber and vinyl ester. As described in Table 4-6, an increase in adhesion resulted when fibers were coated with the polyurethane materials. Polyurethane beads could not be debonded from carbon fibers to evaluate sizing/fiber adhesion directly due to the low modulus of the polyurethane. For an unsized fiber, 28±8 MPa was required to debond the vinyl ester network from the carbon fiber. When the carbon fiber was coated with a polyurethane using the polycaprolactone soft segment, the force necessary to break the bond between the vinyl ester matrix and the fiber increased to 57±8.7 MPa. The polyurethane prepared from the polytetramethylene oxide without the phosphine oxide component resulted in less significant improvement in strength (41.10±3.4 MPa). The reduction in adhesive strength was not surprising due to removal of the strongly hydrogen bonding phosphine oxide that interacted with heteroatoms on the fiber surface.

Table 4-6. Interfacial shear strengths for carbon fiber/vinyl ester model composites from microdebond testing.

Sizing Material	DPPO (eq)	MDEA (eq)	BD (eq)	Interfacial Shear Strength (MPa)
PCL	1	1	0	56.7±7.5
PTMO	1	1	0	50.29±9.2
	1	0.25	0.75	46.92±7.9
	0	1	1	41.10±3.4

While the rapid interdiffusion would have suggested that polyurethane was no longer at the fiber surface, on the small scale of the fiber debond experiment diffusion may have been altered. Each bead was 30-50μm, which was less than the interdiffused region seen in the bilayers. Particularly near the edges of the bead, which were thinner, an interphase region may have developed to improve the shear strength.

4.5.3.4. Composite Characteristics

Composite panels $(0°/90°)_{7S}$ were prepared from polyurethane sized carbon fibers and vinyl ester resin. The polycaprolactone polyurethane investigated was chosen due the high interfacial shear strength found for this polyurethane by microdebond experiments. Composite fatigue performance, determined using fully reversed (R = -1) notched fatigue tests, has been found particularly sensitive to changes in the fiber-matrix interface[8]. Improved fatigue performance is evident by a decrease in the slope of the stress-cycle curve and increases in the stress level at which the material survives 10^6 cycles.

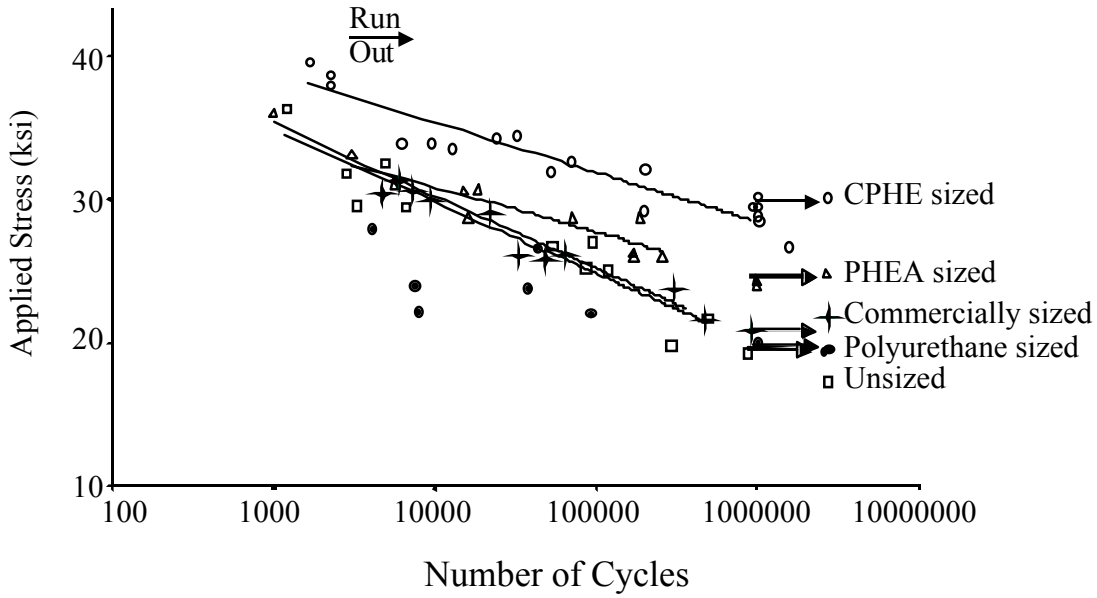

Figure 4-25. Durability of composite panels made from sized fibers, determined from cyclic fatigue tests; run out was defined as the stress at which a sample could undergo a million cycles without failure.

In cyclic fatigue testing the durability of the composite prepared from polyurethane sized fibers showed no improvement over the unsized system (Figure 4-25).

Although fiber/matrix adhesion was enhanced in microdebond, this improvement was not transferred to composite performance. This was likely due to the fact that there was no interphase region, but rather the polyurethane completely dissolved into the vinyl ester matrix. In the composite panel, there was a larger concentration of vinyl ester resin in which the polyurethane sizing could dissolve compared to the microdebond system. This lack of interphase was also suggested by the appearance of the failed specimens. Increased longitudinal splitting of the failed samples resulted in a 'broom' appearance of the fibers for both the unsized fiber and polyurethane sized fiber composites in which the fibers were not adhered together. On the other hand, modified poly(hydroxyether) sized fibers yielded brittle failure of the composite due to stress concentrations, where the fibers to either side of the failure were still adhered together. The polyurethane sized fiber composite performance was not improved most likely because no polyurethane remained at the fiber surface, which led to poor fiber/matrix adhesion in the actual composite system.

4.5.3.5. Conclusions

The series of water dispersible polyurethanes were obtained by incorporation of at least 0.25 mol % tertiary amine. By protonating the amine with acetic acid, a stable aqueous dispersion with a broad range of particle sizes was prepared and used to size carbon fibers. While the phosphine oxide concentration did not affect the water dispersibility of the polyurethane, the glass transition temperatures of the polyurethanes and the fiber/matrix adhesion of sized fibers increased with phosphine oxide incorporation. The strongly hydrogen bonding phosphine oxide resulted in increased interactions within the thermoplastic altering the glass transition and between the fiber surface and the polyurethane, improving adhesion.

While each of the polyurethanes synthesized was too miscible in the vinyl ester resin to form an interphase region, limitations of the microdebond test were encountered in this research. The single fiber debond is a good method for probing the interfacial shear strength directly; however, the results may not accurately reflect those found in the composite. As seen with the polyurethane sized fibers, an increase in debond interfacial shear strength did not result in improved composite properties. The small amount of vinyl ester resin in a single bead may have allowed an interphase to form in the

microdebond test system, leading to an apparent increase in fiber/matrix adhesion. When the vinyl ester resin was introduced in the composite to a thin layer of polyurethane on the fiber, the polyurethane dissolved, leaving no interphase or gradient of properties and thus no increase in composite fatigue properties.

4.6. Conclusions

Composite durability was improved through the addition of a tough ductile sizing that facilitated the development of an interphase region with a stiffness gradient. It appears to be critical to composite performance to maintain a layer of sizing material at the fiber surface. Both carboxy modified poly(hydroxyether) and poly(hydroxyether ethanolamine) sizings resulted in an interphase region with sizing material at the fiber surface. Composite durability was improved with these sizings compared to the unsized fiber composites. When fibers were coated with a miscible polyurethane sizing no interphase region formed because of the rapid interdiffusion of the polyurethane and the vinyl ester resin. Without an interphase region, composite durability was the same as for unsized fibers.

Increased adhesion between the fiber and bulk matrix further increased the composite durability. Both the fiber/sizing and sizing/matrix interactions must be considered when trying to improve interfacial adhesion. While differences among the poly(hydroxyether) structures did not affect the fiber/sizing adhesion, which was greater than the vinyl ester/fiber adhesion, the interactions with the matrix resin were more sensitive to changes in the poly(hydroxyether) structure. The carboxy modified poly(hydroxyether) showed limited miscibility with the vinyl ester resin at the elevated cure temperatures and the poly(hydroxyether ethanolamine) showed no interaction with the vinyl ester resin. The low sizing/matrix adhesion between the vinyl ester matrix and the poly(hydroxyether ethanolamine) resulted in poor interfacial shear strength. The limited interdiffusion of the carboxy modified poly(hydroxyether) on the other hand resulted in higher interfacial shear strength. Adhesion was strong on both the fiber/sizing and sizing/matrix sides of the interphase resulting in the most improved composite durability.

Chapter 5. Summary and Conclusions

5.1. Summary

This work has addressed 1) the synthesis and structure-property relationships of new diepoxide thermosets and 2) the design and understanding of fiber reinforced composite interphases. Networks have been prepared from bisphenol-A and triphenyl phosphine oxide epoxy resins using two crosslinking agents, a phenolic novolac or an amine terminated siloxane. Within fiber reinforced composites, the relationship between interphase morphology, due to sizing/vinyl ester resin phase miscibility, and composite fatigue properties has been investigated.

Epoxy Thermosets

A novel aryl phosphine oxide diepoxide was synthesized by reacting bis-(hydroxyphenyl)phenyl phosphine oxide with epichlorohydrin. Strong hydrogen bonding of the polar phosphine oxide bond, confirmed via FTIR, in addition to the rigid triphenyl phosphine oxide backbone affected properties of the resulting thermoset. In networks prepared using an amine terminated siloxane crosslinking agent, which were ~80 wt % epoxy, the incorporation of the phosphine oxide group yielded networks with increased glass transition temperatures and water absorption compared to networks containing a traditional bisphenol-A based diepoxide. Higher char yields were also observed due to the inorganic nature of the phosphorus. As expected offsetting the epoxide/amine stoichiometry resulted in increased molecular weight between crosslinks and improved network toughness. Toughness decreased with incorporation of the phosphine oxide epoxy, which corresponded to increased density and decreased β-transitions, indicating reduced segment mobility.

Networks prepared with the novolac crosslinking agent were ~35 wt % epoxy. Hydrogen bonding, observed using FTIR, was evident even at temperatures above the network T_gs and resulted in increased rubbery moduli with phosphine oxide incorporation. Adhesion, investigated using lap shear tests, increased from ~10 MPa

(1400 psi) with bisphenol-A epoxy to ~13.8 MPa (2000 psi) when the phosphine oxide containing epoxy was incorporated into the network.

Properties of networks crosslinked with the siloxane moiety were more sensitive to incorporation of the phosphine oxide diepoxide. The increased weight % of phosphine oxide in the siloxane networks led to significant increases in water absorption, from 1 wt % to 5.5 wt %, while in the polar novolac networks, water uptake was not altered by addition of the phosphine oxide. In the novolac networks, phosphine oxide hydrogen bonded more strongly with unreacted phenols, which may have limited its interaction with water. In the siloxane networks there was a greater concentration of phosphine oxide and there were no phenol groups present.

The bisphenol-A based siloxane networks were much tougher ($K_{1c} \approx 2$ MPa $m^{1/2}$) than the corresponding novolac networks ($K_{1c} \approx 1$ MPa $m^{1/2}$). The incorporation of the flexible siloxane segment increased chain mobility, as seen in the broader β-relaxation and the decreased glassy densities (1.13 g/ml versus 1.25 g/ml for the novolac network). The siloxane toughness was reduced from 2 to 0.5 MPa $m^{1/2}$ compared to the decrease in novolac networks from 0.6 to 0.3 MPa $m^{1/2}$ by incorporation of 50 mol % phosphine oxide epoxy. In the siloxane networks, the loss of toughness was due to decreased damping caused by decreased β-transitions. The β-relaxations were not affected by the phosphine oxide incorporation in the novolac networks. One possible explanation for the larger decrease in the siloxane network toughness was that the phosphine oxide interacted with the secondary hydroxyl groups, while in the novolac networks, the phosphine oxide hydrogen bonded with phenol groups rather than the aliphatic hydroxyl moieties.

Interestingly, the lap shear strength in the phosphine oxide containing thermosets appeared to be dominated by network toughness, regardless of the crosslinking agent used. A linear correlation was found between fracture toughness and adhesive lap shear strength in samples showing cohesive failure for networks prepared with either siloxane or novolac crosslinking agents.

Composite Interphases

Within carbon fiber/vinyl ester composites, a series of tough ductile thermoplastics and a series of one-phase polyurethanes were investigated as carbon fiber sizings. The sizing was incorporated into the composite to tailor the chemical structure, morphology and mechanical properties of the interphase region. In order to alleviate residual stress that developed during cure shrinkage, the optimum interphase region appeared to require a material gradient thus leading to a gradient in mechanical properties. Good adhesion on both sides of the interphase, between the fiber and sizing and the sizing and matrix, led to good load transfer between the matrix and fiber. The tough, ductile poly(hydroxyether) interphase materials investigated had similar mechanical properties but resulted in three different types of interphase regions. Light crosslinking of the carboxylate modified poly(hydroxyether) sizing during the fiber drying process limited the region of interdiffusion between the sizing and resin to ~5 μm. This system showed an increase in fiber/matrix adhesion and the composite fatigue durability was improved by ~50 % compared to composites containing unsized carbon fibers. Using a poly(hydroxyether ethanolamine), which was not miscible with the resin even at elevated temperatures, a sharp sizing/vinyl ester matrix interface developed. The adhesion was not improved through the use of this sizing and the composite durability increased only a moderate amount, ~ 25%. A series of polyurethane sizings based on isophorone diisocyanate was synthesized and investigated in the composite system. Each of the polyurethanes was miscible with the vinyl ester resin. This miscibility resulted in broad interdiffused regions, >60μm, in polyurethane/vinyl ester bilayers. Fatigue durability in composite panels was not improved by the addition of the polyurethane sizings. The favorable interactions between the polyurethane and vinyl ester resin probably led to complete dissolution of the polyurethane sizing into the matrix so that there was no interphase region to affect composite performance. Thus, interdiffusion of a sizing and matrix provided excellent sizing-matrix adhesion by promoting a graded interphase region. However, limiting such interdiffusion through light crosslinking was desirable to ensure that sufficient amounts of the interfacial agent remained on the fiber surface after processing.

5.2. Conclusions

The strong hydrogen bonding nature of the phosphine oxide moiety led to decreased chain mobility and increased polarity in cured epoxy networks. Toughness was reduced and density increased due the segment interactions and reduced mobility. The higher polarity of the phosphine oxide containing thermosets compared to the bisphenol-A based epoxy thermosets resulted in higher water absorption and improved adhesion to steel.

Composite cyclic fatigue performance of fiber reinforced composites was improved by coating fibers with a sizing that had limited miscibility with the vinyl ester resin. It was necessary for the matrix and the sizing to interact to promote good adhesion between the sizing and matrix; however, the miscibility must be limited to maintain the sizing in the interphase near the fiber.

Chapter 6. Future Work

The tough bisphenol-A based epoxy/siloxane networks show promise as adhesives with their high toughness, low water absorption and reasonable cure. Improvements in the surface preparation of the steel adherends should now be investigated to increase adhesion between the steel adherend and the epoxy network, in an attempt to achieve cohesive failure.

While incorporation of the phosphine oxide moiety into the epoxy network led to a brittle network, adhesion was improved. Therefore, addition of the phosphine oxide to a network that does not contain other hydrogen bonding moieties, such as a resin that can be cured via a free radical process, may lead to increased adhesion without the decrease in network toughness. The addition of tougheners might also be considered as a means of improving the properties of the phosphine oxide containing epoxy networks. The differences between the theoretical and the experimental molecular weight between crosslinks within the phosphine oxide containing networks were larger than those found in the bisphenol-A containing networks. This suggests that the network structure was more open possibly due to a difference in the mechanism of the resin cure. It would therefore be of interest to investigate the amine/epoxide reaction in the presence of phosphine oxide.

Within the area of the composite materials, further research should address reducing the miscibility of the polyurethane with the vinyl ester resin. This might be accomplished by incorporating a functionality, such as a carbon-carbon double bond, that could lightly crosslink the polyurethane sizing prior to introduction of the resin.

Bibliography

1. J. J. Aklonis and W. J. MacKnight, Introduction to Polymer Viscoelasticity, 2nd edition, 1983, John Wiley and Sons, New York.
2. M. Anand and A. L. Srivastava, Synthesis and characterization of epoxy resins containing transition metals. *Polymer*, 1993, **34**(13), 2860-2864.
3. M. Anand and A. K. Srivastava, Synthesis of zinc-containing epoxy resin. *Journal of Applied Polymer Science*, 1994, **51**, 203-211.
4. S. Andjelic and J. Mijovic, Dynamics of carbonyl-modified-epoxy/amine networks for FTIR and dielectric relaxation spectroscopy. *Macromolecules*, 1998, **31**, 8463-8473.
5. W. R. Ashcroft, Curing agents for epoxy resins, Chemistry and Technology of Epoxy Resins, 1st edition, Ed. B. Ellis, Chapman & Hall, New York, 1993, 37-71.
6. K. E. Atkinson and C. J. Jones, A study of the interphase region in carbon fibre/epoxy composites using dynamic mechanical thermal analysis. *Journal of Adhesion*, 1996, **56**, 247-260.
7. K. E. Atkinson and C. Kiely, The influence of fibre surface properties on the mode of failure in carbon-fibre/epoxy composites. *Composite Science and Technology*, 1998, **58**(12), 1917-1922.
8. G. G. Barclay, S. G. McNamee, C. K. Ober, K. I. Papathomas, and D. W. Wang, Liquid-crystalline epoxy thermosets based on dihydroxymethylstilbene-synthesis and characterization. *Journal of Polymer Science: Part A: Polymer Chemistry*, 1992, **30**(9), 1831-1843.
9. B. C. Benicewicz, M. E. Smith, J. D. Earls, R. D. Priester, Jr., S. M. Setz, R. S. Duran, and E. P. Douglas, Magnetic field orientation of liquid crystalline epoxy thermosets. *Macromolecules*, 1998, **31**, 4730-4738.
10. J. Berg and F. R. Jones, The role of sizing resins, coupling agents and their blends on the formation of the interphase in glass fibre composites. *Composites*, 1998, **29A**(9-10), 1261-1272.
11. M. Bikales, Ed., Encyclopedia of Polymer Science and Engineering, **13**, John Wiley & Sons, New York, 243-252.
12. T. A. Bogetti, T. Wang, M. R. VanLandingham and J. W. Gillespie Jr., Characterization of nanoscale property variations in polymer composite systems: 2. Numerical modeling. *Composites*, 1999, **30A**(1), 85-94.
13. U. M. Bokare and K. S. Gandhi, Effect of simultaneous polyaddition reaction of the curing of epoxides, *Journal of Polymer Science: Polymer Chemistry Edition*, 1980 **18**, 857-870.
14. A. Bolshakov, W. C. Oliver, and G. M. Pharr, Finite Element Studies of the Influence of Pile-Up on the Analysis of Nanoindentation Data. *Materials Research Society Symposium Proceedings,* 1997, **436**, 141-146.
15. N. S. Broyles, R. Chan, R. M. Davis, J. J. Lesko, and J. S. Riffle, Sizing and Characterization of Carbon Fibers with Aqueous Solutions of Poly(vinylpyrrolidone). *Polymer*, 1998, **39**(12), 2607-2613.
16. N. S. Broyles, K. E. Verghese, S. V. Davis, H. Li, R. M. Davis, J. J. Lesko, and J. S. Riffle, Designed Polymeric Interphases in Carbon Fiber-Vinyl Ester Composites. *Polymer*, 1998, **39**(15), 3417-3424.

17. H. Li, E. Burts, K. Bears, Q. Li, J. J. Lesko, D. A. Dillard, and J. S. Riffle, Network Structure and properties of dimethacrylate-styrene matrix materials. *Journal of Composite Materials*, 2000, 34(18), 1512-1528.
18. G. Canche-Escamilla, J. I. Cauich-Cupul, E. Mendizabal, J. E. Puig, H. Vazquez-Torres and P. J. Herrera-Franco, Mechanical properties of acrylate-grafted henequen cellulose fibers and their application in composites. *Composites*, 1999, **30A**(3), 349-359.
19. K. Chung, T. Takata, and T. Endo, Anionic cross-linking of polymers having an epoxy group in the side chain with bicyclic and spirocyclic bis(γ-lactone)s. *Macromolecules*, 1997, **30**, 2532-2538.
20. Civil Engineering Research Foundation, Partnership for the advancement of infrastructure and its renewal: transportation component (PAIR-T) technology & investment plan. *Civil Engineering Research Foundation white paper*, 1998a.
21. R. L. Clark, R. G. Kander, and B. B. Sauer, Nylon 66/poly(vinyl pyrrolidone) reinforced composites: 1. Interphase microstructure and evaluation of fiber-matrix adhesion. *Composites*, 1999, **30A**(1), 27-36.
22. R. L. Clark Jr., R. G. Kander and S. Srinivas, Morphological changes in polyamide/PVP blends. *Polymer*, 1998, **39**(3), 507-516.
23. Y. Cohen, D. M. Rein, L. E. Vaykhansky and R. S. Porter, Tailoring the interface in polyethylene fiber/matrix composites: surface-entangled interfacial layer. *Composites*, 1998, **30A**, 19-25.
24. S. G. Corcoran, Quantitative nanoindentation: bridging the gap between the nanomechanics and AFM communities. *Application Note, Hysitron Inc*.
25. J. V. Crivello, The discovery and developments of onium salt cationic photoinitiators. *Journal of Polymer Science*, 1999, **37**(A), 4241-4254.
26. N. Dilsiz and J. P. Wightman, Surface analysis of unsized and sized carbon fibers. *Carbon*, 1999, 37(7), 1105-1114.
27. J. I. DiStasio, Ed., Epoxy Resin Technology-Developments Since 1979, Noyes Data Corp., Park Ridge, NJ, 1982.
28. M. F. Doerner and W. D. Nix, A method for interpreting the data from depth-sensing indentation instruments. *Journal of Materials Research*, 1986, **1**, 601.
29. L. T. Drzal, M. J. Rich, M. F. Koenig and P.F Lloyd, Adhesion of graphite fibers to epoxy matrices: II. The effect of fiber finish. *Journal of Adhesion*, 1983, **16**, 133-152.
30. L. T. Drzal, M. J. Rich and P. F. Lloyd, Adhesion of graphite fibers to epoxy matrices: I. The role of fiber surface treatment. *Journal of Adhesion*, 1982, **16**, 1-30.
31. B. Ellis, Ed., Chemistry and Technology of Epoxy Resins, 1st edition, 1993, Chapman & Hall, New York.
32. B Ellis, Introduction to the chemistry, synthesis, manufacture and characterization of epoxy resins, Chemistry and Technology of Epoxy Resins, 1st edition, Ed. B. Ellis, , Chapman & Hall, New York, 1993, 1-36.
33. T. Emrick, H.-T. Chang, and J. M. J. Frechet, An $A_2 + B_3$ approach to hyperbranched aliphatic polyethers containing chain end epoxy substituents. *Macromolecules*, 1999, **32**, 6380-6382.

34. E. W. Flick, Epoxy Resins, Curing Agents, Compounds, and Modifiers, 1987, Noyes Publications, Park Ridge, NJ.
35. A. Gao and K. L. Reifsnider, Tensile failure of composites: Influence of interface and matrix yielding. *Journal of Composites Technology and Research*, 1992, **14**(4), 201-210.
36. J. Gassan and A. K. Bledzki, Influence of fiber surface treatment on the creep behavior of jute fiber-reinforced polypropylene. *Journal of Thermoplastic Composite Materials*, 1999, **12**, 388-398.
37. J. F. Gerard, Characterization and role of an elastomeric interphase on carbon fibers reinforcing an epoxy matrix. *Polymer Engineering Science*, 1988, **28**, 568-577.
38. R.J. Good, N. R. Srivatsa, M. Islam, H. T. L. Huang and C. J. Van Oss, Theory of the acid-base hydrogen-bonding interactions, contact angles, and the hysteresis of wetting-application to coal and graphite surfaces. *Journal of Adhesion Science and Technology*, 1990, **4**(8), 607-617.
39. G. Gray and G. Savage, Advanced Thermoplastic Composite Materials. *Metals and Materials*, 1989, **5**, 513.
40. R. B. Grubbs, M. E. Broz, J. M. Dean, and F. S. Bates, Selectively epoxidized polyisoprene-polybutadiene block copolymers. *Macromolecules*, 2000, **33**, 2308-2310.
41. R. B. Grubbs, J. M. Dean, M. E. Broz, and F. S. Bates, Reactive block copolymers for modification of thermosetting epoxy. *Macromolecules*, 2000, **33,** 9522-9534. .
42. K. Hakala, R. Vatanparast, S. Li, C. Peinado, P. Bosch, F. Catalina, and H. Lemmetyinen, Monitoring of curing process and shelf life of the epoxy-anhydride system with TICT compounds by the fluorescence technique. *Macromolecules*, 2000, **33**, 5954-5959.
43. Y. Han , S. Schmitt and L. Friedrich, Microfriction of various phases in a carbon fiber, polytetrafluoroethylene, graphite and polyetheretherketone composite blend as measured by atomic force microscopy. *Tribology International*, 1998, **31**(12), 715-725.
44. J. C. Hedrick, N. M. Patel, and J. E. McGrath, Toughening of Epoxy-Resin Networks with Functionalized Engineering Thermoplastics, Toughened Plastics I: Science and Engineering, Advances in Chemistry Series (233), C.K. Riew and A. J. Kinloch, Ed., 1993, American Chemical Society, Washington DC, 293-304.
45. C. L. Heisey, Adhesion of Novel High Performance Polymers to Carbon Fibers: Fiber Surface Treatment, Characterization, and Microbond Single Fiber Pull-out Test. *Virginia Tech dissertation,* 1993.
46. P. J. Herrera-Franco and L. T. Drzal, Comparison of methods for the measurement of fiber matrix adhesion in composites, *Composites*, 1992, **23**(1), 2-27.
47. H. Ho, J. J. Lesko, J. Morton, K. L. Reifsnider, S. Wilkinson and T.C. Ward, Effect of fiber treatment on the in-plane shear properties of composite materials. *Journal of Adhesion*, 1993, **42**, 39-53.
48. J. L. Hopewell, University of Queensland Dissertation, Brisbane, Australia, 1997.
49. K. Jayaraman, K. L. Reifsnider and R. E. Swain, Elastic and thermal effects in the interphase: Part I. Comments on characterization methods. *Journal of Composites Technology and Research*, 1993, **15**(1), 14-22.

50. T. D. Juska and P. M. Puckett, Matrix resins and fiber/matrix adhesion, Composites Engineering Handbook, Ed. P.K. Mallick 1997, Marcel Dekker, Inc., New York
51. D. H. Kaelble, J. Moacanin and A. Gupta, Physical and Mechanical Properties of Cured Resins, Epoxy Resins: Chemistry and Technology, C. A. May, Ed., 1988, Marcel Dekker, Inc., 603-651.
52. J. Kaji, K. Nakahara, K. Ogami, T, Endo, Synthesis of a novel epoxy resin containing pyrene moiety and thermal properties of its cured polymer with phenol novolac. *Journal of Applied Polymer Science*, 2000, 75, 528-535.
53. M. Kaji, K. Nakahara, K. Ogami, and T. Endo, Synthesis of a novel epoxy resin containing diphenylether moiety and thermal properties of its cured polymer with phenol novolac. *Journal of Polymer Science: Part A: Polymer Chemistry*, 1999, **37**, 3687-3693.
54. M. Kaji, T. Endo, Synthesis of a novel epoxy resin containing naphthalene moiety and properties of its cured polymer with phenol novolac. *Journal of Polymer Science: Part A: Polymer Chemistry*, 1999, **37**, 3063-3069.
55. E. T. Kang, Z. H. Ma, K. L. Tan, O. N. Tretinnikov, Y. Uyama, and Y. Ikada, Surface hardness of pristine and modified polyaniline films. *Langmuir*, 1999, **15**(16), 5389-5395.
56. H. M. Kang, T. H. Yoon, M. Bump, and J. S. Riffle, Effect of solubility and miscibility on the adhesion behavior of polymer-coated carbon fibers with vinyl ester resins. *Journal of Applied Polymer Science*, 2001, **79**(6), 1042-1053.
57. I.-C. Kim and T.-H. Yoon, Enhanced interfacial adhesion of carbon fibers to vinyl ester resin using poly(arylene ether phosphine oxide) coatings as adhesion promoters, *Journal of Adhesion Science and Technology*, 2000, **14**(4), 545-559.
58. A. Korjakin, R. Rikards, F.-G. Buchholz, H. Wang, A. K. Bledzki and A. Kessler, Comparative study of interlaminar fracture toughness of GFRP with different fiber surface treatments. *Polymer Composites*, 1998, **19**(6), 793-806.
59. M. Kobayashi, F. Sanda, and T. Endo, Application of phosphonium ylides to latent catalysts for polyaddition of bisphenol A diglycidyl ether with bisphenol A: model system of epoxy-novolac resin. *Macromolecules*, 1999, 32(15), 4751-4756.
60. M. Kobayashi, F. Sanda, and T. Endo, Application of (triphenylphosphinemethylene)boranes to thermally latent catalysts for polyaddition of bisphenol A: model system of epoxy-novolac resin. *Macromolecules*, 2001, **34**, 1134-1136.
61. V. Lacrampe, J. P. Pascault and J. F. Gerard, Physicochemical characterization of interphase created from sizings in glass fibers based epoxy composites. *Polymer Preprints*, 1995, **36**, 813-814.
62. B. K. Larson and L. T. Drzal, Glass fibre sizing/matrix interphase formation in liquid composite moulding: effects on fibre/matrix adhesion and mechanical properties. *Composites*, 1994, **25**, 711.
63. P. Lemoine and J. McLaughlin, Surface Topography Applications. *Application Note Burleigh Instruments, Inc.*, **16**, March 1998.
64. H. Lee and K. Neville, Handbook of Epoxy Resins, 1967, McGraw-Hill, Inc., New York.
65. J. J. Lesko, A. Rau, and J. S. Riffle, Proc. 10th American Society of Composites, 18-20 Sept., 1995, 53-62.

66. J. J. Lesko, R. E. Swain, J. M. Cartwright, J. W. Chin, K. L. Reifsnider, D. A. Dillard and J. P. Wightman, Interphases developed from fiber sizings and their chemical-structural relationship to composite compressive performance. *Journal of Adhesion*, 1993, **45**, 43-57.
67. C. H. Lin and C. S. Wang, Novel phosphorus-containing epoxy resins Part I. Synthesis and properties. *Polymer*, 2001, **42**(5), 1869-1878.
68. J.-F. Lin, C.-F. Ho, and S. K. Huang, Thermal characterization of the phosphorus-containing sulfone-modified epoxy resins by thermogravimetric analysis and direct pyrolysis-GC/MS measurement of the thermally degradative volatiles. *Polymer Degradation and Stability*, 2000, **67**, 137-147.
69. Y.-L. Liu, G.-H. Hsuie, Y.-S. C, R.-J. Jeng and L.-H. Perng, Phosphorus-containing epoxy for flame retardant. I. Synthesis, thermal, and flame-retardant properties, *Journal of Applied Polymer Science*, 1996, **61**, 613-621.
70. I. Luzinov, D. Julthongpiput, A. Liebmann-Vinson, T. Cregger, M. D. Foster, and V. V. Tsukruk, Epoxy-terminated self-assembled monolayers: molecular glues for polymer layers. *Langmuir*, 2000, **16**, 504-516.
71. M. S. Madhukar and L. T. Drzal, Fiber-matrix adhesion and its effect on composite mechanical properties: I. Inplane and interlaminar shear behavior of graphite/epoxy composites. *Journal of Composite Materials*, 1991, **25**(8), 932-957.
72. M. S. Madhukar and L. T. Drzal, Fiber-matrix adhesion and its effects on composite mechanical properties: IV. Mode I and mode II fracture toughness of graphite/epoxy composites. *Journal of Composite Materials*, 1992, **26**, 936-968.
73. S. Magonov, Studies of polymer surfaces with atomic force microscopy. *Application Note*, *Digital Instruments,* October 1995.
74. J. Mahy, L. W. Jeneskens and O. Grabandt, The fibre/matrix interphase and the adhesion mechanism of surface-treated Twaron® aramid fibre. *Composites*, 1994, 25(7), 653-660.
75. S. Maiti, S. Banerjee, and S. K. Palit, Phosphorus-containing polymers, *Progress in Polymer Science*, 1993, **18**, 227-261.
76. J. J. Mallon and P. M. Adams, Synthesis and characterization of novel epoxy monomers and liquid crystal thermosets. *Journal of Polymer Science: Part A: Polymer Chemistry*, 1993, **31**, 2249-2260.
77. C. A. May, Ed., Epoxy Resins: Chemistry and Technology, 1988, Marcel Dekker, Inc. New York.
78. C. A. May, Introduction to Epoxy Resins, Epoxy Resins: Chemistry and Technology, C. A. May, Ed., Marcel Dekker, Inc. New York, 1988.
79. P. F. M. Meurs, B. A. G. Schrauwen, P. J. G. Schreurs and T. Peijs, Determination of the interfacial normal strength using single fibre model composites. *Composites*, 1998, **29A**(9-10), 1021-1026.
80. J. Mijovic, X. Chen, and J.-W Sy, Dipole dynamics in liquid crystalline epoxies by broad-band dielectric relaxation spectroscopy. *Macromolecules*, 1999, **32**, 5365-5374.
81. T. F. Mika and R. S. Bauer, Curing Agents and Modifiers, Synthesis and Characteristics of Epoxides, Epoxy Resins: Chemistry and Technology, C. A. May, Ed., 1988, Marcel Dekker, Inc. New York.

82. M. Miwa, A. Takeno, K. Yamaguchi, and A. Watanabe, Relation between shear strength of the fibre-matrix interphase and shear properties of the resin matrix. *Journal of Material Science*, 1995, **30**(8), 2097-2100.
83. S. I. Moon and J. Jang, The effect of the oxygen-plasma treatment of UHMWPE fiber on the transverse properties of UHMWPE-fiber/vinyl ester composites. *Composites Science and Technology*, 1999, **59**(4), 487-493.
84. M. Munz, H. Sturm, E. Schulz and G. Hinrichsen, The scanning force microscope as a tool for the detection of local mechanical properties within the interphase of fibre reinforced polymers. *Composites*, 1998, **29A**(9-10), 1251-1259.
85. L.E. Nielsen, Cross-linking – Effect on physical properties of polymers, *Journal of Macromolecular Science – Reviews Macromolecular Chemistry*, 1969, **C3**(1), 69-103.
86. C. Ortiz, R. Kim, E. Rodighiero, C. K. Ober, and E. J. Kramer, Deformation of a polydomain, liquid crystalline epoxy-based thermoset. *Macromolecules*, 1998, **31**, 4074-4088.
87. N. Oya and H. Hamada, Axial compressive behavior of reinforced fibres and interphase in glass/epoxy composite materials. *Journal of Material Science*, 1998, **33**(13), 3407-3417.
88. G. M. Pharr, W. C. Oliver, and F. R. Brotzen, On the generality of the relationship among contact stiffness, contact area, and elastic modulus during indentation. *Journal of Materials Research*, 1992, **7**, 1564.
89. M. R. Piggott, Failure processes in the fibre-polymer interphase. *Composites Science and Technology*, 1991, **42**, 57-76.
90. W. G. Potter, Epoxide Resins, 1970, Springer-Verlag, New York.
91. S.K.Rajaraman, W.A.Mowers, and J.V.Crivello, Novel hybrid monomers bearing cycloaliphatic epoxy and 1-propenyl ether groups. *Macromolecules*, 1999, **32**, 36-47.
92. V. Rao, P. Herrera-Franco, A. D. Ozzello and L. T. Drzal, A direct comparison of the fragmentation test and the microbond pull-out test for determining the interfacial shear strength. *Journal of Adhesion*, 1991, **34**, 65-77.
93. A. Renner and J.-A Cotting, Novel epoxy resins based on cyclohexanone-aldehyde condensation products. *Journal of Applied Polymer Science*, 1990, **39**, 789-802.
94. J. S. Riffle, J. Yilgor, C. Tran, G. L. Wilkes, J. E. McGrath and A. K. Banthia, Elastomeric Polysiloxane Modifiers for Epoxy Networks: Synthesis of Functional Oligomers and Network Formation Studies. Epoxy Resin Chemistry, ACS Symposium Series (221), 1983, R. S. Bauer, Ed., 21-54.
95. D. J. Riley, Synthesis and Characterization of Phosphorus Containing Poly(arylene ether)s, *Virginia Tech Dissertation*, 1997.
96. D. J. Riley, A. Gungor, S. A. Srinivasan, M. Sankarapandian, C. Tchatchoua, M. W. Muggli, T. C. Ward, J. E. McGrath, and T. Kashiwagi, Synthesis and characterization of flame resistant poly(arylene ether)s. *Polymer Engineering and Science*, 1997, **37**(9), 1501-1511.
97. J. C. Salamone, Ed., Polymeric Materials Encyclopedia, CRC Press, Boca Raton, 1996.
98. C. C. Schmitt and J. R. Elings, Nanoindenting, scratching, and wear testing using scanning probe microscopy. *Application Note, Digital Instruments*, April 1997.

99. S. J. Shaw, Additives and Modifiers for epoxy resins, Chemistry and Technology of Epoxy Resins, 1st edition, B. Ellis, Ed., Chapman & Hall, New York, 1993, 117-143.
100. A. Sjogren, R. Joffe, L. Berglund and E. Mader, Effects of fibre coating (size) on properties of glass fibre/vinyl ester composites. *Composites*, 1999, **30A**, 1009-1015.
101. B. Starr, E. Burts, J. R. Upson and J. S. Riffle, Polyester dimethacrylate oligomers and networks. 2001, submitted to *Polymer*.
102. S. Subramaniam, J. J. Lesko, K. L. Reifsnider and W. W. Stinchcomb, Characterization of the fiber-matrix interphase and its influence on mechanical properties of unidirectional composites. *Journal of Composite Materials*, 1996, **30**(3), 309-332.
103. N. B. Sunshine, Flame retardancy of phenolic materials, Flame Retardancy of Phenolic Resins and Urea- and Melamine-formaldehyde Resins, Vol. 2, W.C. Kurlya and A. J. Papa, Eds., 1973.
104. Y. Tanaka, Synthesis and Characteristics of Epoxides, Epoxy Resins: Chemistry and Technology, C. A. May, Ed., Marcel Dekker, Inc. New York, 1988.
105. Y. Tanaka and R. S. Bauer, Curing Reactions, Synthesis and Characteristics of Epoxides, Epoxy Resins: Chemistry and Technology, C. A. May, Ed., Marcel Dekker, Inc. New York, 1988.
106. C. Tan, H. Sun, and B. M. Fung, Properties of liquid crystal epoxy thermosets cured in a magnetic field. *Macromolecules*, 2000, **33**, 6249-6254.
107. P. M. Thangamathesvaran and S. R. Jain, Synthesis and characterization of thiocarbononhydrazone-based epoxy resins. *Journal of Polymer Science, Part A: Polymer Chemistry*, 1991, **29**, 261-267.
108. M. N. Tillie, T. M. Lam and J. F. Gerard, Insertion of an interphase synthesized from a functionalized silicone into glass-fibre/epoxy composites. *Composites Science and Technology*, 1998, **58**(5), 659-663.
109. C. Tran, Modification of Polymers I. Polysiloxane Modified Epoxies II. Segmented Polyurethane Blends, *Virginia Tech Dissertation*, 1984.
110. T. Y. Tsui, W. C. Oliver, and G. M. Pharr, Nanoindentation of Soft Films on Hard Substrates: The Importance of Pile-Up. *Materials Research Society Symposium Proceedings*, 1997, **436**, 207-212.
111. C. S. Tyberg, Void-Free Flame Retardant Phenolic Networks: Properties and Processability, Virginia Tech Dissertation, 2000.
112. C. S. Tyberg, K. Bergeron, M. Sankarapandian, P. Shih, A. C. Loos, D. A. Dillard, J. E. McGrath, J. S. Riffle, and U. Sorathia, Structure-property relationships of void-free phenolic-epoxy materials, *Polymer*, 2000, **41**, 5053-5062.
113. U.S. Department of Transportation, Bureau of Transportation Statistics, web site, http://www.bts.gov/aboutbts.html, 2001.
114. A. Valadez-Gonzalez, J. M. Cervantes-Uc, R. Olayo and P. J. Herrera-Franco, Effect of fiber surface treatment on the fiber-matrix bond strength of natural fiber reinforced composites. *Composites*, 1999, **30B**(3), 309-320.
115. M. R. VanLandingham, R. R. Dagastine, R. F. Eduljee, R. L. McCullough and J. W. Gillespie Jr., Characterization of nanoscale property variations in polymer composite systems: 1. Experimental results. *Composites*, 1999, **30A**(1), 75-83.

116. M. R. Vanlandingham, S. H. McKnight, G. R. Palmese, J. R. Elings, X. Huang, T. A. Bogetti, R. F. Eduljee and J. W. Gillespie Jr., Nanoscale indentation of polymer systems using the atomic force microscope. *Journal of Adhesion*, 1997, **64**, 31.
117. P. C. Varelidis, R. L. McCullough and C. D. Papaspyrides, The effect of temperature on the single-fiber fragmentation test with coated carbon fibers. *Composite Science and Technology*, 1998, **58**(9), 1487-1496.
118. T. Vu-Khanh and S. Frikah, Influence of processing on morphology, interface, and delamination in PEEK/carbon composites. *Journal of Thermoplastic Composite Materials*, 1999, **12**, 84-95.
119. I.-Y. Wan, J. E. McGrath and T. Kashiwagi, Triarylphosphine oxide containing Nylon 6,6 copolymers, Fire and Polymers II Materials and Tests for Hazard Prevention, ACS Symposium Series (599), G. L. Nelson, Ed., 1995, 29-40.
120. C. Wang and C.-R. Liu, Transcrystallization of polypropylene composites: nucleating ability of fibres. *Polymer*, 1999, **40**(2), 289-298.
121. C. S. Wang and C. H. Lin, Novel phosphorus-containing epoxy resins. Part II: curing kinetics, *Polymer*, 2000, **41**, 8579-8586.
122. C. S. Wang and C. H. Lin, Novel phosphorus-containing epoxy resins. Part I: synthesis and properties, *Polymer*, 2001, **42**, 1869-1878.
123. C.-S. Wang and J.-Y. Shieh, Synthesis and properties of epoxy resins containing bis(3-hydroxylphenyl) phenyl phosphate, *European Polymer Journal*, 2000, **36**, 443-452.
124. C. –S. Wang and J.-Y.Shieh, Synthesis and properties of epoxy resins containing 2-(6-oxid-6H-dibenz<c,e><1,2>oxaphosphorin-6-yl)1,4-benzenediol. *Polymer*, 1998, **39**, 5819.
125. S. Wang, Phosphorus-containing polymers, their blends, and hybrid nanocomposites with poly(hydroxyether), metal chlorides, and silica colloids, Virginia Tech Dissertation, 2000.
126. S. Wang, T. E. Glass, H. Zhuang, M. Sankarpandian, Q. Ji, A. R. Shultz, and J. E. McGrath, Miscibility of phosphine oxide containing poly(imide) and bisphenol-A poly(hydroxyether). *American Chemical Society Polymer Preprints*, 1998, **40**(2), 744-745.
127. S. Wang, Q. Ji, C. T. Tchatchoua, A. R. Shultz, and J. E. McGrath, Synthesis and characterization of poly(arylene ether phosphine oxide/sulfone) statistical copolymers and their blends with poly(hydroxyethers)("phenoxy resin"), *American Chemical Society Polymer Preprints*, 1998, **39**(2), 410-411.
128. S. Wang, Q. Ji, C. T. Tchatchoua, A. R. Shultz, and J. E. McGrath, Phosphonyl/hydroxyl hydrogen bonding-induced miscibility of poly(arylene ether phosphine oxide/sulfone) statistical copolymers with poly(hydroxy ether) (phenoxy resin): Synthesis and characterization, *Journal of Polymer Science Part B – Polymer Physics*, 1999, **37**(15), 1849-1862.
129. S. F. Waseem, S. D. Gardner, G. Je, W. Jiang and U. Pittman Jr., Adhesion and surface analysis of carbon fibres electrochemically oxidized in aqueous potassium nitrate. *Journal of Materials Science,* 1998, **33**(12), 3151-3162.

130. H. R. Wu, D. W. Dwight and N. T. Huff, Effects of silane coupling agents on the interphase and performance of glass-fiber-reinforced polymer composites. *Composites Science and Technology*, 1997, **57**(8), 975-983.
131. S. Yang, J.-S. Chen, H. Korner, T. Breiner, C. K. Ober, and M. D Poliks, Reworkable epoxies: thermosets with thermally cleavable groups for controlled network breakdown. *Chemistry of Materials, Communications*, 1998, **10**(6), 1475-1482.
132. X. Yang, P. C. Painter, and M. M. Coleman, Equilibrium constants and predictions of mixcibility windows and maps for polymer blends involving p-(hexafluoro-2-hydroxy-2-propyl)styrene with methacrylate and acetoxy groups. Macromolecules, 1992, 25(8), 2156-2165.
133. E. Yilgor and I. Yilgor, 1,3-Bis(γ-aminopropyl)tetramethyldisiloxane modified epoxy resins: curing and characterization. *Polymer*, 1998, **39**(8-9), 1691-1695.
134. H. S. Yu, T. Yamashita, and K. Horie, Synthesis and chemically amplified photo-cross-linking reaction of a polyimide containing an epoxy group. *Macromolecules*, 1996, **29**, 1144-1150.
135. H. Zhuang, Synthesis and Characterization of Aryl Phosphine Oxide Containing Thermoplastic Polyimides and Thermosetting Polyimides with Controlled Reactivity, Dissertation Virginia Tech, 1998.

Vita

Born in 1973 to Gary and Brenda Bobbitt, Maggie enjoyed growing up with her sister Callie in the beautiful Blue Ridge Mountains of southwestern Virginia. She attended Floyd County High School, graduating first in her class in 1991. Maggie pursued her bachelor degree at Virginia Polytechnic Institute and State University. While at VPI & SU, she also received her teaching certificate in secondary education, worked at Burrough's Wellcome (Research Triangle Park, NC) as a cooperative education student, and met her future husband, Greg Bump. After completing her undergraduate work in 1996, Maggie and Greg were married. Maggie returned to VPI&SU for graduate study in the field of synthetic polymer chemistry. In 2001, she completed her doctoral degree and is looking forward to teaching chemistry.